THE IMPACT OF WATER CONTENT AND OTHER ENVIRONMENTAL PARAMETERS ON TOLUENE REMOVAL FROM AIR IN A DIFFERENTIAL BIOFILTRATION REACTOR

A thesis

submitted in the partial fulfilment

of the requirements for the Degree

of

Doctor of Philosophy in Chemical and Process Engineering

in the

University of Canterbury

by

Abraham L. Beuger

Department of Chemical and Process Engineering
University of Canterbury
2008

Abstract

In this work, a differential reactor was used to expose all the biofilter packing material (compost) to a uniform toluene concentration in air. The reactor was combined with water content control using the suction cell principle and traditional inlet concentration, temperature and humidity control.

The matric potential was controlled using the suction cell principle between -5 to -300 cm H_2O which controlled the water content between 0.99 and 2.30 g g^{-1} (dry weight). Two types of compost were used, with different water retention curves with no observed difference in elimination capacity. The elimination capacity varied between 2.7 g m^{-3}_r hr^{-1} and 21 g m^{-3}_r hr^{-1} with low potential causing low removal rates. The reduction in EC at low matric potentials was attributed to several factors: loss of water availability to the organisms, water redistribution in the medium, non-adaptable micro-organisms, and reduced mass transfer.

Cultures isolated from compost were used to inoculate the reactor to create a biofilm. A maximal observed surface EC of is 0.17 g m^{-2}_r hr^{-1} and a specific removal rate of 1250 g m^{-3}_b hr^{-1} is measured. These values were used in modelling the biofilter performance.

The EC was dependent on the residual toluene concentration. The EC increased with increasing toluene concentration until reaching a critical concentration. Above this concentration, 100 – 300 ppm (0.37- 1.11 g m^{-3}) depending on biofilm thickness and area of coverage, the EC was constant. Three toluene dependency curves were fitted using a zero order and a composite model using a weighted average of a zero and first order component. From the data the critical concentration (C_{crit}) and the EC_{crit} was found and used to determine the biofilm thickness. It was estimated to be between 68 and 134 μm. Using a q_{max} of 1250 g m^{-3}_b hr^{-1} and optimising the model a K_s of $1.3 \cdot 10^{-1}$ g m^{-3}_g was found. This was comparable to values found in the literature. There was no significant difference in the fit between both models. The K_s was low compared to the majority of the data, which means that the zero order part of the composite model dominated.

Nitrogen and other nutrients were added to investigate their influence on the elimination capacity (EC) of toluene. Also the effect of temperature on the EC was investigated between 14 and 60 °C. Maximal removal rates were found between 25 and 55 °C. The EC decreased by 90% going from 55 to 60 °C and took many weeks to recover.

Without any extra nitrogen added to the media, the EC averaged around 6 ± 0.3 g m^{-3}_r h^{-1}. Although the average EC was lower than most reports for toluene removal, it was still in the general range reported. When NH_4Cl (1 g l^{-1}) was added to the reactor, the EC increased to 41 ± 1.7 g m^{-3}_r hr^{-1}. Similar effects were observed with nitrate addition; the steady state EC doubled from 30.1 ± 0.9 g m^{-3}_r hr^{-1} to 76.3 ± 2.5 g m^{-3}_r hr^{-1}. Other macronutrients tested like phosphate, sulphate, magnesium, calcium and iron did not increase the EC.

Table of contents

List of Figures

List of Tables

Acknowledgements

The first person to thank is my supervisor Dr. Peter Gostomski. Not only for tricking me into doing a PhD, but also in supporting me with advice and direction. Also thanks for introducing me to the Staff volleyball.

I would like to thank the mechanical and electronic workshop; Ray Allen, Peter Jones, Leigh Richardson, Bob Gordon and Tim Moore. Without your expertise the experimental design would not have become reality. Also thanks to Tony Allen, for the ever available computer support. And thanks to Trevor Berry and David Brown for your general support and analytical wisdom.

I would also like to thank two undergrad students for helping me along the way; Lars Madsen from Odense University in Denmark and Anas Saudi, a CAPE 3rd Pro-Student. Thanks to you both for collecting valuable data.

Especially I would thank my friends and colleagues within the department. A special mention goes out to Rahul Shastry, my office mate, for never a dull moment even during experimental no-mans-land and John Gabites for Friday beers. As well as Justin Nijdam for making lunch more enjoyable and in acknowledging the fact that people are annoying.

Financial assistance was gratefully acknowledged from the University of Canterbury Targeted Scholarship fund.

Thanks to my partner Amber. Without her support I would never dreamed about undertaking this journey. And for staying in your home town for me!

Finally, I would like to thank my parents for ‘giving’ me up for 3 ½ years. Pap en Mam bedankt!

natura non facit saltus

Nature does not make jumps

plebeius es incommodo

Chapter 1: Introduction

1.1 Air pollution control

VOC's are known environmental pollutants that are often toxic and/or carcinogenic as well as contributors to odour problems, global warming and ozone depletion (Sercu *et al.*, 2005). They are mostly released in the air by commercial processes and transportation. Examples of industrial operations with large VOC emissions are: printing and coating, plastics, electronics and paint manufacturing (Yoon and Park, 2002), the automobile industry (Morgado *et al.*, 2004), wastewater and solid waste treatment facilities (Moe and Irvine, 2001b) and the petrochemical industry.

Several biological and non-biological methods are available to remove odours and VOC's from waste air streams. Non biological methods include dispersion, condensation, scrubbing, incineration, absorption and UV oxidation. (Kennes and Veiga, 2001). Advantages include possible pollutant recovery and removal of non biodegradable pollutants. These techniques are preferred at high (>1000ppm) pollutant concentrations. Many of these methods are very costly, especially in energy requirements. Biological air pollution control techniques include biofilters, biotrickling filters and membrane reactors. One of the advantages of using biological air pollution control methods is that the pollutants are actually destroyed by biological oxidation. A downside is that some pre-treatment of the air and pollutant may be required, for example pre-filtration for particulates, temperature adjustments and humidification of the gas flow (Leson and Winer, 1991). Biofiltration, depending on the contaminant concentration and gas flow rate, can be the most suitable method to remove pollutants.

1.2 Biofiltration

The first reports on the use of a biological method to remove odour from an air stream in a waste water treatment plant were found in 1923 in Germany (Leson and Winer, 1991). Until the 1970's, biological degradation of pollutants was mainly used in soil and waste water treatment. From the mid 70's, the technique of removing pollutants from waste air streams by biological degradation became more common. A driving

force behind these developments was more stringent regulations of odour and pollutant emissions. A reason for these new regulations, especially in Europe was the decreased separation of industrial and residential areas. The regulations and financial support for biofiltration projects increased the use of biofiltration in the late 70's to the mid 80's (Leson and Winer, 1991). From then on, more research was done and new applications were discovered.

The pollutants are oxidised by the wide variety of micro-organisms normally present in natural biofilter packing (Juteau *et al.*, 1999). If an inert packing material is used, specialist strains can be added (Acuna *et al.*, 1999; Prado *et al.*, 2002; Sakuma *et al.*, 2006). Pollutants that are degraded vary from malodorous (H_2S, NH_3) to highly toxic compounds and solvents. Although biofiltration is a simple process, the degradation of gaseous emissions is a complex phenomenon. It involves three phases (packing material, water and gas) and biological kinetics (Fig. 1.1) (Morgado *et al.*, 2004). The emissions treated can be odours, VOCs or a combination of the two.

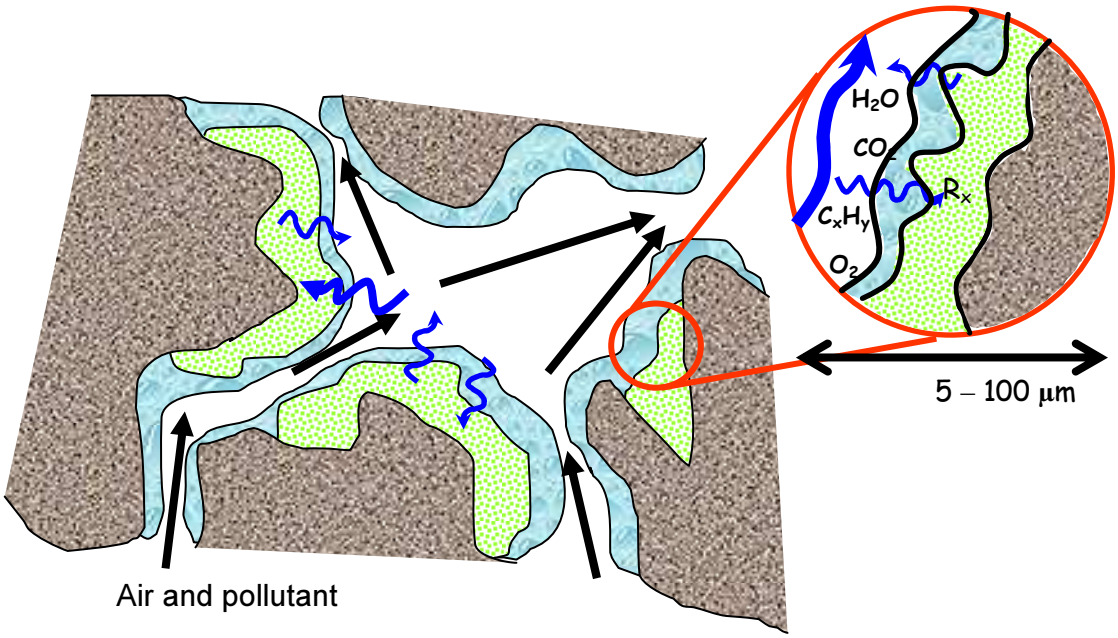

***Figure 1.1**: Schematic presentation of the mass transfer and removal of pollutants in a biofilter. The pollutant (C_xH_x) and oxygen diffuse through the water layer into the biofilm where the pollutant is oxidised with rate R_x into CO_2 and water.*

1.2.1 Odour control

In meat rendering plants, the inlet gasses of a biofilter contains over 400 different compounds, 40 of which are odorous. (Luo and Van Oostrom, 1997). These components are mostly sulphur containing compounds like H_2S, mercaptans and organic sulphide and nitrogen-based compounds like ammonia, amines, indole and skatole. Other odorous compounds like volatile fatty acids, alcohols and aldehydes are also produced (McGahan *et al.*, 2002). Biological treatment destroys the odorous emissions and does not hide or store them. The micro-organisms oxidise the odorous compounds into CO_2 and H_2O and other non-odorous products such as nitrates and sulphates (Schlegelmilch *et al.*, 2005).

1.2.2 VOC control

The main commercial applications for biofiltration have been in low concentrations of VOC's ($\leq$ 1,000 ppm) in large volumetric gas flows (1,000 to 150,000 $m^3\ hr^{-1}$) (Leson and Winer, 1991). Biological removal of pollutants in waste air streams has some advantages over more traditional removal techniques; it is inexpensive; both in capital and operating costs, versatile, reliable and importantly environmental friendly (Ottengraf and Vandenoever, 1983).

1.3 Thesis outline

Although biofiltration is a simple concept, the processes involved are very complex. Not only is the mass transfer between three phases important but also the microbial kinetics. They are both dependent on environmental parameters like packing type, substrate and nutrient concentrations, water content and temperature. To investigate the effect of these parameters on the performance of a biofilter, a suitable experimental apparatus is required.

1.3.1 Reactor development

In order to rigorously control environmental parameters, the differential reactor technique, commonly used in catalysis research, was extended to biofiltration. A differential reactor exposes all of the solid catalytic phase (compost) to the same environmental parameters (water content, contaminant concentration, temperature, etc.). Applying this concept to biofiltration was complicated by the need to control

water content. This was accomplished by using a very thin bed of compost hydraulically connected to a water reservoir. This reactor system is in contrast to a traditional long column (integral) laboratory biofilter where most of the parameters change along the length of the reactor.

The reactors and experimental setup are discussed in Chapter 2 and are the first report of a differential reactor with rigorous water content control in biofiltration research. With this reactor system, the environmental parameters discussed in the following sections are investigated.

1.3.2 Water

A critical aspect of biofilter operation is the control of the water content of the bed material (Devinny *et al.*, 1999). Although this is widely recognized, water content control has received little attention. Too little water will reduce microbial activity and irreversibly damage the packing material. Too much water fills the biofilter pores and reduces the mass transfer of nutrients, oxygen and waste products (Bohn and Bohn, 1999). High water content also leads to structural problems, increased pressure drops in the biofilter bed and excessive leachate.

Structured investigations on the influence of water content are limited (Cox *et al.*, 1996; Holden *et al.*, 1997a; Krailas *et al.*, 2000; Stark and Firestone, 1995; Sun *et al.*, 2002; Wang and Govind, 1997). Wang and Govind (1997) found the highest performance at a moisture content between 47 – 60% dry weight for compost and between 60 – 70% dry weight for peat. They also found that if the bed material became severely dried, irreversible damage to the bacterial community and the packing material occurred. There are several ways that water content directly and indirectly influences biofiltration. For example low water content alters cell morphology, which influences micro-colony size and ultra-structure (Auerbach *et al.*, 2000; Chang and Halverson, 2003) and water is also a primary controller of the oxygen availability (Holden, 2001).

Chapter 3 will discuss the influence of the water content or more accurately matric potential on the removal of toluene. The best removal rates are seen at matric

potentials between -10 and -100 cm H_2O, with a maximum at -20 cm H_2O. At higher and lower matric potentials the removal rate is reduced.

1.3.3 Microbiology

Most biofiltration media are natural products with an extensive microbial community such as compost and soil. Compost has not only bacteria present, but also a multitude of yeast, moulds, protozoa, and even algae and microscopic worms. These other organisms can play a role in the effectiveness of the biofilter. Natural selection plays an important role in a biofilter. If the pollutant is a source of energy, strains that can use it will usually dominate. The acclimatisation to steady state removal can take several days (Torkian *et al.*, 2003) to several months (Li and Liu, 2006; Torkian *et al.*, 2003). Many research groups try to reduce acclimation time by creating an inoculum separately from the biofilter.

The isolation of toluene degraders from compost will be discussed in Chapter 4. The cultures are directly applied in the reactor to form a biofilm. These experiments will give some insight in specific removal rates which are similar to literature values.

1.3.4 Pollutant

The main objective of a biofilter is to remove pollutants in the gas phase. For good operation, the pollutant has to be transferred from the gas phase into a biologically active layer. In this layer, the pollutant is oxidised and serves as a source of energy and occasionally anabolic processes. Traditionally, the degradation kinetics in a biofilm are described using growth and maintenance by the model proposed by Jacques Monod in the 1940s (Rittmann and McCarty, 2001). The concentration of the pollutant plays an important role in the rate of degradation. It was proposed by Ottengraf and Vandenoever (1983) that at low pollutant concentrations, the removal is limited by mass transfer and at high concentrations by the available biomass.

In Chapter 5 the impact of pollutant concentration is explored. Using toluene as the model compound, the removal rate increases with increasing toluene concentration until a critical concentration is reached. Above this concentration, 100 – 300 ppm depending on biofilm thickness and area of coverage, the EC is constant. The data is

fitted with a zero, first and composite models. Both the zero and composite models give a good fit and show that the theory proposed by Ottengraf and Vandenoever (1983) is valid.

1.3.5 Nutrients

Micro-organisms need a source of carbon, nitrogen, potassium and sulphur to increase their biomass. Often other elements are also required for protein and nucleic acids synthesis (Rittmann and McCarty, 2001). Biofilter bed media are mostly natural materials like compost or peat. They support a wide variety of micro-organisms and have an amount of major and minor nutrients (Cherry and Thompson, 1997). The amount of nutrients is often considered sufficient for microbial survival (Leson and Winer, 1991), but at high loading rates nutrient addition is sometimes required (Morales *et al.*, 1998).

After carbon (50%) and excluding water, nitrogen (13%) is the second most common element or compound in bacterial cell mass (Delhomenie *et al.*, 2001b; Morgenroth *et al.*, 1996). The availability of nitrogen to the microbial flora is very important in biological systems, like biofiltration. Although the total nitrogen concentration in biofiltration media can be large, the total available nitrogen is the important parameter. The total available nitrogen in compost is mainly present as ammonium and nitrate (Corsi and Seed, 1995). Addition of nitrogen to the biofilter media can significantly improve biofilter operation (Corsi and Seed, 1995; Morales *et al.*, 1998)

The effect of nutrients like ammonia, nitrate, phosphate buffer, magnesium sulfate, iron sulfate and calcium chloride on the removal rate is explored in Chapter 6. The most significant effect for the compost tested is observed with ammonia and nitrate.

1.3.6 Temperature

The degradation of pollutants in biofilters is mostly accomplished by mesophilic organisms, especially if the biofilter is in the open air exposed to ambient conditions. Thermophilic organisms are also found, but to a lesser extent. In general, degradation of the pollutant is predicted to increase with temperature until an optimum is reached. This optimum lies between 20 and 40 °C (Leson and Winer, 1991).

The effect of temperature is investigated in Chapter 6. The range explored is between 14 and 60 °C. The removal rate is constant over a wider range (25 to 55 °C) than reported elsewhere. Above 55 °C, the removal rate decreases by 90%.

1.3.7 Future work

The future work will be discussed in the specific chapters, but will be summarised in Chapter 7. Also in this chapter; future experiments that did not fit in a specific chapter or overlap within chapters will be discussed.

1.4 References

Acuna, M. E., F. Perez, R. Auria, and S. Revah. 1999. Microbiological and kinetic aspects of a biofilter for the removal of toluene from waste gases. *Biotechnology and Bioengineering* 63: 175-184.

Auerbach, I. D., C. Sorensen, H. G. Hansma, and P. A. Holden. 2000. Physical morphology and surface properties of unsaturated *Pseudomonas putida* biofilms. *Journal of Bacteriology* 182: 3809-3815.

Bohn, H. L., and K. H. Bohn. 1999. Moisture in biofilters. *Environmental Progress* 18: 156-161.

Chang, W. S., and L. J. Halverson. 2003. Reduced water availability influences the dynamics, development, and ultrastructural properties of *Pseudomonas putida* biofilms. *Journal of Bacteriology* 185: 6199-6204.

Cherry, R. S., and D. N. Thompson. 1997. Shift from growth to nutrient-limited maintenance kinetics during biofilter acclimation. *Biotechnology and Bioengineering* 56: 330-339.

Corsi, R. L., and L. Seed. 1995. Biofiltration of BTEX: Media, substrate, and loadings effects. *Environmental Progress* 14: 151-158.

Cox, H. H. J., F. J. Magielsen, H. J. Doddema, and W. Harder. 1996. Influence of the water content and water activity on styrene degradation by *Exophiala jeanselmei* in biofilters. *Applied Microbiology and Biotechnology* 45: 851-856.

Delhomenie, M. C., L. Bibeau, S. Roy, R. Brzezinski, and M. Heitz. 2001. Influence of nitrogen on the degradation of toluene in a compost-based biofilter. *Journal of Chemical Technology and Biotechnology* 76: 997-1006.

Devinny, J. S., M. A. Deshusses, and T. S. Webster. 1999. *Biofiltration for air pollution control*. Lewis Publishers, Boca Raton, Fla.

Holden, P. A. 2001. Biofilms in unsaturated environments. *Microbial Growth in Biofilms, Pt B* 337: 125-143.

Holden, P. A., L. J. Halverson, and M. K. Firestone. 1997. Water stress effects on toluene biodegradation by *Pseudomonas putida*. *Biodegradation* 8: 143-151.

Juteau, P., R. Larocque, D. Rho, and A. LeDuy. 1999. Analysis of the relative abundance of different types of bacteria capable of toluene degradation in a compost biofilter. *Applied Microbiology and Biotechnology* 52: 863-868.

Kennes, C., and M. C. Veiga. 2001. *Bioreactors for waste gas treatment*. Kluwer Academic, Dordrecht ; Boston.

Krailas, S., Q. T. Pham, R. Amal, J. K. Jiang, and M. Heitz. 2000. Effect of inlet mass loading, water and total bacteria count on methanol elimination using upward flow and downward flow biofilters. *Journal of Chemical Technology and Biotechnology* 75: 299-305.

Leson, G., and A. M. Winer. 1991. Biofiltration - an innovative air-pollution control technology for VOC emissions. *Journal of the Air & Waste Management Association* 41: 1045-1054.

Li, L., and J. X. Liu. 2006. Removal of xylene from off-gas using a bioreactor containing bacteria and fungi. *International Biodeterioration & Biodegradation* 58: 60-64.

Luo, J. F., and A. Van Oostrom. 1997. Biofilters for controlling animal rendering odour - a pilot-scale study. *Pure and Applied Chemistry* 69: 2403-2410.

McGahan, E., C. Kolominskas, K. Bawden, and R. Ormerod. 2002. Strategies to reduce odour emissions from meat chicken farms. Pages 27-39. *Poultry Information Exchange Conference*.

Moe, W. M., and R. L. Irvine. 2001. Polyurethane foam based biofilter media for toluene removal. *Water Science and Technology* 43: 35-42.

Morales, M., S. Revah, and R. Auria. 1998. Start-up and the effect of gaseous ammonia additions on a biofilter for the elimination of toluene vapors. *Biotechnology and Bioengineering* 60: 483-491.

Morgado, J., G. Merlin, Y. Gonthier, and A. Eyraud. 2004. A mechanistic model for m-xylene treatment with a peat-bed biofilter. *Environmental Technology* 25: 123-132.

Morgenroth, E., E. D. Schroeder, D. P. Y. Chang, and K. M. Scow. 1996. Nutrient limitation in a compost biofilter degrading hexane. *Journal of the Air & Waste Management Association* 46: 300-308.

Ottengraf, S. P. P., and A. H. C. Vandenoever. 1983. Kinetics of organic-compound removal from waste gases with a biological filter. *Biotechnology and Bioengineering* 25: 3089-3102.

Prado, O. J., J. A. Mendoza, M. C. Veiga, and C. Kennes. 2002. Optimization of nutrient supply in a downflow gas-phase biofilter packed with an inert carrier. *Applied Microbiology and Biotechnology* 59: 567-573.

Rittmann, B. E., and P. L. McCarty. 2001. *Environmental biotechnology : principles and applications*. McGraw-Hill, Boston.

Sakuma, T., T. Hattori, and M. A. Deshusses. 2006. Comparison of different packing materials for the biofiltration of air toxics. *Journal of the Air & Waste Management Association* 56: 1567-1575.

Schlegelmilch, M., J. Streese, and R. Stegmann. 2005. Odour management and treatment technologies: An overview. *Waste Management* 25: 928-939.

Sercu, B., K. Demeestere, H. Baillieul, H. Van Langenhove, and W. Verstraete. 2005. Degradation of isobutanal at high loading rates in a compost biofilter. *Journal of the Air & Waste Management Association* 55: 1217-1227.

Stark, J. M., and M. K. Firestone. 1995. Mechanisms for soil-moisture effects on activity of nitrifying bacteria. *Applied and Environmental Microbiology* 61: 218-221.

Sun, Y. M., X. Quan, J. W. Chen, F. L. Yang, D. M. Xue, Y. H. Liu, and Z. H. Yang. 2002. Toluene vapour degradation and microbial community in biofilter at various moisture content. *Process Biochemistry* 38: 109-113.

Torkian, A., R. Dehghanzadeh, and M. Hakimjavadi. 2003. Biodegradation of aromatic hydrocarbons in a compost biofilter. *Journal of Chemical Technology and Biotechnology* 78: 795-801.

Wang, Z., and R. Govind. 1997. Biofiltration of isopentane in peat and compost packed beds. *Aiche Journal* 43: 1348-1356.

Yoon, I. K., and C. H. Park. 2002. Effects of gas flow rate, inlet concentration and temperature on biofiltration of volatile organic compounds in a peat-packed biofilter. *Journal of Bioscience and Bioengineering* 93: 165-169.

Chapter 2: Reactor development

2.1 Introduction

The system for accurate moisture control developed by Ranasinghe and Gostomski (2003) is modified for continuous operation. This chapter will lay out the design and operation of the reactors used in this research.

The purpose of this work is to rigorously control environmental parameters, especially water content and contaminant concentration (toluene) to investigate their effect on volumetric removal rates. To accomplish this, the differential reactor technique, commonly used in catalysis research, is extended to biofiltration. A differential reactor exposes all of the solid catalytic phase (compost) to the same environmental parameters (water content, contaminant concentration, temperature, etc.). The conversion per pass through the bed is negligible but a high rate of mixing (or recycle) effectively exposes the entire bed to the same reactant concentration while generating a measurable conversion (Carberry, 1964).

Catalytic studies are mainly conducted using differential or integral reactors. Integral reactors can rarely be operated isothermally and analysis of the data is complicated. Although the differential reactor provides good kinetic data, even small analytical errors often lead to inaccurate rates (Tajbl *et al.*, 1966).

An ideal reactor can be defined as a reactor operated isothermally over a wide range of steady state conversions. This has to apply to both catalysts and reactants. The residence time has to be clearly defined and from it, direct rate laws can be determined (Carberry, 1964). Using this definition for an ideal reactor, new reactors have been developed in order to get more accurate kinetic data. These include mixed flow reactors, recycle reactors and batch recycle reactors (Levenspiel, 1999).

Applying this concept to biofiltration is complicated by the need to control water content. This is accomplished by using a very thin bed of compost hydraulically connected to a water reservoir. This reactor system is in contrast to a traditional long column (integral) laboratory biofilter where most of the parameters change along the

length of the reactor. Toluene is used as the model contaminant because of the availability of extensive literature results for comparison.

2.1.1 Recycle reactor

The elements of a recycle reactor are a catalyst bed, a circulation pump and tubing to form a loop (Fig. 2.1). The recycle rate (recycle flow / inlet flow) has to be large to achieve small conversion rates per pass.

The average overall rate of conversion can be described by Eq. 2.1. The nomenclature can be found in Sec. 2.9.

$$R = \frac{(C_{in} - C_{out})F_g}{V} \qquad [2.1]$$

The advantage of this type of reactor is when operated at high recycle rates, the high velocities and low conversion per pass leads to negligible gradients within the bed (Carberry, 1964).

One of the hard parameters to decide on is the recycle ratio. This ratio is dependent on the process parameters like reactor volume, packing volume and flow rates and is defined as the recycle flow rate divided by the volumetric flow rate into the system. As a general rule a recycle ratio of 20 is suggested by Gillespie and Carberry (1966), although disputed by Wedel and Villadsen (1983) as this number can lead to large errors in the catalytic rates.

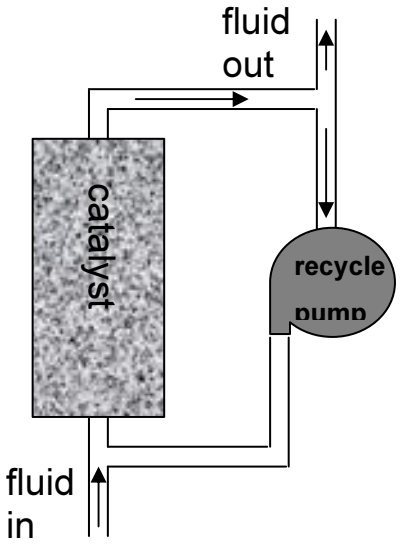

***Figure 2.1**: Schematic design of the recycle reactor.*

Other problems with this type of reactor include difficulties in temperature control, leakages and large dead volumes that can lead to slow response to transient changes (Berty, 1974).

2.1.2 Batch reactors

The above recycle system can be modified into a batch reactor. By removing the in- and outlet flow and adding a reservoir, a reactor system as used by Butt *et al.* (1962) (Fig 2.2) is created.

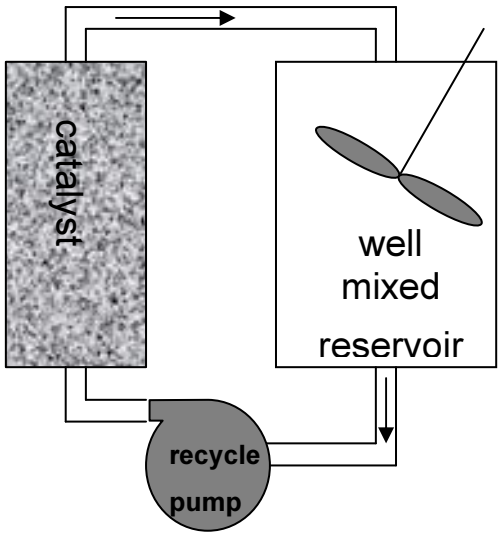

***Figure 2.2**: Schematic design of the batch reactor.*

In order to get good experimental data, the concentration throughout has to be uniform and the conversion per pass very small (Levenspiel, 1999). Ranasinghe and Gostomski (2003) based their experimental work on this type of reactor system.

2.1.3 Mixed flow reactors

Mixed flow reactors require a uniform composition of the fluid throughout the reactor for accurate data to be collected. Several types of the mixed flow reactor are described in the literature. One reactor is an internal recycle reactor, or gradient-less reactor (Fig. 2.3) described by Berty (1974), the other a basket-type reactor (Fig. 2.4).

The Berty reactor is an internal recycle reactor that circulates gas past a stationary catalyst bed using a vane blower. It is very suitable for high temperature and pressure reactions. This design is commercially available from Autoclave Engineers, USA.

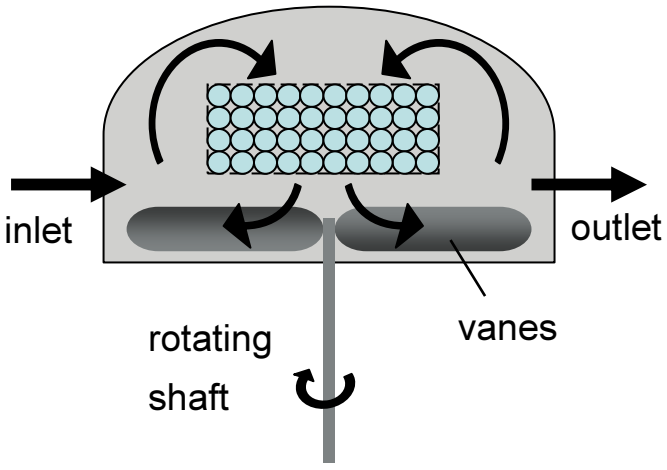

***Figure 2.3**: Berty reactor.*

A related reactor type is a basket-type mixed flow reactor. In this reactor, developed by Carberry (1964), the catalyst is packed in mesh baskets attached to a shaft. This shaft rotates and the baskets with the catalyst are stirred through the gas phase to produce perfect mixing. Both these reactors give excellent control of volume, temperature and flow rates.

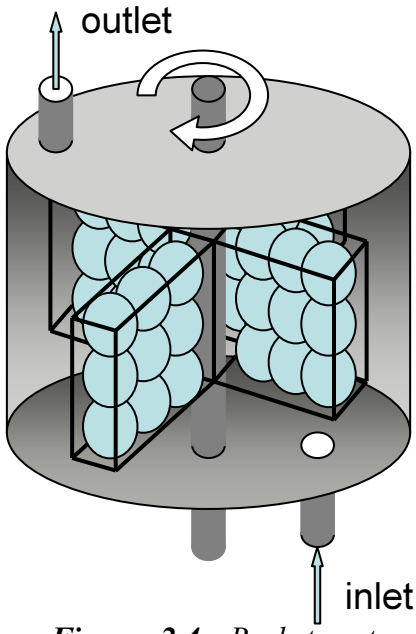

***Figure 2.4**: Basket – type mixed flow reactor*.

One important parameter to control in this study is the water content of the catalyst; in this case compost. None of the continuous reactors described to date provide any obvious means to control the water content.

2.1.4 Control of the water content

Water in soil and other porous media is retained largely by matric forces in pores and as films on particle surfaces. At saturation water content or zero tension, all of the pores are filled with liquid water and the matric potential, ψ_m, is zero (Papendick and Campbell, 1981). When an external force or tension (vacuum, pressure or gravity) is applied to the porous media, an equilibrium between the force and the matric force in the media will form. Every soil has a unique relationship between the matric potential and the physical amount of water in the soil. By controlling the matric potential, the water content can be controlled.

Like the catalysts studies in the mixed flow reactors, the amount of compost should be small. The advantage of a small amount distributed in a thin layer is that the water distribution is more uniform. To control the water content of the compost, it has to be in direct contact with the water without becoming saturated. Techniques used in soil physics to measure matric potential, like the pressure plate (Hanks, 1992; Kirkham and Powers, 1972) and tension plate (Hillel, 1982) can be adapted for matric potential control.

The suction cell (Fig. 2.5) is a relatively simple but accurate approach to control the water content in the compost. The compost is placed on a semi-permeable material which provides hydraulic contact with a water reservoir in a chamber directly below. The membrane is permeable to water, but not to air. Most hydrophilic filtration membranes operated at differential pressures below their bubble point can be used. The chamber is connected to an external water reservoir placed below the membrane. By changing the height between the reservoir and the membrane, a vacuum is applied to the membrane.

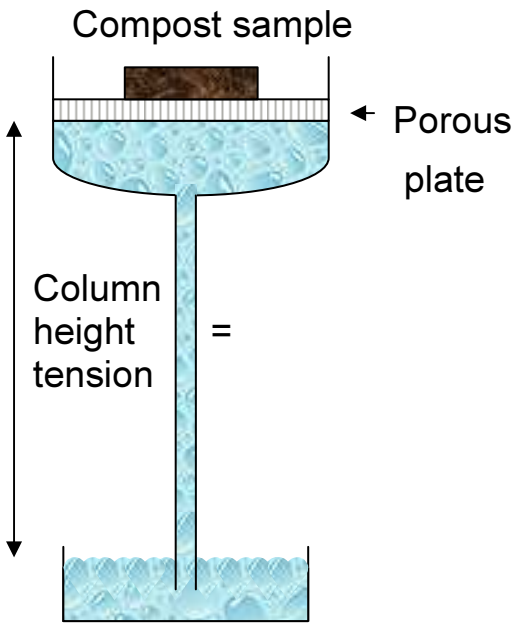

***Figure 2.5**: Suction cell assembly.*

The water potential in the compost will equilibrate to the water potential in the chamber. If the potential in the compost is smaller ('wet' compost), excess water from the compost will be drained away. If the water potential in the compost is higher ('dry' compost) than the water potential in the chamber, the compost will pull water up to equilibrate. The supply reservoir at the bottom of Fig. 2.5 provides excess water capacity so that water movement in either direction does not effectively change the tension applied at the membrane surface.

The capability of water content control of the tension plate and the mixed flow reactor are combined into a continuous well mixed laboratory-scale biofilter. In this reactor environmental parameters like water content, contaminant concentration and temperature are controlled.

2.2 Reactor design

The reactor is based on a similar design as reported by Ranasinghe and Gostomski (2003). Although the control of the water potential is based on the same principle, the reactors and experimental setup are modified to obtain a continuous system. This design will make it the only differential reactor that includes rigoruous water control in biofiltration. The reactors are mainly constructed out of glass and are operated continuously.

2.2.1 Initial Reactor design

The reactor is based on a two part glass filtration funnel (Fig. 2.6) (Cole-Parmer, Vernon Hills, IL). The bottom part (B) is a glass funnel with a sintered disk as a membrane support which fits a 90 mm membrane. The top part (A) is a funnel with a volume of 1000 ml. The top edge of this funnel is ground down to create a flat surface to facilitate a gasket. A stainless steel ring in two parts (parts A1 and A2 in Fig. 2.7) is placed around the bottom lip of part A. This enables part A to be clamped tightly to part B.

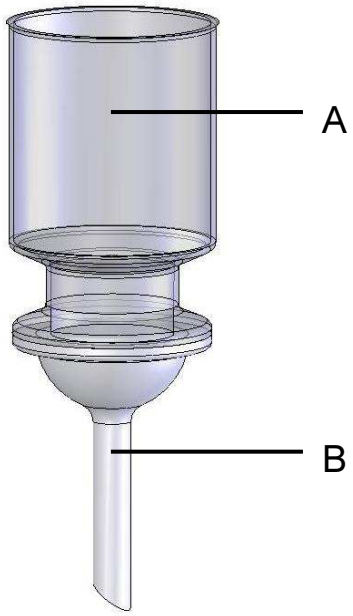

***Figure 2.6**: The filtration funnel basis of the reactor design.*

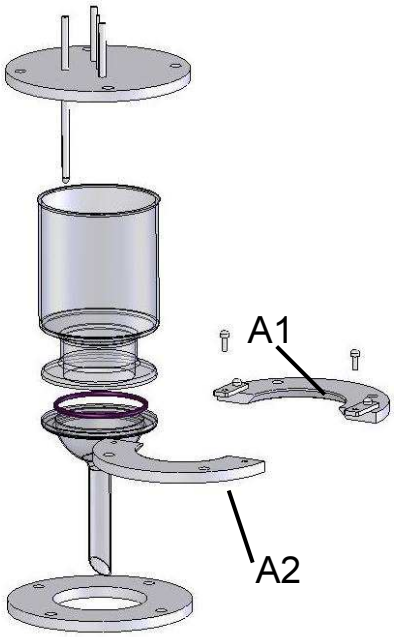

***Figure 2.7**: The filtration funnel with stainless rings and head plate.*

Glass was chosen instead of the stainless steel of the previous reactor (Ranasinghe and Gostomski, 2003) for visual inspection of the interior during the run. Changes in water content influence the colour of the compost. Also excess water condensation on the walls and air bubbles trapped underneath the membrane can be observed. These air bubbles can disrupt the conductivity of the water across the membrane.

The two glass parts are kept together with two stainless steel rings and a head-plate, fastened by three threaded rods and nuts (Fig. 2.7). Between the two glass parts, a membrane (Mixed cellulose ester, diameter 90 mm, pore size 0.45 μm, Advantec MFS Inc. Dublin, CA) is placed and on top of the membrane a Viton o-ring to prevent leaks and glass-on-glass grinding.

The head-plate has a groove in which a Viton o-ring (ID 80mm, 2.35 mm cross section, Dotmar Engineering Plastics Ltd, Christchurch, NZ) is placed. Also three ports; two ¼" gas ports and a 1/8" liquid port, and a thermo-well, made out of ¼" tubing are welded in. All three ports are all fitted with ¼" brass Swagelok fittings (Swagelok, Solon, OH).

After extensive leak testing, the bottom glass part (part B) of the design did not prove to be robust. The tests included submerging the whole system in a water bath and pressurizing it to approximately 0.5 bar. It was left overnight and the bottom part was found shattered in the morning. Additional details are described in App. A.

2.2.2 Reactor 1

The lack of robustness (App. A) of the initial design resulted in a redesign of the bottom reservoir (Fig. 2.8 part C). A 50 mm long piece of OD 100 mm (thickness 5 mm) glass (part C3) is clamped between two stainless steel plates (C2 and C4) and sealed by Viton o-rings (ID 91 mm, 2.35 mm cross section, Dotmar Engineering Plastics Ltd, Christchurch, NZ). The bottom plate (C4) has two pieces of 1/8" stainless steel tubing welded in. One is used for the connection to the water reservoir, the other one for removal of air bubbles under the membrane. The top part of this tube is connected to a small piece of 1/8" Viton tubing with a Y-connector (Fig. 2.9). This Y-connector has two pieces of Viton tubing, which are in contact with the bottom of

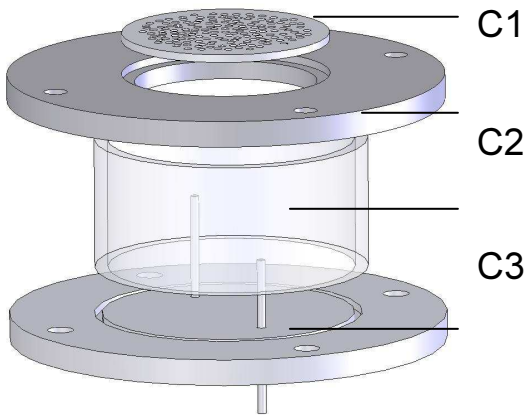

***Figure 2.8**: The final design of the bottom reservoir (part C) and membrane support.*

the membrane support to be able to remove all entrapped air. The top plate (C2) holds an 80 mm diameter stainless steel perforated disk (C1), which functions as the support for the membrane.

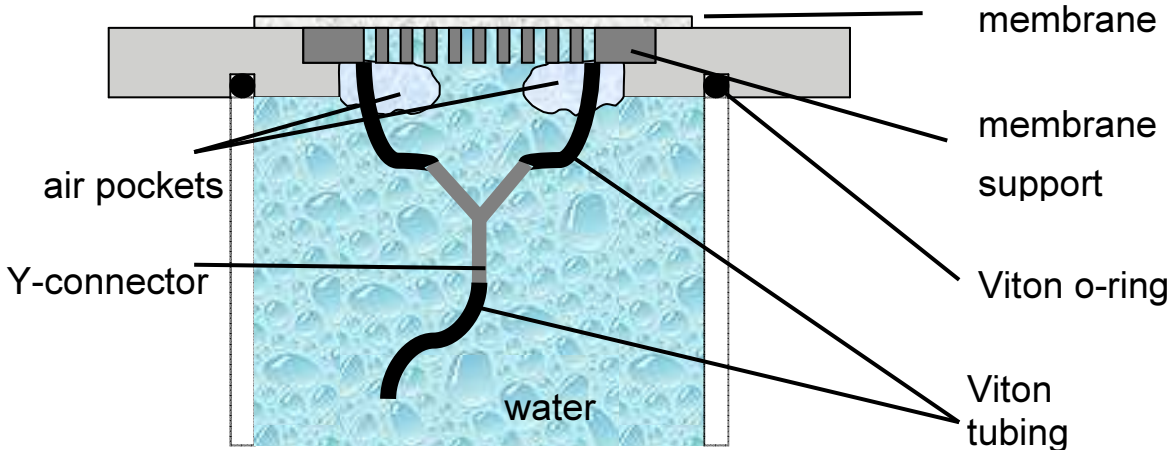

***Figure 2.9**: Open–cut of the bottom part (C) of the reactor. The Y piece and tubing is used to remove any trapped air from underneath the membrane.*

The membrane is placed on top of the support and a Viton o-ring (ID 80mm, 2.35 mm cross section, Dotmar Engineering Plastics Ltd, Christchurch, NZ) is used to create a seal. The glass top part of the filtration funnel is placed on top of the o-ring (Fig. 2.10) and fastened by tightening the nuts on the threaded rods. The head-plate is placed on top and can be removed without disturbing the seal on the membrane.

Agitation of the head space is provided by an external diaphragm pump (flow rate 22.6 L min^{-1}) (Thomas Pumps, 107CD18-198A, Sheboygan, WI) with a Teflon liner.

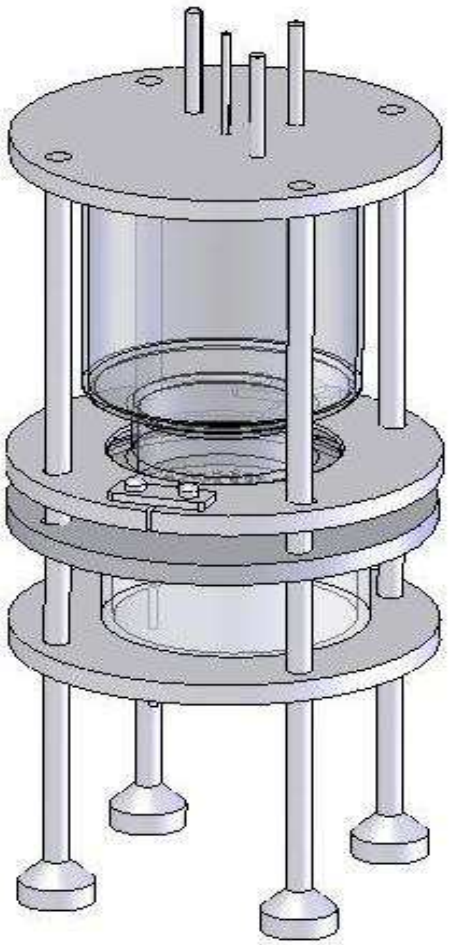

***Figure 2.10**: Reactor 1 assembly.*

2.2.3 Reactor 2

The second version of the reactor (Fig 2.11) uses direct agitation of headspace driven by a magnetically coupled drive (Fig 2.12) (AMAR Equipments PVT. LTD, QM64, India) and an electric motor.

The magnetic coupled drive is a zero leakage drive originally designed for high pressure, high temperature operation. The drive consists of an external magnet rotor,

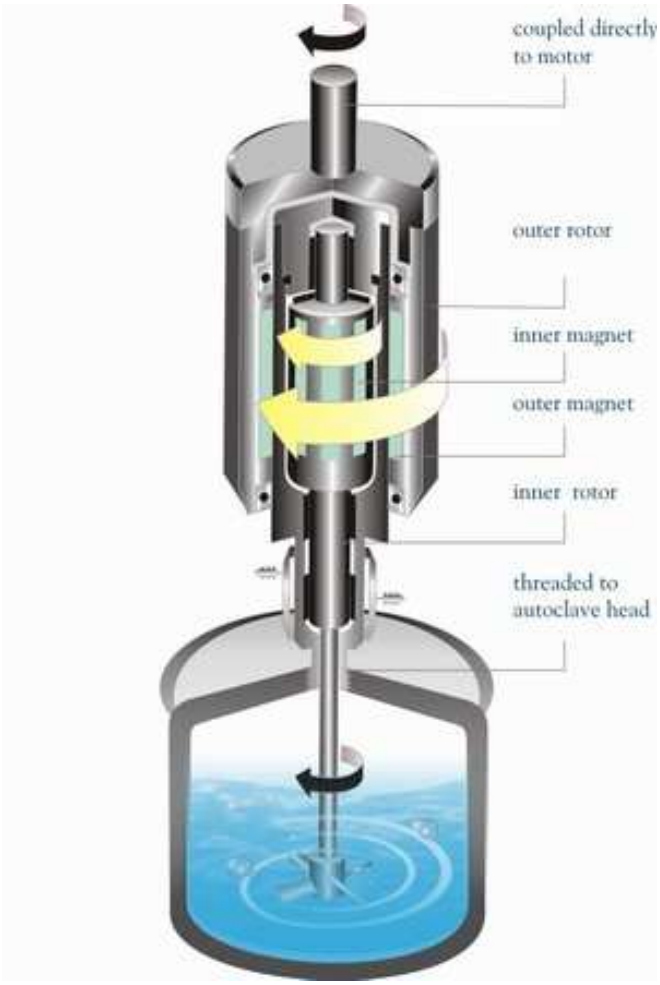

***Figure 2.12**: Section view of the magnetic drive, courtesy of Amar Equipment Ltd.*

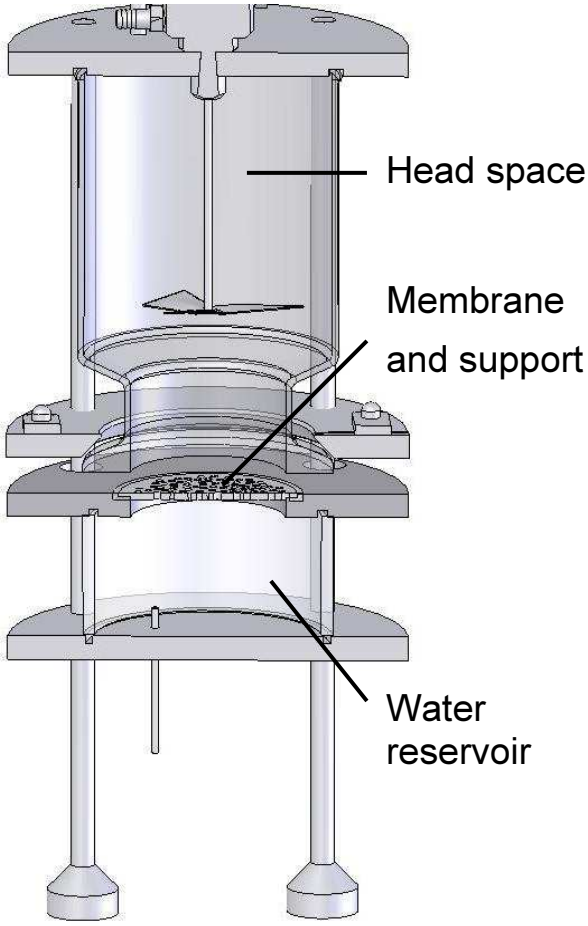

***Figure 2.11**: Section view of Reactor 2 showing the direct agitation.*

which is driven by the motor. A stationary shell is threaded to the head plate of the reactor. So the external rotor is completely isolated from the inner rotor. As the external rotor rotates, the internal rotor, to which the shaft is threaded, rotates in synchrony.

The head plate has two ¼" gas ports and a thermo-well, made out of ¼" tubing welded in. Both ports are fitted with stainless steel Swagelok fittings (Swagelok, Solon, OH).

2.2.4 Reactor 3

The third version of the reactor used direct agitation of headspace, without a magnetic drive. A shaft is inserted through the head-plate. A Viton rotary seal (SealJet New Zealand Ltd, Christchurch, NZ) provides the air tight seal between the shaft and the reactor (Fig 2.13). The shaft is driven by an electric motor (model: 50D522-70A, 1300 rpm, FASCO Asia Pacific, Australia) through a sprocket and belt assembly.

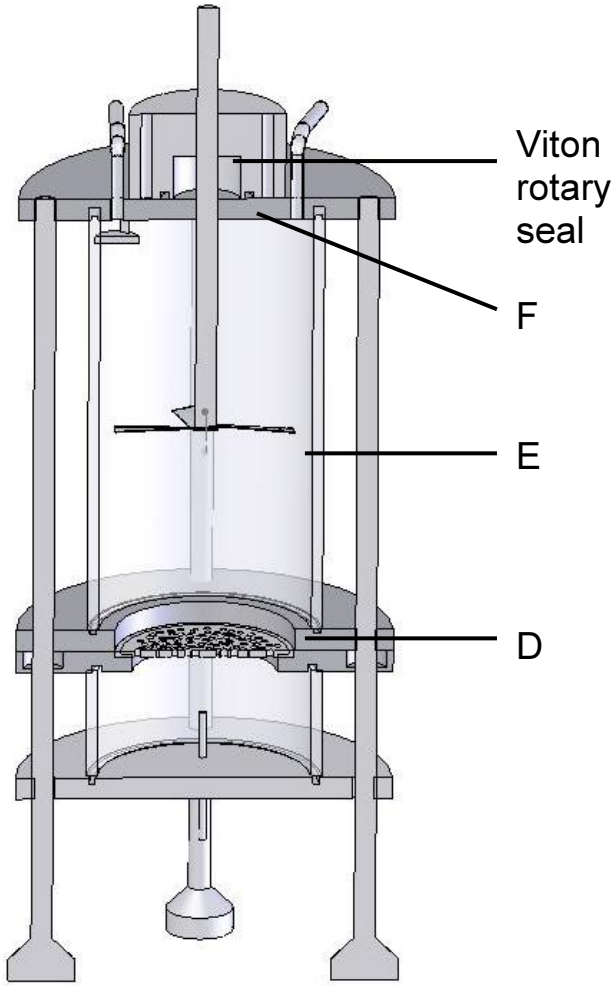

***Figure 2.13**: New design of reactor version 3. Direct agitation sealed by a rotary seal. This includes the new design of the gas reservoir.*

The other design change was in the top reservoir. Instead of the filtration funnel, a larger piece of the glass tubing (same as the water reservoir) is used. The tubing (E) is clamped between the bottom plate (D in Fig. 2.13) and the top head plate (F). The advantages of this revised design were lower cost and flexibility in the volume. The head plate (F) and the glass tube (E) can be removed without disturbing the compost or the membrane. This improves the access to the compost.

2.2.5 Column reactor

The column reactor is similar to integral biofilters widely used in research. It consists of a 60 cm, 1” ID Quickfit glass pipe. The top and bottom are connected to 1” to QVF reducers. Between the bottom reducer and the pipe two layers of fine steel mesh provide support for the bed material.

2.3 Diffusion tube

Several different methods are available to create a dilute concentration of a volatile contaminant in a gas stream when the pure contaminant is liquid at ambient conditions. The most widely used system bubbles the inlet gas stream through a pure liquid contaminant. This system, when properly designed, will generate a constant contaminant concentration (nearly saturated). This gas stream can be diluted to the appropriate level. This design although simple, has two significant drawbacks. First as the liquid level drops, the contact time of the gas and the liquid reduces and the contaminant concentration will decrease. Second the temperature of the liquid contaminant must be controlled to maintain a constant vapour pressure and the near saturated air stream must not be allowed to cool below its dew point prior to dilution.

Another widely used system is a syringe pump. A syringe is filled with the liquid contaminant and slowly the liquid is brought in contact with the gas phase. Due to cohesion of the liquid, a drop will form at the tip of the syringe. This drop falls into the tube and greatly increasing the surface area for evaporation. This causes fluctuations in the concentration of the contaminant in the gas phase. These fluctuations can be up to 25% (Ergas *et al.*, 1999).

An easier method is to use a compressed gas bottle comprising of air and a known amount of the contaminant. Most contaminants used in biofiltration are available. This is only a practical at low gas flow rates. While straight forward, obtaining consistent bottles from suppliers can sometimes be difficult (App. A.6).

A novel technique for biofiltration research, although widely used in chromatography uses a diffusion tube. Gases and vapours diffuse through tubes at a uniform rate if the temperature, concentration gradients, and tube geometry remain unchanged. Diffusion tubes are a convenient method of producing low concentrations of solvent vapours in a moving gas stream (Nelson, 1971).

Diffusion tubes come in a wide variety of configurations. As long as the length and cross sectional area are known, the diffusion rates can be calculated. A rule of thumb for the geometry is that the area to length ratio should be less than 0.3. The diameter

of the tube should not be larger than 20 mm as this will cause turbulence which decreases the effective diffusion path length.

The driving force of diffusion is the concentration gradient up the tube. The liquid contaminant reservoir acts as the source governed by the temperature at which the reservoir is maintained. This temperature defines the partial vapour pressure above the liquid (Altshuller and Cohen, 1960).

The diameter of the tube is another important design parameter. The tube cannot be too thin. A thin tube causes a strong capillary effect, which changes the effective diffusion length. Large tube diameters in combination with high flow rates of the gas phase will cause turbulence or eddies at the tube outlet. This will extend the region of vapour free gas down into the tube which leads to a decrease in effective diffusion length. The optimal range of the tube diameter according to Altshuller and Cohen (1960) is between 0.2 and 2 cm.

The diffusion coefficient is affected by the temperature (T in K) and pressure (P in bar) of the diffusion tube system. The diffusion coefficient is (D) calculated from Eq. 2.2 (Nelson, 1971).

$$D = D_{298}\left(\frac{T}{298}\right)^{n}\frac{1}{P} \qquad [2.2]$$

The value of coefficient *n* varies between 1.6 and 2. According to Chen and Othmer (1964) a coefficient of 1.81 is used. The change in temperature will also lead in a change in vapour pressure (p_v) of the toluene and is described by the Antoine relationship:

$$\ln p_v = A - \frac{B}{T + C} \qquad [2.3]$$

The factors A, B and C are found in the literature (Table 2.1) and p_v is the vapour pressure at temperature T. The coefficients used are from Pitzer and Scott (1943).

***Table 2.1**: Antoine coefficients for toluene, according to the National Institute of Standards and Technology. These values will give a vapour pressure in bar.*

Temperature (K)	A	B	C	Reference
273.1 – 297.9	4.23679	1426.448	-45.957	Besley and Bottomley, 1974
303.0 – 343.0	4.08245	1346.382	-53.508	Gaw and Swinton, 1968
420.0 - 580.0	4.54436	1738.123	0.394	Ambrose *et al*., 1967
308.5 - 384.7	4.07827	1343.943	-53.773	Williamham *et al*., 1945
273.0 – 323.0	4.14157	1377.578	-50.507	Pitzer and Scott, 1943

If assumed that the concentration of the toluene vapour at the tube exit remains near zero by the air flow and that the vapour in the diffusion tube is saturated, the volumetric flow rate of toluene (q_d) can be calculated with Eq. 2.4 and the concentration generated (C_{dif}) with Eq. 2.5 (Nelson, 1971).

$$q_d = \frac{D \cdot A_t \cdot \ln\left(\frac{P}{P - p_v}\right)}{L} \qquad [2.4]$$

$$C_{dif} = \frac{q_d}{F_g} 10^6 \qquad [2.5]$$

The concentration of toluene (C_{dif}) into the system is controlled in three ways;

1. Changes in temperature will lead to changes in vapour pressure and the diffusion coefficient; hence in diffusion rate.
2. The second variable is the gas flow rate (F_g). Increasing the gas flow rate will decrease the concentration exiting the diffusion tube. However, the diffusion rate will remain constant, which means that the overall mass of toluene per time is constant as well.
3. The third method of controlling the concentration is by changing the dimensions (area A_t and length L) of the diffusion tube itself.

The diffusion tube (Fig 2.14) is constructed from a stainless steel block with two ¼" SS pieces of tubing and a third SS piece of tubing to form a tee. Three different versions of diffusion tubes are constructed (Table 2.2).

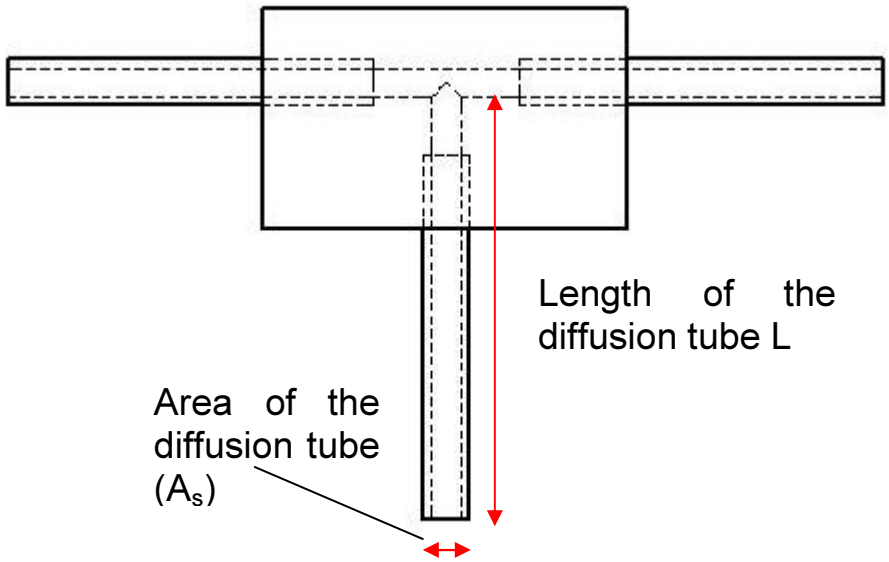

***Figure 2.14**: Cross section of the diffusion tube.*

***Table 2.2**: The diffusion tube dimensions and the theoretical concentration generated by the diffusion tubes at a gas flow rate of 22 ml min^{-1}.*

Diffusion tube	**Tube ID (cm)**	**Tube area A_s (cm^2)**	**Tube length L (cm)**	**Concentration at 5 °C (ppm)**	**Concentration at 50 °C (ppm)**
Small	0.15	0.018	17.0	5	66
Medium	0.395	0.123	17.0	18	250
Large	0.64	0.332	11.6	69	961

The feed air is passed continuously through the two horizontal tubes across the top of the vertical tube. The vertical tube is connected to a 1 L flask containing approximately 30 ml of liquid toluene allowing free diffusion of toluene vapour. This system (Fig. 2.15) is submerged in a temperature-controlled (GD100, Grant Instruments, Cambridge, England) water bath.

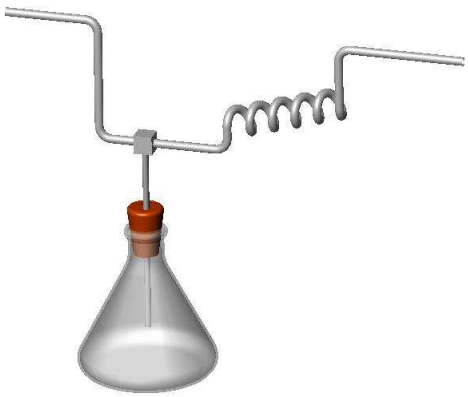

***Figure 2.15**: The submerged diffusion tube assembly.*

The temperature range in which the diffusion tubes are used is between 5 and 59 ºC. The concentrations generated by the diffusion tubes in the experiments and the theoretical predictions can be found in App. C.1. The concentrations agreed (Fig. C.1) for the small and medium diffusion tube with the theoretical concentrations (gas flow = 22 ml min^{-1}), but a discrepancy between the theoretical and the generated concentrations of the large diffusion tube were found (App. C.1).

2.4 Humidifier

The toluene-laden gas entering the reactor is humidified with a shell-in-tube humidifier (Fig. 2.16) (Perma Pure LLC, Toms River, NJ). Water vapour is transferred between a liquid water supply and a flowing gas stream, driven by the partial pressure of the water vapour on opposing sides of the Nafion membrane.

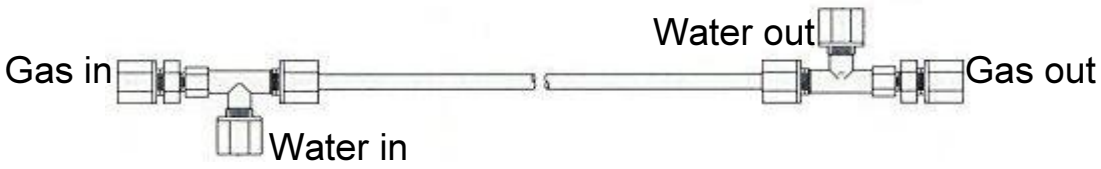

Figure 2.16*: Schematic of the Perma Pure Humidifier (Courtesy of Perma Pure).*

The humidifier can handle an air flow up to 10 L min^{-1}. The air flow used in the experiments is between 5 and 50 ml min^{-1}. The exit air at these low flow rates has a dew point close to the reactor temperature and no extra heating of the humidifier is needed.

The water is supplied to the humidifier by a siphon method. A reservoir with de-ionized water is placed approximately 50 cm above the humidifier and connected to the water inlet with Viton tubing. A short piece of the Viton tubing is connected to the water outlet and capped off. By pulling a vacuum at this end the shell is filled with de-ionized water. As the water in the humidifier is evaporated into the gas, the water is replenished from the reservoir.

The gas entering the column reactor is humidified by bubbling air through a 50 cm column of water.

2.5 Water retention apparatus

Two different experimental apparatuses are used to determine the water retention curves. Two apparatuses as described by Ranasinghe and Gostomski (2003) are used and three apparatuses constructed out of mainly Quickfit fittings (Fig. 2.17).

The Quickfit apparatuses are based on a glass 3" to a 1" reducer. On the 3" side of the reducer a glass 3" sieve plate is placed. To ensure a proper seal, Vaseline is applied to the contact areas. On top of the distributor, a stainless steel mesh is placed, which acts as a support for the membrane. The membranes are the same type as used in the reactors.

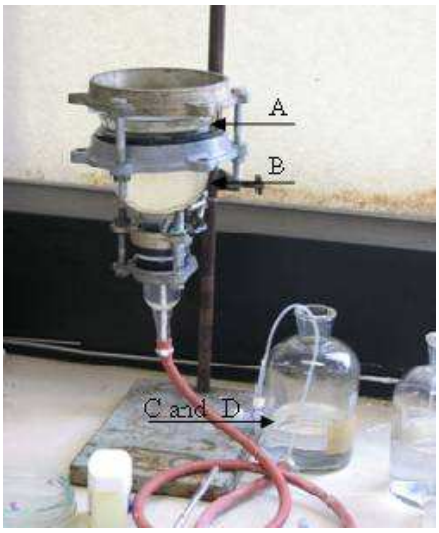

***Figure 2.17**: Photo of the suction cell apparatus used to determine the water retention curves. Membrane (A), Quickfit reducer, (B), Water reservoir (C) and tubing (D).*

The 1" side of the reducer is attached to a 1" to hose barb connection, clamped together using 1" backing flanges. A silicon hose connects the barb connection and the water reservoir. Through the silicon tubing a small diameter tube is fed. One end sits just below the membrane and the other end protrudes from the external water reservoir. This end is closed by a three way valve. The tubing is used to remove any trapped air bubbles trapped below the membrane that can cause a disruption of the water transfer to the compost. A schematic of the setup can be seen in Fig 2.18.

A membrane is placed on top of support mesh and water is sprayed on to saturate the membrane. The edges of the wet membrane rest on the glass edge of the membrane support and create a seal when the external water reservoir is placed lower than the membrane. To prevent a membrane failure, this reservoir cannot be placed higher than the membrane. If it is raised above, water flows freely from beneath the membrane.
Air is evacuated from the water reservoir in contact with the membrane using a 60 ml plastic syringe to fill the reservoir slowly with water. If the water level drops during this process, a leak is present and has to be fixed before commencing. If no leaks are

found, the whole reservoir can be filled. Any air that is trapped underneath the membrane can be removed by slightly tilting the reactor and removing the air bubbles through the tubing.

A glass ring is placed on top of the membrane for support of the compost and to act as a spacer. A Plexiglas plate is placed on top to the glass ring to reduce air drying. Another 3" backing flange is placed on top of the plate and 8 mm threaded rods and nuts clamp the whole setup together.

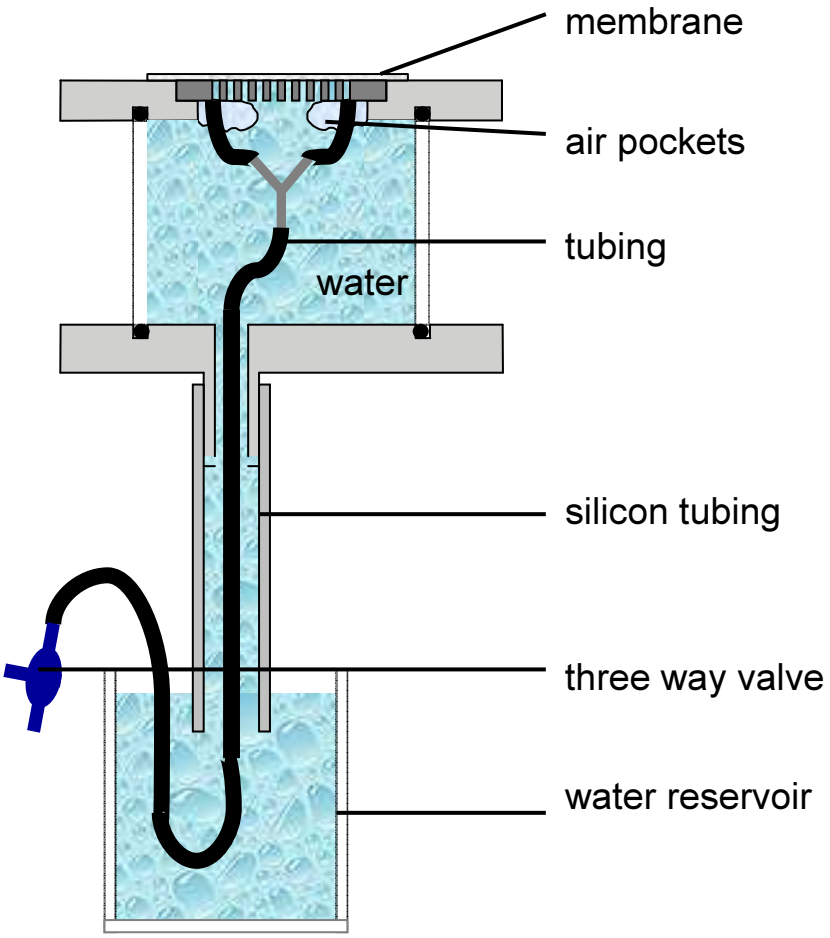

***Figure 2.18**: Schematic of the suction cell apparatus used to determine the water retention curves.*

2.6 Experimental setup

All stainless steel or copper tubing between the individual parts and the reactors are connected using Swagelok fittings. The exact setup of each individual reactor is discussed in the following sections. Larger flow diagrams can be found in App. A.9.

2.6.1 Reactor 1

The reactor and humidifier are placed in a Styrofoam box to control their temperature independent from the lab (Fig. 2.19). The temperature in the box is controlled by a temperature controller (Model: 2186-25A, Cole-Parmer, Vernon Hills, IL) turning two 100W light bulbs off and on. A cooling load is applied to the system when temperatures near or below room temperature are required by passing a small flow of chilled water through a copper coil at the back of the box. Two rotary computer fans circulate the air in the box. As discussed in Sec 2.2.2, agitation of the head space is provided by an external diaphragm pump. Toluene is supplied to Reactor 1 by using a compressed air cylinder supplemented with 100 ppm toluene (BOC Ltd, NZ). A manual flow controller (32505 Series, Cole Parmer, Vernon Hills, IL) in combination with a flow meter (250 ml, Gilmont, Accucal, Barrington, IL) controls the inlet flow rate. All tubing is ¼" copper or stainless steel.

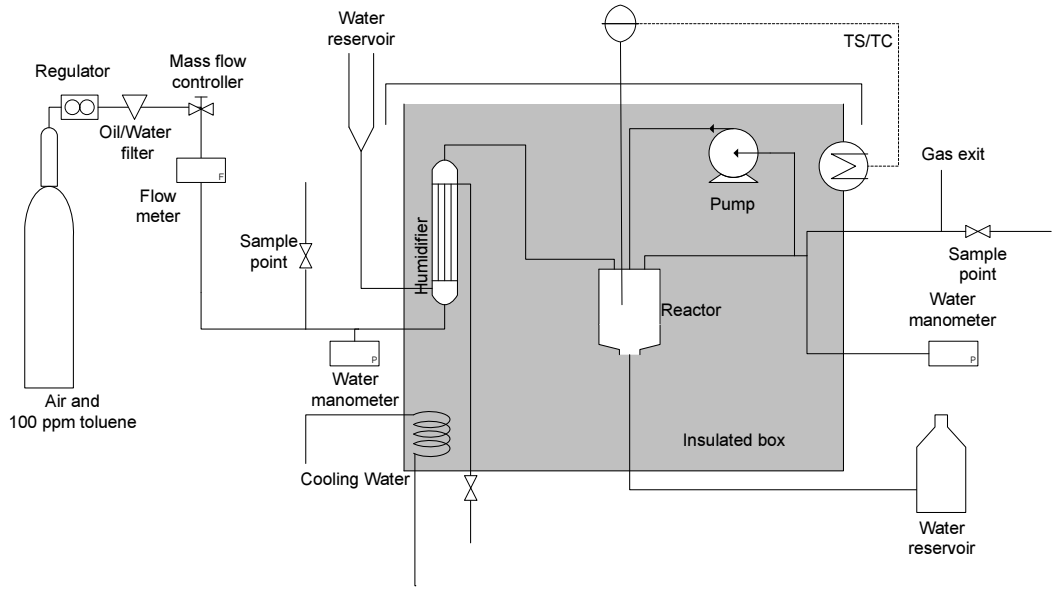

Figure 2.19: *The experimental setup of Reactor 1.*

The inlet flow is sampled through a 1/8” septum injector nut (Valco Instrument Co., Inc., Houston, TX) attached to a Swagelok 1/4” female branch tee to 1/8” female NPT (SS-400-3TTF) and Swagelok bored-through male connector (SS-200-1-2BT). The septa used are GC septa (Blue 3/8”, Alltech Associates Ltd., Deerfield, IL). Initially valves isolated the septa, but the dead volume this created interfered with the sampling accuracy.

A water manometer is connected before the humidifier (see Sec. 2.3). The humidified air and toluene stream enters the reactor through the 1/8” port in the reactor head plate.

The gas is circulated through the reactor by a diaphragm pump (Thomas Pumps, Sheboygan, WI) fitted with a Teflon diaphragm liner. The pump is connected by ¼” stainless steel tubing and placed outside the insulated box. At the outlet of the reactor a tee provides a pressure measurement point for the reactor headspace. The exiting air flow is sampled similar to the inlet. Finally a glass bubble flow meter is attached in order to determine the gas flow rate accurately.

Tension is applied onto the compost by placing the external water reservoir below the membrane as explained in Sec. 2.1.4. The reservoir is open to the atmosphere. In the tension calculations, the values will be corrected for the pressure in the reactor headspace. Pressure differences between the headspace and atmospheric pressure are the equivalent of changing the height of the reservoir.

2.6.2 Reactor 2

Similar to Reactor 1, Reactor 2 and its humidifier are placed inside a Styrofoam box with temperature control and a cooling coil (Fig. 2.20). Compressed air from a gas cylinder (BOC Ltd, NZ) is passed through a regulator and connected to a flow meter with a valve on the outlet (King Instrument Co, Garden Cove, CA, model: 74C-104G042-1-2-3-7-2-0) with 1/8” stainless steel tubing and Swagelok fittings.

The flow is introduced into a water bath through a coil of ¼" copper tubing to ensure that the gas is equilibrated to the water bath temperature before it enters the diffusion tube. After toluene is added, the gas flow is passed through a 9 L stainless steel mixing vessel to dampen small concentration fluctuations. This vessel also reduces any disturbance on the flow by sampling.

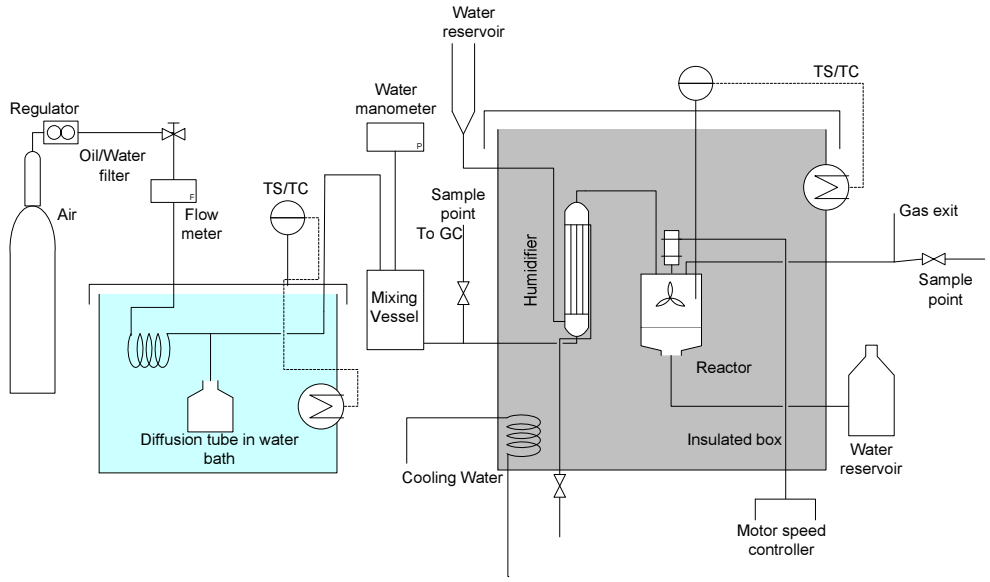

***Figure 2.20**: The experimental setup of Reactor 2.*

A sampling port is installed before the insulated box. The gas is humidified as described before. The flow enters the reactor through a ¼" SS tube. At the exit port, the reactor pressure is monitored with a water manometer. The flow exits the box through ¼" SS tubing and passes another sampling port. Similar to Reactor 1, a glass bubble flow meter is attached to periodically determine the gas flow rate accurately.

2.6.3 Reactor 3

Reactor 3 is in setup very similar to Reactor 2 (Fig. 2.21). The major differences are that the box is made of medium density fibre board (MDF) insulated with Styrofoam and that no water manometers are installed.

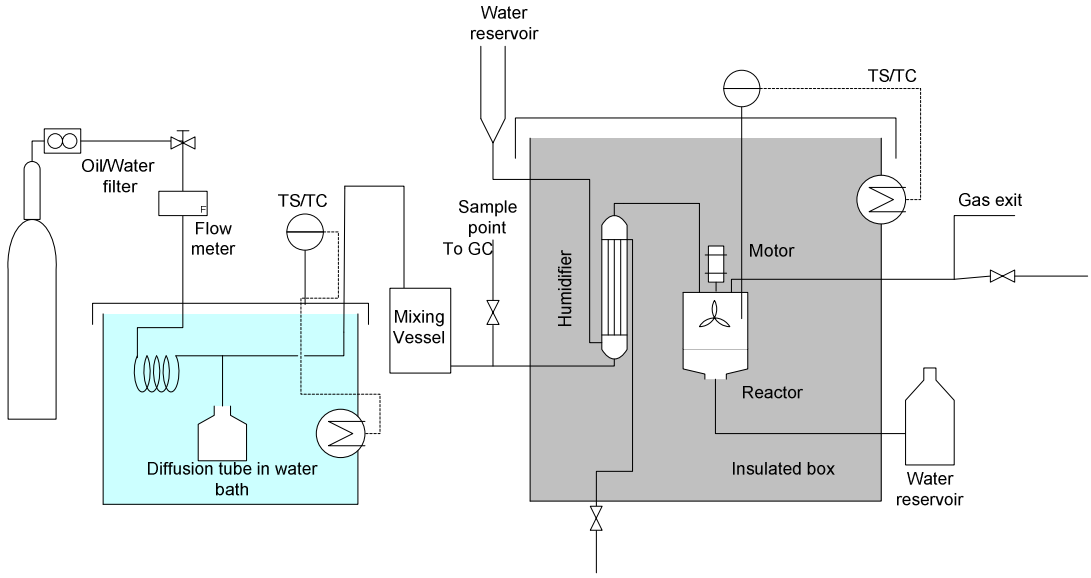

***Figure 2.21**: The experimental setup of Reactor 3.*

2.6.4 Column Reactor

The column reactor is of a similar setup as commonly reported in the literature (Fig. 2.22). A gas flow is generated by an aquarium pump and split into two. The majority goes through a flow meter with a valve on the outlet (King Instrument Co, Garden Cove, CA, model: 74C-111G082323720) and the smaller flow goes through a valve and flow meter.

The larger flow is introduced through the humidifier as described before and enters a mixing vessel. The smaller flow bubbles through a 2 cm deep liquid toluene to saturate the air stream, after which also it also enters the mixing vessel. Both flows are combined before entering the column itself. A water trap at the inlet prevents any condensation blocking the tubing. Sample ports are available at the inlet and outlet and the flow is measured periodically by a bubble flow meter.

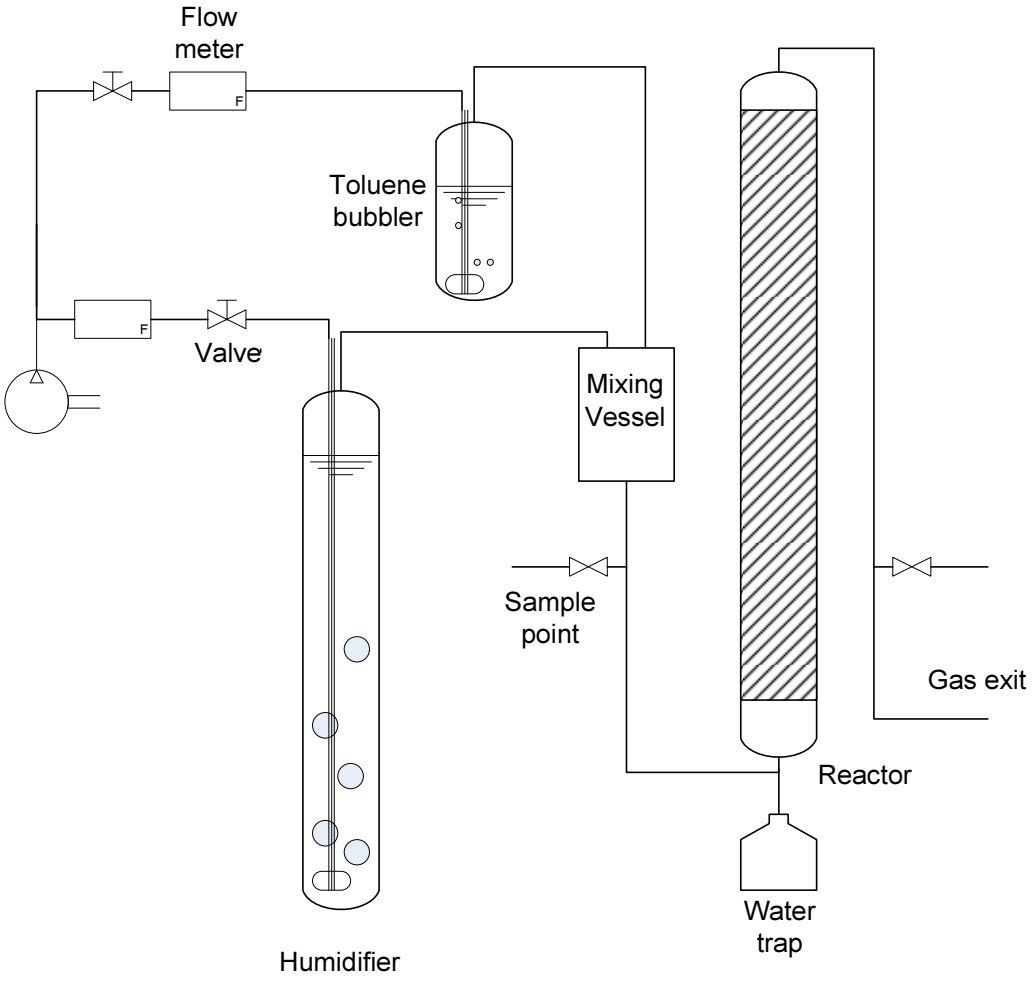

***Figure 2.22**: The experimental setup of the Column Reactor.*

2.7 Troubleshooting

The system components and the reactor were extensively tested. The results of these tests can be found in Appendix A. Discussed are:

- The robustness of the reactor design.
- Testing for leaks in the system
- Control experiments without compost
- The operation of sampling and sample points
- Diffusion tube test
- Gas bottles discrepancies
- Humidifier test
- Mass transfer resistance in the compost layer

2.8 Reactor assembly and loading

All three reactors are designed similarly although the specific assembly and operation is slightly different. The whole reactor including o-rings is autoclaved for 20 minutes at 121 °C prior to final assembly and compost addition to minimize any microbial growth in places other than the compost layer.

The reactor is assembled from the bottom up. The first part is the bottom plate (part C4) which stands on legs (Fig. 2.8). A Viton o-ring is placed inside the groove which forms the seal between the glass tubing (C3) and the metal plate. The support ring (C2 with Viton o-ring in groove) is lined up on top of the glass so the threaded rods can be put in place. The Y-piece with the tubing (Fig 2.9) has to be lined up so it sits just below the perforated membrane support (C1). The nuts on the threaded rods are fastened to seal the water reservoir.

The membrane is wetted out and placed on top of the support. Even without clamping the membrane should seal the reservoir so it can be filled with water. The external water reservoir is filled with autoclaved tap water (121°C for 20 min) to minimize any microbial growth in both water reservoirs. The external reservoir is placed lower than the reactor to prevent a pressure build-up under the membrane.

The air is evacuated from the reactor water reservoir using a 60ml plastic syringe. The reservoir will slowly fill up with water. If the water level in the internal water reservoir drops during this process, a leak is present. If no leaks are found, the whole reservoir can be filled. Any air that is trapped underneath the membrane can be removed by slightly tilting the reactor to move the air towards the tubing. With a syringe the last of the air bubbles can be removed.

The next step for Reactor 1 and 2 is placing the Viton o-ring on top of the membrane on which the glass reservoir with the metal ring (part A1 and A2) rests. Using the threaded rods and nuts, it is fastened to the water reservoir. For reactor 3 part D is placed on top of the o-ring and fastened with the rods and nuts.

A known weight of sieved compost (no. 6 mesh) is loaded into a stainless steel ring which is placed on to of the membrane. The use of this ring makes the packing of the compost easier as the exact volume is known. The rings have a diameter of 2" and a height of 1.6, 3 and 5 mm. In most experiments, the 3 mm high ring is used. The compost is lightly packed in order to get a good contact between the compost and the membrane. After the compost is packed, the metal ring is removed.

In case of Reactor 3, the glass gas reservoir (E) is placed on top of the o-ring in part D. Next the lid is fitted and the reactor is made gas tight by screwing the nuts hand-tight.

The reactor is placed in the temperature controlled box and all ports on the reactor are connected to the in- and outlet tubing, and the temperature probe is placed in the thermo-well. The external water reservoir is placed at the appropriate height. An It is important that the reservoir is never placed higher than the membrane or the compost will flood.

After installation of Reactor 1, the gas flow rate is set, the circulation pump and the temperature controller are switched on. For Reactors 2 and 3, the direct agitation can be started. To generate the required toluene concentration with the diffusion tube, the temperature of the water bath is set to the appropriate temperature.

2.9 Nomenclature

A_t	diffusion tube cross sectional area	m^2
C_{dif}	concentration at the exit of the diffusion tube	ppm
C_{in}	concentration at the inlet	$g\ m^{-3}_g$
C_{out}	concentration at the outlet	$g\ m^{-3}_g$
D	diffusion coefficient at pressure P and temperature T	$m^2\ s^{-1}$
D_{298}	diffusion coefficient at 25 ºC and 1 atm.	$m^2\ s^{-1}$
F_g	gas flow rate	$m^3_g\ s^{-1}$
n	temperature coefficient	-
P	pressure in the diffusion cell	bar
q_d	diffusion rate	$m^3\ s^{-1}$

R	rate of conversion	$g\ m^{-3}_r\ s^{-1}$
T	absolute temperature	K
x	diffusion tube length	m
V	volume of the reactor	m^3

Subscripts

g	of gas
r	of bed volume in the reactor

2.10 References

Altshuller, A. P., and I. R. Cohen. 1960. Application of diffusion cells to the production of known concentrations of gaseous hydrocarbons. *Analytical Chemistry* 32: 802-810.

Berty, J. M. 1974. Reactor for vapor-phase catalytic studies. *Chemical Engineering Progress* 70: 78-85.

Butt, J. B., H. Bliss, and C. A. Walker. 1962. Rates of reaction in a recycling system - Dehydration of ethanol and diethyl ether over alumina. *Aiche Journal* 8: 42-47.

Carberry, J. J. 1964. Designing laboratory catalytic reactors. *Industrial and Engineering Chemistry* 56: 39-46.

Chen, N. H., and D. F. Othmer. 1964. Correlations for coefficients of gaseous diffusion. *Industrial & Engineering Chemistry Fundamentals* 3: 279-280.

Ergas, S. J., L. Shumway, M. W. Fitch, and J. J. Neemann. 1999. Membrane process for biological treatment of contaminated gas streams. *Biotechnology and Bioengineering* 63: 431-441.

Gillespie, B., and J. J. Carberry. 1966. Influence of mixing on isothermal reactor yield and adiabatic reactor conversion. *Industrial & Engineering Chemistry Fundamentals* 5: 164-171.

Hanks, R. J. 1992. *Applied soil physics : soil water and temperature applications*. Springer-Verlag, New York.

Hillel, D. 1982. *Introduction to soil physics*. Academic Press, Orlando ; New York ; Sydney.

Kirkham, D., and W. L. Powers. 1972. *Advanced soil physics*. Wiley-Interscience, New York.

Levenspiel, O. 1999. *Chemical reaction engineering*. Wiley, New York.

Nelson, G. O. 1971. *Controlled test atmospheres; principles and techniques*. Ann Arbor Science Publishers, Ann Arbor, Mich.,.

Papendick, R. I., and G. S. Campbell. 1981. Theory and measurement of water potential in J. F. Parr, W. R. Gardner, and L. F. Elliott, eds. *Water potential relations in soil microbiology, SSSA special publication number 9*. Soil science society of America, Madison.

Pitzer, K. S., and D. W. Scott. 1943. The thermodynamics and molecular structure of benzene and its methyl derivatives. *Journal of the American Chemical Society* 65: 803-829.

Ranasinghe, M. A., and P. A. Gostomski. 2003. A novel reactor for exploring the effect of water content on biofilter degradation rates. *Environmental Progress* 22: 103-109.

Tajbl, D. G., J. B. Simons, and J. J. Carberry. 1966. Heterogeneous Catalysis in a Continuous Stirred Tank Reactor. *Industrial & Engineering Chemistry Fundamentals* 5: 171-&.

Wedel, S., and J. Villadsen. 1983. Falsification of kinetic-parameters by incorrect treatment of recirculation reactor data. *Chemical Engineering Science* 38: 1346-1349.

Chapter 3: Water in biofilters

3.1 Introduction

One of the most critical aspects of biofilter operation is the control of the water content (Devinny *et al.*, 1999). Although this is recognized as an important aspect, it has received little attention. In operating a biofilter, operators rely on experience to control water content. Too little water will reduce microbial activity; too much water fills the biofilter pores and reduces the mass transfer of nutrients, oxygen and waste products (Bohn and Bohn, 1999).

The moisture content has an important or even a dominating effect on the magnitude of the biomass in soil (Wardle and Parkinson, 1990b). The moisture content (gravimetric or volumetric) plays a role in the sustainability of biomass by transporting nutrients, waste products, salts and other molecules. The key parameter is not the moisture content itself, but the availability of the water to the biomass.

For organic biofilter media 50 - 60% moisture content (wet weight basis) typically provides good biofilter performance. It is dependent on the bulk density, size of particles and pores and the amount and nature of the bulking agent (Bohn and Bohn, 1999). This does make it difficult to compare optimal water contents between different types of media compositions.

An independent way of describing the water in biofilter media is using the water potential (ψ). The potential describes the free energy of the water in a system and is the summation of several components: osmotic potential (ψ_π), matric potential (ψ_m), gravitational potential (ψ_g), pressure potential (ψ_p) and overburden potential (ψ_Ω) (Papendick and Campbell, 1978). These components will be described in detail in Sec. 3.2.3.

Water in soil and other porous media is mainly retained by matric forces in pores and as films on particle surfaces. At saturation, all of the pores are filled with liquid water and the matric potential, ψ_m, is zero (Papendick and Campbell, 1981). When water flows out of the pores, the water potential is reduced and it becomes more difficult

for micro-organisms to use the water. Micro-organisms exposed to osmotic and matric stresses adjust their intracellular osmolyte concentrations to maintain the proper cellular turgor pressure. Cellular dehydration causes protein denaturation, DNA damage and phase transitions in membranes. Bacteria also increase their extracellular polysaccharide production, presumably for their water holding capacity (van de Mortel and Halverson, 2004).

Most bacteria experience reduced metabolic activity at water potentials below $-4 \cdot 10^4$ cm H_2O (Bloom and Richard, 2002). Optimal decomposition and mineralisation rates in soil have been observed to be in the range between -100 and -500 cm H_2O (Rodrigo *et al.*, 1997). However, Stark and Firestone (1995) found that at a water potential of -600 cm H_2O, substrate limitation occurred and caused major inhibition of bacterial activity. This shows that the water potential plays an important role in finding optimal degradation rates.

3.2 Definitions of water in porous media

Water studies in soil use mainly three different measures of the amount of water present; soil water content, the percentage of pore space filled with water and matric potential (Rodrigo *et al.*, 1997). All three measures have their advantages and disadvantages.

3.2.1 Water content

Water content is often used in soil research as it is a parameter that is easily measured. It is defined as the amount of water that is retained in the pores of the soil (Fredlund and Xing, 1994).

The % water content (ω) of a soil on a dry weight basis is calculated with Eq. 3.1. The details of the symbols and units are described in the nomenclature Sec. 3.8.

$$\omega = \frac{W_{water}}{W_{soil}} \cdot 100 \qquad [3.1]$$

The water content of a soil on a volume basis is defined as:

$$\theta = \frac{V_{water}}{V_{soil} + V_{void}} \qquad [3.2]$$

The relationship between Eq. 3.1 and 3.2 is:

$$\theta = \frac{\omega}{100} \cdot \frac{\rho_{bulk}}{\rho_{water}} \qquad [3.3]$$

The advantage of using water content is that it can be simple and accurately measured. A disadvantage is that water content does not give any information on the amount of water available to micro-organisms or plants. Two porous materials at the same water content can have considerably different availabilities of water. Other measures like water activity and water potential can describe the available water. This will be discussed in more detail in Sec 3.2.3 and Sec. 3.4.3

3.2.2 Degree of saturation

The degree of saturation is a measure of the percentage of the voids in the soil that are filled with water. The relationship is described as follows:

$$S = \frac{V_{water}}{V_{void}} \qquad [3.4]$$

The degree of saturation is used in soil-water relations when aerobic versus anaerobic activity is discussed (Linn and Doran, 1984). An advantage is that this measure can be used for varying conditions of incubation period, bulk density and clay content, but it is not accurate near saturation, which is the water content these experiments are investigating (Franzluebbers, 1999).

3.2.3 Soil-Water potential

Water potential is important to any process where there is movement of soil water such as infiltration and redistribution within the soil, or the removal of water from the

soil by evaporation or plant uptake. The soil-water potential was defined by Buckingham (1907) as the amount of work required per unit weight of water to pull the water away from a mass of soil. The capillary forces are the main contributor to the force holding the water in the soil.

The relationship between the water potential ψ (J m^{-3}), the chemical potential μ (J kg^{-1}) and the matric head H (m) is given as (Tuller and Or, 2005a):

$$\mu = \frac{\psi}{\rho_w} = gH \qquad [3.5]$$

Water potential consists out of several components (Papendick and Campbell, 1981):

- Osmotic potential (ψ_π), due to solutes in the water is defined as,

$$\psi_\pi = \phi \cdot \gamma \cdot R \cdot T \cdot c \qquad [3.6]$$

- Matric potential (ψ_m), includes both adsorption and capillary effects of the solid phase.
- Gravitational potential (ψ_g), proportional to the elevation differences from the reference. Is equal to $\rho_{water} \cdot g \cdot h$. g = gravitational constant and h = height above free water surface.
- Pressure potential (ψ_p), resulting from external gas or hydraulic pressure applied to the water.
- Overburden potential (ψ_Ω), caused by the weight from overlying matter on water present in a non-rigid porous body.

This gives the total water potential (Papendick and Campbell, 1981):

$$\psi = \psi_\pi + \psi_m + \psi_g - \psi_p + \psi_\Omega \qquad [3.7]$$

In most soil systems, only the matric and osmotic potentials contribute significantly to the overall water potential. They have the largest effect on the availability of the water to micro-organisms. The other components are assumed to be constant. (Papendick and Campbell, 1981)

To manipulate the matric potential, the sample is hydraulically connected to a water reservoir. The sample is separated from the water by a barrier that is permeable to water but not to air, for example a semi-permeable membrane. By applying a force to the barrier a vacuum is applied to the membrane and thus to the sample. This can be done by either placing the water reservoir under suction or by applying a pneumatic pressure. The suction in the reservoir can be applied by non-permeating solutes like PEG (Holden *et al.*, 1997a) or lowering the water reservoir in relation to the barrier. The matric potential in the sample will equilibrate to the pressure applied.

To control the osmotic potential in soil or agar media the initial salt concentration must be known. The osmotic potential is then calculated using a modified Van 't Hoff relation (Papendick and Campbell, 1981). Osmotically active components can be added to achieve the desired potential.

Both osmotic and matric potential have an affect on microbial activity, although not to the same extent. The activity is reduced more at low matric potentials then at low osmotic potentials. A possible explanation is that the matric potential has an effect on micro-organisms by reducing available nutrients (Chenu and Roberson, 1996).

3.2.4 Water and the pollutant

An important parameter for the effective removal of a pollutant is the dimensionless partition coefficient, or Henry coefficient. In Table 3.1 common pollutants and their Henry coefficients are presented. In general, pollutants with a Henry coefficient higher than 1 are considered less suitable for removal by a biofilter (Deheyder *et al.*, 1994). These pollutants are often highly volatile and can travel through a biofilter bed without being degraded (Davis *et al.*, 2001). So the rate of removal of pollutants with a high Henry coefficient is controlled by the mass transfer between the vapor phase and the biofilm (Zhu *et al.*, 2004). The mass transfer is also dependent on the amount

of water present in the biofilter. High water content results in a thick liquid film surrounding the cells, which increases the mass transfer resistance in the stagnant of toluene to the cells, and therefore lowers the removal rate. Hodge and Devinny (1994) did see that the water content of the bed media has an influence on the sorptive properties of the bed material. At high water contents there will be more sorptive capacity in the bed, especially components with small Henry coefficients.

***Table 3.1**: Henry coefficients and experimental EC's for selected VOC's (Johnson and Deshusses, 1997).*

Pollutant	**Henry Coefficient**	**EC_{max}**
	g in air g^{-1} in water	g m^{-3}_{r} hr^{-1}
Hexane	$7.4\ 10^{1}$	5
Isopentane	$5.6\ 10^{1}$	8
Benzene	$2.2\ 10^{-1}$	8
Toluene	$2.8\ 10^{-1}$	15
Xylene	$3.6\ 10^{-1}$	17
Ethyl benzene	$3.6\ 10^{-1}$	32
Butyl acetate	$1.4\ 10^{-2}$	32
Isobutyl acetate	$1.9\ 10^{-2}$	75
Acetone	$1.6\ 10^{-3}$	67
MEK	$2.4\ 10^{-3}$	32
Ethyl acetate	$5.5\ 10^{-3}$	200
MIBK	$5.7\ 10^{-3}$	45
Methanol	$1.9\ 10^{-4}$	70
Ethanol	$2.6\ 10^{-4}$	150
1-propanol	$2.8\ 10^{-4}$	150
2-propanol	$3.5\ 10^{-4}$	120
2-butanol	$4.2\ 10^{-4}$	140

In the removal of ethane (Henry coefficient = 10.2) a higher removal rate is seen at a lower water content (< 40%) in a granular activated carbon biobed, then at a higher (> 40%) water content. Although the maximal removal rates are higher at the drier

conditions, this removal rate can not be maintained for long periods. Intermittent water (and nutrients) additions did correct the decrease in EC after dry periods (Deheyder et al., 1994). Their results show that for ethane, an optimal water content for removal exists, but it is lower than expected. The water content at this optimum was not measured, but as the bed dries, the water layer thickness is reduced. This also will reduce the mass transfer resistance of the ethane through the water layer.

3.3 Effects of water content on the microbial environment

A strong link between soil water and the activity of soil microbial life exists (Skopp *et al.*, 1990). The effect of the water content conveys itself directly and indirectly on the individual cells and the population.

3.3.1 Direct effects on micro-organisms

Soil micro-organisms are often subjected to low water potentials. According to thermodynamics, the water potential in the micro-organisms has to be equal to the water potential of their surroundings (Kieft *et al.*, 1987). The response to a change in water potential can be either passive or active. Organisms can be divided into several classes, which have different type of responses against water potential changes (Table 3.2).

***Table 3.2**: Microbial classes for water potential responses (Harris, 1981).*

Class	Response	Types
I	No compatible solute production	Some Gram-negative
II	Inducible compatible solutes	Most Gram-negative
III	Constitutive compatible solutes production	Some Gram-positive, lichens, free living fungi, yeasts, algae
IV	Inducible and constitutive solutes production	Most Gram-positive, yeasts, soil fungi, algae, halophilic bacteria and algae

Passive control of internal water potential can occur by cellular plasmolysis. This is when the cell loses water and thus turgor pressure. In situations of low water potential, this can lead to a loss of physiological activity and may lead to cell death (Harris, 1981; Kieft *et al.*, 1987).

Active response against decreasing water potential includes the accumulation of inducible and/or constitutive compatible solutes (Table 3.3). These solutes, like amino acids and polyols are produced or accumulated to control the intracellular water potential (Harris, 1981). These organisms often have strong cell walls as an extra protection. Even at high concentration, compatible solutes allow enzymes to function effectively (Jennings and Burke, 1990).

***Table 3.3**: Compatible solutes found in different organisms.*

Organism	**Compatible solute**	**Reference**
Fungi	Glycerol, mannitol, sorbitol, proline	Jennings and Burke, 1990
F. graminearum	Arabitol, glycerol	Ramirez *et al.*, 2004
Procaryotes	Amino acids	Harris, 1981
Eucaryotes	Polyols	Harris, 1981

Drying often occurs gradually, so the micro-organisms have time to adjust to the water potential. But if a dry soil is wetted fast, because of a downpour, the water potential increases rapidly. This rapid rewetting is called downshock (Harris, 1981) and can lead one or more of the following responses of the micro-organisms (Kieft *et al.*, 1987):

- The cell takes up water to equilibrate to the water potential, but the influx of water is so large that it breaks the cell membrane and the cell lyses.

- The intracellular compatible solutes will rapidly be catabolised to CO_2.

- The active or passive transport of intracellular solutes out of the cells. In extreme cases all cell solutes are released and the cell dies. These solutes can be scavenged by other surviving organisms.

After soil rewetting, an increase in CO_2 production is often observed. This is mainly attributed to the release and mineralisation of the intracellular components (Fierer and Schimel, 2003; Kieft *et al.*, 1987; Sorensen, 1974). What happens to the cells during the up- or downshock is a function of the severity, the level of intracellular

constitutive compatible solutes, the strength of the cell wall/membrane and the availability of stress solutes to counterbalance dehydration. Borken *et al.* (2003) found that the more severe the downshock is, the more CO_2 as well as for a longer period is released.

Scott's (1957) generalizations state that when the ψ is reduced below an optimum level, an increase in the lag phase of microbial growth, a decrease in the rate of growth and a decrease in the amount of cell biomass synthesized occur. This means that all micro-organisms are likely to have a characteristic optimum ψ at which growth occurs most rapidly (Harris, 1981).

3.3.2 Indirect effects on micro-organisms

A reduction in microbial activity is attributed more to an indirect effect on substrate availability and transport of metabolic products than a direct effect of water potential on micro-organisms. The reduction in water potential by lowering the matric potential has a larger effect on the diffusion of nutrients to and waste products from the cells then lowering the osmotic potential. In nitrification, small reductions in water potential (< 2000 cm H_2O) can substantially reduce the rate of nitrification. It is not likely that the microbial metabolic processes are influenced by such small changes in water potential (Papendick and Campbell, 1981).

The water in soil is essential for microbial growth. It not only plays a role as a medium but is also needed for a variety of cell processes. The major roles it plays are (Tate, 1994):

- Essential material: Enzymes need water for their processes, like hydrolysis and hydroxylations.
- Affecting gas exchange: If all pores are filled with water, oxygen limitations can occur.
- Microbial nutrient supply: Water is a transport medium for nutrients to the cell and waste products away from the cell.

- Soil temperature: Water has a high heat capacity. When the water content in the soil is high, the soil temperature will be less influenced by air temperature fluctuations.
- Growth medium for microbial colonies: Micro-organisms function in the water layer on soil particles or within soil pores. Soil is a particulate system, but micro-organisms live in an aquatic world. The water layer might consist only of a micro-film or the micro- and macro-pores are completely filled. For the micro-organism to function properly, it must be completely submerged in water.
- As a transport mechanism of cells to colonise different parts of the soil (Holden and Fierer, 2005).

Soil micro-organisms are often surrounded by a layer of extracellular polysaccharides (EPS). A popular hypothesis is that this layer protects the organism against desiccation. Roberson and Firestone (1992) did see an increase in EPS production at drier conditions. The EPS layer can trap water and nutrients and protect the cell from drying. At higher water potentials the EPS layer could restrict the diffusion of nutrients, but at low matric potentials, diffusion rates of nutrients in the EPS can be higher than in the soil itself (Chenu and Roberson, 1996).

3.3.3 Effects on population

Drying is a selective factor in the microbial population in soils (Sparling *et al.*, 1989). For example fungi prefer drier conditions than bacteria do. Table 3.4 shows some of the effects of the matric potential on microbial activity. When the matric potential is lower than $-4.0 \cdot 10^4$ cm H_2O, bacterial growth is slowed down or even stopped. Maintaining a low matric potential for an extended time will cause the microbial community to change; the number of bacteria will be reduced and the biofilter will be dominated by yeasts and other fungi.

The relationship between soil matrix potential (ψ_m) and soil water content is defined by the soil water retention isotherm properties of the soil, taking into account the consideration of hysteresis effects. Soil ψ_m of -100 cm H_2O is normally associated with water saturation of soil capillaries $\leq$ 30 μm in diameter; -300 cm H_2O < 4 μm;

and at < -5000 cm H_2O the soil water tends to be distributed as a film only a few water molecules thick. The decreasing matric potential will empty narrower and narrower pores and thereby reducing the physical amount of water present.

Drying and wetting cycle experiments were conducted by Fierer *et al.* (2003) to investigate the effect on the community structure, diversity and richness. Their results did not indicate a large shift in the community. It was possible that their soil samples had been exposed to many cycles before testing and the community had already adapted. Other experiments by Fierer and Schimel (2002) saw a change in the community after water stress experiments, especially an increase in the number of nitrifiers. Exposing a soil to fluctuating water contents can lead to a significant loss in nitrogen. The nitrogen could be lost by leaching NO_3^- or a loss of gaseous nitrogen.

***Table 3.4**: Microbial tolerance to matric-controlled water stress* (Coyne, 1999).

Max tolerance (cm H_2O**)**	**Water film thickness (µm)**	**Microbial activity affected**
$-3.0\ 10^2$	4.0	Denitrification
$-1.0\ 10^3$	1.5	Movement of protozoa/bacteria
$-5.0\ 10^3$	0.5	Nitrification
$-1.5\ 10^4$	$30\ 10^{-4}$ (10 water molecules)	Sulphur oxidation
$-4.0\ 10^4$	$<30\ 10^{-4}$	Bacterial/actinomycete growth
$-1.0\ 10^5$	$<15\ 10^{-4}$ (< 5 water molecules)	Fungal growth
$-4.0\ 10^5$	$< 9\ 10^{-4}$ (< 3 water molecules)	Fungal growth

Sun *et al*. (2002) investigated the microbial presence under different moisture contents. They quantified bacteria, yeasts, moulds and actinomycetes. With increasing moisture content, the CFU g^{-1} decreased for the moulds and actinomycetes, while it increased for the bacterial count.

3.4 Water in biofilters

One of the most critical aspects of biofilter operation is the control of the water content (Devinny *et al.*, 1999). Approximately 75% of problems in biofilters is attributed to poor control of the water content (Auria *et al.*, 1998; Sun *et al.*, 2002). Although recognized as an important aspect, it has received little specific attention. Too little water will reduce microbial activity; too much water fills the biofilter pores and reduces the mass transfer of nutrients, oxygen and waste products (Bohn and Bohn, 1999).

The optimal water content in biofiltration is subject to the type of bed material, the pollutant, the microbial community present, humidification, etc. The water content has been demonstrated to have an important or even a dominating effect on the biomass in a biofilter (Wardle and Parkinson, 1990a). As seen in the previous section; the physical amount of water (g g^{-1}, m^3 m^{-3}) is not the key parameter but the availability of the water to the biomass is. The availability of the water is dependent on the properties of the bed material. It controls the relationship between the water content and available water for the micro-organisms.

3.4.1 Influence of bed material

To make any statements about the moisture contents in a biofilter bed, the medium has to be identified. Many different media are used; compost (Cardenas-Gonzalez *et al.*, 1999; Sercu *et al.*, 2005), wood bark (du Plessis *et al.*, 2003; Knauf and Zimmer, 1994; Vaiskunaite *et al.*, 2005; Vanlangenhove *et al.*, 1986), peat (Hartikainen *et al.*, 1996; Morgado *et al.*, 2004; Yoon and Park, 2002), polyurethane foam (Moe and Irvine, 2001b) and a combination between organic and inorganic media (Chan and Lu, 2003). All these media have different moisture retaining properties and optimal values for optimal removal rates (Table 3.5). For organic biofilter media, 50 - 60% moisture content on wet weight basis yields a good biofilter performance. This range depends on the bulk density, size of particles and pores and the amount and nature of the bulking agent (Bohn and Bohn, 1999).

***Table 3.5**: Water content reported for different biofilter media.*

Material	Water content	Reference
Wood bark	60-65%	Van Langenhove *et al.*, 1986
Compost	30-55%	Cardenas-Gonzalez *et al.*, 1999
Compost	51-58%	Sercu *et al.*, 2005
Polyurethane foam	65%	Moe and Irvine, 2001
Peat	40-60%	Morgado *et al.*, 2004
Peat	57-68%	Yoon and Park, 2002

As Buckingham (1907) stated in his famous 1907 bulletin:

> "The capillary potential for a given water content varies from soil to soil; the retentiveness of different soils, or even of the same soil in different states of structure, is different. To put it in another way, if we subject the different soils to the same force, gravitational or other, tending to pull water away from them, we find that this force drains some soils drier than others. But the final value of capillary potential must be the same in all, because it just balances the same outside pull. Hence in some soils the water content has to be run down lower than in others to raise the capillary potential to a given value. These soils, in other words, are less retentive of water than the others."

Although the quote is made over a hundred years ago, it indicates the importance of describing water content of the biofilter medium as a function of the external forces acting on the medium.

3.4.2 Mechanisms of water retention

Water is retained in packed beds in two ways; bound and free water. The bound water is unavailable to any higher or micro-organisms and thus not of any significant influence in biofiltration. This water is in equilibrium with free water and can under certain conditions convert into free water and vice-versa. Removal of this water can only be achieved by heating the medium (soil) above 105 °C for extended periods of time. The bound water is retained by three mechanisms (Krasil'nikov, 1958).

1. Hygroscopic water is physically bound to the soil particles by ways of molecular cohesion. This layer covers the soil particles and is strongly bound.

2. Film water is also physically bound to the soil. The water molecules are not as strongly bound to the soil as the hygroscopic water. It moves as a liquid but has different properties than liquid water; a higher viscosity and lower freezing point. This water is unavailable for plant life due to the strong binding. It is unknown if this water can be used by microbial cells.

3. Chemical bound water is present. It has entered the composition of minerals and is unavailable for any organisms.

The free water is present in two ways: gravitational water and capillary water. Both these are available to micro-organisms. The gravitational water is the water present in the soil that can move freely. This water is subject to the gravitational pull and slowly filters downward. The capillary water is water that fills the pores of the soil and moves by way of capillary force. The capillary force on the water is dependent on the structure and size of the soil particles (Krasil'nikov, 1958).

3.4.3 Water retention curves

A measure of the ability of the bed material to hold water can be described by the water retention curve. This is a fundamental property unique for every material. An example of the water characteristic curve for three different types of soil can be found in Fig. 3.1.

The relation between the water content and matric potential is non-linear and therefore the relationship has to be determined for the full range in which the bed material will be used. Hysteresis and the structural changes to the material can influence the relationship (Hanks, 1992).

To characterize the relationship between water content and matric potential, an equilibrium between the two has to be established (Lal, 2002). Two common laboratory methods are the hanging water column (Sec. 2.1.4) and the pressure plate

apparatus (Banin *et al.*, 1968; Tuller and Or, 2005b). In situ methods include tensiometers (Banin *et al.*, 1968; Richards, 1960), psychrometers, piezometers, time domain reflectometry (TDR) (Hillel, 1982) and electrical resistivity (Pozdnyakov *et al.*, 2006).

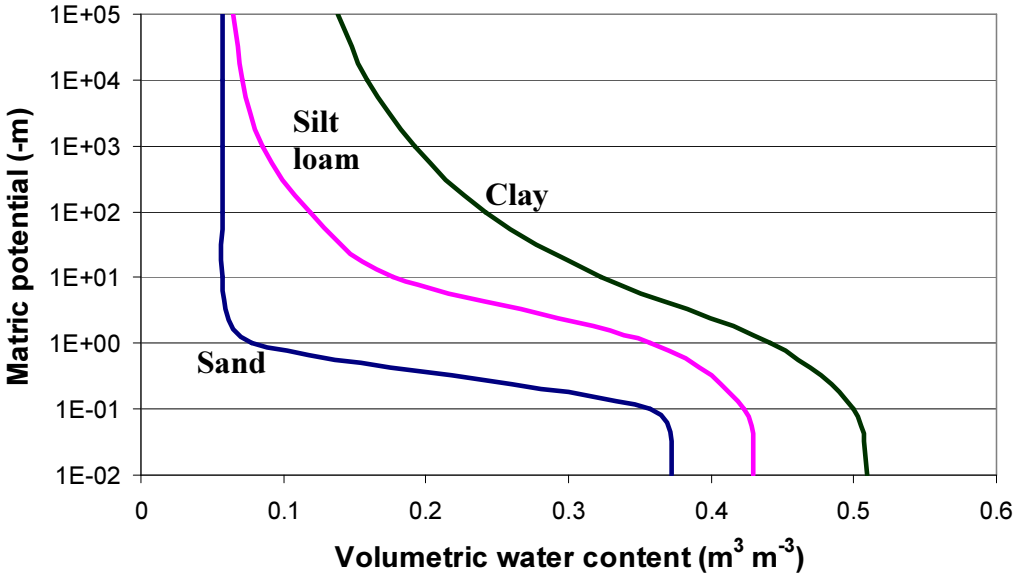

***Figure 3.1**: Typical water potential – water content relationships for different soils. (Tuller and Or, 2005b).*

These water retention curves are not unique and depends whether the curve was obtained by wetting (sorption) or drying (desorption) of the soil. This phenomenon is commonly referred to as hysteresis and is attributed to several causes including non-uniformity of pores, differences in radius and curvature between advancing and receding menisci, effects of entrapped air, and differential changes in soil structure during sorption and desorption (Hillel, 1982).

3.4.4 Hydraulic conductivity

The hydraulic conductivity is a measurement of the ability of the porous medium to conduct the flow of water. It varies due to many factors such as temperature, particle size, and pore properties (Iwata *et al.*, 1988). Although hydraulic conductivity is an important factor in soil-water relations, it is less of a factor in this research as only steady state water contents are used.

3.4.5 Water in biofilters in the literature

Most papers in the biofiltration literature only superficially look at the effect of water content. Although they recognise the importance, relatively little research into this topic has been done. In general the range of water content in compost biofiltration is reported is between 40% and 60%. Often it is unclear if they are based on a dry or wet weight basis. This makes direct comparison difficult. Kennes and Thalasso (1998) presented a table of the water content of several biofilter materials.

Holden *et al.* (1997a) have done experiments in the matric potential range between 0 to $-1.5 \cdot 10^4$ cm H_2O. They found that at a slightly negative matric potential (-2,500 cm H_2O) the bacterial cultures had the highest growth rates. The other observation was that the matric potential had little effect on VOC degradation rates.

The experiments conducted by Ranasinghe and Gostomski (2003) controlled the matric potential over a smaller range at wetter conditions (-6 to -36 cm H_2O). The elimination capacity (EC) dropped from 155 to 24 g m^{-3}_r hr^{-1} as the matric potential decreased. This means a six-fold reduction of elimination capacity over a small range of matric potentials.

Krailas *et al.* (2000) found that a downward flow biofilter is easier to compensate for water loss during operation. Also the water content was more evenly distributed. When the airstream was introduced from the top, the top part of the bed worked as a humidifier. When water was supplied to the top part, the relative humidity of the airstream did get close to saturation. Any excess water, not transferred into the gas phase, slowly seeped through the column. During upflow operation, the airstream removed the moisture from the packing material in the bottom of the column and the packing material dried out.

Lu *et al.* (2002) mentioned that at a low relative humidity in the biofilter, the availability of water for the micro-organisms is very low. Only tolerant micro-organisms can survive. But more important for the current research is that with less water, all nutrients and dissolved salts will be concentrated. This leads to a decrease in water potential. Lower water potential means a reduction of the degradation. They

also looked at the effect of counter-current and co-current flow on performance. Their removal efficiencies for BTEX were 79% and 81% respectively. They noticed a difference in performance over the length of the column. This can be directly linked to the water availability.

Veiga and Kennes (2001) used perlite as an inert packing material. Inlet humidification and regular nutrient addition maintained the water content between 40% and 60%. After a prolonged period without water addition, the water content dropped below 40% and a reduction in elimination capacity was observed. This was reversed after the watering was resumed. Not only water content would have played a role, but as perlite does not have any nutrients available, nutrient limitation could have played a significant role in reduction of the EC.

The effect of drying on the performance of a biofilter was investigated by Morales *et al.* (2003). They implemented a dynamic one dimensional model to describe the drying and its effect on the biofilter. They introduced critical water content, which is a standard drying term. This is the moisture content when the transport of the liquid phase in the material is due to internal capillary forces. The surface of the peat was dry and vapour reached the surface by molecular diffusion through the bed. At this point the water activity in the biofilm was decreased and the toluene degradation was reduced. In their case for peat, the critical water content was 0.8 g water per gram dry peat.

Klapkova *et al.* (2006) found a maximal removal of a toluene/xylene mixture in a compost/perlite biofilter at a bed moisture content of 70%. It was not reported is if this was on a dry or wet basis. Drier conditions did lead to a decrease in removal.

For components with a small Henry coefficient or a high affinity for water like ethanol, the water content in a biofilter is important for the absorbance into the bed material. Dry materials have a much lower capacity to absorb ethanol (Auria *et al.*, 1998; Hodge and Devinny, 1994). Auria *et al.* (1998) observed that below a water content of 49% (dry weight), the EC dropped significantly. They speculated that this reduction was a combination of several factors caused by water content; change in the partition coefficient, change in the porosity, hydrodynamic air flow and biomass

activity. These factors were not readily reversible and preventing bed drying was an important step.

Most groups have seen the highest removal at the highest operating water content. Wang and Govind (1997) found an optimum removal rate for isopentane at a water content of 0.536 g water g^{-1} dry compost and 0.645 g water g^{-1} dry peat. At lower water contents, the removal dropped away steeply as seen in other research. But at high water content, the drop was more gradual. It is important to maintain the water content near its optimum at all times to retain high removal efficiencies.

Poulsen and Jensen (2007) investigated the removal of ammonia using a sewage sludge compost and yard waste compost. Their conclusions were that the sewage sludge compost had to have a higher water content to be as effective as the yard waste compost. Their argument was that the sewage sludge compost has a larger internal pore volume which has to be filled with water in order to become effective. If they had determined the matric potential instead, they might have been able to compare the composts more direct. This again shows that the water content itself is only a guideline for optimal biofilter operation.

3.5 Experimental methods

The only variable component of the water potential in this work was the matric potential. The matric potential was changed by applying a force on the compost. In these experiments that force was applied by the suction cell principle (Klute, 1986). The principle was described before in Sec. 2.1.4.

3.5.1 Water retention curves

The setup of the apparatuses was described in Sec. 2.5 and was placed in the lab at room temperature. The two types of compost were tested, Compost 1 (“Results”, a general commercial brand) and Compost 2 (“Plus Extra”, Parkhouse Garden Supplies, produced from bark, animal effluent and grass). Both composts were sieved using a mesh no. 6 (3.36 mm opening). No other compost characteristics were determined.

A layer of approximately 5 mm thick and 70 mm diameter (~ 6 g wet weight) was placed on top of the polymer membrane or ceramic disk. The matric potential was applied between -5 and -300 cm H_2O. At the lower matric potentials, air was removed regularly from the water side of the membrane. Changes in matric potential were chosen randomly in magnitude as well as the wetting or drying direction. After equilibrating for approximately 7 days, about a third of the compost was removed. The water content was determined by oven drying at 105 °C for 24 hours or by a moisture analyser (Sartorius MA-30, Goettingen, Germany).

3.5.2 Matric potential in the biofiltration reactors

The reactors used to determine the influence of matric potential on the performance of biofiltration were Reactor 1 and 2 (Sec 2.2.2 and Sec. 2.2.3). The inlet concentration and flow were kept as constant as possible and the only variable was the matric potential applied to the compost. The matric potential was controlled by lowering the external water reservoir to the desired height below the membrane. The matric potential of -300 cm H_2O was accomplished by closing the head space of the external water reservoir and reducing the gas pressure in the head space. The pressure was monitored using a pressure transducer (Setra 280E, Setra Systems Inc, Acton, MA).
The water content in the compost at the start of each run, as well as the mass loaded is found in Table 3.6. In the run R3r1, data was collected at three different thicknesses of the compost layer and thus different mass loadings. The measured dry bulk densities are similar to what Mysliwiec *et al.* (2001) reported (298 kg m^{-3}).

Table 3.6*: Initial compost parameters in the reactor runs.*

Run	Compost type	Initial water content (g H_2O g^{-1} dry compost)	Compost loaded (g dry)	Bulk density (kg m^{-3} dry weight)
R1r2	1	1.22	1.70	257
R1r4	1	1.78	1.88	284
R1r5	1	1.50	1.56	236
R2r1	2	1.16	1.96	296
R3r1a	2	1.14	2.85	258
R3r1b	2	1.65	1.79	270
R3r1c	2	2.20	0.91	249

3.6 Results and discussion

3.6.1 Water retention curves

The relationship between matric potential and gravimetric water content was determined for both composts (Fig. 3.2 and Fig. 3.3 and combined in A.8). All water contents were determined after a minimum equilibration time of 7 days. In both cases, a decrease in matric potential from -5 cm to -50 cm H_2O did lower the water content rapidly. This was attributed to drainage of the large interparticle pore spaces. These spaces hold large quantities of water but are easily drained. The decrease in matric potential from -50 cm to -300 cm showed a much smaller decrease in water content, most likely due to the high capillary forces generated by small pores in the individual compost particles. Compost 1 clearly showed higher water contents as the matric potential increased, however at lower matric potentials, both compost types approached water contents of approximately 1.1 g g^{-1} (~50 % wet basis). Little hysteresis in water content was observed for either compost. A typical change in matric potential between two data points was 5 to 30 cm H_2O. Large matric potential changes (> 100 cm H_2O) were not investigated and further work is required.

Several empirical relationships are developed to estimate the relation between water content and matric potential (Hon, 1999). One of the relationships (Eq. 3.8) is developed by Van Genuchten (Tuller and Or, 2005b). The data was fit to Eq. 3.8.

$$\Theta = \frac{\theta - \theta_r}{\theta_s - \theta_r} = \left[\frac{1}{1 + (\alpha \psi_m)^n} \right]^m \qquad [3.8]$$

With: $m = 1 - \frac{1}{n}$

The parameters of the model (Table 3.7) were determined using the least squares method (Eq. C.10) on all data points. As no experimental data was collected above a matric potential of -5 cm H_2O, it was difficult to validate the model in that very wet region.

***Table 3.7**: Fitted parameters of the Van Genuchten model.*

Parameter	Compost 1	Compost 2
α (cm^{-1})	0.654	3.673
n (-)	1.484	1.294
Θ_s ($g\ g^{-1}$)	4.566	3.174
Θ_r ($g\ g^{-1}$)	0.598	0.759

The shape of the curves was comparable to the shapes of the typical water retention curves in Fig. 3.1. Soils of different textures have a very different soil-water retention curves and absolute values are difficult to compare.

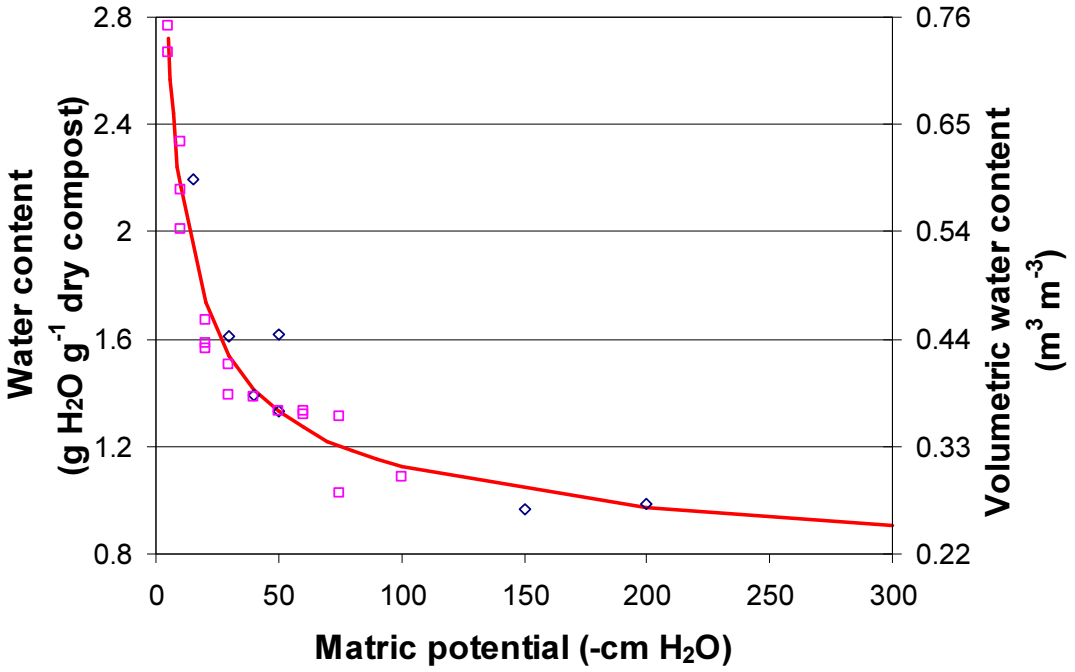

***Figure 3.2**: Water retention curves for Compost 1. The drying curve (open blue diamonds (◊)) and the wetting curve (open pink squares (□). The red solid line is the Van Genuchten model fit. The bulk density used is 270 kg m^{-3}.*

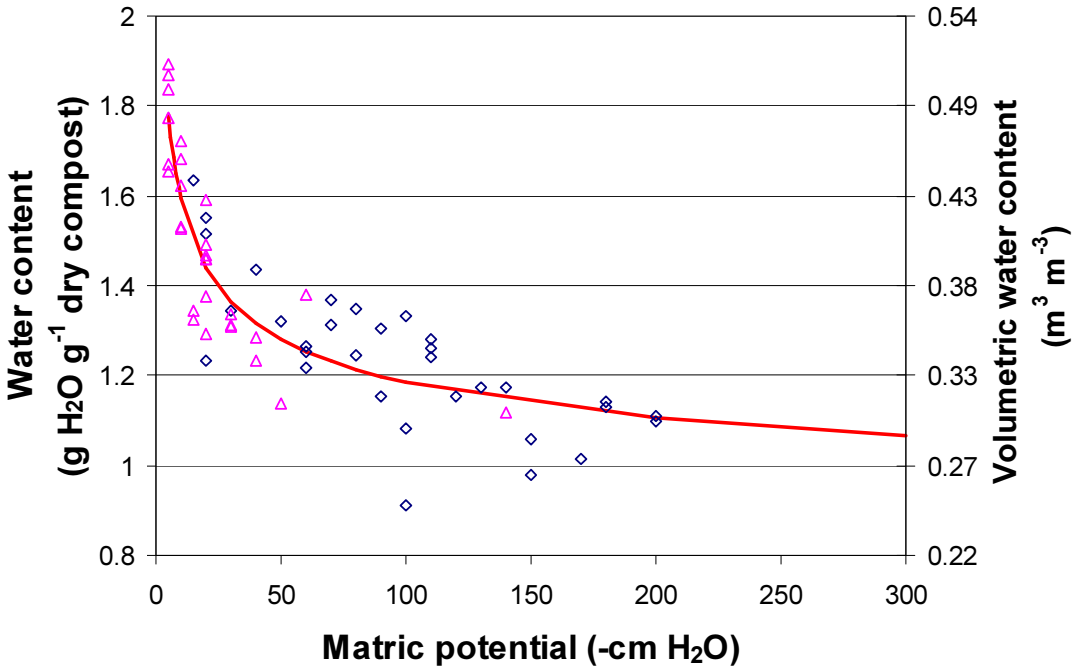

***Figure 3.3**: Water retention curves for Compost 2. The drying curve (open blue diamonds (◊)) and the wetting curve (open pink squares (□). The red solid line is the Van Genuchten model fit. The bulk density used is 270 kg m^{-3}.*

3.6.2 Water content of the compost in the reactors

At the end of the experimental runs in the reactors degrading toluene, the water content was measured to confirm the validity of the assumption that the reactor controls the water content accurately (Table 3.8). At first glance the reactors during the runs did not perform as well as expected. But there were several explanations when for some of the large delta ψ_m. The $\Delta\psi_m$ was determined by using the Van Genuchten model (Eq.3.8) to predict ψ_m which were compared to the ψ_m set on the reactor. A negative $\Delta\psi_m$ means that the compost in the reactor was drier then expected. The water contents in R1r3, R1r5 b and R3r1 are all within the expected range. The average of Compost 1 in the tension reactors at -20 cm H_2O varied from 1.57 to1.61 g g^{-1}.

During R1r2 the compost was at a matric potential of -300 cm for 26 days before it was increased to -20 cm H_2O. Because of the extended period at a low matric potential the compost could have become hydrophobic, so it possibly did not rewet to the same water content. The drier conditions of the compost could have stimulated the

growth of fungi. These fungi can also cause hydrophobicity in soils (Cardenas-Gonzalez *et al.*, 1999; King, 1981).

***Table 3.8**: Water content in reactors when measured immediately after the experiment.*

Run	**Reason end**	**Water content (g H_2O g^{-1} dry compost)**	**Matric potential measured (cm H_2O)**	**$\Delta \psi_m$**
R1r1	Membrane rupture	-	-	-
R1r2	EC loss	1.37	-45	-25
R1r3	Temp control failure	1.60	-26	-6
R1r4	Air leak	1.42	-39	+81
R1r5a	Test water content	1.31	-53	+72
R1r5b	Test water content	1.67	-23	-3
R2r1	Not opened			
R3r1a	Removed layer	1.65	-8	+12
R3r1b	Removed layer	2.20	-2	+18
R3r1c	Removed layer	2.13	-2	+18

In R1r4 the reactor was kept at -120 cm H_2O for only 2 days until the run was stopped because of a leak in one of the welds of the bottom plate. The matric potential before was kept at -60 cm H_2O for 23 days. The compost was much wetter than expected. No direct reason for this could be found but it is possible that the water content did not reach equilibrium yet.

When the reactor in R1r5a was opened, water drops fell from the top surface of the ring that clamps the membrane (The red area in Fig. 3.4) onto the compost. The compost absorbed the water and the water content turned out to be higher then

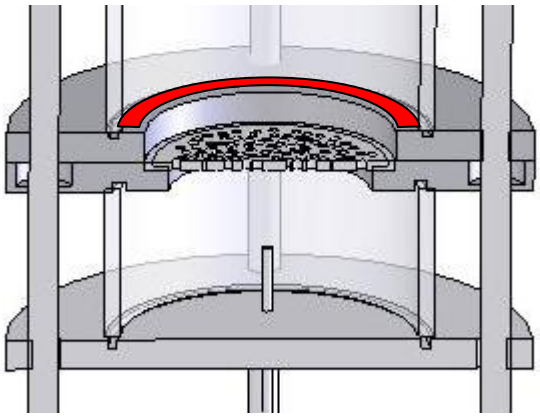

***Figure 3.4**: Cutaway of R1. The red surface indicates the location of the water accumulation. The surface was tapered after the run.*

expected. The reactor was reassembled with the remaining compost. Care was taken in disassembling at the end of the second part of the run, and the water content was as expected. The surface was tapered after the run to prevent this in the future.

As Reactor 1 and 3 had the same design of the clamping plate (D in Fig 2.13), water fell onto the compost while disassembling R3r1b and R3r1c. Both water contents were therefore higher then expected. The results showed that without experimental errors, the water content in the reactors corresponded with the water retention curves.

3.6.3 Influence of matric potential on biofilter performance: Reactors

The results for Compost 1 (Fig. 3.5) and Compost 2 (Fig. 3.6) clearly indicate that by decreasing the matric potential the EC dropped. While outlet concentrations did vary during these experiments between 20 and 60 ppm, results discussed in Chapter 5 will support that matric potential was the dominant parameter.

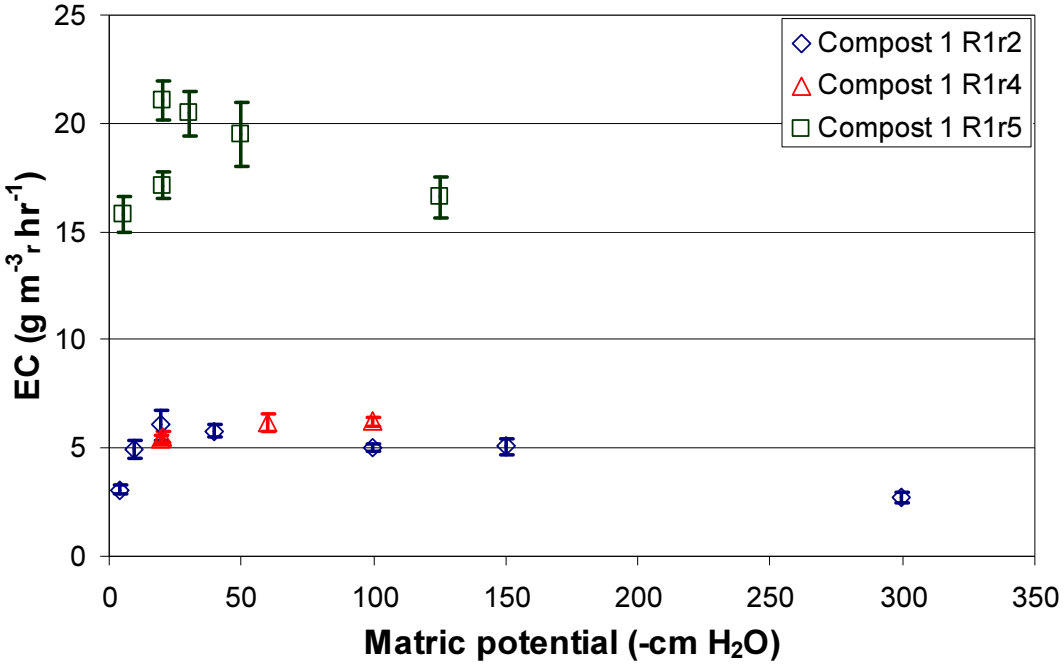

***Figure 3.5**: Influence of the matric potential on the elimination capacity for Compost 1 in Reactor 1 run 2 (open blue diamonds (◊)), Reactor 1 run 4 (open red triangles (Δ)) and Reactor 1 run 4 (open green squares (□)). The error bars represent 95% confidence interval.*

The maximum EC occurred at approximately -20 cm H_2O for both compost types, but with a fairly broad maximum. The removal rates for toluene for both compost types were not very high. This low value is not an artefact of the reactor system, as comparable EC's were observed in a traditional integral reactor (Sec 3.5.4). However, reported EC values for toluene vary considerably. Auria *et al.* (2000) showed EC's between 15 and 150 g m^{-3}_r hr^{-1}, Morales *et al.* (1998) reported EC's between 8 and 190 g m^{-3}_r hr^{-1} and Sun *et al.* (2002) between 0 and 40 g m^{-3}_r hr^{-1}. The results for R1r5 show much higher EC's than the other two runs and is discussed in Sec 3.6.3.1. The figure showing the EC as a function of water content can be found in Sec 3.6.5.

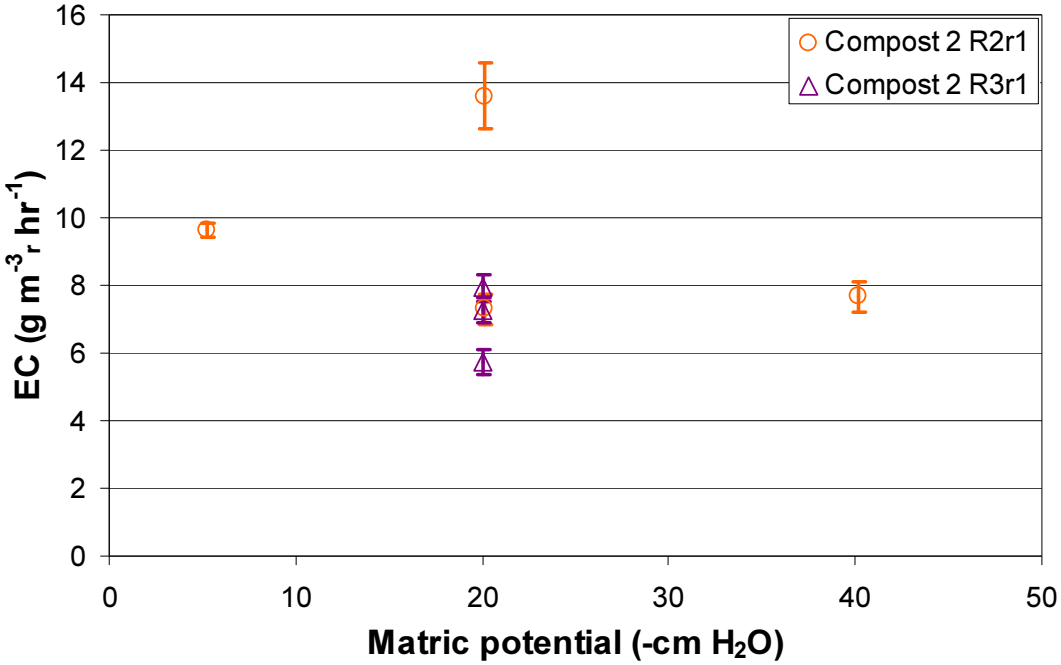

***Figure 3.6**: Influence of the matric potential on the elimination capacity for Compost 2 in Reactor 2 run 1 (open orange circles (○)), Reactor 3 run 1 (open purple triangles (Δ)). The error bars represent 95% confidence interval.*

3.6.3.1 The effect of the type of water on the average EC

The water below the membrane during R1r2 and R1r4 was autoclaved de-ionized (DI) water. This could have caused the low EC's in comparison with R1r5 where autoclaved tap water was used. The reduced mineral concentration of DI water has a higher water potential than tap water. So exposure of the compost to the DI water could have caused an upshock which could have damaged the whole population,

including the toluene degraders in the compost. The integral reactor (Sec. 3.6.4) showed a similar low steady state EC (4.8 ± 0.3 g m^{-3}_{r} hr^{-1}). It is possible that the tap water contained small amounts of trace elements and salts that had a large influence on the biomass.

3.6.3.2 The effect of a low matric potential on the EC

After reaching a matric potential in R1r2 of -300 cm H_2O (1 g g^{-1} dry weight), the EC dropped significantly to 2.7 g m^{-3}_{r} hr^{-1} (Fig. 3.5). After increasing the matric potential to -20 cm (Fig. 3.7), the EC did not recover. The water content in the reactor was measured after the experiment and was found to be 1.37 (g g^{-1} dry weight). Results of the water retention experiments (Fig. 3.2) showed that the equilibrium water content at -20 cm H_2O was 1.58 (g g^{-1} dry weight). Even after 27 days equilibrating at -20 cm H_2O, the compost in the reactor clearly did not fully rewet. The EC was unable to recover due to water content hysteresis (not rewetting to the original water content) and possibly damage to the microbial cultures. Bed materials like compost have hydrophobic surfaces with high air-water-solid contact angles, which are difficult to re-wet when dry. The hydrophobic surfaces repel the water spreading through the compost and prevent water entering the pores (Kennes and Veiga, 2001). Additional experiments at the low potentials are required to explore hydrophobicity issues.

Lowering the matric potential lowers the amount of available water. As cell membranes are permeable, water will leak out of the cell, causing a stress. In contrast to water stress by osmotic potential, no compatible solute molecules are available to reduce the stress by adjusting the intracellular water potential. That is why many groups have seen a larger sensitivity to matric then to osmotic stress (Adebayo and Harris, 1971; Ramos *et al.*, 1999). If the cells do not have compatible solute production, they have no defence against the lower water potential (Harris, 1981). The organism widely attributed to toluene removal; the *Pseudomonas* genera, do not in general accumulate any intracellular polysaccharides to protect against drying (Roberson and Firestone, 1992). Even when the cells can produce intracellular solutes, these solutes can inhibit enzyme activity by lowering enzyme hydration (Rattray *et al.*, 1992; Stark and Firestone, 1995). These responses could all contribute to lower removal rates at low matric potentials. To test this hypothesis experiments with pure cultures and analysis of intracellular components are required.

The initial recommended optimal moisture content in composting ranges from 40-65% (w/w) (Rynk, 1992). Thus, the microbial cultures in the compost are acclimatised to this moist environment. Drying of compost can have a significant influence on the bacterial community present. If a significant percentage of toluene degraders do not easily adapt to drier conditions, for example by compatible solutes, a reduction in EC will likely occur.

In soil drying experiments conducted by Bottner (1985), it was found that after drying the soil biomass was reduced by 1/3 to 1/4. The decay was mostly found within the more active biomass. The dormant biomass seemed to have a higher resistance against drying and a larger fraction of this type of biomass survived. The decay released carbon as well as nitrogen into the soil, which got partly re-metabolized. Microbial cultures in environments that have been regularly exposed to drying are invariable more resilient to water stress, than cultures in moist environments (Wardle, 1992). Therefore, a large part of the microbial community could have been susceptible to water changes and did not recover well from the -300 cm H_2O matric potential. Further work to determine the ratio between living and dead cells similar to experiments by Tresse *et al.* (2003) would be required to confirm this hypothesis.

This effect has been noted by several other groups. Holden *et al.* (1997a) used solutes (NaCl and PEG-8000) to put pure cultures of toluene degraders under water stress. The highest rate in toluene degradation was observed at 0 cm water potential. At a water potential of -2,500 cm H_2O, an optimum in the growth rate was seen, but at lower potentials, the growth and degradation of toluene slowed down considerably. Although the water potentials they used were much lower (0 to -15,000 cm H_2O) than that used in this research (0 to -300 cm H_2O), the trend was comparable.

3.6.3.3 Mass transfer effects

A lower water content will reduce the thickness of the water film surrounding the biofilm. This will reduce the mass transfer resistance of toluene to the biofilm. This could explain why the EC at lower matric potentials does not drop dramatically. The water content between -20 and -300 cm H_2O (compost 1) is reduced by 52%. As the amount of compost and the area are constant, the thickness of the water layer is also

reduced. Halving the water film thickness does reduce the mass transfer resistance proportionally.

Roberson and Firestone (1992) did see an increase in EPS at drier conditions. Although the cells are more protected from drying, the mass transfer resistance to the cells did increase. Changing water potential could lead to a change in the hydration of the biofilm, which can lead to a change in diffusion coefficient of toluene. The effect of the water potential on the diffusion coefficient of toluene through a *Pseudomonas putida* biofilm was investigated by Holden *et al.* (1997b). Their results did show a lower diffusion coefficient through the biofilm as compared through pure water. No significant difference was seen in the diffusion coefficient measured at a water potential between 0 and $-1.5 \cdot 10^4$ cm H_2O. The total mass transfer is proportional to the resistance from all these factors; water layer thickness, EPS (and thus biofilm) thickness and biofilm hydration. It is not easy to determine which one will influence the degradation of, in this case toluene, the most.

3.6.3.4 Reduction due to water redistribution

After rewetting the compost, although the water content may be the same, the location of the water can be different. During rewetting compost, the water can fill the larger pores more readily then the smaller ones, causing air to be trapped (Bloom and Richard, 2002). A change in water distribution changes the availability of the water for the degraders. If they are present in the small pores where there will be less water, the degradation will be reduced. If the degraders are in the large pores, more water will be available and degradation will increase. A change in the overall removal rate will depend on the ratio of degraders present in large or small pores. The experiments investigated long term steady states, so entrapped air from large water content changes is not be a big factor.

3.6.3.5 Reduction of the EC due to water potential increase

After 27 days at -300cm H_2O the matric potential was increased to -20 cm H_2O. As can be seen in Fig 3.7, initially the EC increased from 2.7 to 4.8 g m^{-3}_r hr^{-1}. However, after three days, the EC dropped significantly to around 0.8 g m^{-3}_r hr^{-1}, after which it recovered to similar values as the -300 cm steady state. No data was taken for two

weeks, but after that the EC still not had recovered. The expectation was that the EC would drop ever further and the run was stopped.

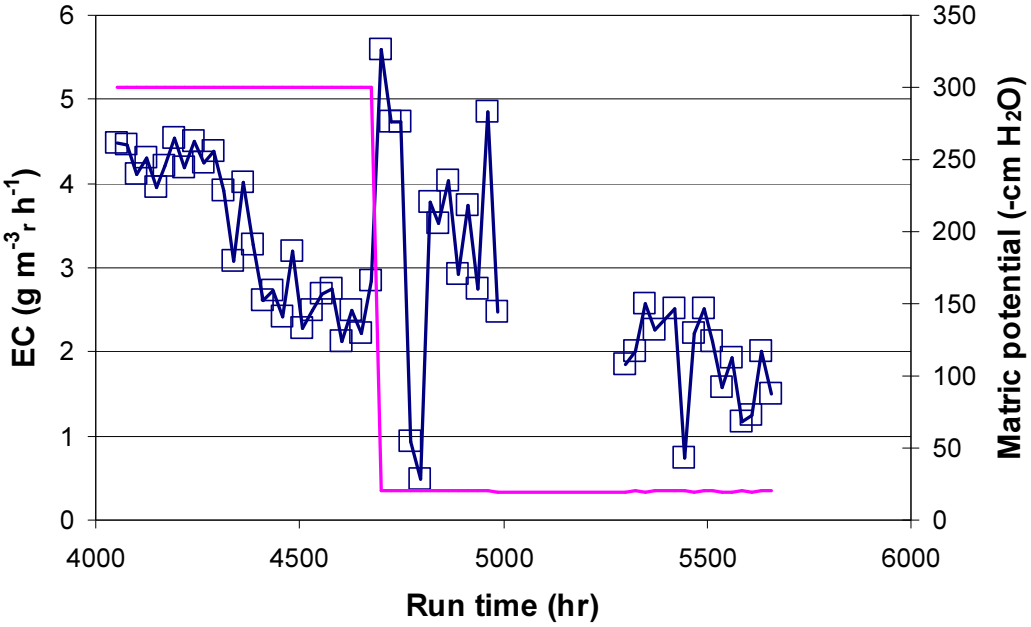

***Figure 3.7**: Data from R1r2 to illustrate the inability for the EC to recover after a high matric potential. The EC (blue squares and line) and corresponding matric potential (pink line).*

A similar trend has occurred in R2r1 (Fig 3.8). After a steady state at -20 cm H_2O, the matric potential was reduced to -5 cm H_2O. This led initially to a significant drop in EC and only after twelve days the EC recovered to higher values.

Initially an increase in the available water did improve the degradation. This could be due to enzyme hydration and energy savings in maintaining the turgor pressure. As the water content had not reached steady state, the thickness of the water film surrounding the biofilm increased as well. Toluene is a hydrophobic compound and increasing the thickness of the water layer increased the mass transfer resistance. This increase in mass transfer resistance caused a reduction in elimination capacity (Bagherpour *et al.*, 2005).

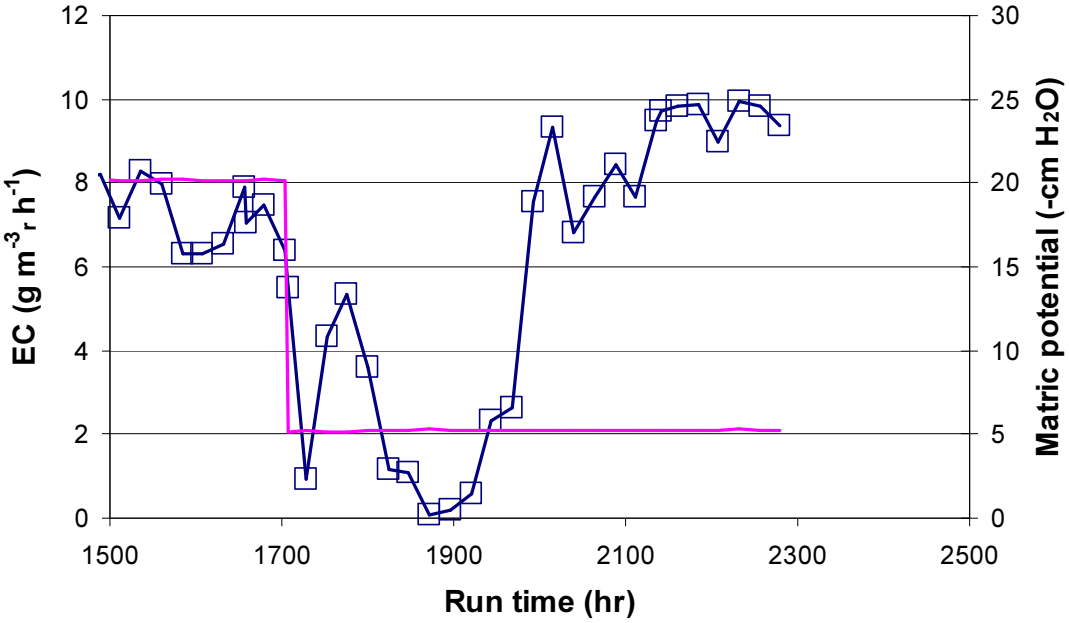

***Figure 3.8**: Data from R2r1 to illustrate the time for the EC to recover after rewetting. The EC (solid blue line) and corresponding matric potential (solid pink line).*

The drop in EC at steady state at high matric potential (high water contents) matches observations elsewhere (Leson and Winer, 1991; Wang and Govind, 1997). In biofilters, excess water fills the biofilter pores and reduces the mass transfer of nutrients, oxygen and waste products (Bohn and Bohn, 1999). It also increases the pressure drop through the bed, bed compaction, formation of anaerobic zones (Krailas et al., 2000) and breakthrough of the pollutant. As the pores in the compost layer in at high potentials start filling with water, the additional mass transfer resistance of the extra water could reduce the removal rates.

3.6.4 Influence of matric potential on biofilter performance: Column

For the first run in the column reactor the column was loaded with Compost 1 at a water content of 1.13 g g^{-1}. Over the initial four days, the outlet and inlet concentrations were not significantly different, and the EC was negligible. The water content was equivalent to a matric potential of -97 cm H_2O. After this initial period, the column was disassembled and the water content confirmed. The water content had dropped marginally to 1.08 g g^{-1} or matric potential of -119 cm H_2O.

The compost was wetted to a water content of 1.54 g g^{-1} (ψ_m = -30 cm H_2O) and repacked. Significant removal of toluene was evident within 2 days (Fig 3.9). The EC peaked after 6 days and slowly trailed of to reach a steady state of 4.8 ± 0.7 g m^{-3}_r hr^{-1}. This confirms that the low EC seen before in the reactors was due to the compost and not an artefact from the differential reactor configuration. It is not uncommon to require two to three weeks to achieve steady state (Morales *et al.*, 1998) with a previously non-adapted microbial population. This steady state was maintained for 20 days. During this time, the load was periodically changed from 30 to 5 g m^{-3}_r hr^{-1}. The trend of a short initial peak in EC followed by lower steady state was observed by Morales *et al.* (1998). In their experiments, the EC reached a maximum value of 180 g m^{-3}_r hr^{-1} shortly after start-up, which reduced to 8 g m^{-3}_r hr^{-1} at steady state.

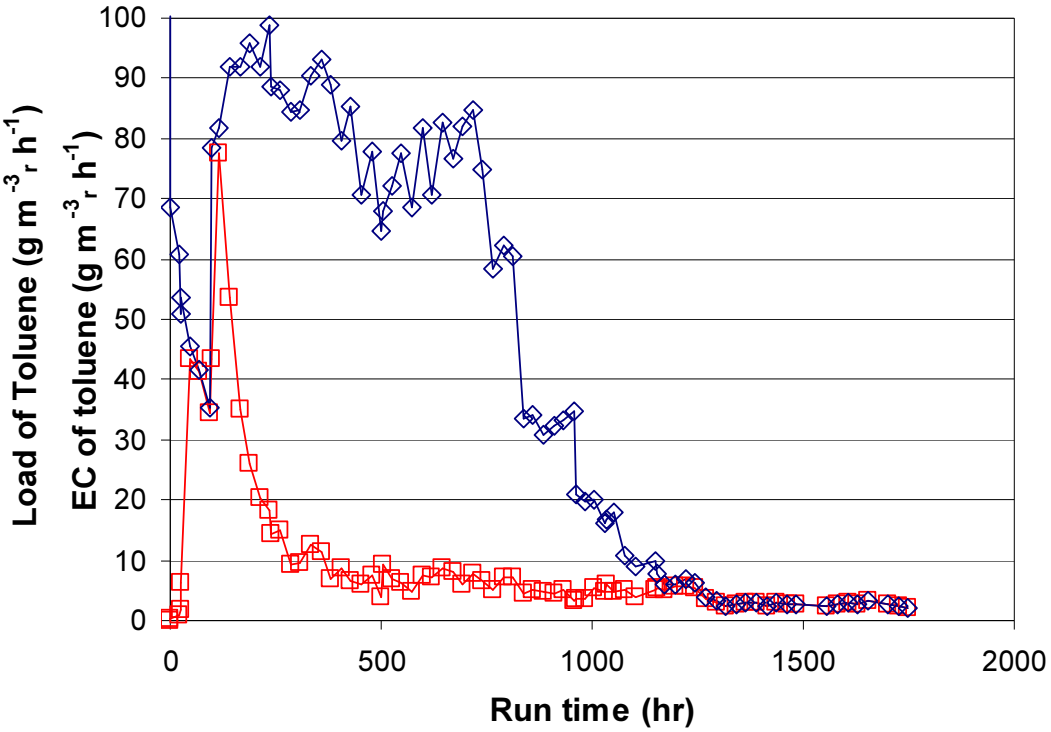

***Figure 3.9**: Elimination capacity (open red squares (□) and load (open blue diamonds (◊) of RC run 2.*

The water content after the run was 1.26 g g^{-1} (ψ_m = -62 cm H_2O). Over the 1750 hour run the matric potential decreased by 32 cm H_2O. As can be seen in Fig. 3.5, the EC between a matric potential of -20 to -100 cm H_2O did not vary significantly. So the increase in water potential was believed not to have a significant impact on the EC.

3.6.5 Water potential vs. water content

Although both composts had different water holding capacities especially at higher potentials, they resulted in similar EC's at the same water potential. As can be seen in Fig.3.10, the composts have different EC's at the same water contents. The maximum EC occurred at approximately -20 cm H_2O for both compost types, which corresponds with 1.73 g g^{-1} and 1.44 g g^{-1} for Compost 1 and Compost 2 respectively. These differences are small because of the similarity of the water release curves. The differences would be more obvious if materials with significantly different water release curves like peat or soil were investigated.

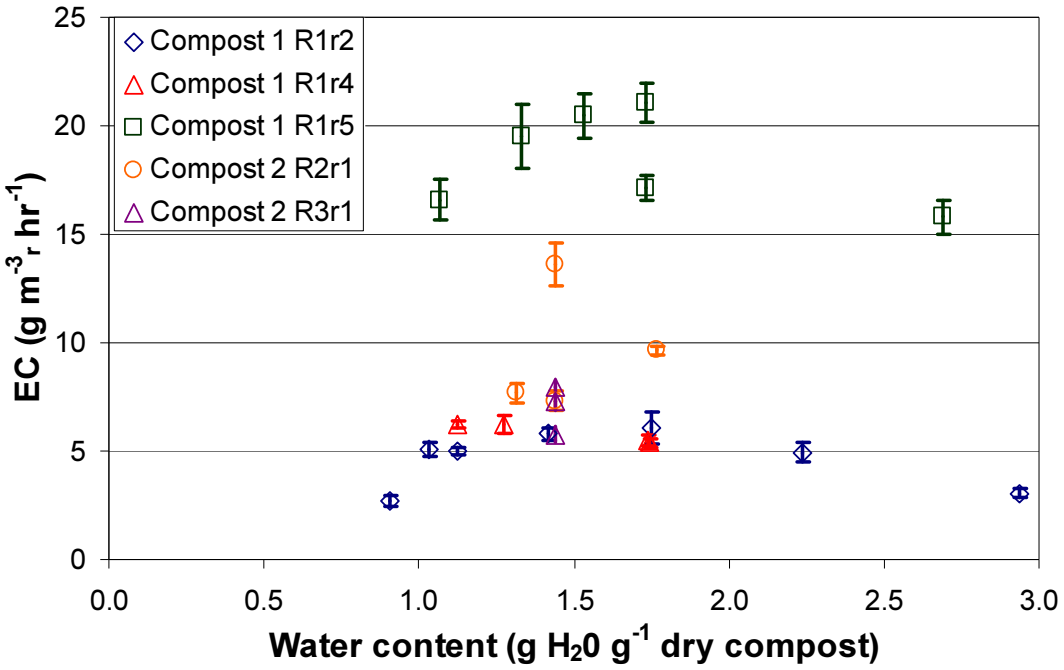

***Figure 3.10**: Influence of the water content on the elimination capacity for Compost 1: R1r 2 (open blue diamonds (◊)), R1r4 (open red triangles (Δ)) and R1r5 (open green squares (□)) and Compost 2: R2r1 (open orange circles (○)), R3r1 (purple crosses (x)). The error bars represent 95% confidence interval.*

Therefore, water potential and not water content was the predominant factor affecting degradation in these systems. Wang and Govind (1997) investigated the effect of water content on removal of isopentane in peat and compost. Both bed materials showed a similar maximal removal rate (EC = 6 g m^{-3}_r hr^{-1}), but at different water contents, 66% (peat) and 56% (compost) respectively. Although they did not

investigate the water holding capacity; peat generally holds more water at a given potential than compost (Mandelbaum *et al.*, 1993). Their results support that water potential and not water content controls elimination capacity for simple hydrocarbons. Obviously two composts could have different communities and available nutrients and further work is required to determine the wider applicability of this hypothesis.

3.7 Conclusions

Water content does have an influence on the elimination capacity of toluene in compost. More accurately, water potential and not water content was the predominant factor affecting degradation. Optimal removal rates were seen at a matric potential between -10 and -100 cm H_2O, with a maximum at -20 cm H_2O. A reduction in water potential to -300 cm H_2O led to a 60% reduction in EC. At water potentials above -10 cm H_2O, the EC also was reduced. This reduction was attributed to several factors: loss of water availability to the organisms, water redistribution in the medium, non-adaptable micro-organisms, and reduced mass transfer.

3.8 Nomenclature

c	concentration of the solute	mol kg^{-1}
g	acceleration of gravity	m s^{-2}
m	$1-\frac{1}{n}$	-
n	empirical shape parameter	-
n_m	number of moles	-
R	universal gas constant	J mol^{-1} K^{-1}
T	temperature	K
V_{soil}	volume of the soil	m^3
V_{void}	volume of the void in the soil	m^3
V_{water}	volume of the water in the soil	m^3
W_{soil}	weight of the dry soil	kg
W_{water}	weight of the water in the soil	kg
α	empirical shape parameter	-
γ	number of osmotically active particles per molecule solute	-
ϕ	osmotic coefficient	-

Θ	normalised water content at matric head h	-
θ_r	residual water content	$m^3\ m^{-3}$
θ_s	saturated water content	$m^3\ m^{-3}$
θ	water content	$m^3\ m^{-3}$
ψ_m	matric potential	-
ρ_{bulk}	density of the bulk soil (= W_{soil} / (V_{soil} + V_{void}))	$kg\ m^{-3}$
ρ_{water}	density of water	$kg\ m^{-3}$
ρ_w	density of water	$kg\ m^{-3}$

Subscripts

r	of reactor

3.9 References

Adebayo, A. A., and R. F. Harris. 1971. Fungal Growth Responses to Osmotic as Compared to Matric Water Potential. *Soil Science Society of America Proceedings* 35: 465-469.

Auria, R., A. C. Aycaguer, and J. S. Devinny. 1998. Influence of water content on degradation rates for ethanol in biofiltration. *Journal of the Air & Waste Management Association* 48: 65-70.

Auria, R., G. Frere, M. Morales, M. E. Acuna, and S. Revah. 2000. Influence of mixing and water addition on the removal rate of toluene vapors in a biofilter. *Biotechnology and Bioengineering* 68: 448-455.

Bagherpour, M. B., M. Nikazar, U. Welander, B. Bonakdarpour, and M. Sanati. 2005. Effects of irrigation and water content of packings on alpha-pinene vapours biofiltration performance. *Biochemical Engineering Journal* 24: 185-193.

Banin, A., B. G. Davey, and P. F. Low. 1968. Effect of membrane pore size on measurement of water tension in bentonite suspension. *Soil Science Society of America Proceedings* 32: 306-309.

Bloom, E., and T. L. Richard. 2002. Relative humidity and matric potential constraints on composting microbial activity. *Proceedings 2002 ASEA annual international meeting*, Chicago, Illinois.

Bohn, H. L., and K. H. Bohn. 1999. Moisture in biofilters. *Environmental Progress* 18: 156-161.

Borken, W., E. A. Davidson, K. Savage, J. Gaudinski, and S. E. Trumbore. 2003. Drying and wetting effects on carbon dioxide release from organic horizons. *Soil Science Society of America Journal* 67: 1888-1896.

Bottner, P. 1985. Response of microbial biomass to alternate moist and dry conditions in a soil incubated with C-14-labeled and N-15-labelled plant-material. *Soil Biology & Biochemistry* 17: 329-337.

Buckingham, E. 1907. Studies on the movement of soil moisture. *USDA, Bureau of soils* Bulletin 38.

Cardenas-Gonzalez, B., S. J. Ergas, M. S. Switzenbaum, and N. Phillibert. 1999. Evaluation of full-scale biofilter media performance. *Environmental Progress* 18: 205-211.

Chan, W. C., and M. C. Lu. 2003. A new type synthetic filter material for biofilter: Poly(vinyl alcohol)/peat composite bead. *Journal of Applied Polymer Science* 88: 3248-3255.

Chenu, C., and E. B. Roberson. 1996. Diffusion of glucose in microbial extracellular polysaccharide as affected by water potential. *Soil Biology & Biochemistry* 28: 877-884.

Coyne, M. 1999. *Soil microbiology: an exploratory approach*. Delmar Publishers Inc., Albany, NY.

Davis, L. C., C. Pitzer, S. Castro, and L. E. Erickson. 2001. Henry's constant, Darcy's law and contaminant loss. *Conference on Environmental Research*, Manhattan, Kansas.

Deheyder, B., A. Overmeire, H. Vanlangenhove, and W. Verstraete. 1994. Ethene removal from a synthetic waste-gas using a dry biobed. *Biotechnology and Bioengineering* 44: 642-648.

Devinny, J. S., M. A. Deshusses, and T. S. Webster. 1999. *Biofiltration for air pollution control*. Lewis Publishers, Boca Raton, Fla.

du Plessis, C. A., J. M. Strauss, E. M. T. Sebapalo, and K. H. J. Riedel. 2003. Empirical model for methane oxidation using a composted pine bark biofilter. *Fuel* 82: 1359-1365.

Fierer, N., and J. P. Schimel. 2002. Effects of drying-rewetting frequency on soil carbon and nitrogen transformations. *Soil Biology & Biochemistry* 34: 777-787.

Fierer, N., and J. P. Schimel. 2003. A proposed mechanism for the pulse in carbon dioxide production commonly observed following the rapid rewetting of a dry soil. *Soil Science Society of America Journal* 67: 798-805.

Fierer, N., J. P. Schimel, and P. A. Holden. 2003. Influence of drying-rewetting frequency on soil bacterial community structure. *Microbial Ecology* 45: 63-71.

Franzluebbers, A. J. 1999. Microbial activity in response to water-filled pore space of variably eroded southern Piedmont soils. *Applied Soil Ecology* 11: 91-101.

Fredlund, D. G., and A. Q. Xing. 1994. Equations for the soil-water characteristic curve. *Canadian Geotechnical Journal* 31: 521-532.

Hanks, R. J. 1992. *Applied soil physics : soil water and temperature applications*. Springer-Verlag, New York.

Harris, R. F. 1981. Effect of water potential on microbial growth and activity in J. F. Parr, W. R. Gardner, and L. F. Elliott, eds. *Water potential relations in soil microbiology, SSSA special publication number 9*. Soil science society of America, Madison.

Hartikainen, T., J. Ruuskanen, M. Vanhatalo, and P. J. Martikainen. 1996. Removal of ammonia from air by a peat biofilter. *Environmental Technology* 17: 45-53.

Hillel, D. 1982. *Introduction to soil physics*. Academic Press, Orlando ; New York ; Sydney.

Hodge, D. S., and J. S. Devinny. 1994. Biofilter treatment of ethanol vapors. *Environmental Progress* 13: 167-173.

Holden, P. A., and N. Fierer. 2005. Microbial processes in the vadose zone. *Vadose Zone Journal* 4: 1-21.

Holden, P. A., L. J. Halverson, and M. K. Firestone. 1997a. Water stress effects on toluene biodegradation by *Pseudomonas putida*. *Biodegradation* 8: 143-151.

Holden, P. A., J. R. Hunt, and M. K. Firestone. 1997b. Toluene diffusion and reaction in unsaturated *Pseudomonas putida* biofilms. *Biotechnology and Bioengineering* 56: 656-670.

Hon, A. S. Y. 1999. Hydraulic properties of biologically active media. *Chemical and Process Engineering*. Univerisity of Canterbury, Christchurch.

Iwata, S., B. P. Warkentin, and T. Tabuchi. 1988. *Soil-water interactions : mechanisms and applications*. Dekker, New York, N.Y.

Jennings, D. H., and R. M. Burke. 1990. Compatible Solutes - the Mycological Dimension and Their Role as Physiological Buffering Agents. *New Phytologist* 116: 277-283.

Johnson, C. T., and M. A. Deshusses. 1997. Quantative structure-activity relationships for VOC biodegradation in biofilters. *4th In-situ and On-site Bioremediation Symposium*. Batellle Press.

Kennes, C., and F. Thalasso. 1998. Waste gas biotreatment technology. *Journal of Chemical Technology and Biotechnology* 72: 303-319.

Kennes, C., and M. C. Veiga. 2001. *Bioreactors for waste gas treatment*. Kluwer Academic, Dordrecht ; Boston.

Kieft, T. L., E. Soroker, and M. K. Firestone. 1987. Microbial biomass response to a rapid increase in water potential when dry soil is wetted. *Soil Biology & Biochemistry* 19: 119-126.

King, P. M. 1981. Comparison of methods for measuring severity of water repellence of sandy soils and assessment of some factors that affect its measurement. *Australian Journal of Soil Research* 19: 275-285.

Klapkova, E., M. Halecky, M. Fitch, C. R. Soccol, and J. Paca. 2006. Impact of biocatalyst and moisture content on toluene/xylene mixture biofiltration. *Brazilian Archives of Biology and Technology* 49: 347-352.

Klute, A. 1986. *Methods of soil analysis, Part 1-Physical and mineralogical methods*. Soil Science Society of America, Inc, Madison, Wisconsin.

Knauf, S., and H. Zimmer. 1994. Biofiltration at a temperature above 40-degrees-C - Comparison of the biofilter materials bark compost and wood chips. *Staub Reinhaltung Der Luft* 54: 41-44.

Krailas, S., Q. T. Pham, R. Amal, J. K. Jiang, and M. Heitz. 2000. Effect of inlet mass loading, water and total bacteria count on methanol elimination using upward flow and downward flow biofilters. *Journal of Chemical Technology and Biotechnology* 75: 299-305.

Krasil'nikov, N. A. 1958. *Soil microorganisms and higher plants*. Academy of Sciences of the USSR, Israel Program for Scientific Translations, Moscow.

Lal, R., ed. 2002. *Encyclopedia of soil science*. Marcel Dekker, New York.

Leson, G., and A. M. Winer. 1991. Biofiltration - an innovative air-pollution control technology for VOC emissions. *Journal of the Air & Waste Management Association* 41: 1045-1054.

Linn, D. M., and J. W. Doran. 1984. Effect of water-filled pore-space on carbon-dioxide and nitrous-oxide production in tilled and nontilled soils. *Soil Science Society of America Journal* 48: 1267-1272.

Lu, C. S., M. R. Lin, and C. H. Chu. 2002. Effects of pH, moisture, and flow pattern on trickle-bed air biofilter performance for BTEX removal. *Advances in Environmental Research* 6: 99-106.

Mandelbaum, R., Y. Hadar, and Y. Chen. 1993. Simple apparatus to study microbial activity in organic substrates under constant water potential. *Soil Biology & Biochemistry* 25: 397-399.

Moe, W. M., and R. L. Irvine. 2001. Polyurethane foam based biofilter media for toluene removal. *Water Science and Technology* 43: 35-42.

Morales, M., S. Hernandez, T. Cornabe, S. Revah, and R. Auria. 2003. Effect of drying on biofilter performance: Modeling and experimental approach. *Environmental Science & Technology* 37: 985-992.

Morales, M., S. Revah, and R. Auria. 1998. Start-up and the effect of gaseous ammonia additions on a biofilter for the elimination of toluene vapors. *Biotechnology and Bioengineering* 60: 483-491.

Morgado, J., G. Merlin, Y. Gonthier, and A. Eyraud. 2004. A mechanistic model for m-xylene treatment with a peat-bed biofilter. *Environmental Technology* 25: 123-132.

Mysliwiec, M. J., J. S. VanderGheynst, M. M. Rashid, and E. D. Schroeder. 2001. Dynamic volume-averaged model of heat and mass transport within a compost biofilter: I. Model development. *Biotechnology and Bioengineering* 73: 282-294.

Papendick, R. I., and G. S. Campbell. 1981. Theory and measurement of water potential in J. F. Parr, W. R. Gardner, and L. F. Elliott, eds. *Water potential relations in soil microbiology, SSSA special publication number 9*. Soil science society of America, Madison.

Poulsen, T. G., and A. H. B. Jensen. 2007. Gaseous ammonia uptake in compost biofilters as related to compost water content. *Journal of the Air & Waste Management Association* 57: 940-946.

Pozdnyakov, A. I., L. A. Pozdnyakova, and L. O. Karpachevskii. 2006. Relationship between water tension and electrical resistivity in soils. *Eurasian Soil Science* 39: S78-S83.

Ramirez, M. L., S. N. Chulze, and N. Magan. 2004. Impact of osmotic and matric water stress on germination, growth, mycelial water potentials and endogenous accumulation of sugars and sugar alcohols in *Fusarium graminearum*. *Mycologia* 96: 470-478.

Ramos, A. J., N. Magan, and V. Sanchis. 1999. Osmotic and matric potential effects on growth, sclerotia and partitioning of polyols and sugars in colonies and spores of *Aspergillus ochraceus*. *Mycological Research* 103: 141-147.

Ranasinghe, M. A., and P. A. Gostomski. 2003. A novel reactor for exploring the effect of water content on biofilter degradation rates. *Environmental Progress* 22: 103-109.

Rattray, E. A. S., J. I. Prosser, L. A. Glover, and K. Killham. 1992. Matric potential in relation to survival and activity of a genetically modified microbial inoculum in soil. *Soil Biology & Biochemistry* 24: 421-425.

Richards, L. A. 1960. Advances in soil physics. *7th Internal congress of soil science* Madison, Wisc.

Roberson, E. B., and M. K. Firestone. 1992. Relationship between desiccation and exopolysaccharide production in a soil *Pseudomonas* Sp. *Applied and Environmental Microbiology* 58: 1284-1291.

Rodrigo, A., S. Recous, C. Neel, and B. Mary. 1997. Modelling temperature and moisture effects on C-N transformations in soils: comparison of nine models. *Ecological Modelling* 102: 325-339.

Rynk, R. 1992. *On-farm composting handbook*. NRAES, Ithaca, NY, USA.

Scott, W. J. 1957. Water relations of food-spoilage microorganisms. *Advances in Food Research* 7: 83-127.

Sercu, B., K. Demeestere, H. Baillieul, H. Van Langenhove, and W. Verstraete. 2005. Degradation of isobutanal at high loading rates in a compost biofilter. *Journal of the Air & Waste Management Association* 55: 1217-1227.

Skopp, J., M. D. Jawson, and J. W. Doran. 1990. Steady-state aerobic microbial activity as a function of soil-water content. *Soil Science Society of America Journal* 54: 1619-1625.

Sorensen, L. H. 1974. Rate of decomposition of organic-matter in soil as influenced by repeated air drying-rewetting and repeated additions of organic material. *Soil Biology & Biochemistry* 6: 287-292.

Sparling, G. P., A. W. West, and J. Reynolds. 1989. Influence of soil-moisture regime on the respiration response of soils subjected to osmotic-stress. *Australian Journal of Soil Research* 27: 161-168.

Stark, J. M., and M. K. Firestone. 1995. Mechanisms for soil-moisture effects on activity of nitrifying bacteria. *Applied and Environmental Microbiology* 61: 218-221.

Sun, Y. M., X. Quan, J. W. Chen, F. L. Yang, D. M. Xue, Y. H. Liu, and Z. H. Yang. 2002. Toluene vapour degradation and microbial community in biofilter at various moisture content. *Process Biochemistry* 38: 109-113.

Tate, R. L. 1994. *Soil microbiology*. Wiley, New York.

Tresse, O., S. Lescob, and D. Rho. 2003. Dynamics of living and dead bacterial cells within a mixed-species biofilm during toluene degradation in a biotrickling filter. *Journal of Applied Microbiology* 94: 849-855.

Tuller, M., and D. Or. 2005a. Water films and scaling of soil characteristic curves at low water contents. *Water Resources Research* 41: -.

Tuller, M., and D. Or. 2005b. Water retention and characteristic curve in D. Hillel, ed. *Encyclopedia of soils in the environment*. Elsevier/Academic Press, Oxford, UK ; Boston.

Vaiskunaite, R., P. Baltrenas, and V. Spakauskas. 2005. Mathematical modeling of biofiltration in activated pine-bark charge of a biofilter. *Environmental Science and Pollution Research* 12: 297-301.

van de Mortel, M., and L. J. Halverson. 2004. Cell envelope components contributing to biofilm growth and survival of *Pseudomonas putida* in low-water-content habitats. *Molecular Microbiology* 52: 735-750.

Vanlangenhove, H., E. Wuyts, and N. Schamp. 1986. Elimination of hydrogen-sulfide from odorous air by a wood bark biofilter. *Water Research* 20: 1471-1476.

Veiga, M. C., and C. Kennes. 2001. Parameters affecting performance and modeling of biofilters treating alkylbenzene-polluted air. *Applied Microbiology and Biotechnology* 55: 254-258.

Wang, Z., and R. Govind. 1997. Biofiltration of isopentane in peat and compost packed beds. *Aiche Journal* 43: 1348-1356.

Wardle, D. A. 1992. A comparative-assessment of factors which influence microbial biomass carbon and nitrogen levels in soil. *Biological Reviews of the Cambridge Philosophical Society* 67: 321-358.

Wardle, D. A., and D. Parkinson. 1990a. Comparison of physiological techniques for estimating the response of the soil microbial biomass to soil-moisture. *Soil Biology & Biochemistry* 22: 817-823.

Wardle, D. A., and D. Parkinson. 1990b. Determination of bacterial and fungal fumigation Kc factors across a soil-moisture gradient. *Soil Biology & Biochemistry* 22: 811-816.

Yoon, I. K., and C. H. Park. 2002. Effects of gas flow rate, inlet concentration and temperature on biofiltration of volatile organic compounds in a peat-packed biofilter. *Journal of Bioscience and Bioengineering* 93: 165-169.

Zhu, X. Q., M. T. Suidan, A. Pruden, C. P. Yang, C. Alonso, B. J. Kim, and B. R. Kim. 2004. Effect of substrate Henry's constant on biofilter performance. *Journal of the Air & Waste Management Association* 54: 409-418.

Chapter 4: Toluene degrader isolation and biofilm reactor

4.1 Introduction

The reactors are developed to investigate the performance of porous biofilter media. These media act as a carrier and nutrient supply for a microbial population. This medium can be eliminated and the microbial cells can be placed directly onto the membrane. Unlike most biofilm reactors, which operate with saturated biofilms (England *et al.*, 2005; Kim and Kim, 2005; Parvatiyar *et al.*, 1996), this reactor system is suitable to investigate unsaturated biofilms. Unsaturated biofilms could have an increased removal rate as the mass transfer resistance to the biofilm surface is lower. The results from the experiments will give insight in this hypothesis as well as give specific degradation rates that can be used in biofilm modelling.

In this section, the following experiments are discussed. Toluene degraders are isolated from compost and cultivated to a high cell concentration to inoculate the reactors. The cells are placed on the membrane in the reactor to establish a biofilm. The reactors are operated in the same way as before, measuring gas flow, inlet and outlet concentrations. From the results, a surface elimination capacity is calculated and compared to values in the literature. Measuring the thickness by scanning electron microscopy gives a specific degradation rate that is used in the models in Chapter 5.

4.2 Microbiology in biofilters

4.2.1 Microbial community

Most biofiltration media are natural products with an extensive microbial community. Compost has not only bacteria present, but also a multitude of yeast, moulds, protozoa, and even algae and microscopic worms. These other organisms can play a role in the effectiveness of the biofilter. Natural selection plays an important role in the effectiveness of a biofilter. If the pollutant is a major source of energy, like toluene, strains that can use this source will be favoured and will usually dominate. As well as the pollutant, environmental parameters like water content, temperature and pH are important selectors.

Biofilter acclimation times to reach a steady state removal rate vary from several days (Torkian *et al.*, 2003) to several months (Li and Liu, 2006; Torkian *et al.*, 2003). Many research groups try to reduce acclimation time by creating an inoculum for the biofilter. The inoculums types include the direct use of activated sludge (Corsi and Seed, 1995; Hartikainen *et al.*, 1996; Krishnakumar *et al.*, 2007; Lin *et al.*, 2007; Singh *et al.*, 2006), acclimatized activated sludge (Govind *et al.*, 1993; Singh *et al.*, 2006; Yoon and Park, 2002), cultures isolated from activated sludge (Jeong *et al.*, 2006; Lin *et al.*, 2007), from other biofilters (Garcia-Pena *et al.*, 2005; Song and Kinney, 2005), from soil (Park *et al.*, 2002; Smet *et al.*, 1996), from industrial sites (Morgado *et al.*, 2004) and pure and mixed cultures from databanks (Jorio *et al.*, 2000b; Zilli *et al.*, 2000). Inoculums are always used when the bed materials have limited amounts of natural microbial activity, but have good properties like affordability, low pressure drops, biofilm adherence and large surface areas. Like polyurethane foam (Moe and Irvine, 2001b), ceramics (Sakuma *et al.*, 2006) and perlite (Prado *et al.*, 2002).

The longest start-up time reported in any of the inoculated biofilters is 9 days (Garcia-Pena *et al.*, 2001), which was attributed to the use of a fungus. Other reports vary between 2 and 7 days. Inoculation reduces in most cases the start-up times (Acuna *et al.*, 1999; Smet *et al.*, 1996). Acclimatised cultures can also increase the maximal removal rates. Zilli *et al.* (2000) did see 10-21% higher toluene removal rates then elsewhere, using a bed inoculated with a toluene degrader. Similar results were obtained by Jeong *et al.* (2006) removing p-xylene.

4.2.2 Microbial degradation: aerobic

Organic carbon sources can be oxidised to generate energy. The oxidation mechanism or metabolism is distinguished by which electron acceptor the organisms use. The mechanisms are aerobic, anaerobic and anoxic. In the case of aerobic degradation, oxygen is used as the electron acceptor.

Many organisms are obligate aerobes; only oxygen can serve as the electron acceptor. Oxidation using oxygen is most commonly seen in biofiltration. Most biofilters operate at high air flows (1,000- 150,000 m^3 hr^{-1}) with low pollutant concentrations (<

1000 ppm) (Leson and Winer, 1991). This makes the lack of oxygen in the biofilter bed not likely. Anaerobic zones can be present. This can happen when biofilters are partially clogged with excess biomass or when the solubility is reduced due to a temperature increase or when the air stream bypass parts of the bed.

Oxygen is present in the air at around 210,000 ppm (21%), while contaminants are typically present up to 1000 ppm. As shown in Eq. 4.1, the removal of a mole of toluene requires nine moles of oxygen. At a toluene concentration of 1000 ppm, 9000 ppm of molecular oxygen is stoichiometrically required to fully oxidize the toluene. Reactions using other electron acceptors have been observed in the literature and are discussed in the following paragraph.

$$C_7H_8 + 9O_2 + 3H_2O \rightarrow 7HCO_3^- + 7H^+ \qquad [4.1]$$

4.2.3 Microbial degradation: anaerobic

Anoxic metabolism use oxidized inorganic compounds like nitrate (NO_3^-), nitrite (NO_2^-), sulphate (SO_4^{2-}) (Cattony *et al.*, 2005; Rabus *et al.*, 1993) and iron (Fe(III)) (Chakraborty *et al.*, 2005; Lovley and Lonergan, 1990) as the electron acceptor. Generally the energy production of the anoxic metabolism per mole of oxidised compound is lower compared to aerobic metabolism. Chackraborty *et al.* (2005) showed toluene oxidation in the presence of nitrate and chlorate by *Dechloromonas* strain RCB (Eq. 4.2). .

$$C_7H_8 + 4.5SO_4^{2-} + 2H^+ + 3H_2O \rightarrow 7HCO_3^- + 4.5H_2S \qquad [4.2]$$

Toluene can be degraded under different terminal electron accepting conditions (adapted to toluene from Tan *et al.* (2003)) as demonstrated in the following reaction equations. The energy generated is lowest for Eq. 4.3 and highest for Eq. 4.7.

$$5C_7H_8 + 18SO_4^{2-} + 33H_2O \rightarrow 35HCO_3^- + 18HS^- + 53H^+ \qquad [4.3]$$

$$C_7H_8 + 18NO_3^- + 3H_2O \rightarrow 7HCO_3^- + 18NO_2^- + 7H^+ \qquad [4.4]$$

$$C_7H_8 + 6NO_3^- + 3H_2O \rightarrow 7HCO_3^- + 3N_2 + 7H^+ \quad [4.5]$$

$$C_7H_8 + 36Fe^{3+} + 21H_2O \rightarrow 7HCO_3^- + 36Fe^{2+} + 43H^+ \quad [4.6]$$

$$C_7H_8 + 6ClO_3^- + 3H_2O \rightarrow 7HCO_3^- + 6Cl^- + 7H^+ \quad [4.7]$$

Energetically the aerobic degradation (Eq. 4.1) is favourable. In the presence of oxygen, aerobic degradation will be the dominant mechanism. No examples of anaerobic biofiltration treating a gas stream are reported. Most applications for anaerobic removal of toluene are in waste water treatment. Cattony *et al.* (2005) used a horizontal-flow anaerobic immobilised biomass reactor to remove ethanol and toluene under sulphate-reducing conditions. Other electron acceptors used in the literature are summarised in Table 4.1.

Table 4.1*: Different terminal electron acceptors investigated in the literature.*

Terminal electron acceptor	**Reference**
CO_2/CH_4	Edwards and Grbicgalic, 1994
SO_4^{2-}/H_2S	Rabus *et al.*, 1993
NO_3^-/NO_2^-	Evans *et al.*, 1991; Fries *et al., 1994* ;
NO_3^-/N_2	Martinez *et al.*, 2007
Fe^{3+}/ Fe^{2+}	Lovley and Lonergan, 1990; Lovley *et al.*, 1994
O_2/H_2O	Tsao *et al.*, 1998
Mn	Langenhoff *et al.*, 1997
ClO_3^-/Cl^-	Chakraborty *et al.*, 2005

4.3 Biofilms in unsaturated media

Micro-organisms and particular bacteria prefer a community structure over individual living cells. These communities form what is generally known as a biofilm. Observations of biofilms generally show micro-organisms embedded in an extracellular polysaccharide (EPS) matrix. This matrix can be attached to almost any surface in an aqueous environment, varying from rock, soil, plants, or any surface that is wetted periodically. A submerged or saturated biofilm is in an environment that has two phases: water and solid. The unsaturated biofilm has an extra phase in the form of a gas or air phase, which is usually the main phase (Holden, 2001).

4.3.1 Biofilms

Biofilm and multicellular aggregates are common in nature. The main reason for forming aggregates is survival. Forming a colonies helps in survival in unfavourable environmental conditions and to protect against protozoan grazing and antibiotics (Webb *et al.*, 2003).

The EPS matrix comprises mainly of carbohydrates or proteins, but also lipids, DNA and humic substances. The matrix plays different roles; it can absorb organic molecules, ions, water and offer a mass transfer resistance. The EPS matrix controls the environment in which the micro-organisms live. It can affect cell-physiology, cell quorum-sensing and protein expression. Oxygen limitation (Steinberger and Holden, 2004) and low matric potential (Chang and Halverson, 2003; Roberson and Firestone, 1992) increases the production of EPS.

4.3.2 Biofilms and biofiltration

Biofilters are beds packed with a porous material which supports microbial cultures. These cultures will develop into a heterogeneous biofilm on the bed material. During the operation of the biofilter, a pollutant in the gas phase flows through the bed, where the pollutant is transferred into the biofilm and degraded by the micro-organisms present (Acuna *et al.*, 2002).

The bed material is often a natural material that has sufficient nutrients present to maintain the biofilm. But the use of non-natural materials is not uncommon either.

Activated carbon (Lim *et al.*, 2005), Biosol (Jeong *et al.*, 2006), vermiculite (Garcia-Pena *et al.*, 2001) and ceramic pellets are some examples. These materials do not contain any nutrients, so in order to maintain an active biofilm, regular nutrient addition is required.

The biofilm grows in the voids and pores of the bed material. If sufficient nutrients and a high pollutant concentration are available, the pores and voids will slowly fill up with a thicker layer of biomass. This increase in thickness can lead to a reduction in the area of the biofilm exposed to the pollutant. The mass transfer into the biofilm is dependent on the area, so a smaller area will decrease the mass transfer into the biofilm and thus in a reduction in removal (Alonso *et al.*, 2001). Mature biofilms can increase in thickness without increasing cell numbers. This increase in thickness is a result of accumulation of EPS, leakage and cell lysis products (Tresse *et al.*, 2003). A biomass increase can lead to blockage of more the pores and voids. This leads to increased pressure drops and a loss in removal rates of the pollutant (Okkerse *et al.*, 1999). It is difficult to remove the excess biomass and often the bed material in the biofilter has to be replaced.

A different approach for removing air pollutants is the use of a biotrickling filter. The main difference from a biofilter is the continuous recirculation of a liquid medium (Tresse *et al.*, 2003). The packing material is usually a synthetic or inert material, like plastic rings, foam cubes, lava rocks, etc. (Kennes and Veiga, 2001). A build-up of excess biomass does not immediately result in the replacement of the bed. A biotrickling filter has the ability to remove excess biomass with backwashing (Okkerse *et al.*, 1999; Smith *et al.*, 1996). Backwashing uses a high circulation rate of the medium in order to achieve high shear forces to remove the biofilm from the packing material. The bed can be enlarged by 40% during the fluidisation, which can cause a problem. Another problem is that backwashing generates a large quantity of high BOD wastewater (Cox and Deshusses, 1999). Other options for excess biomass removal include protozoan predation and chemical washing. Both options can lead to a reduction in microbial activity and hence a reduction in removal rates (Vinage and von Rohr, 2003a).

4.3.3 Other biofilms reactors

Biofilms can be grown directly on membranes (Fig. 4.1) and other surfaces. The main interest for membrane bioreactors (MBR) is the high VOC removal rates with relatively small volumes. The presence of a water phase directly in contact with the biofilm allows for optimal moisture in the biomass layer and removal of degradation products (Kumar *et al.*, 2008a). Other advantages of MBRs are (Kennes and Veiga, 2001):

- Easy to prevent clogging
- Control of liquid phase, pH, and nutrients to support the biofilm
- Separation of the biomass from the air stream to prevent carry-over
- Sensitive or special microbial strains can be used
- Low pressure drop
- Compact modular design

Disadvantages include:

- Only small scale experience
- High capital as well as operating costs

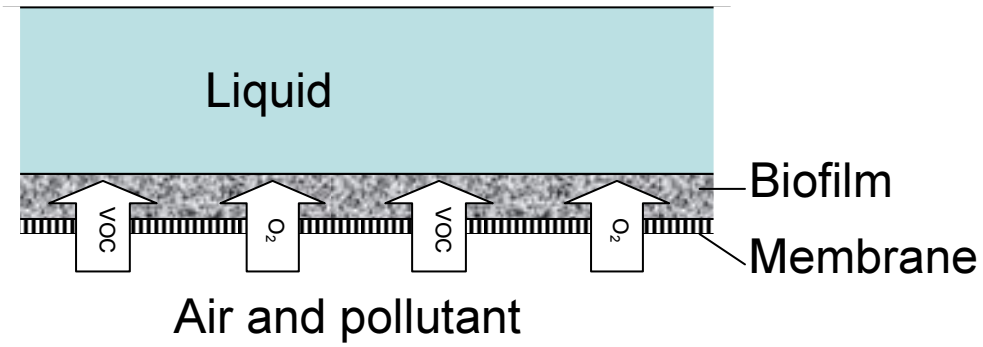

***Figure 4.1**: Principle of the membrane bioreactor.*

Villaverde *et al.* (1997) used a Flat Plate Vapour Phase Biological Reactor (VPBR) for their experiments. The gas phase over the biofilm is considered plug flow. The saturated biofilm was covered by 4 mm of medium, through which the toluene had to diffuse.

Holden *et al.* (1997b) developed a batch reactor with a biofilm growing on a membrane. Similar to the setup in this research, the biofilm was unsaturated. They placed their biofilm on one side of a membrane and placed medium amended with poly-ethylene glycol (PEG) on the back side to control the water potential. They also measured the diffusion rates and toluene depletion at different water potentials.

Hollow fibre membrane bioreactors offer a large surface area for mass transfer. Ergas *et al.* (1999) used a bundle of 2400 hollow fibres for their reactor. A nutrient solution with microbial cells was circulated on the outside of the fibres, with VOC-laden gas passing on the tube side. The toluene removal reached a maximum of 42 g m^{-3}_{r} hr^{-1}. Another reactor system that utilises biofilms is the rotating biological contactor or RBC. The RBC was used by Vinage and Von Rohr (2003a) to remove toluene from an air stream. They observed a stable removal of 30 g m^{-3}_{r} hr^{-1} for more then 200 days.

4.5 Experimental methods

4.5.1 Microbial isolation

The toluene degraders were isolated from commercially available composts. No attempt was made to identify the cultures or determine the purity of the cultures. Agar plates (App. B.3) were inoculated from compost samples and placed in a desiccator. The desiccator ensured an enclosed environment, so toluene vapor could be provided as the sole carbon source. The whole desiccator was incubated at 30 °C. Liquid toluene (100 µl) was added daily or when opening the desiccator to inspect the plates.

Colonies from the plates were used to inoculate serum bottles (App. B.4) with liquid medium (App B.1). Serum bottles (160 ml) were chosen because a toluene-rich environment could easily be maintained and monitored. A volume of 25 ml liquid medium was transferred into 160 ml serum bottles and closed with a butyl stopper and an aluminium cap. Further details of used methods and materials can be found in Appendix B.

4.5.2 Reactor loading

Neither the cell concentration nor the relative numbers of viable to non-viable cells in each of the serum bottles were determined. Visual inspection of the cloudiness and toluene depletion rates (App. B.4) indicated the most active serum bottles.

The setup of Reactor 1 (Sec. 2.6.1) was used for the biofilm experiments. The procedure for loading the reactor was similar to the method described in Sec 2.8. Without compost present additional nutrients had to be provided. The water in the reservoir was replaced with a compost extract, to provide a similar nutrient composition. Equal parts of compost and water were thoroughly mixed and filtered through a Whatman no. 1 filter to remove any solids. The compost extract was autoclaved at 121 °C for 20 minutes.

For the first run, 10 ml of each cell suspension from bottles A, 1A and 1E were transferred from the serum bottles into a 20 ml disposable syringe and sprayed slowly onto the membrane. The second run had a loading of 15 ml of cell suspension from bottle 1E. Normal biofilm development has three distinct phases: a lag phase for biofilm attachment, biofilm establishment and a maturation phase where the cell number remains constant (Tresse et al., 2003). By placing the cells directly on the membrane, the first two phases were shortened if not eliminated.

The excess medium was drained away as the membrane was under a negative matric potential. After applying the biomass, the reactor was reassembled and installed into the temperature controlled box. The toluene concentration fed to the reactor was constant due to the use of a toluene in air bottle (BOC Ltd, NZ). Variation between different gas bottles did exist, see App. A.6. Control of the residual toluene concentration was achieved by adjusting the flow rate and thus the load.

4.5.3 Biomass dry weight determination

A tension apparatus (Sec. 3.5.1) was used to determine the dry weight of cells loaded on the membrane. A 12 ml sample from each bottle (A, 1E and 1F) was loaded in the same way as before. The membrane was weighed before and after oven drying at 102 °C for 24 hours. The dry biomass was 14 ± 1 mg dry weight spread over 38.5 cm^2. As

a smaller sample of cells was loaded, the dry biomass in the first run of the reactor was an estimated 11 ± 1 mg.

4.5.4 SEM of the biofilm

After the first run ended, the membrane with the biofilm was removed from the reactor. A small piece of the membrane and biofilm was mounted using a carbon tab to allow observation of the fractured surface and covered with conducting carbon paint using a Polaron 5000 sputter coater. An SEM microscope (Leica S440) was used to observe the samples at standard magnifications in all cases. All micrographs have a micron scale to indicate the actual magnification.

4.6 Results and discussion

4.6.1 Removal of toluene in serum bottles

After the bottles were incubated at 30 °C for 11 days, the toluene concentration was measured per method in App. A.3. All bottles except for bottle F had approximately 0.02 % of the initial toluene present. No measurements were taken until day 38 (Fig. B.2) when 5 µl of liquid toluene was added with fresh air. Toluene (10 µl) was added (day 49) to achieve a gas phase concentration of 14,000 ppm. After three days the concentration in the bottles was halved. Hardly any toluene was removed in the four days thereafter. The suspected reason for the low removal rate was oxygen limitation. In total 22,000 ppm or 0.14 mmol toluene was removed, this means that stoichiometrically, nine times that amount of oxygen (1.27 mmol) was consumed (Sec. 4.2.2). In the serum bottle with a headspace of 130 ml, only 1.14 mmol of oxygen is present. This means that the removal was limited by oxygen depletion.

After 57 days, the toluene concentration did not significantly change. The overpressure was relieved and the bottles were flushed three times with fresh sterile air. The bottles were pressurised to approximately 1.5 atm. The freshly added toluene was depleted in bottles B and R within 2 days. No significant removal was seen in bottles A and F. The first 2 days after the adding the air, bottle E did not remove any toluene. But a day later 93% was removed.

The microbial suspensions in the serum bottles were kept alive for more than a year. Even by neglecting them for 8 months, toluene removal activity was still observed. Fresh air and toluene were added on day 287, which was removed by bottles A and B within 48 hours (Fig B.3). Two days later bottle E did see an increase in removal, but F and R showed little activity.

The bottles were kept into the incubator for another two weeks. Fresh air and toluene were added after 305 days and thereafter the bottles were sampled regularly (Fig. B.4). The suspensions chosen for inoculation were bottles A, 1A and 1E, as they demonstrated the highest removal rates.

4.6.2 Removal of toluene by the biofilm

Within 24 hours after reactor start-up, the toluene removal was 95% at a flow rate of 18 ml min^{-1} and an inlet concentration of 40 ppm. The rapid acclimatization was attributed to the cultivation of the cell on toluene as the sole carbon source.

To explore the maximal EC, the load was increased by increasing the gas flow rate. The highest EC during the first run was reached after 500 hours, at a residual concentration of 9 ppm. As will be discussed in Chapter 5, the EC at this concentration was probably not the maximal EC possible. Before the load could be increased further, the temperature controller in the box failed at hr 546 and the reactor was exposed to temperatures in excess of 60 °C and the EC dropped significantly. The reactor was disassembled and SEM photographs were taken of the membrane and biofilm (Sec. 4.6.3).The reactor was restarted for the second run with a reduced amount of biomass loaded.

Several different types of biofilm reactors have been reported for VOC control. Examples are flat plate reactors (FP) (Jacobs *et al.*, 2004; Studer and von Rohr, 2008), hollow fibre membrane bioreactors (HF) (England *et al.*, 2005; Ergas *et al.*, 1999; Kim and Kim, 2005; Parvatiyar *et al.*, 1996), hollow tube (HT) (England et al., 2005) and rotating biological contactors (RBC) (Vinage and von Rohr, 2003a). All these membrane biofilm reactors (MBR) are integral reactors. As toluene concentrations are not uniform throughout the whole reactor, the specific rates of toluene removal are

averages over the whole reactor. No differential reactor results were found to compare results with directly.

To compare the values of the toluene removal rates in the different systems, the EC based on the biofilm volume would be optimal, but biofilm thickness and area are rarely reported. More common is to base the EC on the total membrane surface area.

The Surface Elimination Capacity is defined as:

$$SEC = \frac{(C_{in} - C_{out})Flow}{A_m} \qquad [4.1]$$

4.6.2.1 Reactor results

The SEC and Surface Loading are plotted in Fig. 4.2 and Fig. 4.3 for the two runs. The removal efficiency is between 80 to 96%. The residual toluene concentration at the highest SEC (second biofilm run) was 20 ppm.

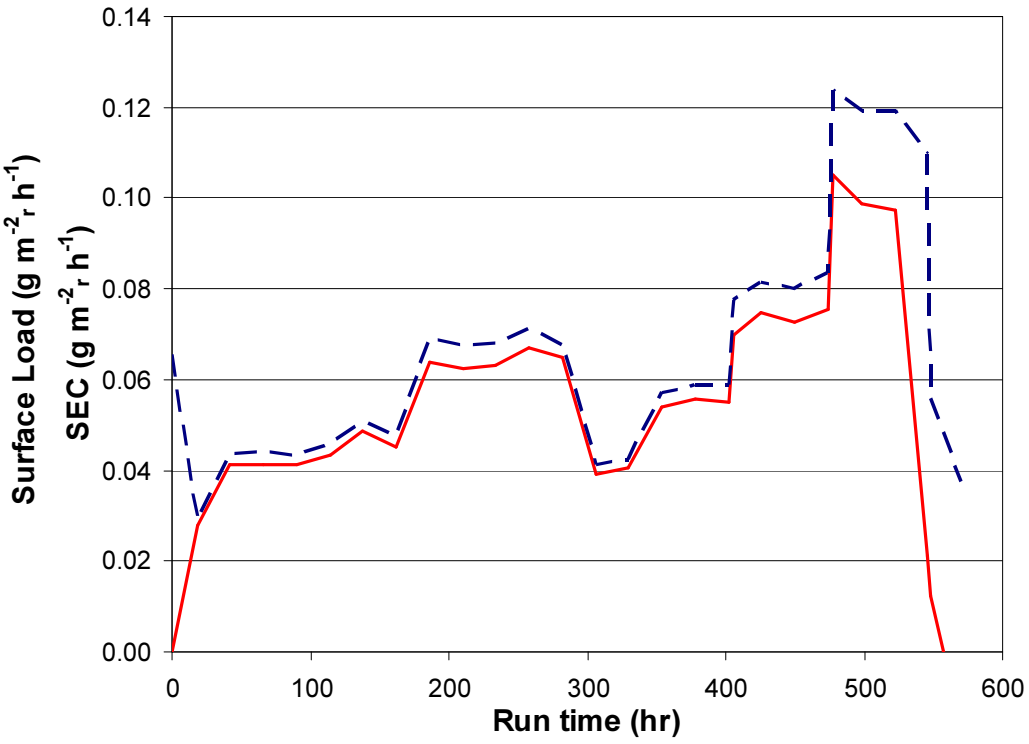

***Figure 4.2**: The Surface Load (blue dotted line) and corresponding SEC (red solid line) of the first biofilm run in Reactor 1.*

Results in Chapter 5 will show that maximal removal rates are observed at residual concentrations above 100 ppm. Both biofilm runs ended before a higher residual concentration and thus maximal EC was achieved.

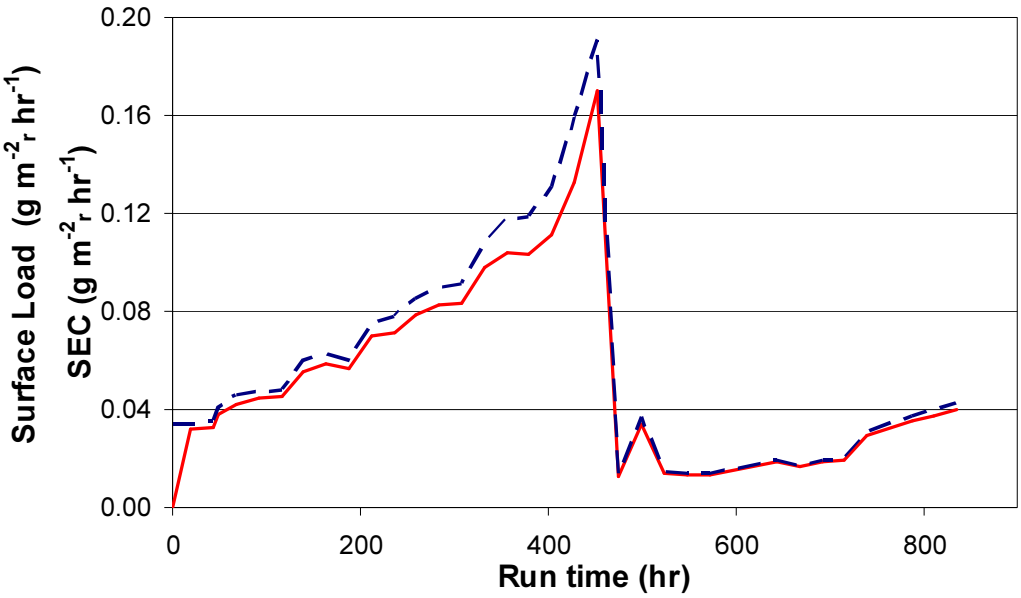

***Figure 4.3**: The Surface Load (blue dotted line) and corresponding SEC (red solid line) of the second biofilm run in Reactor 1.*

The relationship between the outlet concentration (i.e. residual concentration) and the steady state SEC is plotted (Fig. 4.4). Ottengraf and Vandenoever (1983) presented three scenarios to describe the toluene concentration profile in the biofilm. First, at gas concentrations below a critical concentration (C_{crit}), the biofilm is not fully utilized. The component is degraded quicker than it can diffuse through the entire biofilm. Second, at C_{crit} the whole biofilm is utilised, and the concentration in the biofilm reaches zero at the interface between the biofilm and the carrier material. Third, by increasing the gas concentration, no extra removal will be seen as the whole biofilm is already active. From C_{crit} upwards, the degradation is biological limited.

As predicted by theory, the SEC increases with an increasing toluene concentration. The highest concentration measured is expected to be below the C_{crit} and thus both biofilms are only partly utilised. If both biofilms have similar properties like cell concentration, diffusion coefficients and specific degradation rates, the same thickness

of biofilm is used to degrade the toluene. Even if the actual biofilm thicknesses are different, below the lowest C_{crit} the removal rate will be the same.

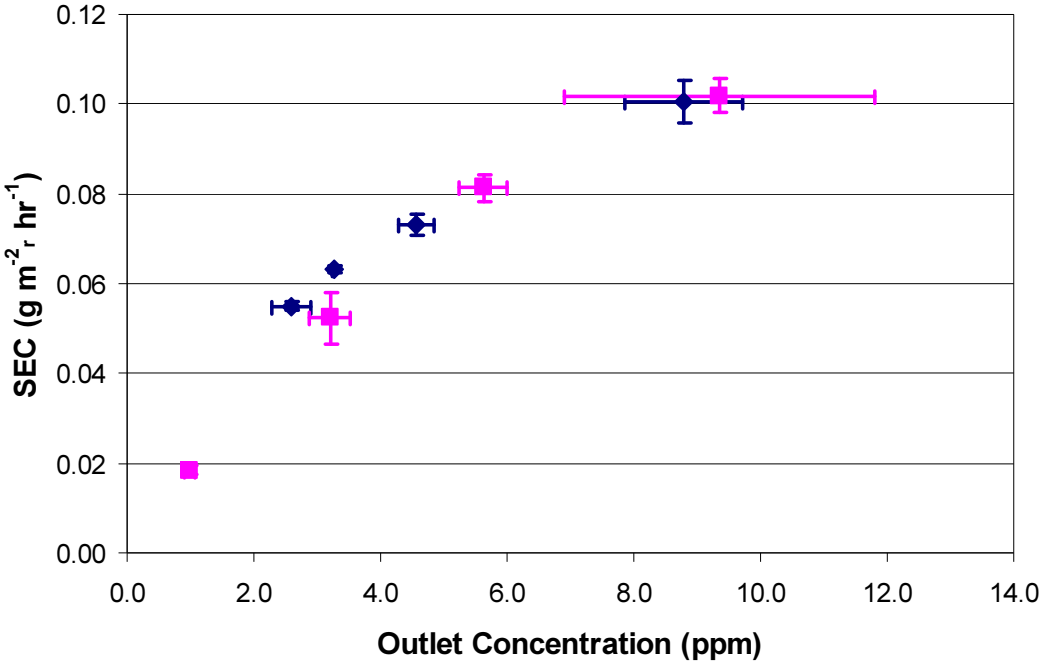

***Figure 4.4**: The dependency of the steady state SECs on the outlet (or residual) concentration. The blue diamonds (♦) is the data for Run 1 and the pink squares (■) for Run 2. The error bars represent 95% confidence interval.*

The maximum SEC measured (not a steady state) was 0.17 g m^{-2}_{r} hr^{-1} (load of 0.19 g m^{-2}_{r} hr^{-1}). This value was in the same range as reported in the literature (Table 4.2). Only England *et al.* (2005) have reported values significantly higher than any other groups. But their toluene loading was almost a factor of 100 higher than any other group.

The highest observed SEC will be used in Chapter 5 for modelling purposes. Together with the biofilm thickness (Sec. 4.6.3) a maximal removal rate per biofilm volume was calculated. This resulted in a specific EC of 1250 g m^{-3}_{b} hr^{-1}.

***Table 4.2**: Literature loading and SEC values.*

Reference	**Reactor type**	**Loading ($g\ m^{-2}_r\ hr^{-1}$)**	**SEC ($g\ m^{-2}_r\ hr^{-1}$)**
Parvatiyar *et al.*, 1996	HF	0.03 to 0.24	0.02 to 0.2
Studer and von Rohr, 2008	FP[1]	3.3	0.6
Ergas *et al.*, 1999	HF	0.07 to 0.35	0.04 to 0.12
Kim and Kim, 2005	HF	0.12 to 0.63	0.12 to 0.54
England *et al.*, 2005	HT	4.7 to 18.3	1.72 to 2.56
Holden *et al.*, 1997	FP	N/A	0.02 to 0.22
Van Langenhove *et al.*, 2004	FP	0.06 to 0.65	0.06 to 0.5
Moller *et al.*, 1996	Biotrickling	0.12	0.06 to 0.11
Vinage and Von Rohr., 2003	RBC	0.74	0.44
Kumar *et al.*, 2008b	FP	1.48	1.2

[1] Use of absorbent between biofilm and waste gas stream

4.6.2.2 Saturated versus unsaturated biofilms

All membrane reactors in the literature, except for Holden *et al.* (1997b) had the biofilm positioned in the liquid phase (Fig. 4.1). Holden *et al.* (1997b) found that between a matric potential of 0 and $-1.0 \cdot 10^4$ cm H_2O the removal rates on a protein basis were constant. But if their removal rates are based on membrane area, the lower matric potentials resulted in lower SECs. As discussed in Chapter 3, lowering the water potential will reduce enzymatic and growth rates and increases EPS production. Any of these could change the degradation and mass transfer characteristics to the cells (Chenu and Roberson, 1996; Holden *et al.*, 1997b).

There is no significant difference in the removal rates (Table 4.2) between reactors using unsaturated or saturated biofilms. The saturated MBR have an extra mass transfer resistance in the form of the membrane between the gas phase and the biofilm. But in general, the overall mass transfer coefficient is considered to be dominated by the resistance in the liquid phase (Ergas and McGrath, 1997). More experiments with unsaturated biofilms have to be done to investigate if it has any mass transfer advantages compared to saturated biofilms.

4.6.2.3 Stability

In order to use a MBR successfully in a commercial application, the long term stability has to be proven (Table 4.3). The longest run time found in the literature was 339 days (Jacobs *et al.*, 2004). After this time, the removal efficiencies were lower than measured in their earlier experiments.

The RBC used by Vinage and Von Rohr (2003a) was operated in excess of a year at stable removal rates. Their inoculum consisted out of *P. putida* and *R. erythropolis*, but after some time the biofilm had evolved into a mixed culture. The mixed culture did not show loss in performance.

***Table 4.3**: Run times of MBRs in the literature.*

Reference	**Total run time**	**Culture**
Parvatiyar *et al.*, 1996	N/A	Mixed
Studer and von Rohr, 2008	162 days	*P. putida* and *R. globerus*
Ergas *et al.*, 1999	N/A	Mixed
Ergas and McGrath, 1997	3 months	*P. putida*
Jacobs *et al.*, 2004	339 days	*P. putida*
Kim and Kim, 2005	150 days	*P. putida*
England *et al.*, 2005	50 days	Mixed
Holden *et al.*, 1997	10 hours	*P. putida*
Van Langenhove *et al.*, 2004	20 days	*P. putida*
Kumar *et al.*, 2008b	144 days	*B. vietnamiensis* G4

Although most of the reactors have been operated in controlled laboratory conditions, only Jacobs *et al.* (2004) reported issues on the reduction of performance from contamination. Nitrifiers were detected and caused a reduction in performance by producing inhibiting levels of nitrite, reducing pH and consuming oxygen in the biofilm. Changing from ammonium to nitrate in the nutrient solution eliminated any nitrification.

4.6.3 SEM photo's and biofilm thickness estimates

When the first biofilm run failed, a SEM of the membrane was performed (Fig. 4.5 and 4.6). The organisms in the biofilm had the expected rod-shape (Fig 4.8) of a *Pseudomonas* strain. The length was between 1.5 and 3 µm and the width between 0.5 to 0.9 µm. The micrographs look similar to results obtained by Shapiro (1985). The thickness of the membrane (Table 4.4) (Mixed Cellulose Ester, A045A090C, Advantec MFS, Inc) is confirmed in Fig 4.6.

Table 4.4*: Properties of the membrane.*

Property	**Value**
Material	cellulose nitrate and cellulose acetate
Diameter (mm)	90
Thickness (µm)	145
Pore diameter (µm)	0.45
Porosity (% open area)	78
Bubble point (Mpa)	≥0.24

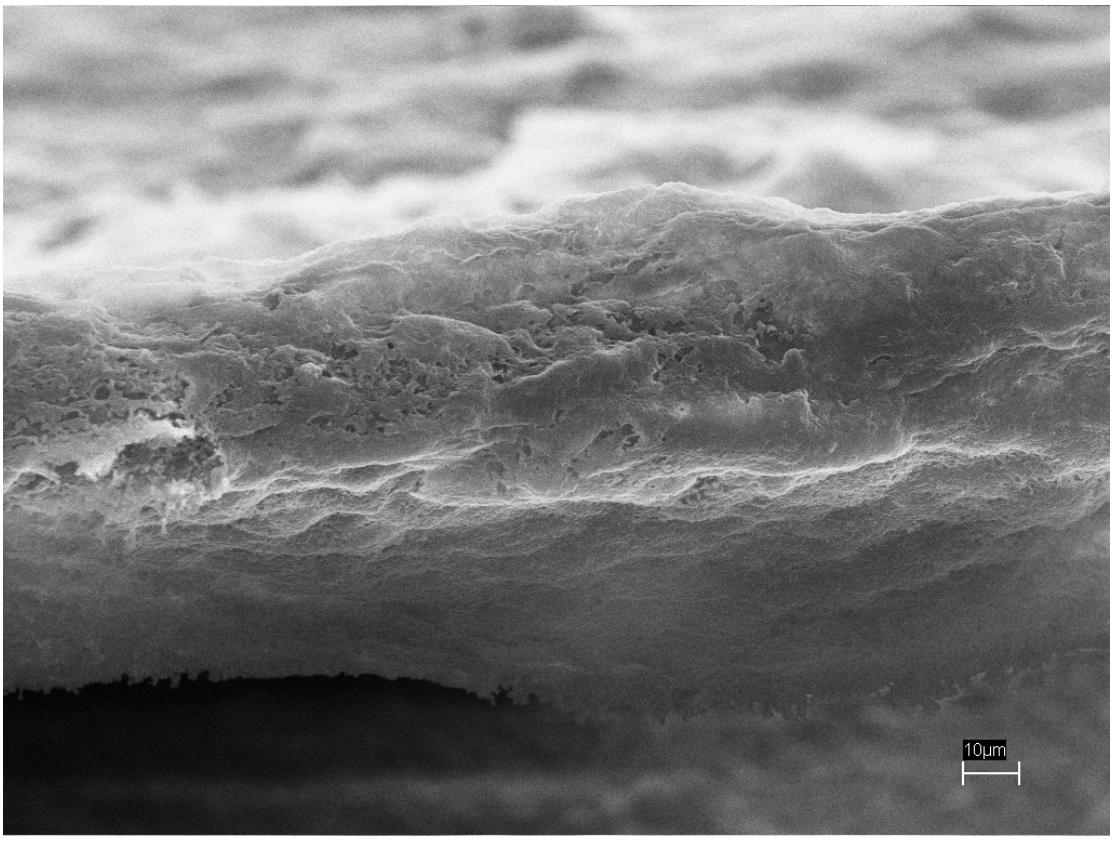

Figure 4.5*. : SEM photo of the side of the biofilm.*

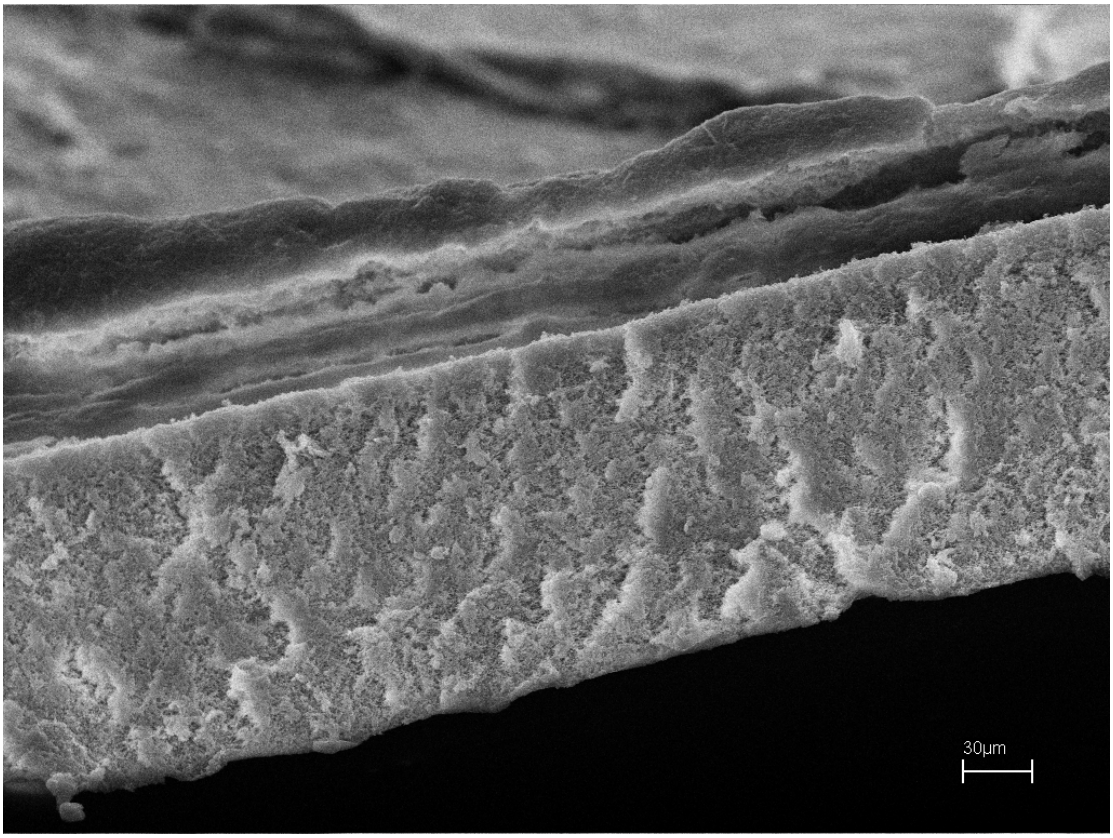

***Figure 4.6**: SEM photo of the biofilm on top of the membrane.*

The biofilm thickness was measured from the micrographs and varied between 75 and 95 µm, with an average of 80 ± 5 µm (Fig 4.5). Biofilm thickness measurements and estimates are numerous, such as an estimate by England *et al.* (2005) of 100 µm and a measured value of 500 µm by Studer and Von Rohr (2008). Vayenas *et al.* (2002) observed biofilm thickness between 71 and 239 µm in their experiments of biofilm thickness in porous media.

A certain percentage of the cells placed on the membrane might not have been active in degrading toluene. According to Tresse *et al.* (2003) in a mature biofilm degrading toluene, only 51% of the cells are actually alive. As no cell viability measurements were performed, the biofilm in this work was assumed to be completely active.

The thickness in the reactor was dependent on the amount of biomass that has been put on the membrane at start-up, the run time and concentration of the carbon and other nutrients. Due to different cell mass loading, the biofilm thickness of the two runs was expected to be different as well. Although the thickness of the biofilm in

Run 2 was not measured, the two runs have identical surface load removal curves (Fig. 4.7). But as discussed in Sec.4.6.2.1, not enough data was collected to comment on the actual biofilm thickness of run 2.

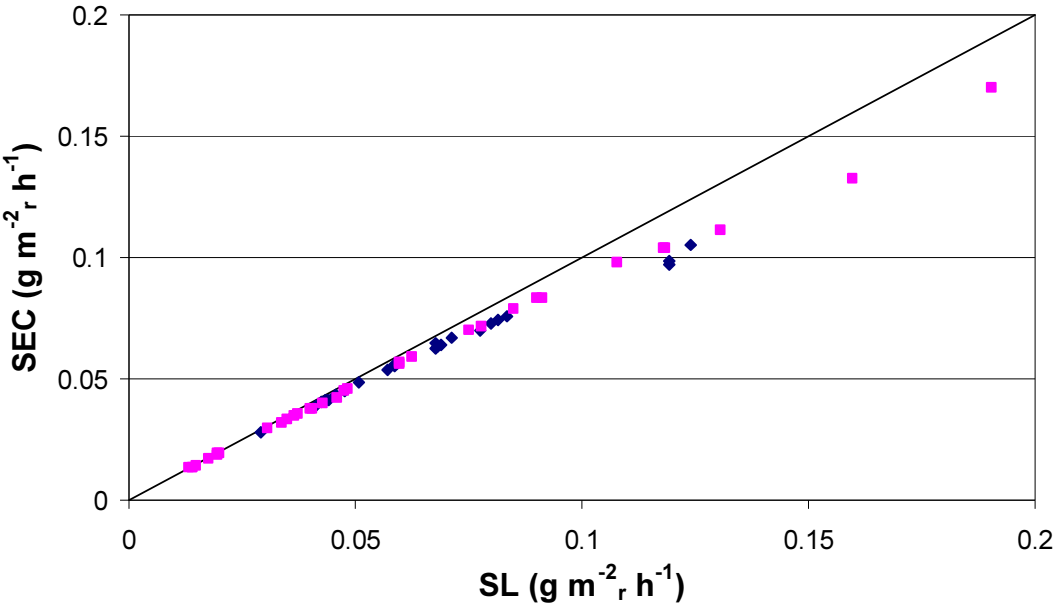

Figure 4.7*: Relationship between the Surface Loading and the Surface Elimination Capacity for Run 1(blue diamonds (♦)) and Run 2 (pink squares (■)). The solid line represents 100% removal rate.*

In most MBR reactors, the biofilm is on the liquid side of the membrane. That means that the superficial velocity of the liquid over the biofilm can be controlled. The velocity will incur shear stress on the biofilm and at higher velocities, the biofilm will detach. (Studer and von Rohr, 2008). This gives a way to control thickness. In the current reactor no shear force can be exerted, so no control of the thickness is possible. A very thick biofilm could lead to mass transfer issues and an underestimate of the degradation rates per biofilm volume.

The shape of the biofilm interface is an important aspect in the mass transfer of nutrients and oxygen. The rougher the interface is, the larger the area exposed to the gas phase. In comparison to Holden *et al.* (1997b) where the interface was very flat, the observed biofilm interface was much rougher and full of cavities (Fig. 4.8). They

also applied a liquid inoculum directly to the membrane, so the surface interface was not an artefact of the experimental technique.

The structure of a biofilm can depend on the substrate concentration. A high concentration leads to fast biofilm growth and a less dense structure (Horn and Hempel, 1998). In biofilters this will lead to rapid clogging of the filter bed. As there is only limited data available on the biofilm structure, no conclusion in relation to structural changes due to substrate concentration can be given. Although this is an interesting point to investigate in the future.

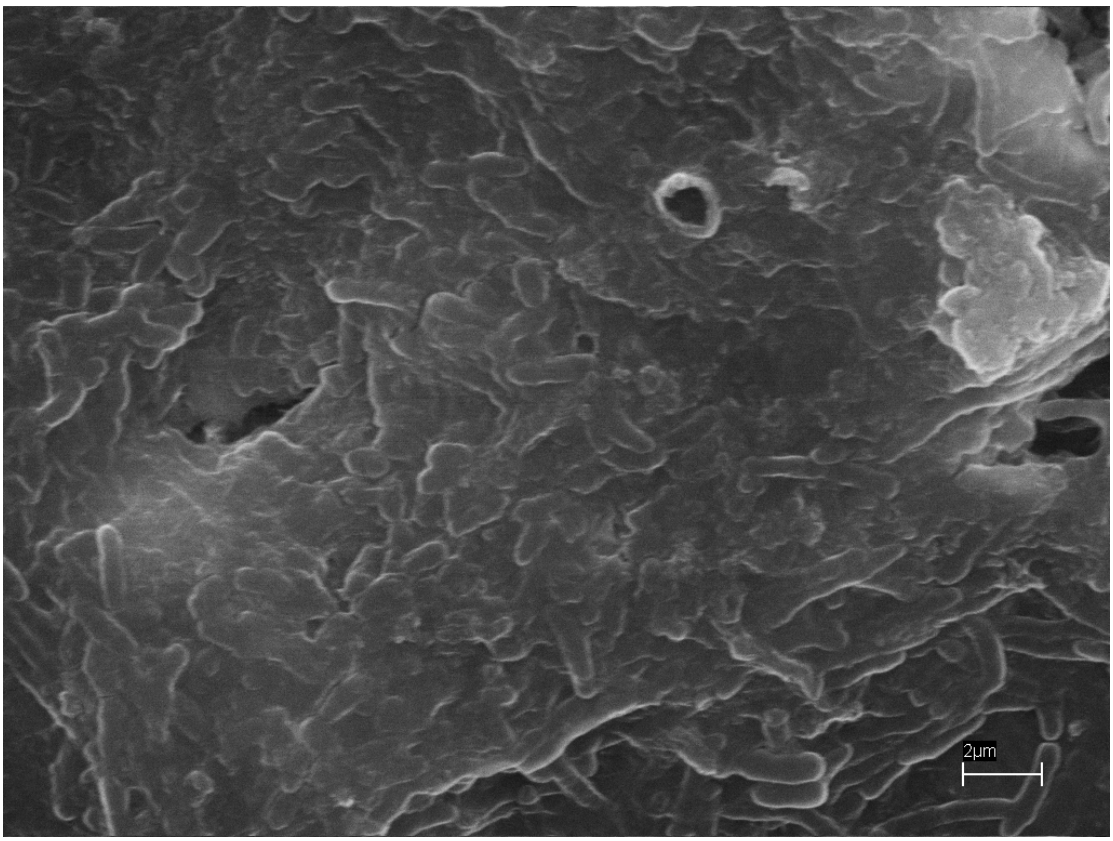

Figure 4.8*: SEM photo of the biofilm- air interface.*

4.7 Conclusions

Toluene degraders were isolated from compost using a basic minimal medium with a toluene atmosphere. Although no attempt to identify the cultures was made, SEM pictures of the biofilm showed the expected rod-shape of a *Pseudomonas* strain. The biofilm thickness varied between 75 and 95 μm and was used to calculate the specific removal rate.

The results from the biofilm runs in the reactor did give similar results in terms of removal of toluene as compared to the literature. These experiment resulted in a maximal observed SEC of is 0.17 g m^{-2}_r hr^{-1} and a specific removal rate of 1250 g m^{-3}_b hr^{-1} and are used in modelling biofilm performance. This was the highest observed rate, but probably not the maximal possible. Both biofilm runs ended before a higher residual concentration (>100 ppm) was achieved. Above this concentration, a maximum in the EC is expected.

4.7 Nomenclature

A_m	Area of the membrane	m^2
C_{in}	Inlet concentration	g m^{-3}_g
C_{out}	Outlet concentration	g m^{-3}_g
Flow	Gas flow rate	m^3_g hr^{-1}
SEC	Surface elimination capacity	g m^{-2}_r hr^{-1}

Subscripts

b	of biomass
g	of gas
r	of reactor

4.8 References

Acuna, M. E., F. Perez, R. Auria, and S. Revah. 1999. Microbiological and kinetic aspects of a biofilter for the removal of toluene from waste gases. *Biotechnology and Bioengineering* 63: 175-184.

Acuna, M. E., C. Villanueva, B. Cardenas, P. Christen, and S. Revah. 2002. The effect of nutrient concentration on biofilm formation on peat and gas phase toluene biodegradation under biofiltration conditions. *Process Biochemistry* 38: 7-13.

Alonso, C., X. Q. Zhu, M. T. Suidan, B. R. Kim, and B. J. Kim. 2001. Mathematical model of biofiltration of VOCs: Effect of nitrate concentration and backwashing. *Journal of Environmental Engineering-Asce* 127: 655-664.

Cattony, E. B. M., F. A. Chinalia, R. Ribeiro, M. Zaiat, E. Foresti, and M. B. A. Varesche. 2005. Ethanol and toluene removal in a horizontal-flow anaerobic immobilized biomass reactor in the presence of sulfate. *Biotechnology and Bioengineering* 91: 244-253.

Chakraborty, R., S. M. O'Connor, E. Chan, and J. D. Coates. 2005. Anaerobic degradation of benzene, toluene, ethylbenzene, and xylene compounds by *Dechloromonas* strain RCB. *Applied and Environmental Microbiology* 71: 8649-8655.

Chang, W. S., and L. J. Halverson. 2003. Reduced water availability influences the dynamics, development, and ultrastructural properties of *Pseudomonas putida* biofilms. *Journal of Bacteriology* 185: 6199-6204.

Chenu, C., and E. B. Roberson. 1996. Diffusion of glucose in microbial extracellular polysaccharide as affected by water potential. *Soil Biology & Biochemistry* 28: 877-884.

Corsi, R. L., and L. Seed. 1995. Biofiltration of BTEX: Media, substrate, and loadings effects. *Environmental Progress* 14: 151-158.

Cox, H. H. J., and M. A. Deshusses. 1999. Biomass control in waste air biotrickling filters by protozoan predation. *Biotechnology and Bioengineering* 62: 216-224.

Edwards, E. A., and D. Grbicgalic. 1994. Anaerobic degradation of toluene and o-xylene by a methanogenic consortium. *Applied and Environmental Microbiology* 60: 313-322.

England, E., M. Fitch, M. Mormille, and M. Roberts. 2005. Toluene romoval in membrane bioreactors under recirculating and non-recirculating liquid conditions. *Clean Technology and Environmental Policy* 7: 259-269.

Ergas, S. J., and M. S. McGrath. 1997. Membrane bioreactor for control of volatile organic compound emissions. *Journal of Environmental Engineering-Asce* 123: 593-598.

Ergas, S. J., L. Shumway, M. W. Fitch, and J. J. Neemann. 1999. Membrane process for biological treatment of contaminated gas streams. *Biotechnology and Bioengineering* 63: 431-441.

Evans, P. J., D. T. Mang, K. S. Kim, and L. Y. Young. 1991. Anaerobic degradation of toluene by a denitrifying bacterium. *Applied and Environmental Microbiology* 57: 1139-1145.

Fries, M. R., J. H. Zhou, J. Cheesanford, and J. M. Tiedje. 1994. Isolation, Characterization, and Distribution of Denitrifying Toluene Degraders from a Variety of Habitats. *Applied and Environmental Microbiology* 60: 2802-2810.

Garcia-Pena, E. I., S. Hernandez, E. Favela-Torres, R. Auria, and S. Revah. 2001. Toluene biofiltration by the fungus *Scedosporium apiospermum TB1*. *Biotechnology and Bioengineering* 76: 61-69.

Garcia-Pena, I., S. Hernandez, R. Auria, and S. Revah. 2005. Correlation of biological activity and reactor performance in biofiltration of toluene with the fungus *Paecilomyces variotii CBS115145*. *Applied and Environmental Microbiology* 71: 4280-4285.

Govind, R., V. Utgikar, W. Zhao, Y. Shan, M. G. Parvatiyar, and D. F. Bishop. 1993. Development of novel biofilters for treatment of volatile organic compounds (VOCs). *IGT Symposium on Gas, Oil and Environmental Biotechnology*, Colorado Springs, CO.

Hartikainen, T., J. Ruuskanen, M. Vanhatalo, and P. J. Martikainen. 1996. Removal of ammonia from air by a peat biofilter. *Environmental Technology* 17: 45-53.

Holden, P. A. 2001. Biofilms in unsaturated environments. *Microbial Growth in Biofilms, Pt B* 337: 125-143.

Holden, P. A., J. R. Hunt, and M. K. Firestone. 1997. Toluene diffusion and reaction in unsaturated *Pseudomonas putida* biofilms. *Biotechnology and Bioengineering* 56: 656-670.

Horn, H., and D. C. Hempel. 1998. Modeling mass transfer and substrate utilization in the boundary layer of biofilm systems. *Water Science and Technology* 37: 139-147.

Jacobs, P., I. De Bo, K. Demeestere, W. Verstraete, and H. Van Langenhove. 2004. Toluene removal from waste air using a flat composite membrane bioreactor. *Biotechnology and Bioengineering* 85: 68-77.

Jeong, E., M. Hirai, and M. Shoda. 2006. Removal of p-xylene with *Pseudomonas* sp NBM21 in biofilter. *Journal of Bioscience and Bioengineering* 102: 281-287.

Jorio, H., L. Bibeau, G. Viel, and M. Heitz. 2000. Effects of gas flow rate and inlet concentration on xylene vapors biofiltration performance. *Chemical Engineering Journal* 76: 209-221.

Kennes, C., and M. C. Veiga. 2001. *Bioreactors for waste gas treatment*. Kluwer Academic, Dordrecht ; Boston.

Kim, D. J., and H. Kim. 2005. Degradation of toluene vapor in a hydrophobic polyethylene hollow fiber membrane bioreactor with *Pseudomonas putida*. *Process Biochemistry* 40: 2015-2020.

Krishnakumar, B., A. M. Hima, and A. Haridas. 2007. Biofiltration of toluene-contaminated air using an agro by-product-based filter bed. *Applied Microbiology and Biotechnology* 74: 215-220.

Kumar, A., Dewulf, J., and Van Langenhove, H. 2008a. Membrane-based biological waste gas treatment. *Chemical Engineering Journal* 136: 82-91.

Kumar, A., Dewulf, J., Luvsanjamba, M., and Van Langenhove, H. 2008b. Continuous operation of membrane bioreactor treating toluene vapors by *Burkholderia vietnamiensis* G4. *Chemical Engineering Journal* 140: 193-200.

Langenhoff, A. A. M., D. L. BrouwersCeiler, J. H. L. Engelberting, J. J. Quist, J. G. P. N. Wolkenfelt, A. J. B. Zehnder, and G. Schraa. 1997. Microbial reduction of manganese coupled to toluene oxidation. *Fems Microbiology Ecology* 22: 119-127.

Leson, G., and A. M. Winer. 1991. Biofiltration - an innovative air-pollution control technology for VOC emissions. *Journal of the Air & Waste Management Association* 41: 1045-1054.

Li, L., and J. X. Liu. 2006. Removal of xylene from off-gas using a bioreactor containing bacteria and fungi. *International Biodeterioration & Biodegradation* 58: 60-64.

Lim, K. H., S. W. Park, and E. J. Lee. 2005. Effect of temperature on the performance of a biofilter inoculated with *Pseudomonas putida* to treat waste-air containing ethanol. *Korean Journal of Chemical Engineering* 22: 922-926.

Lin, C. W., S. L. Tsai, and S. N. Hou. 2007. Effects of environmental settings on MTBE removal for a mixed culture and its monoculture isolation. *Applied Microbiology and Biotechnology* 74: 194-201.

Lovley, D. R., and D. J. Lonergan. 1990. Anaerobic oxidation of toluene, phenol, and para-cresol by the dissimilatory iron-reducing organism, Gs-15. *Applied and Environmental Microbiology* 56: 1858-1864.

Lovley, D. R., J. C. Woodward, and F. H. Chapelle. 1994. Stimulated Anoxic Biodegradation of Aromatic-Hydrocarbons Using Fe(Iii) Ligands. *Nature* 370: 128-131.

Martinez, S., F. M. Cuervo-Lopez, and J. Gomez. 2007. Toluene mineralization by denitrification in an up flow anaerobic sludge blanket (UASB) reactor. *Bioresource Technology* 98: 1717-1723.

Moe, W. M., and R. L. Irvine. 2001. Polyurethane foam based biofilter media for toluene removal. *Water Science and Technology* 43: 35-42.

Moller, S., A. R. Pedersen, L. K. Poulsen, E. Arvin, and S. Molin. 1996. Activity and three-dimensional distribution of toluene-degrading *Pseudomonas putida* in a multispecies biofilm assessed by quantitative in situ hybridization and scanning confocal laser microscopy. *Applied and Environmental Microbiology* 62: 4632-4640.

Morgado, J., G. Merlin, Y. Gonthier, and A. Eyraud. 2004. A mechanistic model for m-xylene treatment with a peat-bed biofilter. *Environmental Technology* 25: 123-132.

Okkerse, W. J. H., S. P. P. Ottengraf, B. Osinga-Kuipers, and M. Okkerse. 1999. Biomass accumulation and clogging in biotrickling filters for waste gas treatment. Evaluation of a dynamic model using dichloromethane as a model pollutant. *Biotechnology and Bioengineering* 63: 418-430.

Ottengraf, S. P. P., and A. H. C. Vandenoever. 1983. Kinetics of organic-compound removal from waste gases with a biological filter. *Biotechnology and Bioengineering* 25: 3089-3102.

Park, D. W., S. S. Kim, S. Haam, I. S. Ahn, E. B. Kim, and W. S. Kim. 2002. Biodegradation of toluene by a lab-scale biofilter inoculated with *Pseudomonas putida* DK-1. *Environmental Technology* 23: 309-318.

Parvatiyar, M. G., R. Govind, and D. F. Bishop. 1996. Biodegradation of toluene in a membrane biofilter. *Journal of Membrane Science* 119: 17-24.

Prado, O. J., J. A. Mendoza, M. C. Veiga, and C. Kennes. 2002. Optimization of nutrient supply in a downflow gas-phase biofilter packed with an inert carrier. *Applied Microbiology and Biotechnology* 59: 567-573.

Rabus, R., R. Nordhaus, W. Ludwig, and F. Widdel. 1993. Complete Oxidation of Toluene under Strictly Anoxic Conditions by a New Sulfate-Reducing Bacterium. *Applied and Environmental Microbiology* 59: 1444-1451.

Roberson, E. B., and M. K. Firestone. 1992. Relationship between desiccation and exopolysaccharide production in a soil *Pseudomonas* Sp. *Applied and Environmental Microbiology* 58: 1284-1291.

Sakuma, T., T. Hattori, and M. A. Deshusses. 2006. Comparison of different packing materials for the biofiltration of air toxics. *Journal of the Air & Waste Management Association* 56: 1567-1575.

Shapiro, J. A. 1985. Scanning electron-microscope study of *Pseudomonas putida* colonies. *Journal of Bacteriology* 164: 1171-1181.

Singh, R. S., B. N. Rai, and S. N. Upadhyay. 2006. Performance evaluation of an agro waste based biofilter treating toluene vapours. *Environmental Technology* 27: 349-357.

Smet, E., G. Chasaya, H. VanLangenhove, and W. Verstraete. 1996. The effect of inoculation and the type of carrier material used on the biofiltration of methyl sulphides. *Applied Microbiology and Biotechnology* 45: 293-298.

Smith, F. L., G. A. Sorial, M. T. Suidan, A. W. Breen, P. Biswas, and R. C. Brenner. 1996. Development of two biomass control strategies for extended, stable operation of highly efficient biofilters with high toluene loadings. *Environmental Science & Technology* 30: 1744-1751.

Song, J. H., and K. A. Kinney. 2005. Microbial response and elimination capacity in biofilters subjected to high toluene loadings. *Applied Microbiology and Biotechnology* 68: 554-559.

Steinberger, R. E., and P. A. Holden. 2004. Macromolecular composition of unsaturated *Pseudomonas aeruginosa* biofilms with time and carbon source. *Biofilms* 1: 37-47.

Studer, M., and P. R. von Rohr. 2008. Novel membrane bioreactor: Able to cope with fluctuating loads, poorly water soluble VOCs, and biomass accumulation. *Biotechnology and Bioengineering* 99: 38-48.

Tan, N., W. Van Doesburg, and F. Stam. 2003. Anaerobic biodegradation of benzene in contaminated soils Wageningen University, Wageningen.

Torkian, A., R. Dehghanzadeh, and M. Hakimjavadi. 2003. Biodegradation of aromatic hydrocarbons in a compost biofilter. *Journal of Chemical Technology and Biotechnology* 78: 795-801.

Tresse, O., S. Lescob, and D. Rho. 2003. Dynamics of living and dead bacterial cells within a mixed-species biofilm during toluene degradation in a biotrickling filter. *Journal of Applied Microbiology* 94: 849-855.

Tsao, C. W., H. G. Song, and R. Bartha. 1998. Metabolism of benzene, toluene, and xylene hydrocarbons in soil. *Applied and Environmental Microbiology* 64: 4924-4929.

Van Langenhove, H., I. De Bo, P. Jacobs, K. Demeestere, and J. Dewulf. 2004. A membrane bioreactor for the removal of dimethyl sulphide and toluene from waste air. *Water Science and Technology* 50: 215-224.

Vayenas, D. V., E. Michalopoulou, G. N. Constantinides, S. Pavlou, and A. C. Payatakes. 2002. Visualization experiments of biodegradation in porous media and calculation of the biodegradation rate. *Advances in Water Resources* 25: 203-219.

Villaverde, S., R. Mirpuri, Z. Lewandowski, and W. L. Jones. 1997. Study of toluene degradation kinetics in a flat plate vapor phase bioreactor using oxygen microsensors. *Water Science and Technology* 36: 77-84.

Vinage, I., and P. R. von Rohr. 2003. Biological waste gas treatment with a modified rotating biological contactor. I. Control of biofilm growth and long-term performance. *Bioprocess and Biosystems Engineering* 26: 69-74.

Webb, J. S., M. Givskov, and S. Kjelleberg. 2003. Bacterial biofilms: prokaryotic adventures in multicellularity. *Current Opinion in Microbiology* 6: 578-585.

Yoon, I. K., and C. H. Park. 2002. Effects of gas flow rate, inlet concentration and temperature on biofiltration of volatile organic compounds in a peat-packed biofilter. *Journal of Bioscience and Bioengineering* 93: 165-169.

Zilli, M., A. Del Borghi, and A. Converti. 2000. Toluene vapour removal in a laboratory-scale biofilter. *Applied Microbiology and Biotechnology* 54: 248-254.

Chapter 5: Toluene concentration effect on removal

5.1 Introduction

Many researchers have modelled mass transfer in biofilters in the past. They vary from relative simple one component steady state models (Ottengraf and Vandenoever, 1983), to more complex multi-component dynamic models (Deshusses *et al.*, 1995; Dirk-Faitakis and Allen, 2005; Jorio *et al.*, 2003). Biofiltration is a complex process and modelling it accurately is not trivial. Important factors are pollutant concentration, water content, temperature, oxygen transfer, biofilm properties and biological kinetics. These factors influence each other in an ever changing environment and to create a representative model is a real challenge. The reactor system described in Chapter 2 can control the environmental parameters and thus presents a good opportunity to investigate the effect of the toluene concentration on the removal rate and explore the modelling implications.

5.2 Mass transfer in biofilters

The main objective of a biofilter is to remove pollutants from the gas phase. The pollutant is transferred from the gas phase into a biologically active layer. In this layer the pollutant is oxidised and serves as a source of energy and occasionally anabolic processes. The effectiveness of the biofilter depends on the biological layer, the porosity and structure of the bed material, available nutrients and water in the material, the gas flow rate and the concentration of the pollutant.

5.2.1 Substrate consumption rate

The first step in describing or modelling the microbial process in biofiltration is a mass balance over a unit volume of the biomass of the compounds of interest. Oxygen is not regarded as rate-limiting in most cases. Traditionally the degradation kinetics in a biofilm are described using growth by the model proposed by Jacques Monod in the 1940s (Rittmann and McCarty, 2001). The model (Eq. 5.1) relates the growth rate (μ) of bacteria to the limiting substrate concentration (S).

$$\mu = \frac{\mu_{\max} S}{K_S + S} \qquad [5.1]$$

The substrate consumption rate (r_i, Eq. 5.2) is described as a function of the biomass concentration (X) and growth rate through a yield term ($Y'_{X/S}$).

$$-r_i = \frac{\mu X}{Y'_{X/S}} \qquad [5.2]$$

Energy is not only needed for growth but also for essential, but non-growth related processes. Pirt (1975) proposed to call this energy requirement 'maintenance'. This energy requirement is important in degradation kinetics like biofiltration (Hess *et al.*, 1996).

Maintenance can be described as: "the energy consumed for functions other than production of new cell material" (van Bodegom, 2007). This definition includes all terms connected to non-growth:

- RNA and enzyme production due to shifts in metabolic pathways
- Energy spilling reactions
- Cell motility
- Changes in stored polymeric carbon
- Osmoregulation
- Extracellular losses of compounds not involved in osmoregulation
- Proofreading, synthesis and turnover of macromolecular compounds (RNA and enzymes)
- Defence against oxygen stress

The substrate consumption rate in Eq. 5.2 can be modified to include a term for maintenance (Pirt, 1975):

$$-r_i = \frac{\mu X}{Y'_{X/S}} + m_s X \qquad [5.3]$$

In biofiltration, the bed material often is an organic material which holds an array of nutrients. The microbial cultures present can use these nutrients for growth. This

supply is not unlimited and in due course growth of biomass will be limited. It is often assumed in a biofilter operating at steady state that the net growth, or μ is zero (Ottengraf and Vandenoever, 1983). The substrate consumption rate in Eq. 5.3 can be simplified to only a maintenance term (Eq. 5.4).

$$-r_i = m_s X \qquad [5.4]$$

The oxidation of a substrate is an enzymatic reaction and the reaction rate can be described accordingly. The assumption for a non-growing biofilm is that the substrate consumption rate involved is of a Monod-type (Rittmann and Mccarty, 1980):

$$-r_i = \frac{r_{\max} XS}{K_s + S} \qquad [5.5]$$

In nature, microbial life does not experience the controlled environment present in lab experiments. Environmental conditions like temperature and water content change as well as the availability of nutrients. Periods of high nutrient availability are followed by low nutrient availability. To survive these fluctuations, a strategy is essential. During a nutrient 'boom', fast nutrient uptake and growth is crucial as well as energy storage to stay alive and ready for the next nutrient 'boom' (Tappe *et al.*, 1999). Common concepts assume that micro-organisms do not die without external agents, like predators, adverse conditions, toxins or viruses (Drews and Kraume, 2007).

5.2.2 Mass balance over the biofilm

The substrate concentration in the biofilm only changes throughout the thickness or x-direction. Transport of the substrate (*i*) through the biofilm layer is by molecular diffusion and can be described by Eq. 5.6.

In - Out + Production = Accumulation

$$-D_i \frac{\partial C_i(x,t)}{\partial x} + D_i \frac{\partial C_i(x+dx,t)}{\partial x} + r_i(x,t)dx = \frac{\partial C_i(x,t)}{\partial t} dx \qquad [5.6]$$

Expanding the term $C_i(x+dx,t)$ with a Taylor series gives:

$$C_i(x+dx,t) = C_i(x,t) + \frac{\partial C_i(x,t)}{\partial x} dx + \frac{1}{2!} \frac{\partial^2 C_i(x,t)}{\partial x^2} dx^2 + \ldots \quad [5.7]$$

If dx→0 the second-order term can be neglected, and inserting the truncated version of Eq. 5.7 into Eq. 5.6 gives:

$$D_i \frac{\partial^2 C_i(x,t)}{\partial x^2} + r_i(x,t) = \frac{\partial C_i(x,t)}{\partial t} dx \quad [5.8]$$

If there is no accumulation of component *i*, a steady state can be assumed:

$$\frac{\partial C_i(x,t)}{\partial t} = 0 \quad [5.9]$$

This leaves the following mass balance to be solved:

$$D_i \frac{d^2 C_i}{dx^2} - r_i(x,t) = 0 \quad [5.10]$$

In biofilter models, the order of the reaction (r_i) is often assumed zero (Baquerizo *et al.*, 2005; Ottengraf and Vandenoever, 1983) or first order (Park *et al.*, 2004; Parker *et al.*, 1996) to obtain analytical solutions. Biological processes are usually described as Monod or Michaelis-Menten kinetics (Eq. 5.5) for which only numerical solutions exist. In the following sections, the implications of the separate reaction rates are discussed.

5.2.3 Zero order kinetics

Zero order kinetics were proposed by Ottengraf and Vandenoever (1983). They argue that if the substrate concentration is much higher than the K_s value for the majority of the biofilter operation (Eq. 5.5), the reaction can be considered zero order.

The substrate consumption rate can be described by zero order kinetics (assuming no growth of cells) as:

$$r_i = -k_0 \qquad [5.11]$$

Combination with Eq. 5.10 yields:

$$D_i \frac{\partial^2 C_i(x,t)}{\partial x^2} = k_0 \qquad [5.12]$$

The following assumptions are made to obtain boundary conditions for Eq. 5.12. The concentration at the surface of the biofilm layer is in equilibrium with the gas concentration in the bulk gas phase and described by a simple linear relationship:

$$x = 0, \qquad C_{i,0} = \frac{C_{g,i}}{m} \qquad [5.13]$$

There is no mass transfer across the outer boundary of the active layer, or thickness δ (Fig. 5.1).

$$x = \delta, \qquad \frac{dC_i}{dx} = 0 \qquad [5.14]$$

The solution for Eq. 5.12 becomes (Ottengraf and Vandenoever, 1983):

$$\frac{\frac{C_{i,\sigma}}{C_{g,i}}}{m} = 1 + \frac{1}{2}\frac{\phi^2}{\frac{C_{g,i}}{C_{g,in}}}\left(\sigma^2 - 2\sigma\right) \qquad [5.15]$$

Where:

$$\phi = \sqrt{\frac{k_0 m}{D_i C_{g,in}}} \qquad [5.16]$$

With:

$\sigma = \frac{x}{\delta}$ dimensionless length coordinate in the biolayer

$m = \left(\frac{C_g}{C_l} \right)_{equilibrium}$ distribution coefficient according to Henry's law

In an ideal situation, the biofilm has a uniform biomass density, a uniform thickness and the mass transfer resistance is governed by diffusion (Rittmann and McCarty, 2001). Without these assumptions the diffusion coefficient and the specific degradation rate would be a function of *x*; the location in the biofilm. This would make an analytical solution impossible. For zero order kinetics three scenarios can be identified (Fig. 5.1 to 5.3).

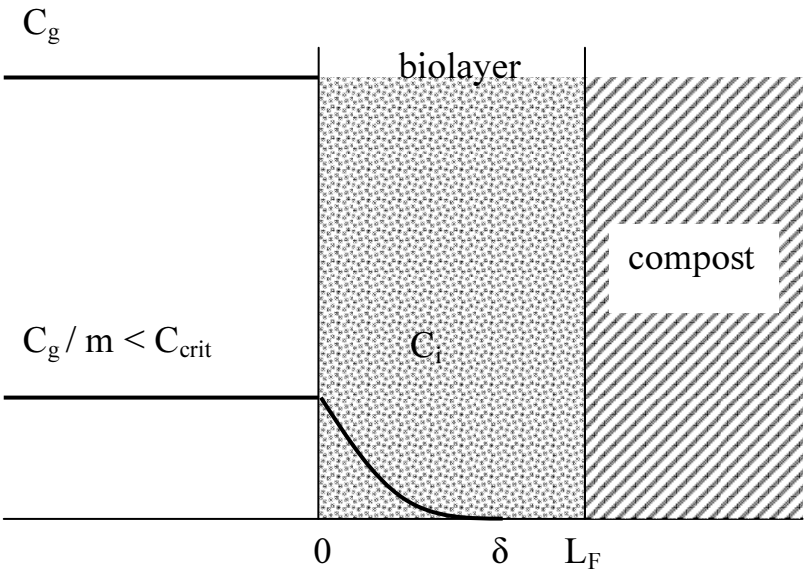

Figure 5.1*: First case: the concentration at the boundary of the biofilm is lower than C_{crit}. This means that the component i does not penetrate the full biofilm. The penetration thickness δ is smaller than the biofilm thickness L_F. The biofilm is not utilised fully. This is what Ottengraf and Vandenoever (1983) called diffusion limitation.*

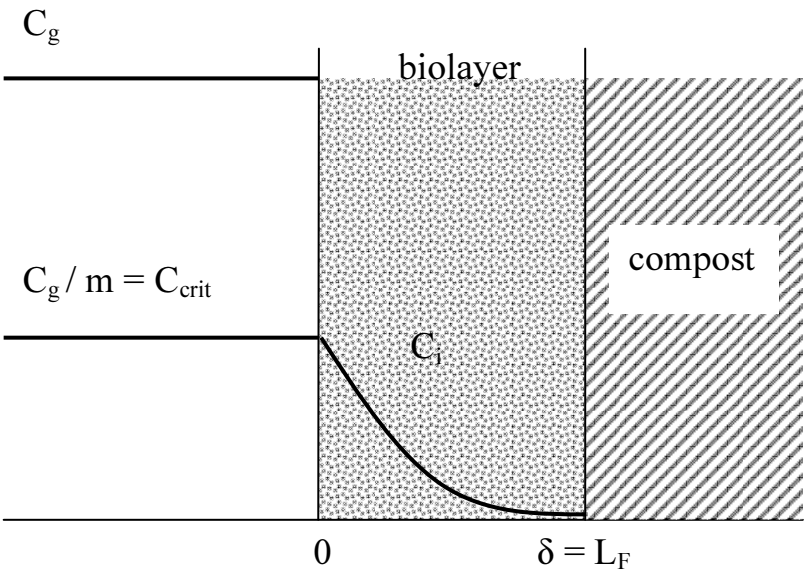

***Figure 5.2**: Second case: the concentration at the boundary of the biofilm is equal to C_{crit}. This means that the component i does exactly penetrate the full biofilm and the penetration thickness δ is equal to the biofilm thickness L_F. The biofilm is fully utilised.*

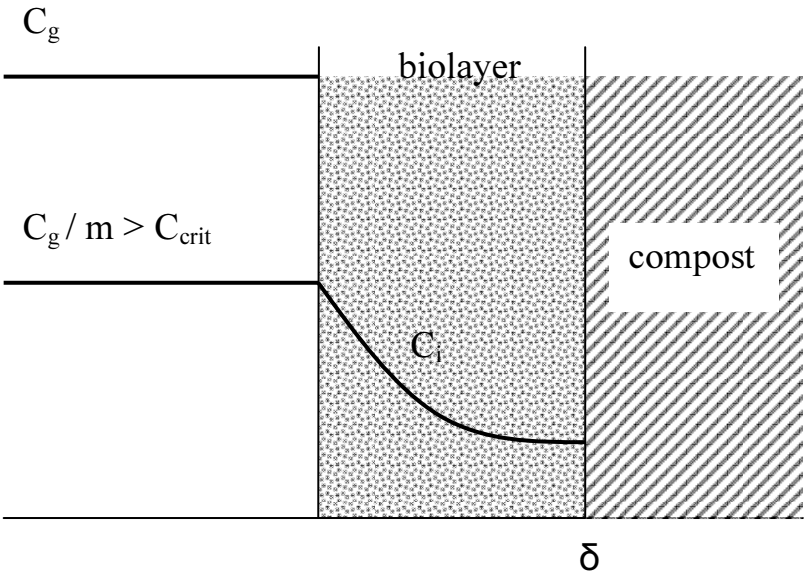

***Figure 5.3**: Third case: the concentration at the boundary of the biofilm is larger then C_{crit}. This means that the component i penetrates the full biofilm and the penetration thickness δ is larger then the biofilm thickness L_F. The biofilm is fully utilised, but an increase in the concentration does not increase the removal. The biofilm is used at its maximal capacity. This is what Ottengraf and Vandenoever (1983) called biological limitation.*

The three situations presented can be collated into a single figure (Fig. 5.4). At concentrations below C_{crit}, the biofilm is not fully utilized. The component is degraded quicker than it can diffuse into the biofilm. At C_{crit}, the whole biofilm is utilised, and the concentration in the biofilm reaches zero at the interface between the biofilm and the carrier material. By increasing the concentration, no extra removal will be seen as the whole biofilm is already active. From C_{crit} onwards, the degradation is biologically limited.

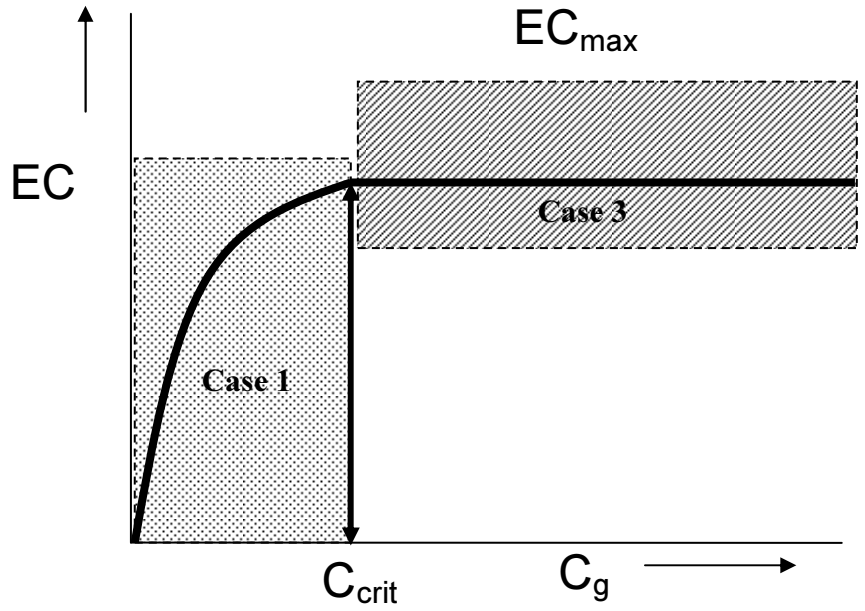

Figure 5.4*: The effect of the gas concentration on the EC in the three cases from Fig. 5.1 (dotted block), Fig. 5.2 (arrow) and Fig. 5.3 (diagonal stripes).*

5.2.4 First order kinetics

Ottengraf and Vandenoever (1983) assumed a zero order reaction, but at very low substrate concentrations Eq. 5.5 becomes first order. Because of the first order nature of the equation, the concentration in the biofilm never becomes equal to zero and therefore no penetration thickness can be defined (Wanner *et al.*, 2006).

The solution for the first order problem is as follows (Riet and Tramper, 1991). The degradation is described by:

$$r_i = -k_1 C_i \qquad [5.17]$$

Combination with Eq. 5.8 yields:

$$D_i \frac{d^2 C_i}{dx^2} - k_1 C_i = 0 \qquad [5.18]$$

A general solution for Eq. 5.18 is:

$$C_i(x) = B_1 e^{-px} + B_2 e^{px} \qquad [5.19]$$

With:

$$p = \sqrt{\frac{k_1}{D'}} \qquad [5.20]$$

Using the same boundary condition (Eq. 5.13), as before it follows:

$$C_i(0) = B_1 e^{p0} + B_2 e^{-p0} = B_1 + B_2 = \frac{C_{g,i}}{m} \qquad [5.21]$$

And the boundary condition in Eq. 5.14:

$$\frac{dC_i}{dx} = -pB_1 e^{-pL_F} + pB_2 e^{pL_F} = 0 \qquad [5.22]$$

$$pB_1 e^{-pL_F} = pB_2 e^{pL_F} \qquad [5.23]$$

$$B_1 = B_2 e^{2pL_F} \qquad [5.24]$$

Combining the result of the first (Eq. 5.21) and the second boundary conditions (Eq. 5.24) gives:

$$\frac{C_{g,i}}{m} = B_2 e^{2pL_F} + B_2 \qquad [5.25]$$

or

$$B_2 = \frac{C_{g,i}/m}{e^{2pL_F} + 1} \qquad [5.26]$$

Combining (Eq. 5.24) and (Eq. 5.26) gives:

$$B_1 = \frac{\left(C_{g,i}/m\right)e^{2pL_F}}{e^{2pL_F} + 1} \qquad [5.27]$$

So the solution for Eq. 5.19 with boundary conditions 5.13 and 5.14 becomes:

$$C_i(x) = \frac{\left(C_{g,i}/m\right)}{e^{2pL_F} + 1}\left(e^{p(2L_F - x)} + e^{px}\right) \qquad [5.28]$$

The concentration profile in the biofilm can be calculated with Eq. 5.28. Unlike the zero order solution the concentration in the biofilm never becomes zero, so no penetration thickness can be calculated.

5.2.5 Composite kinetics

As seen in the previous two sections, analytical solutions for Eq. 5.10 exist when Eq. 5.5 is simplified to either zero or first order reaction kinetics. Without simplifying Eq. 5.5, Eq. 5.10 becomes:

$$D_i \frac{\partial^2 C_i(x,t)}{\partial x^2} + \frac{r_{\max,i} C_i}{K_s + C_i} = \frac{\partial C_i(x,t)}{\partial t} dx \qquad [5.29]$$

No analytical solution for Eq. 5.29 exists. It can only be solved numerically. But by simplifying Eq. 5.5, a solution can be found. At high substrate concentration (C_i >>

K_s) the reaction is considered zero order and at low substrate concentrations ($K_s >> C_i$), the reaction is considered first order (Gapes *et al.*, 2006; Perez *et al.*, 2005; Wanner *et al.*, 2006). The reaction rate changes with substrate concentrations, so using a weighted average of the zero- and first order reaction rate an analytical solution can be found.

5.2.5.1 Zero order flux

The zero order flux is dependent on the thickness of the biofilm in relation to the substrate penetration depth. The substrate penetration depth (δ) is the depth of the biofilm where the substrate concentration becomes zero (Eq. 5.30). Also r_{max} is converted into a specific rate q_{max} in g toluene g^{-1} biomass s^{-1}.

$$\delta = \sqrt{\frac{2D_i \cdot C_{i,0}}{q_{\max,i} \cdot X}} \qquad [5.30]$$

If the actual biofilm thickness is larger then the penetration thickness, only a part of the biofilm is used for removal and the flux ($J^0_{F,i}$) of the substrate into the biofilm is (Perez *et al.*, 2005; Wanner *et al.*, 2006):

$$J^0_{F,i} = \sqrt{2D_i \cdot q_{\max,i} \cdot X} \cdot \sqrt{C_{i,0}} \qquad L_F > \delta \qquad [5.31]$$

At high contaminant concentrations, where the actual biofilm thickness is smaller then the potential penetration thickness, the whole biofilm is used for removal. This means that the flux is independent of concentration:

$$J^0_{F,i} = L_F \cdot q_{\max,i} \cdot X \qquad L_F < \delta \qquad [5.32]$$

5.2.5.2 First order flux

For first order kinetics, no penetration thickness can be calculated as the substrate concentration in the biofilm is never zero. The first order flux can be calculated (Gapes *et al.*, 2006; Perez *et al.*, 2005; Wanner *et al.*, 2006):

$$J_{F,i}^{1} = \frac{q_{\max,i} \cdot X \cdot L_F \cdot C_{i,0}}{K_s} \alpha \qquad [5.33]$$

Where

$$\alpha = \frac{\tanh \beta}{\beta} \quad \text{and} \quad \beta = \sqrt{\frac{q_{\max,i} \cdot X \cdot L_F^{\,2}}{D_i \cdot K_s}} \qquad [5.34]$$

5.2.5.3 Composite flux

To approach the solution of Eq. 5.29, a composite flux through the biofilm can be calculated (Eq. 5.36). This is the weighted average of the zero and first order reaction rates. At low substrate concentrations the first order flux dominates, while at high substrate concentrations the zero order flux does. The advantage of this method over a numerical solution is that the effects of each variable or parameter on the total flux can be investigated (Perez *et al.*, 2005).

$$J_{F,i} = \left(\frac{C_{i,0}}{C_{i,0} + K_s} \right) J_{F,i}^{0} + \left(1 - \frac{C_{i,0}}{C_{i,0} + K_s} \right) J_{F,i}^{1} \qquad [5.36]$$

5.2.6 Mass balance over the gas phase

The removal of the substrate from the perfectly mixed gas phase can be described by the mass balance (Eq. 5.37). The difference between the inlet and outlet represent what is transferred into the biofilm layer where it is degraded. With Eq. 5.38 an elimination capacity can then be calculated.

Accumulation = In - Out

$$V_r \frac{dC_{g,i}}{dt} = F(C_{g,in} - C_{g,i}) - J_{F,i} A_F \qquad [5.37]$$

At steady state Eq. 5.37 transforms into:

$$F(C_{g,in} - C_{g,i}) = J_{F,i} A_F \qquad [5.38]$$

5.3 Experimental setup and methods

The details of the reactor setup are described in Chapter 2. The specific experimental methods are described in the following sections.

5.3.1 Variation of toluene concentration in the reactor.

The reactor used for these experiments is Reactor 2. The matric potential was kept at -5 cm H_2O for the whole experiment. This was chosen to minimise stress on the membrane and reduce the chance of membrane failure. The temperature (30 ± 1.0 °C) and gas flow rate (19.9 ± 1.3 ml min^{-1}) were also kept constant. The toluene inlet concentration was varied by varying the temperature of the water bath in which the diffusion tube was submerged. The temperature was varied between 5 °C and 49 °C using the three diffusion tube designs as described in Sec. 2.3. This resulted in an inlet concentration between 15.5 ± 1.2 ppm and 640.2 ± 22.1 ppm. A comparison between the measured toluene concentration generated by the diffusion tube and the theoretical prediction can be found in App. C.1.

5.3.2 Fitting the data

The data was fit using zero, first and the composite kinetics and using the following assumptions:

- No concentration gradients in the gas phase or in the compost layer. This assumption is a requirement of the differential reactor.
- No oxygen limitation
- The mass transfer resistance through the water layer covering the biofilm is negligible
- The gas/biofilm is in equilibrium according to Henry's Law (Choi and Myung, 2004)
- The reactor is isothermal (Choi and Myung, 2004)
- The biomass concentration and composition are constant (Baquerizo *et al.*, 2005)
- The diffusion coefficient of toluene in the biofilm is the same as in water (Baquerizo *et al.*, 2005)
- No growth; $\mu = 0$ (Baquerizo *et al.*, 2005)

- No change in water content as this is controlled by the reactor
- No accumulation of toluene in the compost or water phase as the system is at steady state

5.4 Results and discussion

5.4.1 Toluene concentration effect on EC

Ottengraf and Vandenoever (1983) presented three scenarios (Fig. 5.1 to 5.3) to describe the toluene concentration profile in the biofilm. First, at gas concentrations below a critical concentration (C_{crit}), the biofilm is not fully utilized. The component is degraded quicker than it can diffuse through the entire biofilm. Second, at C_{crit} the whole biofilm is utilised, and the concentration in the biofilm reaches zero at the interface between the biofilm and the carrier material. Third, by increasing the gas concentration, no extra removal will be seen as the whole biofilm is already active. From C_{crit} upwards, the degradation is biological limited.

The relationship between the outlet concentration (i.e. residual concentration) and the EC was explored (Fig. 5.5 to 5.7 and the combined data in Fig. C.5). As predicted by theory, the EC increased to a critical concentration, after which it remained constant. After initially exploring the range of toluene concentrations (Fig 5.5), an increase in biomass was suspected and a new curve was generated (Fig. 5.6). Next nitrate was added temporarily to the water reservoir to stimulate growth and increase the EC. The nitrate was removed and the system stabilised with a new biomass level (Fig. 5.7) and a new curve generated. All three curves did fit in the scenarios proposed before.

The experiments were initially conducted with the assumption that there would be no change in biomass in the compost layer. The amount of active biomass controls the EC, (Song and Kinney, 2001) so a change in biomass concentration will change the relationship between the residual concentration in the reactor and the EC. Before these experiments started, the reactor was operated for 2000 hr, and any excess nutrients to stimulate growth were assumed depleted.

The first seven points of the experiments are found in Fig. 5.5. The numbers correspond to the order in which the samples were taken. Sample number 1 had a

similar EC as previously observed when the reactor was loaded with the same source of compost. When after point 3 (residual concentration of 83 ppm), the toluene concentration was reduced to 26 ppm (point 4), the EC was higher than seen in points 1 and 2. Although unexpected, these results can be explained. During the earlier experiments (run time 0 to 2,000 hr) the residual concentration did not exceed 66 ppm. It was possible that at point 3, the toluene concentration was high enough to damage non-toluene tolerant cells. Nutrients could have leaked from these cells into the environment. Well adapted cells, probably toluene degraders scavenged these nutrients and a small amount of growth occurred. An increase in toluene degrading biomass would show a higher steady state removal rate.

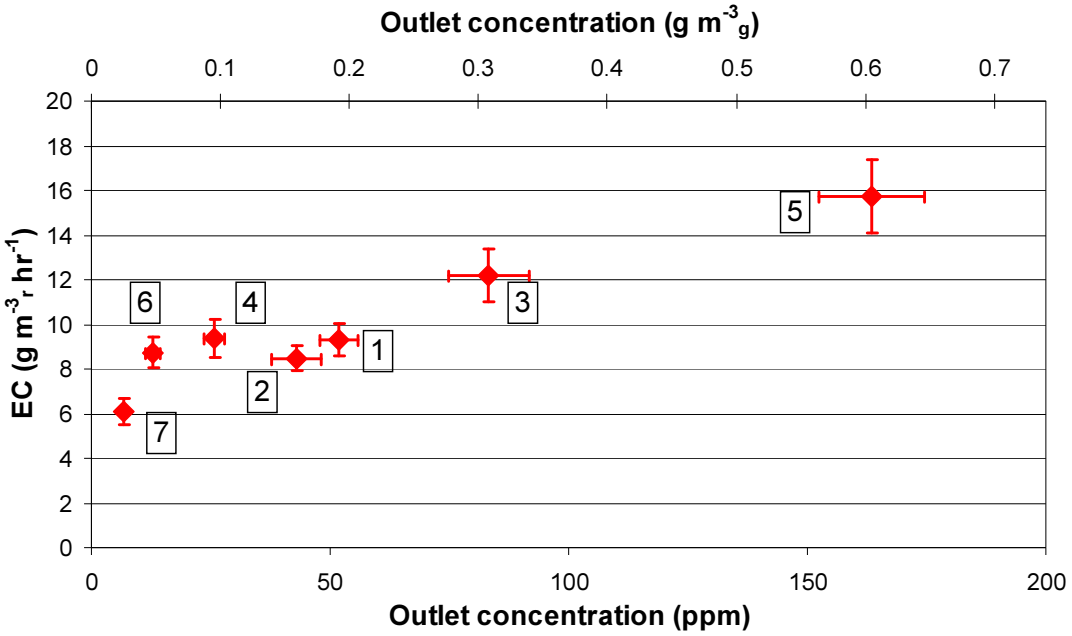

Figure 5.5*: The relationship between the outlet (or residual) concentration on the EC. The numbers represent the order in which the curve was generated. The diamonds are the averages of between 8 and 15 samples, the error bars are one standard deviation. This sample set is called Low and was obtained between hour 2,000 and 5,000.*

Following point 7 (Fig. 5.5), a new curve was started with point 8 after hr 5000 (Fig. 5.6) at a higher residual toluene concentration (287 ppm). The next point (9) after lowering the concentration from 287 ppm to 65 ppm was consistent with the hypothesis that the biomass had increased. The expected EC would have been

between 9.3 ± 0.47 and 12.2 ± 0.73 g m^{-3}_{r} hr^{-1} (point 1 and 3 of Fig. 5.5). The actual measured EC was 15.1 ± 0.6 g m^{-3}_{r} hr^{-1}. This was outside the 95% confidence interval of points 1 and 3. As no other environmental parameters had changed, a release of nutrients by other organisms present in the compost due to a high toluene concentration, which led to growth of the toluene degraders, is the likely explanation. After increasing the residual toluene concentration to 600 ppm, further stimulation of biomass growth was not observed.

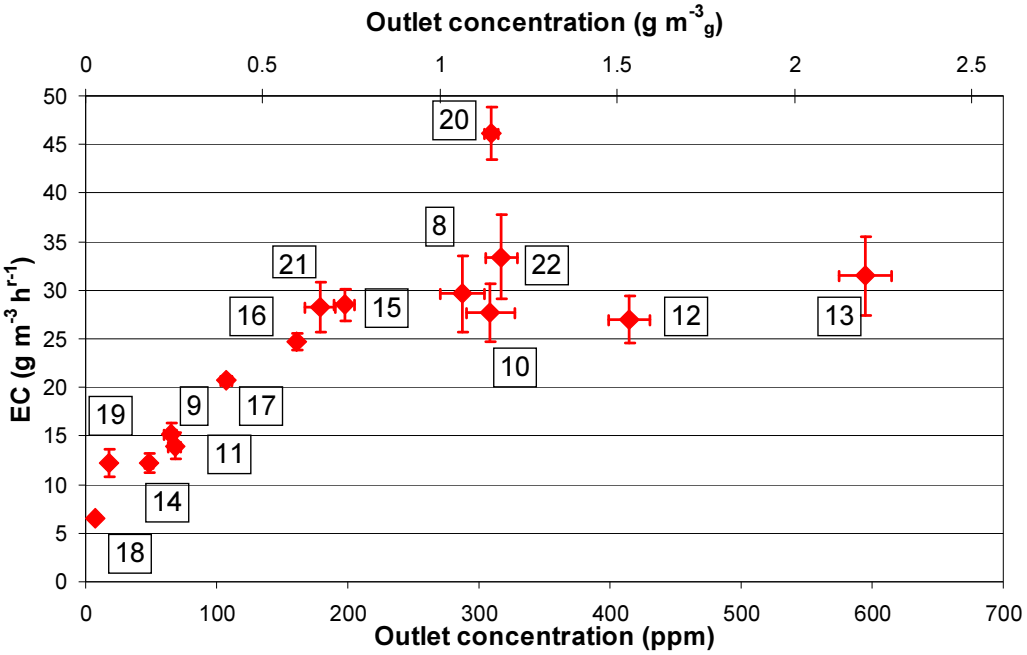

Figure 5.6*: The relationship between the outlet (or residual) concentration on the EC. The numbers represent the order in which the curve was generated. The diamonds are the averages of between 4 and 15 samples, the error bars are one standard deviation. This sample set is called High and was obtained between hour 5,000 and 9,600.*

Toluene is a toxic compound to many micro-organisms at sufficient concentrations. It has an adverse effect on the cytoplasmic membrane (de Bont, 1998). This results in the leakage of proteins, lipids and ions (Ramos *et al.*, 1997; VercelloneSmith and Herson, 1997). Some other organisms, like certain strains and mutants of *P. putida*, *Bacillus* and *Rhodococcus* sp tolerate solvents (de Bont, 1998; Sardessai and Bhosle, 2002). The mechanisms of this resistance include modifications in the cell envelope, increased rates of membrane repair enzymes, solvent inactivating enzymes, active

efflux pumps, release of membrane vesicles with adhering solvent molecules and the production of stress proteins (Sardessai and Bhosle, 2002).

The EC at point 20 was much higher then expected, but there were no obvious reasons for this outlier. The three points before were all at lower concentrations, so a release of nutrients by toluene toxicity was unlikely. As there was approximately 250 ml of water in the reservoir below the membrane, some toluene would be absorbed. Changing the residual concentration from 18 to 309 ppm increased the amount toluene in the water phase (point 19 $\rightarrow$ point 20) by approximately 1 mg (m = 0.27) which would manifest as a higher EC. The EC of point 20 was 46.1 ± 2.3 g m^{-3}_{r} hr^{-1}, which was 12 g m^{-3}_{r} hr^{-1} higher than the expected value, based on previous results. Assuming that this rate of 12 g m^{-3}_{r} hr^{-1} was the rate that the toluene was stored in the water, the time to store 1 mg was much shorter then the 100 hours spent at point 20. So the extra storage of toluene did not fully explain the high EC.

Another reason for the high EC at point 20 could be that the time spent (400 hr) at the lower toluene concentrations changed the affinity of the degraders for toluene. *P. putida* is a soil bacterium that generally lives poor nutrient environments and is well adapted to survive under starvation conditions (Kim *et al.*, 1995). A strain of *P. putida* was found to be fully viable for a month when completely starved for either glucose or nitrogen. Although according to Givskov *et al.* (1994b) starvation of sulphate and phosphate did reduce the survivability significantly. Nutrient limitation can increase the synthesis of membrane-based permeases for the limiting nutrient (Konopka, 2000). Kragelund and Nybroe (1994) observed the appearance of new proteins in the outer membrane after nitrogen or carbon starvation of *P. putida*. These proteins are believed to increase the flux of the nutrient into the cells.

The low residual concentrations of toluene could have induced similar membrane proteins to assist in the capture of toluene. When an abundance of toluene was provided (point 20) extra toluene was transported into the cells and degraded. At an abundance of carbon, these proteins were not needed and production would have stopped. Giskov *et al.* (1994a) did see a reduction in starvation-protein expression within 60 minutes of glucose addition to a carbon starved *P. putida* culture. A lack of

expression of the starvation proteins at higher toluene concentrations could be why the EC did not remain high in the subsequent data points. The EC in point 21 and 22 were in the expected range. Therefore if point 20 had been held longer, a drift of the steady state from an EC of 46.1 to 30 g m^{-3}_{r} hr^{-1} might have been observed. However, the time for point 21 to reach state was not longer than expected. This discounts the hypothesis that extra proteins were expressed.

After collecting the data in point 22 in Fig. 5.6, the water in the reservoir was replaced with a 0.12 g l^{-1} $NaNO_3$ solution. The expectation was that growth would be stimulated and the EC would rise at the same inlet concentration. The EC did increase from 33.4 ± 4.4 to 56.7 ± 6.6 g m^{-3}_{r} hr^{-1}, thus demonstrating nitrogen was the limiting nutrient in the compost at that time. The nitrate solution was removed and replaced with tap water with no change in EC. The residual nitrate concentration was not experimentally determined. The assumption was a full depletion of nitrogen. The residual toluene was again manipulated to generate a new relationship with EC at the new higher biomass loading (Fig. 5.7).

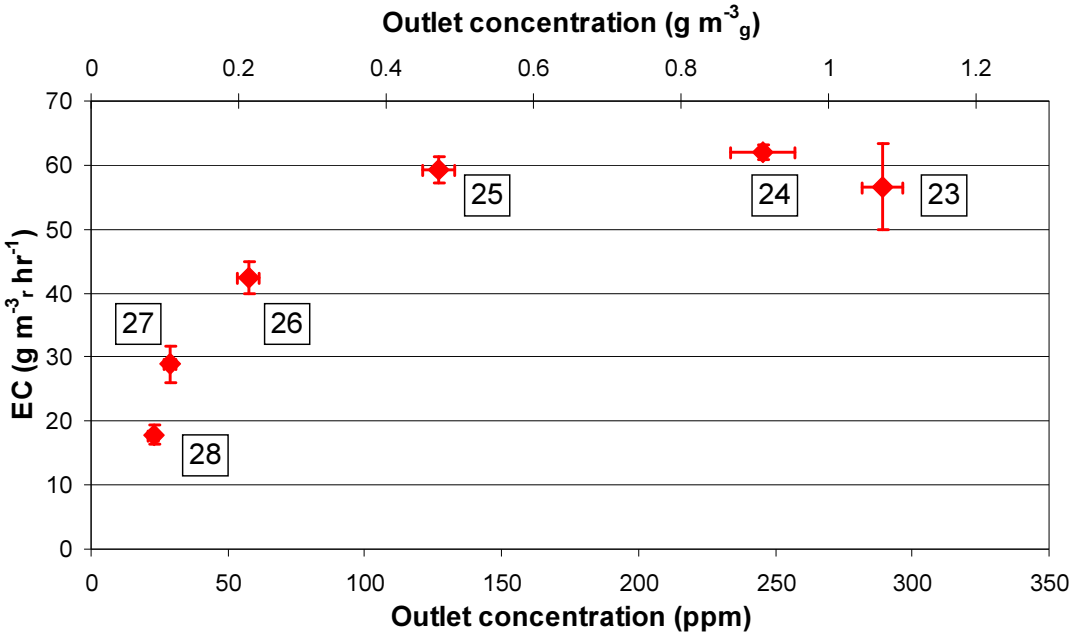

Figure 5.7*: The relationship between the outlet (or residual) concentration on the EC. The numbers represent the order in which the curve was generated. The diamonds are the averages of between 5 to 11 samples, the error bars are one standard deviation. This sample set is called NO_3 and was obtained between hour 9,600 and 10,700.*

Another interesting point to note was after point 23; a failure of the water bath controller with the diffusion tube increased the toluene concentration in the inlet to more then 15,000 ppm for approximately 24 hrs. This spike in toluene concentration decreased the toluene degradation rate to an EC of 3.5 g m^{-3}_{r} hr^{-1} the next day. After three days, the removal returned to its original value. VecelloneSmith and Herson (1997) observed inhibition at toluene concentrations of 130 mg l^{-1} in liquid cultures (= gas phase concentration of 9,500 ppm) and death at a concentration of 267 mg l^{-1} (= gas phase 20,000 ppm) toluene. This demonstrated two things. First, the toluene degraders could handle a large spike in toluene concentrations without any observed long term effects. And second if a large number of toluene sensitive organisms were still present, the toluene spike would have damaged them as discussed earlier. This would have freed up nutrients and would have led to growth and an increase in the steady state EC.

5.4.4 Fit of the models to the experimental data

The data collected on the EC dependency on the outlet concentration was fit using the composite model presented in Sec 5.2.5. The following parameters were chosen (Table 5.1) based on experimental or literature values.

Table 5.1*: Parameter values used for the composite model fit.*

Parameter	Value	Units
Distribution coefficient (m)[1]	0.27	g l^{-1} in air / g l^{-1} in water
Flow rate (Q)	$3.3 \cdot 10^{-7}$	m^3 s^{-1}
Bed volume (V)	$6.6 \cdot 10^{-6}$	m^3
Diffusion coefficient (D)[2]	$8.5 \cdot 10^{-10}$	m^2 s^{-1}
Biomass concentration in biofilm (X)[3]	$3.7 \cdot 10^{4}$	g m^{-3}
Maximal removal rate (q_{max})	$9.3\ 10^{-6}$	g g^{-1} s^{-1}

[1] From Choi and Myung (2004), Shareefdeen and Baltzis (1994)

[2] From Ottengraf and Vandenoever (1983)

[3] From biofilm experiments Sec. 4.4.2 and 4.5.3

The q_{max} was based on the highest measured specific degradation rate in the biofilm experiments (Sec. 4.5.2). The surface elimination capacity (SEC) was 0.1 g m^{-2}_{r} hr^{-1}, which correspond to 1250 g m^{-3}_{b} hr^{-1}. This maximum value was observed at a residual concentration of 9 ppm. As seen in Figs. 5.5-5.7, maximal removal rates are observed at residual concentrations above 100 ppm, thus this q_{max} value is probably a conservative estimate.

The unknown parameters in the models are the concentration that fully penetrates the biofilm (C_{crit}), the EC at C_{crit}, biofilm thickness, biofilm area and the K_s. The q_{max} and K_s are assumed to be constant for the three data sets as the biomass in the biofilm is assumed to be constant in concentration and composition.

In order to find the biofilm thickness and area, the concentration that fully penetrates the biofilm (C_{crit}) and the EC at C_{crit} have to be known. They were first determined graphically (Table C.1) and the R^2 (Eq. C.11) value for every data set is calculated. The sum of the three data sets (R^2_{total}, Eq. C.12) is maximised using the Solver function in Excel. To optimise the K_s value, the least squares (LSM, Eq. C.10) for every data set is calculated. Then the sum of the LSM of the three data is minimised by changing the K_s using the Solver function in Excel. These steps are repeated until conditions C.13 and C.14 are met. More details on the fitting method and the validity of the biofilm area can be found in App. C.3. The results of the parameter values from the fit are in Table 5.2 and 5.3.

***Table 5.2**: Values used for the fitting of the zero order model.*

Parameter	**Low**	**High**	**NO_3**	**Units**
C_{crit}	109	266	136	ppm
Inlet concentration at C_{crit} (C_{in})	132	314	225	ppm
EC at C_{crit}	15.4	32.5	59.3	g m^{-3}_{r} hr^{-1}
Biofilm area (A_F)	$9.5\ 10^{-4}$	$1.3\ 10^{-3}$	$3.3\ 10^{-3}$	m^2
Biofilm thickness (L_F)	$8.6\ 10^{-5}$	$1.3\ 10^{-4}$	$9.6\ 10^{-5}$	m
Sum of squares (S_R)	25	278	115	-
Sum of squares of 95% confidence region	381	441	84	-
EC_{crit} boundaries 95% confidence region	8-14	25-34	45-59	g m^{-3}_{r} hr^{-1}
E_{crit} boundaries 95% confidence region	10-275	159-403	78-194	ppm
R^2 zero order	0.53	0.81	0.95	-

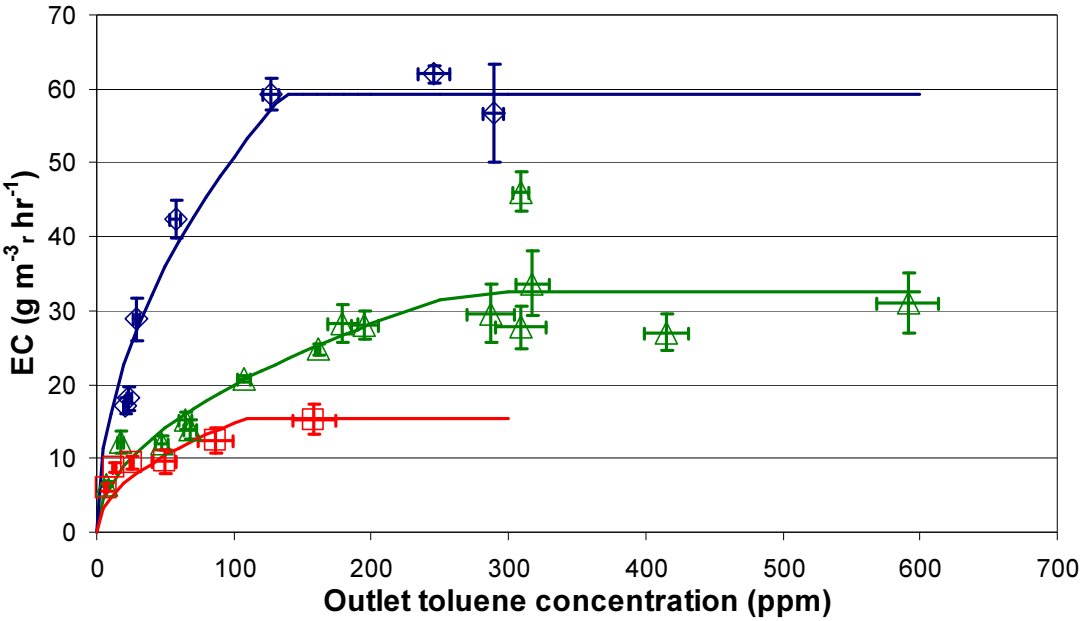

***Figure 5.8**: The zero order model fit for all three data sets. Low is the red open squares (□), High is the open green triangles (Δ) and NO_3 is the open blue diamonds (◊). The error bars represent 95% confidence interval of the data.*

***Table 5.3**: Values used for the fitting of the composite model. The R^2 value for the first order part of the composite model is not shown because of the poor fit.*

Parameter	**Low (Fig. 5.9)**	**High (Fig. 5.10)**	**NO_3 (Fig. 5.11)**	**Units**
C_{crit}	69.0	268	127	ppm
Inlet concentration at C_{crit} (C_{in})	86.7	312	205	ppm
EC at C_{crit}	11.9	29.5	52.1	g m^{-3}_r hr^{-1}
Biofilm area (A_F)	$9.3\ 10^{-4}$	$1.2\ 10^{-3}$	$3.0\ 10^{-3}$	m^2
Biofilm thickness (L_F)	$6.8\ 10^{-5}$	$1.3\ 10^{-4}$	$9.2\ 10^{-5}$	m
K_s	$1.27\ 10^{-1}$			g m^{-3}
Sum of squares (S_R)	40	296	83	-
Sum of squares within 95% confidence region (S_{95})	236	553	496	-
EC_{crit} boundaries 95% confidence region	7-17	28-36	52-66	g m^{-3}_r hr^{-1}
E_{crit} boundaries 95% confidence region	1-103	175-374	101-203	ppm
R^2 composite	0.26	0.80	0.96	-
R^2 zero order of composite	0.31	0.76	0.88	-

All three data sets were fit to the composite model and plotted in Fig. 5.9 to 5.11. The composite fit as well as the zero and first order parts of the model are plotted. The poorest composite fit (R^2 = 0.26) was with the Low data set. As growth occurred during this data set, this data set was not taken at a stable biomass concentration. By omitting point 5 (Fig 5.5) and refitting C_{crit} (5.6 ppm) and EC_{Ccrit} (7.2 g m^{-3}_r h^{-1}), the R^2 value increased to 0.55 for the composite model.

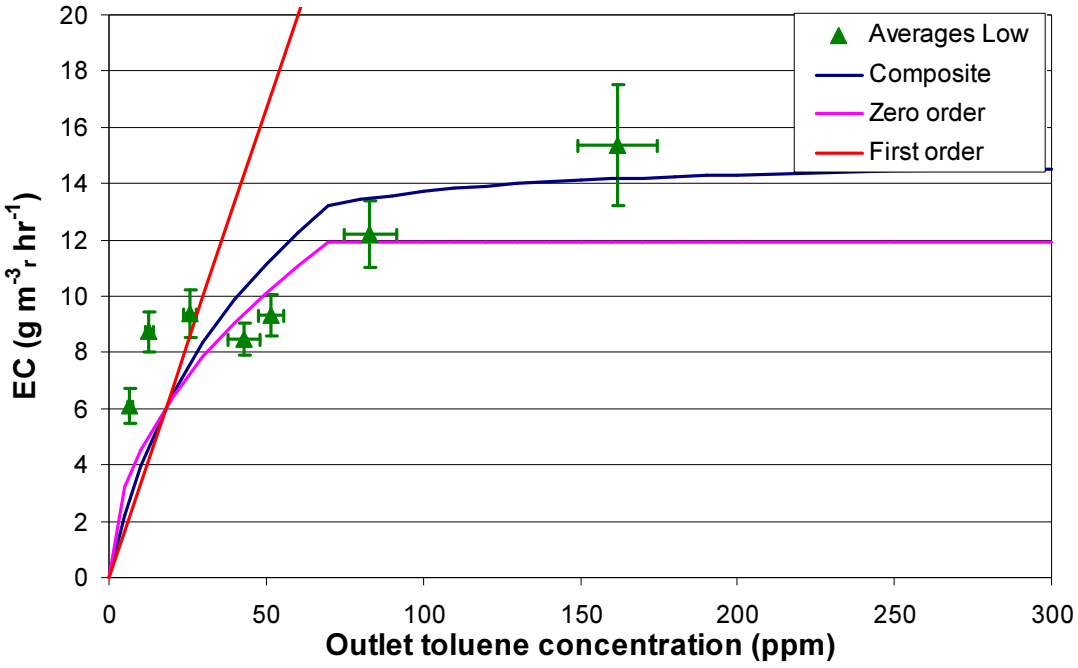

***Figure 5.9**: The relationship between the outlet (or residual) concentration on the EC of the Low sample set fitted with the three parts of the composite model.*

The High fit includes the data point (Fig. 5.10 nr.20) that lies outside the data set. By omitting this point and refitting the C_{crit} (217 ppm) and EC_{Ccrit} (26.7 g m^{-3}_r h^{-1}) it, the R^2 value increased to 0.93 from 0.80 for the composite model.

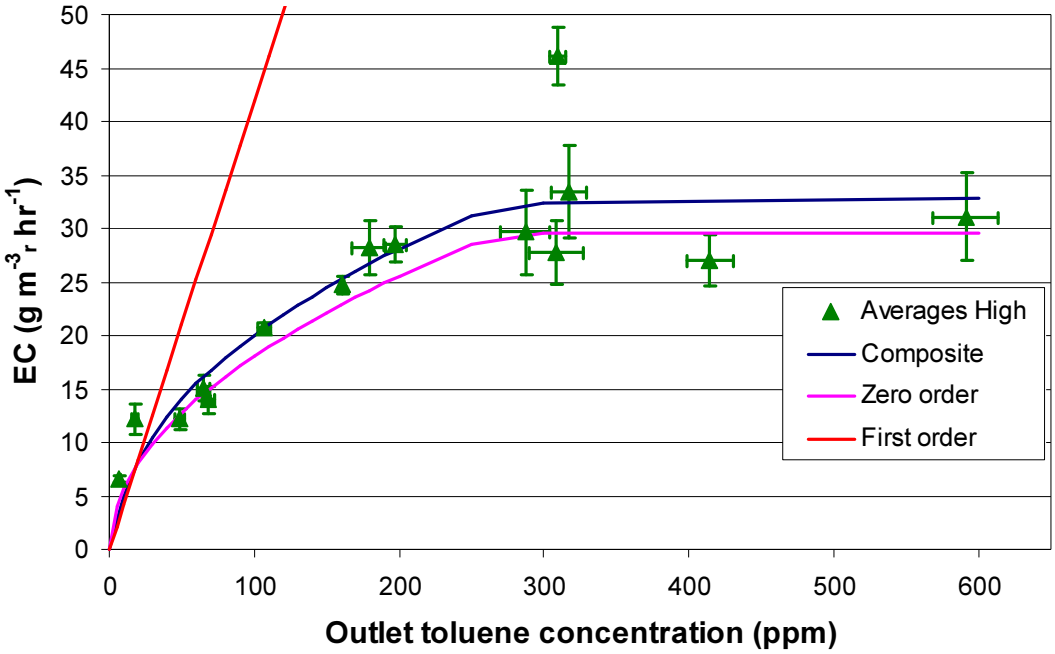

Figure 5.10: *The relationship between the outlet (or residual) concentration on the EC of the High sample set fitted with the three parts of the composite model.*

The fit of the NO_3 data (Fig. 5.11) set is good (R^2 = 0.96). This indicates that the biomass was stable during this run.

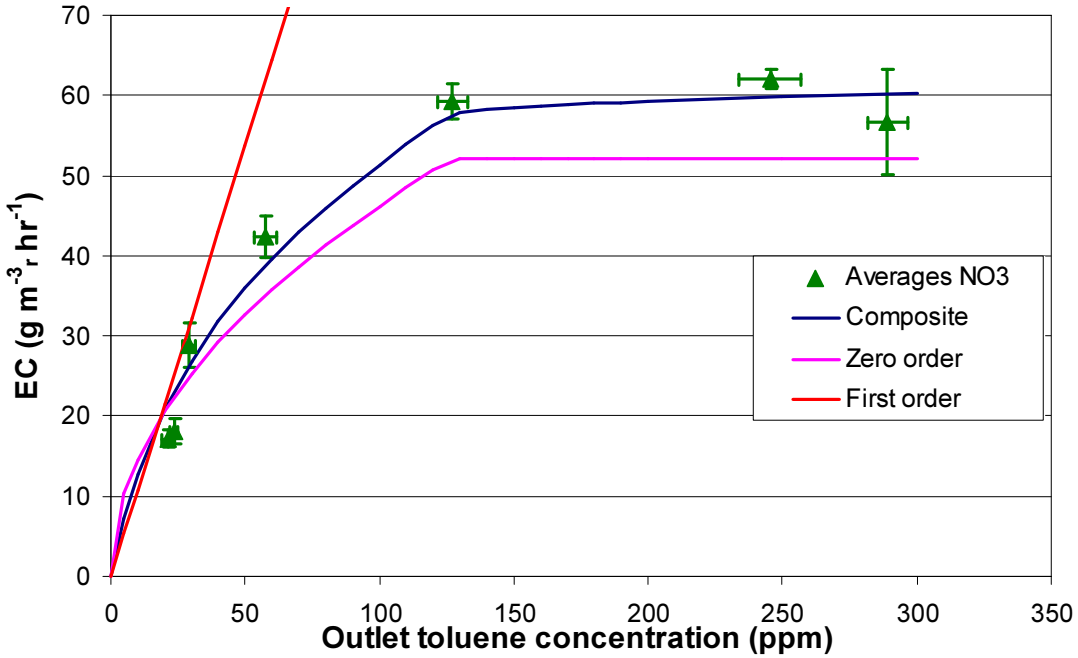

Figure 5.11: *The relationship between the outlet (or residual) concentration on the EC of the NO3 sample set fitted with the three parts of the composite model.*

A possible contributor to the increase in EC post-nitrate addition was not only an increase in biofilm thickness but an increase in biofilm coverage of the compost. After the nitrate addition, the calculated biofilm area increased almost three-fold (Table 5.2). Biofilm growth initially starts with a formation of colonies at fixed locations by clonal growth. After a period of time, the organisms spread out over the substratum and finally form a biofilm covering the substratum (Klausen *et al.*, 2003). Therefore as the biofilm area increased, the new areas covered had a thinner biofilm than the original biofilm. As the biofilm thickness is an average value of the whole biofilm surface, it explains the decrease in biofilm thickness from the High data set (130 μm) to the NO_3 data set (92 μm). The total biomass did increase resulting in an overall increase in EC.

Both the zero order and the composite model fits generated similar curves as can be seen in Figure 5.12. The similarity showed in the similar 95% confidence intervals of the EC_{crit} and C_{crit} in Tables 5.2 and 5.3. The K_s can be varied between 1 10^{-4} and 6.5 10^{-1} g m^{-3} and still kept the composite model fit within the 95% confidence interval. The main reason for this wass that no data was collected below a residual concentration of 7 ppm or 9.6 10^{-2} g m^{-3} and the low concentrations was where the first order part of the model governs. This means overall that for the data collected the zero order model could fit the data just as well as a more complicated composite model.

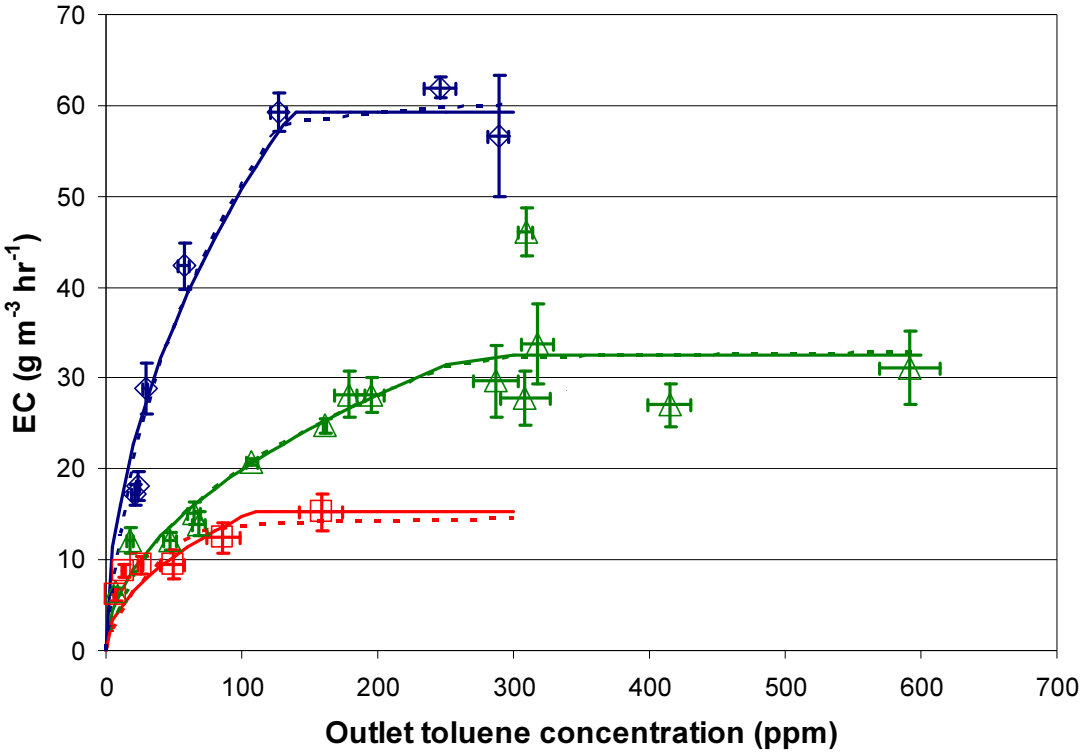

***Figure 5.12**: The zero order (dashed lines) and composite model (solid lines) fit for all three data sets. Low is the red open squares (□), High is the open green triangles (Δ) and NO_3 is the open blue diamonds (◊). The error bars represent 95% confidence interval of the data.*

Both the K_s and q_{max} were kept constant for all three composite data fits. The reasonable fit supports this assumption. This also points to an unchanged composition of the biofilm community. A biofilm in a natural bed material consists of multiple micro-organisms. As seen in Chapter 4, several different colonies were identified. But a constant K_s and q_{max} would be the case for one dominant organism or a stable mixture.

The models allowed K_s to be estimated at 0.127 g m^{-3} or 34 ppm toluene in the gas phase. In general, reported values for K_s vary largely depending on the type of strain, substratum and conditions. The estimate K_s value was within the range reported in literature (Table 5.4) for toluene in biofilms. But as discussed before the calculated K_s has a large 95% confidence interval, so the actual value does not mean much.

***Table 5.4**: K_s values reported in the literature for toluene in biofilms.*

K_s (g m^{-3})	**Culture**	**Reference**
0.18 ± 0.13	Mixed culture	Bielefeldt and Stensel, 1999
0.20 ± 0.04	Mixed culture	Bielefeldt and Stensel, 1999
0.22 ± 0.16	Mixed culture	Bielefeldt and Stensel, 1999
4.0	*P. putida 54G*	Mirpuri *et al.*, 1997
0.10	*P. putida F1* and *Rhodococcus erythropolis PWD1*	Vinage and von Rohr, 2003
2.7 10^{-2}	Mixed culture	Arcangeli and Arvin, 1997
0.10	*P. putida*	Moller *et al.*, 1996

Holden *et al.* (1997a) investigated the kinetic parameters of resting and active growing cells. These are presented as q_m and k_{bio}, respectively. The matric potential according to these results has a large effect on the q_m. The lower the potential, the higher the q_m becomes; more energy is required to keep the cells intact. The growing cells have an opposite trend. Initial experiments (not presented) to repeat the concentration relationship of Fig. 5.7 at a lower matric potential showed that the EC above C_{crit} was 50% lower. This would argue that in contrast to Holden *et al.* (1997a), the water content has indeed a large effect on the removal of a pollutant in a non-growth system.

The predictions of the composite and the zero order models were very similar. As the toluene concentration was much larger then K_s the zero order portion of the model dominated the composite model. Ottengraf and Vandenoever (1983) assumed that biofilters could be accurately described in zero order kinetics, but as seen from these results this is only valid at high toluene concentrations. Biofilters are integral reactors in which the concentration is reduced throughout the column length. At the inlet where the concentration is high, the zero-order model can be used. But nearer the outlet, the concentration will be lower and the first order model will dominate.

The results suggest that to improve biofilter operation, the start-up has to be done with a high toluene concentration. This will assist in the removal of unwanted micro-

organisms and could free up nutrients for toluene degraders. However these results are opposite to what Song and Kinney (2005) observed in their experiments. Over time the increase in heterotrophic organism counts were larger then the increase in toluene degrading organisms. An explanation was their regular addition of a nutrient solution; especially ammonia could have stimulated nitrifyers. In experiments by Villaverde *et al.* (2000) using pure *P. putida* biofilms to degrade toluene, a similar trend was seen. At a 25 fold toluene concentration increase the toluene-culturable cells increased 13 fold, while the total cells increased 200 fold. Their experiments with a pure culture at high toluene concentrations show that the cells may lose their ability to degrade toluene. As no cell counts are performed in this research, no comments can be made on changes in the ratio between toluene degraders and heterotrophic cells.

Streese *et al.* (2005) developed a macrokinetic model and used experimental data to find the kinetic parameters k_1 (hr^{-1}) and k_2 (m^3 mg^{-1}). Their objective was to find a method to determine the size of the biofilter bed for a certain removal and flow. These parameters are part of a concentration dependant shift described by Eq. 5.39. Substituting the k_1 and k_2 from Eq. 5.40 into Eq. 5.39 yields Eq. 5.5. Their k_1 and k_2 were converted into a r_{max} (or EC_{max}) and K_s (Table 5.5).

$$r_i = \frac{k_1 X S}{1 + k_2 S} \qquad [5.39]$$

$$k_1 = \frac{r_{max}}{K_s} \text{ and } k_2 = \frac{1}{K_s} \qquad [5.40]$$

Table 5.5*: Kinetic parameters compared to Streese et al. (2005).*

	Present study			**Streese *et al., 2005***	
	Low (Fig. 5.9)	**High (Fig. 5.10)**	**NO_3 (Fig. 5.11**	**Heather shrub**	**Compost/ wood chip**
K_s ($g\ m^{-3}$)	$1.3\ 10^{-1}$			$5.0\ 10^{-2}$	
r_{max} ($g\ m^{-3}{}_r\ hr^{-1}$)	11.9	29.5	52.1	8.40	8.33

The plots from Streese *et al.* (2005) were based on the logarithmic mean of the inlet and outlet concentration. The validity of this method is taken into question as the order of the reaction throughout the column does change. At high concentrations near the inlet the reaction is zero order and biologically limited and near the outlet the reaction is first-order with a mass transfer limitation. The values of k_1 and k_2 do not have any physical meaning; they are only fitting parameters. Traditional methods of using the load versus the EC plot to determine the biofilter volume do this equally well. One of the main concerns with sizing is changes in removal over time. The short timeframe of the experiments by Streese *et al.* (2005) of 1 day per data point, could have lead to errors in the curve and thus in the biofilter size predictions.

No inhibition by toluene on the removal was observed in the steady state experiments. The maximal residual concentration in the experiments was 600 ppm or a load of 426 ± 11 g m^{-3}_r hr^{-1}. Inhibition was seen by Zilli *et al.* (2000) at a loads above 1000 g m^{-3}_r hr^{-1}.

The EC_{max} was stable over a wide range (100 to 600 ppm) of toluene concentrations. If oxygen limitation did occur, the EC would have dropped at the higher toluene concentration. Although the maximum toluene concentration was 2.2 g m^{-3}, which was higher then the concentration (1.5 g m^{-3}) where Villaverde *et al.* (1997) observed oxygen limitation. This could be because their biofilm was 15 times thicker than the calculated thickness in these experiments. Smith *et al.* (2002) calculated a toluene concentration where oxygen becomes limited. They found limitation at 593 ppm, which was close to the maximum concentration used in these experiments. Schonduve *et al.* (1996) observed the first signs of nutrient and oxygen limitation at a biofilm thickness of 25 μm, while Kirchner *et al.* (1991) did not observe limitations until a biofilm thickness of 100 μm. Both of them investigated a trickle bed. To investigate the oxygen consumption and possible limitation in the biofilm, more experimental work and modelling is needed.

The biofilm thickness calculated by the composite model fit (68 – 134 μm) was within the range reported in the literature (Table 5.6). No reports were found on actual measurements of biofilm thickness in a biofilter. All values reported are theoretical calculations. Amanullah *et al.* (1999) did see in their modelling that the biofilm

thickness was one of the most crucial parameters that influenced removal. They investigated the removal of a biofilm between 5 and 100 µm, but they saw no improvement in removal in a biofilm thicker then 30 µm. The biofilm thickness found by Ottengraf and Vandenoever (1983) was very large and therefore very unlikely to be a real life value.

***Table 5.6**: Literature values of biofilm thickness.*

Biofilm thickness on toluene (µm)	**Reactor**	**Reference**
3.8	Biofilter	Choi and Myung, 2004
1200	Biofilter	Ottengraf and Vandenoever, 1983
93-102	Biofilter	Hwang and Tang, 1997
1400-2300	VPBR	Villaverde *et al.*, 1997
200	RBC	Vinage and von Rohr, 2003

As discussed before, the q_{max} used to calculate the biofilm thickness is probably on the low side. At an outlet concentration of 9 ppm the three curves in Fig. 5.9-5.11 only reach approximately 20% of the maximal EC. If the q_{max} in the model is multiplied by five, the biofilm thicknesses and surfaces are reduced, but still in the reported range (Table 5.7).

***Table 5.7**: Biofilm thickness and area at a q_{max} of 4.7 10^{-5} g g^{-1} s^{-1}.*

Parameter	**Low (Fig. 5.9)**	**High (Fig. 5.10)**	**NO_3 (Fig. 5.11)**	**Units**
Biofilm area (A_F)	4.1 10^{-4}	5.2 10^{-4}	1.3 10^{-3}	m^2
Biofilm thickness (L_F)	3.0 10^{-5}	6.0 10^{-5}	4.1 10^{-5}	m

5.5 Conclusions

The results of the experiments showed that the degradation of toluene is concentration dependent. The relationship demonstrated that at low toluene concentrations the limitation was limited by mass transfer and at high concentrations by the biofilm volume (area and thickness). The concentration at which this transition occurs is

called C_{crit} and was used to calculate a biofilm thickness. This thickness did change over the three data sets collected. As all environmental parameters were kept constant, growth was the likely cause of this increase. Growth can be induced by freeing up nutrients from non-toluene adapted cultures at high toluene concentrations or by nutrient, in this case nitrate, addition.

The data was fit adequately using a zero order and a composite model, comprised of the weighted average of a zero- and first order model. There was no significant difference in the fit between both models. Using the highest measured removal rate from the biofilm experiments, biofilm thicknesses were found to be between 68 and 134 μm. These thicknesses were comparable to literature values. No inhibition by high toluene concentrations or oxygen limitation was observed in the experiments.

5.6 Nomenclature

A_F	area of the biofilm	m^2
C_{crit}	concentration of full penetration	$g\ m^{-3}$
$C_{g,i}$	concentration *i* in the gas phase	$g\ m^{-3}$
$C_{g,in}$	inlet concentration in the gas phase	$g\ m^{-3}$
C_i	concentration *i*	$g\ m^{-3}$
$C_{i,0}$	concentration at the biofilm surface	$g\ m^{-3}$
$C_{i,x}$	concentration at the x	$g\ m^{-3}$
C_l	concentration in the liquid	$g\ m^{-3}$
D_i	diffusion coefficient of *i*	$m^2\ h^{-1}$
F	gas flow rate	$m^3\ h^{-1}$
$J_{F,i}$	flux of component *i*	$g\ m^{-2}\ h^{-1}$
$J^0_{F,i}$	zero order flux of component *i*	$g\ m^{-2}\ h^{-1}$
$J^1_{F,i}$	first order flux of component *i*	$g\ m^{-2}\ h^{-1}$
k_0	zero order reaction constant	$g\ m^{-3}\ h^{-1}$
k_1	first order reaction constant	h^{-1}
K_s	Toluene half-saturation constant	$g\ m^{-3}_g$
K_m	M-M half-saturation constant	$g\ m^{-3}_g$
L_F	biofilm thickness	m
m	Henry distribution coefficient	-

m_s	maintenance coefficient	g substrate g biomass^{-1} h^{-1}
q_{max}	maximum specific degradation rate of *i*	g g$^{-1}_b$ s^{-1}
r_{max}	maximum volumetric consumption rate	g m$^{-3}_r$ h^{-1}
r_s	substrate consumption rate	g m^{-3} h^{-1}
S	substrate concentration	g m^{-3}
S_R	sum of squares	-
S_{95}	sum of squares for the 95% confidence region	-
t	time	h
V_r	reactor volume	m^3
x	length coordinate in the biofilm	m
X	biomass concentration	g m$^{-3}_b$
$Y'_{X/S}$	true yield coefficient	g biomass g^{-1} substrate
δ	penetration depth	m
μ	specific growth rate	h^{-1}
μ_{max}	maximum specific growth rate	h^{-1}
σ	dimensionless length coordinate	-
φ	Thiele number	-

Subscripts

b	of biomass
g	of gas
r	of reactor

5.7 References

Amanullah, M., S. Farooq, and S. Viswanathan. 1999. Modeling and simulation of a biofilter. *Industrial & Engineering Chemistry Research* 38: 2765-2774.

Arcangeli, J. P., and E. Arvin. 1997. Modeling of the cometabolic biodegradation of trichloroethylene by toluene oxidizing bacteria in a biofilm system. *Environmental Science & Technology* 31: 3044-3052.

Baquerizo, G., J. P. Maestre, T. Sakuma, M. A. Deshusses, X. Gamisans, D. Gabriel, and J. Lafuente. 2005. A detailed-model of a biofilter for ammonia removal: Model parameters analysis and model validation. *Chemical Engineering Journal* 113: 205-214.

Bielefeldt, A. R., and H. D. Stensel. 1999. Evaluation of biodegradation kinetic testing methods and longterm variability in biokinetics for BTEX metabolism. *Water Research* 33: 733-740.

Choi, H. S., and S. W. Myung. 2004. Numerical and experimental study on the biofiltration of toluene vapor. *Korean Journal of Chemical Engineering* 21: 680-688.

de Bont, J. A. M. 1998. Solvent-tolerant bacteria in biocatalysis. *Trends in Biotechnology* 16: 493-499.

Deshusses, M. A., G. Hamer, and I. J. Dunn. 1995. Behavior of biofilters for waste air biotreatment .1. Dynamic-model development. *Environmental Science & Technology* 29: 1048-1058.

Dirk-Faitakis, C., and D. G. Allen. 2005. Development and simulation studies of an unsteady state biofilter model for the treatment of cyclic air emissions of an alpha-pinene gas stream. *Journal of Chemical Technology and Biotechnology* 80: 737-745.

Drews, A., and M. Kraume. 2007. On maintenance models in severely and long-term limited membrane bioreactor cultivations. *Biotechnology and Bioengineering* 96: 892-903.

Gapes, D., J. Perez, C. Picioreanu, and M. van Loosdrecht. 2006. Modeling biofilm and floc diffusion processes based on analytical solution of reaction-diffusion equations (vol 39, pg 1311, 2005). *Water Research* 40: 3144-3145.

Givskov, M., L. Eberl, and S. Molin. 1994a. Responses to nutrient starvation in *Pseudomonas-putida Kt2442* - 2-Dimensional electrophoretic analysis of starvation-induced and stress-induced proteins. *Journal of Bacteriology* 176: 4816-4824.

Givskov, M., L. Eberl, S. Moller, L. K. Poulsen, and S. Molin. 1994b. Responses to nutrient starvation in *Pseudomonas putida* Kt2442 - Analysis of general cross-protection, cell-shape, and macromolecular content. *Journal of Bacteriology* 176: 7-14.

Hess, T. F., S. K. Schmidt, and G. M. Colores. 1996. Maintenance energy model for microbial degradation of toxic chemicals in soil. *Soil Biology & Biochemistry* 28: 907-915.

Holden, P. A., L. J. Halverson, and M. K. Firestone. 1997. Water stress effects on toluene biodegradation by *Pseudomonas putida*. *Biodegradation* 8: 143-151.

Hwang, S. J., and H. M. Tang. 1997. Kinetic behavior of the toluene biofiltration process. *Journal of the Air & Waste Management Association* 47: 664-673.

Jorio, H., G. Payre, and M. Heitz. 2003. Mathematical modeling of gas-phase biofilter performance. *Journal of Chemical Technology and Biotechnology* 78: 834-846.

Kim, Y. J., L. S. Watrud, and A. Matin. 1995. A carbon starvation survival gene of *Pseudomonas putida* is regulated by sigma(54). *Journal of Bacteriology* 177: 1850-1859.

Kirchner, K., C. A. Gossen, and H. J. Rehm. 1991. Purification of exhaust air containing organic pollutants in a trickle-bed bioreactor. *Applied Microbiology and Biotechnology* 35: 396-400.

Klausen, M., A. Heydorn, P. Ragas, L. Lambertsen, A. Aaes-Jorgensen, S. Molin, and T. Tolker-Nielsen. 2003. Biofilm formation by *Pseudomonas aeruginosa* wild type, flagella and type IV pili mutants. *Molecular Microbiology* 48: 1511-1524.

Konopka, A. 2000. Microbial physiological state at low growth rate in natural and engineered ecosystems. *Current Opinion in Microbiology* 3: 244-247.

Kragelund, L., and O. Nybroe. 1994. Culturability and expression of outer-membrane proteins during carbon, nitrogen, or phosphorus starvation of *Pseudomonas fluorescens* Df57 and *Pseudomonas putida* Df14. *Applied and Environmental Microbiology* 60: 2944-2948.

Mirpuri, R., W. Sharp, S. Villaverde, W. Jones, Z. Lewandowski, and A. Cunningham. 1997. Predictive model for toluene degradation and microbial phenotypic profiles in flat plate vapor phase bioreactor. *Journal of Environmental Engineering-Asce* 123: 586-592.

Moller, S., A. R. Pedersen, L. K. Poulsen, E. Arvin, and S. Molin. 1996. Activity and three-dimensional distribution of toluene-degrading *Pseudomonas putida* in a multispecies biofilm assessed by quantitative in situ hybridization and scanning confocal laser microscopy. *Applied and Environmental Microbiology* 62: 4632-4640.

Ottengraf, S. P. P., and A. H. C. Vandenoever. 1983. Kinetics of organic-compound removal from waste gases with a biological filter. *Biotechnology and Bioengineering* 25: 3089-3102.

Park, O. H., S. H. Park, and J. H. Han. 2004. Model study based on experiments on toluene vapor removal in a biofilter. *Journal of Environmental Engineering-Asce* 130: 1118-1125.

Parker, W. J., H. D. Monteith, and H. Melcer. 1996. VOCs in fixed film processes .2. Model studies. *Journal of Environmental Engineering-Asce* 122: 564-570.

Perez, J., C. Picioreanu, and M. van Loosdrecht. 2005. Modeling biofilm and floc diffusion processes based on analytical solution of reaction-diffusion equations. *Water Research* 39: 1311-1323.

Pirt, S. J. 1975. *Principles of microbe and cell cultivation*. Blackwell Scientific, Oxford.

Ramos, J. L., E. Duque, J. J. RodriguezHerva, P. Godoy, A. Haidour, F. Reyes, and A. FernandezBarrero. 1997. Mechanisms for solvent tolerance ill bacteria. *Journal of Biological Chemistry* 272: 3887-3890.

Riet, K. v. t., and J. Tramper. 1991. *Basic bioreactor design*. Marcel Dekker, New York.

Rittmann, B. E., and P. L. Mccarty. 1980. Model of steady-state-biofilm kinetics. *Biotechnology and Bioengineering* 22: 2343-2357.

Rittmann, B. E., and P. L. McCarty. 2001. *Environmental biotechnology : principles and applications*. McGraw-Hill, Boston.

Sardessai, Y., and S. Bhosle. 2002. Tolerance of bacteria to organic solvents. *Research in Microbiology* 153: 263-268.

Schonduve, P., M. Sara, and A. Friedl. 1996. Influence of physiologically relevant parameters on biomass formation in a trickle-bed bioreactor used for waste gas cleaning. *Applied Microbiology and Biotechnology* 45: 286-292.

Shareefdeen, Z., and B. C. Baltzis. 1994. Biofiltration of toluene vapor under steady-state and transient conditions - Theory and experimental results. *Chemical Engineering Science* 49: 4347-4360.

Smith, F. L., G. A. Sorial, M. T. Suidan, P. Biswas, and R. C. Brenner. 2002. Development and demonstration of an explicit lumped-parameter biofilter model and design equation incorporating Monod kinetics. *Journal of the Air & Waste Management Association* 52: 208-219.

Song, J., and K. A. Kinney. 2001. Effect of directional switching frequency on toluene degradation in a vapor-phase bioreactor. *Applied Microbiology and Biotechnology* 56: 108-113.

Song, J. H., and K. A. Kinney. 2005. Microbial response and elimination capacity in biofilters subjected to high toluene loadings. *Applied Microbiology and Biotechnology* 68: 554-559.

Streese, J., M. Schlegelmilch, K. Heining, and R. Stegmann. 2005. A macrokinetic model for dimensioning of biofilters for VOC and odour treatment. *Waste Management* 25: 965-974.

Tappe, W., A. Laverman, M. Bohland, M. Braster, S. Rittershaus, J. Groeneweg, and H. W. van Verseveld. 1999. Maintenance energy demand and starvation recovery dynamics of *Nitrosomonas europaea* and *Nitrobacter winogradskyi* cultivated in a retentostat with complete biomass retention. *Applied and Environmental Microbiology* 65: 2471-2477.

van Bodegom, P. 2007. Microbial maintenance: A critical review on its quantification. *Microbial Ecology* 53: 513-523.

VercelloneSmith, P., and D. S. Herson. 1997. Toluene elicits a carbon starvation response in *Pseudomonas putida* mt-2 containing the TOL plasmid pWW0. *Applied and Environmental Microbiology* 63: 1925-1932.

Villaverde, S., F. Fdz-Polanco, and P. A. G. Encina. 2000. Endogenous respiration rate in vapour phase biological reactors (VPBRs) during volatile organic compound (VOC) degradation. *Water Science and Technology* 42: 429-436.

Villaverde, S., R. Mirpuri, Z. Lewandowski, and W. L. Jones. 1997. Study of toluene degradation kinetics in a flat plate vapor phase bioreactor using oxygen microsensors. *Water Science and Technology* 36: 77-84.

Vinage, I., and P. R. von Rohr. 2003. Biological waste gas treatment with a modified rotating biological contactor. II. Effect of operating parameters on process performance and mathematical modeling. *Bioprocess and Biosystems Engineering* 26: 75-82.

Wanner, O., H. Eberl, E. Morgenroth, D. Noguera, C. Picioreanu, B. E. Rittmann, and M. Vanloosdrecht. 2006. *Mathematical modeling of biofilms*. IWA Publishing, London.

Zilli, M., A. Del Borghi, and A. Converti. 2000. Toluene vapour removal in a laboratory-scale biofilter. *Applied Microbiology and Biotechnology* 54: 248-254.

Chapter 6: Nutrient addition and temperature effect on removal

6.1 Introduction

A biofilter is a very complex environment and involves many concurrent physicochemical and biological processes. Understanding the interactions among the various factors involved and identifying the rate-controlling processes is important (Chu *et al.*, 2005). Some factors that could reduce the optimum performance include:

- Low moisture
- Low oxygen
- Low or high pH
- High concentration of waste products
- Presence of toxins
- Lack of nutrients (carbon and inorganic)
- Low or high temperature

The effect of moisture was explored in Chapter 3 and although the oxygen was not directly investigated, theoretical calculations and literature reviews did not show oxygen limitation within the parameters of the experiments. However anaerobic degradation of VOCs is possible as discussed before in Sec. 4.2.3. Electron acceptors like nitrate, sulphate and phosphate could improve removal if anaerobic zones appear in the biofilter.

The pH optimum in biofiltration is considered to be between 6 and 8 for VOCs (Kinney *et al.*, 1999). Some pollutants containing sulphur, nitrogen or chloride produce acidic by-products or intermediates like H_2SO_4, HNO_3 and HCl which result in a decrease in pH and often in removal (Swanson and Loehr, 1997). Although Jin *et al.* (2007) did see 100% removal rates of H_2S at a pH of 2. Control of the pH can be achieved by adding lime or neutralising solutions to the biofilter media.

Toxins can be an issue if the bed materials are contaminated with anti-bacterial compounds like heavy metals. Heavy metals can block essential functional groups or interfere with incorporation of other metal ions into biological molecules. Amor *et al.* (2001) did show that zinc, cadmium and nickel reduced the removal of toluene.

The work described in this chapter controlled environmental parameters, like nitrogen and other nutrients and temperature and investigated their effect on volumetric removal rates. To accomplish this, the differential biofilter was used as described in Chapter 2.

6.2 Nutrients

Micro-organisms need a source of the macronutrients carbon, nitrogen, potassium and sulphur to increase their biomass. Other micronutrients are also required for protein and nucleic acids synthesis (Rittmann and McCarty, 2001). Biofilter bed media are often natural materials like compost or peat. They support a wide variety of micro-organisms and have major and minor nutrients present (Cherry and Thompson, 1997). The amount of nutrients is often considered sufficient for microbial survival (Leson and Winer, 1991), but at high pollutant loading, nutrient supplements are required to maintain a high removal rate (Morales *et al.*, 1998).

In low oxygen conditions, anaerobic micro-organisms can still remove contaminants by using nitrate, sulphate or iron (III) as electron acceptors. Low oxygen conditions do not occur often in biofilters. But in bioremediation the addition of these electron acceptors can increase the removal of pollutants significantly (Jean *et al.*, 2008; Lovley, 2001).

6.2.1 Carbon

Biofiltration can successfully control emissions such as odour, air toxins and volatile organic compounds (VOC). As long as the compounds are volatile and biodegradable, a proper designed biofilter will remove them (Leson and Winer, 1991). VOCs are used for energy and in growth conditions as a carbon source for cell material. Other essential elements have to be supplied by the bed medium or by external supplements (Kennes and Veiga, 2001). Odorous compounds like ammonia and hydrogen sulphide

do provide energy but obviously no carbon. The carbon required is provided by carbon dioxide in the air or by bioavailable carbon in the bed material.

6.2.2 Nitrogen

After carbon (50%) and excluding water, nitrogen (13%) is the second most common element or compound in bacterial cell mass (Delhomenie *et al.*, 2001b; Morgenroth *et al.*, 1996). The availability of nitrogen to the microbial flora is very important in biological systems, like biofiltration. Although the total nitrogen concentration in biofiltration media can be large, the total available nitrogen is the important parameter. Because of its importance, investigations have examined nitrogen availability in the filter bed medium, external addition and the type of nitrogen on performance.

6.2.2.1 Nitrogen in the filter bed medium

The presence of available inorganic nitrogen sources vary greatly between composts of different origin. Kinney *et al.* (1999) show ammonia can vary from 8 to 262 mg kg^{-1} compost and nitrate from 4.5 to 415 mg kg^{-1} compost. For good biofilter performance, the available nitrogen concentration has to be larger than 250 mg kg^{-1} of dry compost. And at elimination capacities larger than 30 g m^{-3}_{r} hr^{-1} even as high as 1000 mg kg^{-1} of dry compost (Kinney *et al.*, 1999).

6.2.2.2 Nitrogen addition and performance

Nitrogen is added to biofilters to improve the removal rate of the pollutant. Song *et al.* (2003) as well as others (Corsi and Seed, 1995; Delhomenie *et al.*, 2001a; Morales *et al.*, 1998) related biofilter performance strongly to nitrogen availability. However, the amount and frequency of nitrogen addition to a biofilter varies widely. Some groups added a nutrient medium to the bed at the start of the experiments (Morales *et al.*, 1998; Morgenroth *et al.*, 1996), others intermittently during the run (Son *et al.*, 2005; Weckhuysen *et al.*, 1993) and trickle bed reactors continuously (Wu *et al.*, 1999). Reported ratios of nitrogen addition are COD:N:P = 200:4:1 (Son *et al.*, 2005) and a C/N ratio of 9.8 by Song and Kinney (2005). Acuna *et al.* (1999) found that the bacterial population in their biofilter increased 20 fold after ammonia addition. This shows that nitrogen was limiting growth.

Nitrogen sources like urea (Delhomenie *et al.*, 2001a), ammonium hydroxide, ammonium chloride (Maestre *et al.*, 2007), gaseous ammonia (Morales *et al.*, 1998) and nitrate (Moe and Irvine, 2001a; Son *et al.*, 2005) can be added to biofilters. Even commercial fertiliser solutions are used (Cherry and Thompson, 1997).

Schonduve *et al.* (1996) investigated the difference between ammonia and nitrate addition on the removal rate of ethyl acetate and toluene and biomass growth. In both cases the ammonia resulted in higher rates then when nitrate was added. Nitrogen is bound in two different oxidation states; -III for ammonium and +V for nitrate. The transformation of nitrate to ammonium requires a high portion of reduction equivalent. This loss of energy resulted in a reduced microbial activity and growth.

Although both ammonium and nitrate can increase removal rates, excess biomass can clog the bed and lower performance. Smith *et al.* (1996) investigated both nitrate and ammonium addition in a trickle bed biofilter. The addition of ammonium caused a tenfold increase in heterotrophic bacteria, compared to the nitrate addition. Both nitrogen sources generated a similar number of toluene degraders. Comparable results were observed by Jorio *et al.* (2000a). Nitrogen supply to two biofilters was either ammonia or nitrate. The EC's observed for the ammonia addition were twice as high as for nitrate. The downside was that the ammonia supplemented biofilter experienced clogging, which ended their experiments.

Zhu *et al.* (2004) used nitrate for nitrogen addition over ammonia because of its lower biomass yield according to Smith *et al.* (1996). Another advantage of nitrate was that it acted as an electron acceptor when oxygen was limited. They showed that only 10% of the consumed nitrate was incorporated into biomass, suggesting that denitrification occurred. They also speculated that an optimum nitrate concentration for maximal removal existed.

Son *et al*, (2005) found that they could increase the removal rate of methyl isoamyl ketone (MIAK) from 55% to 93% by adding a nutrient solution containing potassium nitrate (KNO_3) and potassium phosphate (KH_2PO_4) to supply nitrogen and phosphorus. They did see an increase in removal rates, in particular at high loading rates. At the lower loading rates, addition of the nutrients did not have as much effect.

Morales *et al.* (1998) added gaseous ammonia to their biofilter at a rate of 0.43 mg g^{-1} humid peat hr^{-1}. After a steady state elimination capacity (EC) of 8 g m^{-3}_{r} hr^{-1} was reached, gaseous ammonia was added for 14 hours. No toluene was added simultaneously. The EC after addition increased to reach a maximum of 80 g m^{-3}_{r} hr^{-1} after 2 days, and a steady state of 30 g m^{-3}_{r} hr^{-1} was maintained. Another ammonia injection did not lead to a similar increase in EC.

6.2.3 Phosphate, sulphate and potassium

Phosphorous and sulphur are essential for many processes in the cell. Phosphorous is needed for DNA and for the energy storage molecule ATP. Sulphate is part of many proteins, vitamins and hormones (Schlegel and Zaborosch, 1993). Sorial *et al.* (1997) used phosphate limitation to reduce growth in a trickle bed. The P-limitation resulted in requiring the total bed volume to achieve 99% removal versus only needing 30% of the volume if nutrient-P was supplied. Although sulphate (SO_4^{2-}) has been used widely in the medium additions in biofilters (du Plessis *et al.*, 1998; Schonduve *et al.*, 1996; Weckhuysen *et al.*, 1993), no reports on sulphate being essential for aerobic biofiltration were found.

Potassium plays an important role in the maintenance of intracellular pH and cell turgor as well as protein synthesis (Alahari and Apte, 2004). Like any other nutrient a limitation of potassium leads to a decrease in cell yield. No reports that potassium addition caused an increase in removal in biofilters were found. It was used as a biomass control technique by Wubker and Friedrich (1996). They looked at the removal of *n*-butanol in potassium-limited conditions and saw a reduction in cell yield.

6.2.4 Trace elements and vitamins

Nutrient solutions used in biofilters not only contain major nutrients but also trace elements like magnesium, iron and calcium (Delhomenie *et al.*, 2001a; Morales *et al.*, 1998; Weckhuysen *et al.*, 1993). Prado *et al.* (2002) investigated the effect of vitamin and trace element limitation on a perlite biofilter. Parallel biofilters were operated, in which one received in addition to a macronutrient solution, trace elements and vitamins at start-up. This biofilter had almost double the EC of the one where the

trace elements and vitamins were omitted. Labbé *et al.* (2003) showed that iron in combination with manganese had a significant effect on denitrification. The addition of these trace elements increased the metabolic activity but did not increase growth. Copper, molybdenum and zinc had no effect.

6.2.5 Nutrient problems

Nutrient addition can also lead to problems. If the nutrients are supplied in a liquid form, the biofilter media can become too wet and will result in a reduction in performance, due to an increase in mass transfer resistance and increased pressure drop. Also leachate can remove a large portion of the soluble nitrogen and other nutrients. Ideally, the addition of nutrients to the biofilter has to aid in maintaining the present biomass and not promote growth (Delhomenie *et al.*, 2001a). Growth does result in higher removal rates, but will ultimately lead to failure due to clogging of the bed.

6.3 Temperature

The degradation of pollutants in biofilters is mostly accomplished by mesophilic organisms, especially if the biofilter is in the open air exposed to ambient conditions. Thermophilic organisms are also found, but to a lesser extent. In general, degradation of the pollutant is predicted to increase with temperature until an optimum is reached. This optimum lies between 20 °C and 40 °C (Acuna *et al.*, 1999; Leson and Winer, 1991).

Biodegradation of pollutants is an exothermic process that will increase the temperature in the bed. The heat production is directly linked to the amount of pollutant removed. Removal can be in different zones, so the temperature can vary throughout the bed. A variation up to 4.5 °C between the inlet and outlet temperature has been observed by Morales *et al.* (1998). The temperature at three points in a biofilter removing toluene was monitored by Delhomenie *et al.* (2001a). The temperatures rose from 23, 25 and 26 °C in the lower, middle an upper stage to 26, 29 and 31 °C respectively after extra nitrogen addition caused a five-fold increase in EC.

6.4 Experimental setup and methods

Both experiments of the nutrient addition and the effect of temperature used the setup of Reactor 3 as described in Chapter 2.

6.4.1 Nutrient addition

In these experiments the effect of nutrients on the removal rate were investigated. Different nutrient solutions (Table 6.1) replaced the tap water in the reservoir of the reactor in some experiments. The solutions were autoclaved at 121 °C for 20 minutes.

***Table 6.1**: Details of the nutrient addition experiments.*

Experiment	Nutrient	Conc. ($g\ l^{-1}$)	Duration (days)
1	NH_4Cl	1.0	8
2	NH_4Cl	1.0	10
3	K_2HPO_4	0.8	14
	NaH_2PO_4	0.7	14
4	$MgSO_4 \cdot 7H_2O$	0.4	11
	$FeSO_4 \cdot 7H_2O$	0.0035	11
	$CaCl \cdot 2H_2O$	0.02	11
5	$NaNO_3$	1.0	17

6.4.2 Temperature

The temperature in the insulated box containing the reactor was controlled between 15 and 60 °C. The temperature below ambient was controlled by recirculating water between a chiller (HAAKE WKL26, Thermo Scientific, Waltham, MA) and copper coils in the box and a temperature controller (Model: 2186-25A, Cole-Parmer, Vernon Hills, IL) turning a 200W light bulb off and on. Above ambient temperature, the cooling coil was eliminated. The temperature was changed in 5 °C intervals until steady state was reached. The starting point was 30 °C; the operating temperature for the nutrient and toluene variation experiments.

6.5 Results and discussion

The acclimation time from start-up to the maximal removal rate was 600 hours. A reason for the long acclimation time could have been the small population of toluene degraders in the compost. Or the low nitrogen availability in the compost could have led to slow growth rates, and thus slow acclimation. Morgenroth *et al.* (1996) observed that a lack of nutrients led to a reduced microbial population and thus EC. Therefore the addition of various nutrients was investigated.

6.5.1 Nutrient addition

The run in Reactor 3 was continued after the control experiments with the compost layer thickness (App. A.8). After a steady state EC of 6.0 ± 0.3 g m^{-3}_r hr^{-1} was achieved, a 1.0 g l^{-1} NH_4Cl solution replaced the tap water at hr 1650 (Fig. 6.1).

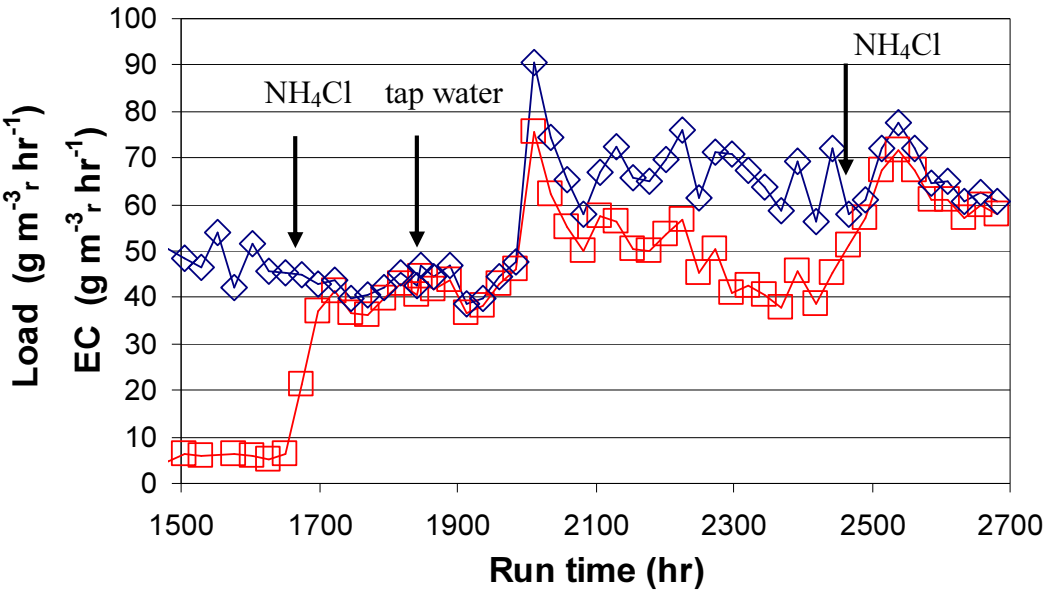

Figure 6.1*: The elimination capacity, open red squares (□) and load, open blue diamonds (◊) for experiment 1: addition of 1.0 g l^{-1} NH_4Cl (first arrow) and tap water (second arrow) and experiment 2: addition of 1.0 g l^{-1} NH_4Cl (third arrow).*

After 24 hours, the EC increased six fold and after 48 hours the EC reached a steady state of 40.9 ± 1.7 g m^{-3}_r hr^{-1}. The toluene removal was 94%. The NH_4Cl solution was removed from the reservoir and replaced with tap water. For five days the EC remained at the same level. The load was increased from 43.3 ± 1.7 g m^{-3}_r hr^{-1} to 68.2 ± 3.5 g m^{-3}_r hr^{-1} at hr 2010. The EC increased initially, but it slowly decreased to a

steady state value at the previous load by hr 2300. Another addition of NH_4Cl solution (1.0 g l^{-1}) at hr 2466 increased the steady state EC to 59.4 ± 1.5 g m^{-3}_r hr^{-1}.

During the removal of the NH_4Cl solution at hr 2682, the membrane started leaking and was replaced. Some of the compost was lost. A portion of the original compost was mixed with fresh compost to reduce the acclimation time. After steady state (EC 30.1 ± 0.9 g m^{-3}_r hr^{-1}) was reached (Fig 6.2) at hour 3162, phosphate buffer (pH 6.5) was added with no significant change in EC. The addition of a solution containing magnesium sulfate, iron sulfate and calcium chloride at hour 3478 also had no effect (Fig. 6.2). However, the addition of 1.0 g l^{-1} $NaNO_3$ (hour 3738) almost doubled the EC. A further increase in the load showed similar results as before, with a maximal EC of 114 g m^{-3}_r hr^{-1}at a load of 120 g m^{-3}_r hr^{-1}. After removing the nitrate solution, a steady state was maintained for 7 days at 76.3 ± 2.5 g m^{-3}_r hr^{-1} (load 97.1 ± 3.1 g m^{-3}_r hr^{-1}). The data from Fig. 6.2 is summarized in Fig. 6.3.

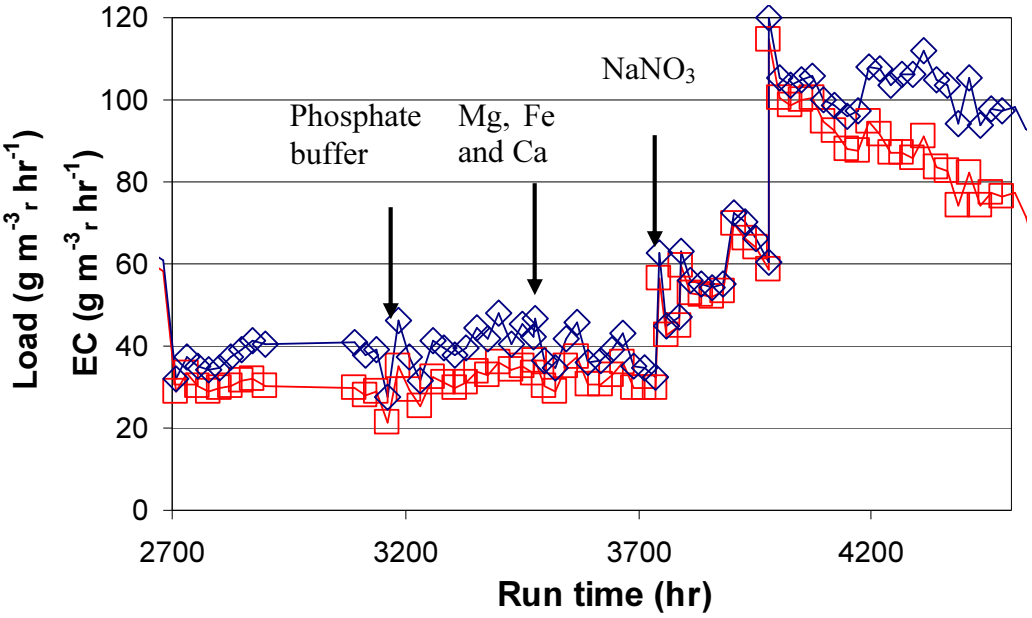

Figure 6.2*: The elimination capacity, open red squares (□) and load, open blue diamonds (◊) for experiment 3: addition phosphate buffer (first arrow), experiment 4: addition of magnesium sulfate, iron sulfate and calcium chloride solution (second arrow) and experiment 5: addition of 1.0 g* l^{-1} *$NaNO_3$ (third arrow).*

The sharp increase in EC after nitrogen addition has been observed before. Morales *et al.* (1998) added gaseous ammonia to their biofilter. After obtaining a steady state toluene EC of 8 g m^{-3}_r hr^{-1}, gaseous ammonia at a rate of 0.43 mg g^{-1} humid peat hr^{-1} was added for 14 hours. No toluene was added simultaneously. The toluene EC subsequently increased to 80 g m^{-3}_r hr^{-1} after 2 days, and a steady state of 30 g m^{-3}_r hr^{-1} was maintained. Cherry and Thompson (1997) also observed a spike in the EC, and small increase in the steady state values after a nutrient injection. Following their logic, the EC profile after nitrogen addition was caused by a transition from maintenance metabolism to growth followed by a return to maintenance metabolism in regards to toluene consumption rates. At steady state, there was no net growth in biomass and all toluene consumption was for maintenance requirements at a relatively low rate. Removal of the nitrogen restricted further growth but the net increase in biomass increased the volumetric toluene consumption for maintenance as well. In this case, the toluene degraders grew when supplemented with both ammonia and nitrate as a nitrogen source. This result was consistent with typical toluene degraders present in compost such as *P. putida* (Schonduve *et al.*, 1996).

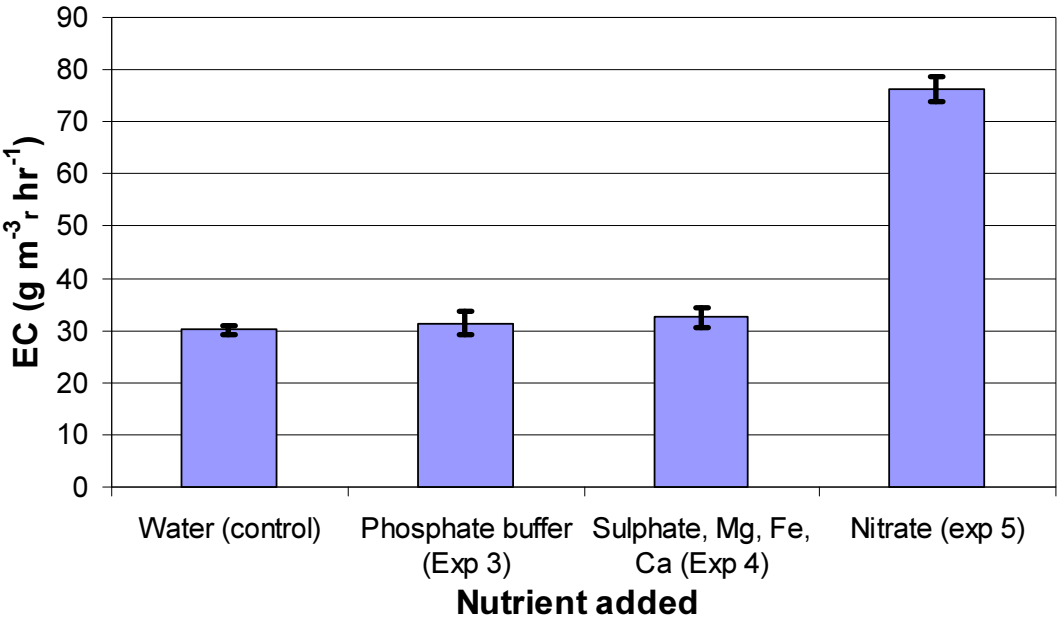

Figure 6.3*: Results of the nutrient addition experiments in Table 6.1 and Fig. 6.2. The error bars represent 95% confidence interval.*

After relieving the nitrogen limitation, carbon became the limiting factor. The removal efficiency in the period after nitrogen addition was 94% at an average load of 43.3 g m^{-3}_{r} hr^{-1}. The load (hr 2010) was increased to an average of 68.2 g m^{-3}_{r} hr^{-1} to confirm that if the EC would increase, the carbon was limited. The EC initially did increase to 75.6 g m^{-3}_{r} hr^{-1}, but the steady state EC after 10 days was 43.0 ± 2.6 g m^{-3}_{r} hr^{-1}.

The temporary increase in EC when the toluene load was increased at hr 2010 was most likely due to a short term production of exopolysaccharide or another energy storage compound, similar to Delhomenie *et al.* (2001a) observed. Morales *et al.* (1998) investigated the carbon products of the consumed toluene and found that approximately 30% was stored in biodegradable polymers. SEM micrographs of biofilter support by Acuna *et al.* (1999) confirmed polymer production at high bacterial activity zones.

Another possibility that could explain the temporary increase in removal during nitrate additions is that nitrate was used as an electron acceptor as discussed in Sec. 4.2.3. If the biofilm covering the compost caused a significant mass transfer resistance, the oxygen might not have penetrated the whole biofilm. The biofilm close to the membrane, were possibly at anoxic conditions. Addition of nitrate could lead to anoxic degradation, and an increased removal of toluene. Depletion of the electron acceptor nitrate would stop this extra removal and the EC will return to the steady state value before the addition. The oxygen limitation can be experimentally validated by increasing the oxygen concentration in the gas phase. If this increases the EC, oxygen was limited in the biofilm.

A third explanation for a temporary EC increase was that by removing the nitrogen limitation, growth did occur and the biofilm became thicker. As the concentration of toluene did not change, the penetration thickness of toluene remained constant as well. Even with a thicker biofilm, the actual active layer thickness did not change and thus the steady state EC did not change. The temporary increase in EC was due to the actual biomass growth.

Nitrate addition experiments with a biofilm instead of compost could provide additional insight because the biofilm thickness could be measured at steady state. There are four likely scenarios that would results from these experiments;

1. No change in thickness and steady state EC; nitrate has no effect on performance.
2. No change in thickness but an increase in steady state EC: nitrate stimulates the activity of toluene degradation. The excess energy production could be stored in storage compounds, which could be visible by SEM.
3. An increase in thickness, but no change in steady state EC: although the thickness increased, the actual penetration thickness did not change. The same volume of biofilm is degrading toluene. The degradation is diffusion limited. This could be confirmed by increasing the residual toluene concentration.
4. An increase in thickness and steady state EC: growth did occur and with it an increase in the maintenance requirements. The system was biologically limited.

6.5.2 Temperature

The effect of the temperature on the EC was investigated (Fig. 6.4). The small amount of compost and the design of the reactor increased the accuracy of the temperature control. Other lab scale integral biofilters can have significant temperature gradients throughout the column. Gostomski *et al.* (1997) did observe a 3 °C variation through the column. These temperature variations could influence the removal rates.

The load during the experiment was kept constant at 97.6 ± 1.3 g m^{-3}_{r} hr^{-1}. The temperature was reduced stepwise from 30 °C to the minimum temperature of 14.3 °C. The corresponding EC was reduced by 60%. The temperature was subsequently increased and the EC recovered rapidly when the temperature returned to 30 °C. Hardly any change in EC was observed between 30 and 55 °C. This range was wider then reported before. At 60 °C, the EC rapidly decreased by 90%. The EC only slowly recovered at 30 °C back to an EC of 30 g m^{-3}_{r} hr^{-1} after a month.

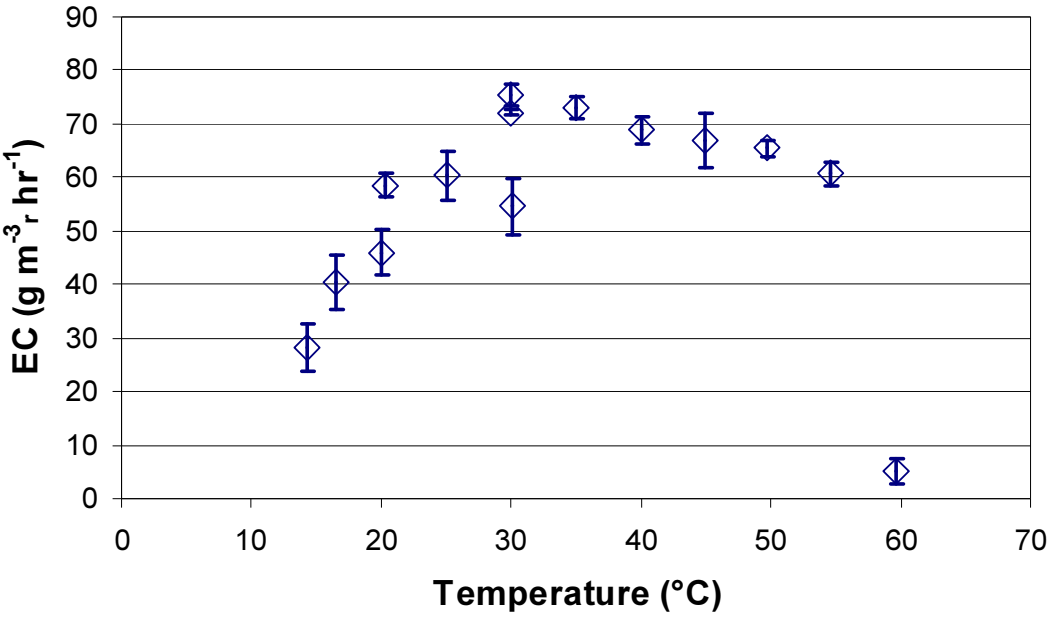

***Figure 6.4**: The effect of temperature on the elimination capacity. The load was kept constant during the experiment (97.5 ± 1.3 g m^{-3}_{r} hr^{-1}). The error bars represent 95% confidence interval.*

The temperature range at which the EC is considered high (> 60 g m^{-3}_{r} hr^{-1}) was wider (25 to 55 °C) then reported elsewhere. Acuna *et al.* (1999) reported a range between 25 and 40 °C, with an optimum at 30 °C. At 45 °C they did see a 15 fold reduction in removal. Wang and Govind (1997) observed that the removal rate increased rapidly until a plateau was reached between 30 and 40 °C. It was shown by Givskov *et al.* (1994) that for *P. putida* growth ceased above a temperature of 45 °C.

Natural bed materials contain a wide variety of micro-organisms. Environmental parameters like water content, temperature and pH are important selectors. It is possible that the community of toluene degraders had a wide range of overlapping optimal temperatures. But above 55 °C, the majority of the community was inhibited.

One of the key mechanisms is the transport of the pollutant from the gas phase into the aqueous phase. The transport can be described by the partition or Henry coefficient (Eq. 6.1).

$$H = \frac{mole/m^3 air}{mole/m^3 water} \qquad [6.1]$$

Generally, pollutants with a Henry coefficient higher than 1 are considered not suitable for biofiltration (Deheyder *et al.*, 1994). These pollutants are often highly volatile and can travel through a biofilter bed without being degraded (Davis *et al.*, 2001).

The Henry coefficient is strongly dependent on the temperature (Eq. 6.2). An increase in the temperature will reduce the concentration of toluene at the biofilm surface.

$$\ln H = a \cdot \frac{1}{T} + b \qquad [6.2]$$

With a and b are for toluene: a = -4362 and b = 13.329 (Dewulf *et al.*, 1999).

The effect of toluene concentration on EC was explored in Chapter 5 and indicated that EC was generally independent of the toluene concentration above a gas phase concentration of 100 ppm (concentration in the liquid at the biofilm surface = 370 ppm). The toluene concentration at the surface in the experiments at 60 °C was approximately 100 ppm. Similar liquid concentrations at lower temperatures showed a much higher EC, so the availability of toluene in the biofilm at higher temperatures was not the cause of the reduced EC.

6.6 Conclusions

The addition of a nitrogen source initially increased the steady state EC significantly. Additions thereafter only resulted in a temporary increase of EC. This temporary increase was most likely the result of a short term production of exopolysaccharide or another energy storage compound. Another explanation of this temporary increase was the limitation of oxygen in the biofilter. These anoxic conditions could have resulted in the use of nitrate as an electron acceptor for toluene degradation. As long as nitrate is available, a larger part of the biofilm is used for toluene degradation.

A wider range in temperature of high activity was seen than reported elsewhere. The broad community of toluene degraders in compost could have had overlapping optimal temperatures but above 55 °C, the majority of that community was greatly inhibited.

6.7 Nomenclature

a	fitting coefficient	-
b	fitting coeffient	-
H	Henry or partition coefficient	mole m^{-3}_{g} / mole m^{-3}_{w}
T	temperature	K

Subscripts

g	of gas
r	of reactor
w	of water

6.8 References

Acuna, M. E., F. Perez, R. Auria, and S. Revah. 1999. Microbiological and kinetic aspects of a biofilter for the removal of toluene from waste gases. *Biotechnology and Bioengineering* 63: 175-184.

Alahari, A., and S. K. Apte. 2004. A novel potassium deficiency-induced stimulon in *Anabaena torulosa*. *Journal of Biosciences* 29: 153-161.

Amor, L., C. Kennes, and M. C. Veiga. 2001. Kinetics of inhibition in the biodegradation of monoaromatic hydrocarbons in presence of heavy metals. *Bioresource Technology* 78: 181-185.

Cherry, R. S., and D. N. Thompson. 1997. Shift from growth to nutrient-limited maintenance kinetics during biofilter acclimation. *Biotechnology and Bioengineering* 56: 330-339.

Chu, M., P. K. Kitanidis, and P. L. McCarty. 2005. Modeling microbial reactions at the plume fringe subject to transverse mixing in porous media: When can the rates of microbial reaction be assumed to be instantaneous? *Water Resources Research* 41: 1-15.

Corsi, R. L., and L. Seed. 1995. Biofiltration of BTEX: Media, substrate, and loadings effects. *Environmental Progress* 14: 151-158.

Davis, L. C., C. Pitzer, S. Castro, and L. E. Erickson. 2001. Henry's constant, Darcy's law and contaminant loss. *Conference on Environmental Research*, Manhattan, Kansas.

Deheyder, B., A. Overmeire, H. Vanlangenhove, and W. Verstraete. 1994. Ethene removal from a synthetic waste-gas using a dry biobed. *Biotechnology and Bioengineering* 44: 642-648.

Delhomenie, M. C., L. Bibeau, J. Gendron, R. Brzezinski, and M. Heitz. 2001a. Toluene removal by biofiltration: Influence of the nitrogen concentration on operational parameters. *Industrial & Engineering Chemistry Research* 40: 5405-5414.

Delhomenie, M. C., L. Bibeau, S. Roy, R. Brzezinski, and M. Heitz. 2001b. Influence of nitrogen on the degradation of toluene in a compost-based biofilter. *Journal of Chemical Technology and Biotechnology* 76: 997-1006.

Dewulf, J., H. Van Langenhove, and P. Everaert. 1999. Determination of Henry's law coefficients by combination of the equilibrium partitioning in closed systems and solid-phase microextraction techniques. *Journal of Chromatography A* 830: 353-363.

du Plessis, C. A., K. A. Kinney, E. D. Schroeder, D. P. Y. Chang, and K. M. Scow. 1998. Denitrification and nitric oxide reduction in an aerobic toluene-treating biofilter. *Biotechnology and Bioengineering* 58: 408-415.

Gostomski, P. A., J. B. Sisson, and R. S. Cherry. 1997. Water content dynamics in biofiltration: The role of humidity and microbial heat generation. *Journal of the Air & Waste Management Association* 47: 936-944.

Jean, J.-S., M.-K. Lee, S.-D. Wang, P. Chattopadhyay, and J. P. Maity. 2008. Effects of inorganic nutrient levels on the biodegradation of benzene, toluene, and xylene (BTX) by *Pseudomonas* spp. in a laboratory porous media sand aquifer model. *Bioresource Technology* In Press.

Jin, Y. M., M. C. Veiga, and C. Kennes. 2007. Co-treatment of hydrogen sulfide and methanol in a single-stage biotrickling filter under acidic conditions. *Chemosphere* 68: 1186-1193.

Jorio, H., L. Bibeau, and M. Heitz. 2000. Biofiltration of air contaminated by styrene: Effect of nitrogen supply, gas flow rate, and inlet concentration. *Environmental Science & Technology* 34: 1764-1771.

Kennes, C., and M. C. Veiga. 2001. *Bioreactors for waste gas treatment*. Kluwer Academic, Dordrecht ; Boston.

Kinney, K. A., R. C. Loehr, and R. L. Corsi. 1999. Vapor-phase bioreactors: Avoiding problems through better design and operation. *Environmental Progress* 18: 222-230.

Labbe, N., S. Parent, and R. Villemur. 2003. Addition of trace metals increases denitrification rate in closed marine systems. *Water Research* 37: 914-920.

Leson, G., and A. M. Winer. 1991. Biofiltration - an innovative air-pollution control technology for VOC emissions. *Journal of the Air & Waste Management Association* 41: 1045-1054.

Lovley, D. R. 2001. Bioremediation - Anaerobes to the rescue. *Science* 293: 1444-1446.

Maestre, J. P., X. Gamisans, D. Gabriel, and J. Lafuente. 2007. Fungal biofilters for toluene biofiltration: Evaluation of the performance with four packing materials under different operating conditions. *Chemosphere* 67: 684-692.

Moe, W. M., and R. L. Irvine. 2001. Effect of nitrogen limitation on performance of toluene degrading biofilters. *Water Research* 35: 1407-1414.

Morales, M., S. Revah, and R. Auria. 1998. Start-up and the effect of gaseous ammonia additions on a biofilter for the elimination of toluene vapors. *Biotechnology and Bioengineering* 60: 483-491.

Morgenroth, E., E. D. Schroeder, D. P. Y. Chang, and K. M. Scow. 1996. Nutrient limitation in a compost biofilter degrading hexane. *Journal of the Air & Waste Management Association* 46: 300-308.

Prado, O. J., J. A. Mendoza, M. C. Veiga, and C. Kennes. 2002. Optimization of nutrient supply in a downflow gas-phase biofilter packed with an inert carrier. *Applied Microbiology and Biotechnology* 59: 567-573.

Rittmann, B. E., and P. L. McCarty. 2001. *Environmental biotechnology : principles and applications*. McGraw-Hill, Boston.

Schlegel, H. G., and C. Zaborosch. 1993. *General microbiology*. Cambridge University Press, Cambridge, [England].

Schonduve, P., M. Sara, and A. Friedl. 1996. Influence of physiologically relevant parameters on biomass formation in a trickle-bed bioreactor used for waste gas cleaning. *Applied Microbiology and Biotechnology* 45: 286-292.

Smith, F. L., G. A. Sorial, M. T. Suidan, A. W. Breen, P. Biswas, and R. C. Brenner. 1996. Development of two biomass control strategies for extended, stable operation of highly efficient biofilters with high toluene loadings. *Environmental Science & Technology* 30: 1744-1751.

Son, H. K., B. A. Striebig, and R. W. Regan. 2005. Nutrient limitations during the biofiltration of methyl isoamyl ketone. *Environmental Progress* 24: 75-81.

Song, J., J. Ramirez, and K. A. Kinney. 2003. Nitrogen utilization in a vapor-phase biofilter. *Water Research* 37: 4497-4505.

Song, J. H., and K. A. Kinney. 2005. Microbial response and elimination capacity in biofilters subjected to high toluene loadings. *Applied Microbiology and Biotechnology* 68: 554-559.

Sorial, G. A., F. L. Smith, M. T. Suidan, A. Pandit, P. Biswas, and R. C. Brenner. 1997. Evaluation of trickle bed air biofilter performance for BTEX removal. *Journal of Environmental Engineering-Asce* 123: 530-537.

Swanson, W. J., and R. C. Loehr. 1997. Biofiltration: Fundamentals, design and operations principles, and applications. *Journal of Environmental Engineering-Asce* 123: 538-546.

Weckhuysen, B., L. Vriens, and H. Verachtert. 1993. The effect of nutrient supplementation on the biofiltration removal of butanal in contaminated air. *Applied Microbiology and Biotechnology* 39: 395-399.

Wu, G., B. Conti, A. Leroux, R. Brzezinski, G. Viel, and M. Heitz. 1999. A high performance biofilter for VOC emission control. *Journal of the Air & Waste Management Association* 49: 185-192.

Wubker, S. M., and C. G. Friedrich. 1996. Reduction of biomass in a bioscrubber for waste gas treatment by limited supply of phosphate and potassium ions. *Applied Microbiology and Biotechnology* 46: 475-480.

Zhu, X. Q., M. T. Suidan, A. Pruden, C. P. Yang, C. Alonso, B. J. Kim, and B. R. Kim. 2004. Effect of substrate Henry's constant on biofilter performance. *Journal of the Air & Waste Management Association* 54: 409-418.

Chapter 7: Recommendations and future work

7.1 Summary

In this work, a differential reactor was used to expose all the biofilter packing material (compost) to a uniform toluene concentration in air. The reactor was combined with water content control using the suction cell principle and traditional inlet concentration, temperature and humidity control.

Water content does have an influence on the elimination capacity of toluene in compost. More accurately, water potential and not water content was the predominant factor affecting degradation. Optimal removal rates were seen at a matric potential between -10 and -100 cm H_2O, with a maximum at -20 cm H_2O. This corresponds to a gravimetric water content for Compost 1 of 1.73 g H_2O g^{-1}dry compost and for Compost 2 of 1.44 g^{-1}dry compost. A reduction in water potential to -300 cm H_2O led to a 60% reduction in EC, which showed to be irreversible. At water potentials above -10 cm H_2O, the EC also was reduced. This reduction was attributed to several factors: loss of water availability to the organisms, water redistribution in the medium, non-adaptable micro-organisms, and reduced mass transfer.

Toluene degraders were isolated from compost using a basic minimal medium with a toluene atmosphere. Although no attempt to identify the cultures was made, SEM pictures of the biofilm showed the expected rod-shape of a *Pseudomonas* strain. The biofilm thickness varied between 75 and 95 μm. The results from the biofilm runs in the reactor did give similar results in terms of removal of toluene as compared to the literature. These experiment resulted in a maximal observed SEC of is 0.17 g m^{-2}_r hr^{-1} and a specific removal rate of 1250 g m^{-3}_b hr^{-1}. This specific rate is used in modelling biofilm performance. This was the highest observed rate, but probably not the maximal possible. Both biofilm runs ended before a higher residual concentration (>100 ppm) was achieved. Above this concentration, a maximum in the EC is expected.

The degradation of toluene is dependent of the residual concentration. The relationship demonstrated that at low toluene concentrations the limitation was limited

by mass transfer and at high concentrations by the biofilm (area and thickness). The concentration at which this transition occurs is called C_{crit} and was used to calculate a biofilm thickness. This thickness did change over the three data sets collected. As all environmental parameters were kept constant, growth was the likely cause of this increase. Growth can be induced by freeing up nutrients from non-toluene adapted cultures at high toluene concentrations or by nutrient, in this case nitrate, addition.

The data was fit adequately using a zero order and composite model, comprised of the weighted average of a zero- and first order model. There was no significant difference in the fit between both models. The best fit K_s ($1.3 \cdot 10^{-1}$ g m^{-3}_g or 34 ppm) was low compared to the majority of the data, which means that the zero order part of the composite model dominated. Using the highest measured removal rate from the biofilm experiments, biofilm thicknesses were found to be between 68 and 134 μm. These thicknesses were comparable to literature values. No inhibition by high toluene concentrations or oxygen limitation was observed in the experiments.

The addition of a nitrogen source initially increased the steady state EC significantly. Additions thereafter only resulted in a temporary increase of EC. This temporary increase was most likely the result of a short term production of exopolysaccharide or another energy storage compound. Another explanation of this temporary increase was the limitation of oxygen in the biofilter. These anoxic conditions could have resulted in the use of nitrate as an electron acceptor for toluene degradation. As long as nitrate is available, a larger part of the biofilm is used for toluene degradation.

A wider range in temperature of high activity was seen than reported elsewhere. The broad community of toluene degraders in compost could have had overlapping optimal temperatures but above 55 °C, the majority of that community was greatly inhibited.

7.2 Water in biofilters

7.2.1 Recommendations

The water potential range in which the removal rate is optimal is very narrow; between -10 and -100 cm H_2O, with a maximum at -20 cm H_2O. A reduction in water potential of -300 cm H_2O leads to a reduction of 60% in EC. This means that accurate moisture control can improve biofiltration significantly.

As seen in Chapter 3, the maximal EC observed is at the same matric potential but at different water contents. Traditionally the volumetric or gravimetric water content is used to determine the water present because of measurement simplicity. Errors can occur when the optimal water content for one media is used for another. In these cases, water potential would avoid the error. A recommendation is that all water in biofilters should be reported in water potentials as this gives a more universal measure of the available water, independent of the medium.

7.2.2 Future work

The duration of the experiments did limit the number of repeated experiments. To show an even clearer picture more matric potential curves at a constant toluene concentration have to be repeated. The residual concentration for the experiments has to be above 100 ppm to be in the maximal EC region. These curves can be used in the model proposed by Ranasinghe (2003) to investigate the effect of water on full scale biofilters.

The region of matric potentials that was investigated varied between -5 and -300 cm H_2O. A broader range of matric potentials has to be investigated to confirm the loss of removal at low (> -300 cm H_2O) matric potentials. This means a redesign of the matric potential control method. There are simple physical constraints locating a water reservoir more than 200 cm below the membrane of the reactor. The system used at -300 cm H_2O was not suitable for long experiments due to small pressure leaks. The reservoir used was a glass flask open to the atmosphere. The flask was sealed with a rubber stopper which did not seal adequately. The reservoir could be of a similar design as the reactor. Two stainless steel plates (part C.4 in Fig 2.8) clamping a piece of glass tubing (part C.3) together. The port in the bottom plate

provides a connection to the water reservoir of the reactor. The ports in the top plate provide a connection to a manometer and a connection to pull a vacuum on the head space

Only compost has been investigated, but other types of medium are used in biofilters, like soil and peat. Soil, sand, compost and peat have a significantly different water retention capacity (Fig. 3.1). Serum bottles were used to choose the compost with the highest degradation. Screened top soil was also tested and found to have similar degradation rates as the tested composts (data not shown). As seen in Chapter 3, the two composts investigated had different water holding capacities especially at higher potentials, but they had similar EC's at the same water potential. The conclusion was that the water potential and not water content was the predominant factor affecting degradation. Different media like peat and soil can be investigated as well to confirm that the matric potential is more important than the water content.

Another interesting experiment is to explore the influence of water content on other compounds with higher and lower solubilities than toluene in water. Two compounds that are becoming more important as environmental problems are methane and ethanol. Methane emissions from landfills are important due to global warming concerns, especially at low concentration when collection is not viable. Ethanol is a common industrial emission in food and beer manufacturing and contributes to smog formation.

7.3 Microbiology

7.3.1 Recommendations

The number of toluene degraders can vary widely in different sources of compost. To achieve high removal rates, a large number would be beneficial. A recommendation to decrease start-up times is using an inoculum, preferably isolation from the same medium. Together with a high toluene concentration at start-up (Sec.7.3.1) and extra nutrient additions (Sec. 7.4.1), inoculation could lead to a significant improvement in removal rates.

7.3.2 Future work

The two experiments with the biofilm (Sec. 4.6.2) did not reach the maximal removal rates due to equipment failure. More experiments are needed to explore the effect of toluene concentration on the removal rate curve. This will give more insight if the assumptions in the models in Chapter 5 are valid.

Using a biofilm instead of compost in the reactor does give some advantages in exploring the different environmental conditions on degradation. Also knowledge about the amount of biomass present does remove any uncertainties and assumptions versus the use of compost or any other bed material. In order to obtain specific rates, the biofilm thickness had to be known. The biofilm thickness was measured before by SEM micrographs. This is a destructive method. It is important for experimental continuity that non-destructive methods to measure biofilm thickness are developed. Options from the literature include scanning confocal laser microscopy (Klausen *et al.*, 2003; Moller *et al.*, 1996; Pamp and Tolker-Nielsen, 2007) and a laser triangulation sensor (Okkerse *et al.*, 2000).

The isolated cultures consisted probably out of multiple strains, so the rates obtained were an average of the microbial cultures present. A detailed study in the composition and dynamics of the mixed cultures would be useful to determine the dominant strain or strains. A comparison in rates between pure and mixed cultures could possibly show that a synergy between cultures is more beneficial, than single cultures. The accurate control of the environmental parameters, easy start-up and sampling make the reactors an ideal tool.

The isolated strains demonstrated high removal rates (Sec. 4.6.2.1) but the high rates could be a direct result of the biofilm being unsaturated. Biofilm reactors like a membrane bioreactor (MBR), a hollow fibre reactor or a rotating biological contactor all operate with a saturated biofilm. More experimental work in comparing the removal rates of the same biofilm under saturated and unsaturated conditions is needed. If these results show a significant improvement, a new type of reactor can be developed. A suggestion for a reactor design would be using horizontal ceramic tubes.

The biofilm can be cultivated on the inside in the air phase, while the matric potential is controlled in the water phase on the shell side.

7.4 Pollutant

7.4.1 Recommendations

Toluene is known to be toxic to many micro-organisms. To improve biofilter operation, a high toluene concentration at start-up could help destroy unwanted cultures. The removal of these cultures will result in releasing nutrients into the biofilter medium. The toluene degraders can use these nutrients to assist in growth. As the number of toluene degraders is directly linked to the amount of toluene removed (Fig 5.9 compared to 5.10), an increase in degraders will increase the EC.

7.4.2 Future work

The variation of the toluene concentration is explored at only one matric potential (Sec 5.4.1). Future work at different matric potentials is currently in progress. Preliminary results show that the shape of the curves does not differ, but the maximal EC is lower supporting the results in Fig. 3.5 and 3.6. A decrease in matric potential from -5 cm H_2O to -40 cm H_2O resulted in a decrease in the maximal EC of 30%. A further drop in matric potential is expected to see even larger reductions in EC. This shows that not only the toluene concentration and amount of biomass have a strong effect on the removal rate, but also the matric potential.

7.5 Nutrients and temperature

7.5.1 Recommendations

For optimal removal rates, this work shows a compost biofilter degrading toluene has to be within a temperature range between 25 and 50 °C (Sec. 6.5.2). Accurate temperature control (0.1°C) is not essential compared to controlling other parameters like matric potential, nutrients and pollutant concentration. The only important aspect in regards to temperature is that is can result in changes in the water content. Proper humidification remains essential.

The addition of nutrients and in particular nitrogen can improve the removal rate dramatically (Sec. 6.5.1). Periodical nitrogen addition, in particular during the start-up

phase will improve the removal capacity. Some problems are also related to nutrient addition. Nutrient solutions can aversely increase the water content of the biofilter bed. This will increase mass transfer resistance and pressure drop, thus a reduction in EC. Also leachate can wash away a large portion of the nutrients. Ideally, the addition of nutrients to the biofilter has to aid in maintaining the present biomass and not promote growth (Delhomenie *et al.*, 2001a). Growth does result in higher removal rates, but will ultimately lead to failure due to clogging of the bed.

7.5.2 Future work

Nutrient availability is variable depending on the source of compost. Although compost is considered to have plenty of nutrients available, more investigation will give insight if adding nutrients is required irrespectively of the compost source. Evaluation of the available nitrogen in different composts and soils and measure their performance after start-up could show that screening the bed material before operation can lead to a significant improvement on the performance.

One of the possible explanations for an increased removal during nitrate addition (Sec. 6.5.1) is the use of nitrate as an electron acceptor in the absence of oxygen. The reactor system gives control of the gas atmosphere, so the oxygen concentration can be controlled. If toluene is removed at low or zero oxygen conditions in the presence of nitrate, anoxic degradation is possible. As well as decreasing the oxygen, an increase in oxygen would help in determining if oxygen is a limiting factor during the experiments.

7.6 General future work

An important parameter is the number of toluene degraders in the compost. In combination with the experiments discussed in Sec. 7.1.2 and 7.4.2, the number of colony forming units (CFU) of the bed material can be determined before and after acclimatisation in the reactor. This will give an insight in reactor start-up times and initial steady states in relation to the number of CFUs on toluene.

An assumption in biofiltration is that at steady state the net growth is zero. This means that all the energy from the consumed pollutant is used for maintenance. To increase

this maintenance demand will result in an increased removal rate. One method, used to reduce activated sludge production in waste water treatment is the use of chemical uncouplers or protonophores. Although a biofilter is not an actively growing system, the principle should be explored.

Oxidation of a substrate creates a proton motive force across the intracellular cytoplasm membrane which creates a driving force for the oxidative phosphorylation. The chemical uncouplers carry protons through the membrane and remove the driving force that is needed for the chemiosmotic mechanism of oxidative phosphorylation of ADP to ATP (Low and Chase, 1998; Wei *et al.*, 2003). This means that in order to generate enough ATP for maintenance requirements, more substrate has to be processed. The addition of a chemical uncoupler to a biofilter could result in an increased removal rate without a build-up of excess biomass.

The manual data collection in the current setup is very time consuming. They could be more even more effective if the data collection could be done automatically. The analytical unit could be a GC or online VOC sensor. A multiport valve is needed to switch between the in- and outlets of the reactors.

The carbon dioxide is not monitored regularly. Combining the automation of the gas analysis should include the online analysis of CO_2. The analysis of CO_2 would help close the carbon balance and show if carbon is stored in either biomass or storage compounds.

7.7 References

Delhomenie, M. C., L. Bibeau, J. Gendron, R. Brzezinski, and M. Heitz. 2001. Toluene removal by biofiltration: Influence of the nitrogen concentration on operational parameters. *Industrial & Engineering Chemistry Research* 40: 5405-5414.

Klausen, M., A. Heydorn, P. Ragas, L. Lambertsen, A. Aaes-Jorgensen, S. Molin, and T. Tolker-Nielsen. 2003. Biofilm formation by *Pseudomonas aeruginosa* wild type, flagella and type IV pili mutants. *Molecular Microbiology* 48: 1511-1524.

Low, E. W., and H. A. Chase. 1998. The use of chemical uncouplers for reducing biomass production during biodegradation. *Water Science and Technology* 37: 399-402.

Moller, S., A. R. Pedersen, L. K. Poulsen, E. Arvin, and S. Molin. 1996. Activity and three-dimensional distribution of toluene-degrading *Pseudomonas putida* in a multispecies biofilm assessed by quantitative in situ hybridization and scanning confocal laser microscopy. *Applied and Environmental Microbiology* 62: 4632-4640.

Okkerse, W. J. H., S. P. P. Ottengraf, and B. Osinga-Kuipers. 2000. Biofilm thickness variability investigated with a laser triangulation sensor. *Biotechnology and Bioengineering* 70: 619-629.

Pamp, S. J., and T. Tolker-Nielsen. 2007. Multiple roles of biosurfactants in structural biofilm development by *Pseudomonas aeruginosa*. *Journal of Bacteriology* 189: 2531-2539.

Ranasinghe, M. A. 2003. Modelling the mass and energy balance in a compost biofilter. *Chemical and Process Engineering*. University of Canterbury, Christchurch.

Wei, Y. S., R. T. Van Houten, A. R. Borger, D. H. Eikelboom, and Y. B. Fan. 2003. Minimization of excess sludge production for biological wastewater treatment. *Water Research* 37: 4453-4467.

Appendix A

A.1 Reactor robustness

The initial version of the reactor design used both the components of the 90 mm glass filtration unit (Labglass^{TM} Filtration Assemblies, 90mm diameter, 1000 ml, Cole-Parmer, Vernon Hills, IL). The bottom filter holder was filled with water and a membrane was fitted. The head space was put under a 1 bar overpressure and submerged in a water bath during leak testing. The next day the bottom fritted glass funnel was found shattered. Under normal circumstances the water would remain in place, but a small leak in the membrane released the water. And the pressure difference between the headspace volume and the funnel volume broke the fritted glass disk.

A second funnel broke while using the reactor. After several days into the run, air leaked under the membrane, which reduced the area of contact of the membrane with the water phase. Reduced contact meant a reduced transfer of water into or out of the compost on top of the membrane. When disassembling the reactor, a crack was discovered in the fritted funnel. It is unclear whether this was caused by a manufacturing fault or by over tightening the threaded rods. This resulted into a redesign of the filter holder as seen in Sec. 2.2.2.

The new design was robust. No problems were discovered during the operation. In case of breakage of the glass tubing were easily and cheaply replaced using appropriate diameter glass tubing.

The region of matric potentials that was investigated varied between -5 and -300 cm H_2O. There are simple physical constraints locating a water reservoir more than 200 cm below the membrane of the reactor. The system used at -300 cm H_2O was not suitable for long experiments due to small pressure leaks. The reservoir used was a glass flask open to the atmosphere. The flask was sealed with a rubber stopper which did not seal adequately. A suggestion for a new design is suggested in Chapter 7.

A.2 Leak testing

The leak testing was conducted for the reactors and for the whole system. The reactor was sealed and pressurized using a 60 ml syringe. All possible sources of leaks were sprayed with water and detergent. Any appearance of bubbles indicated a leak. The leak testing was repeated before every run. The complete experimental setup was pressurised and checked for leaks with water and detergent. Long term, slow leaks were detected with the attached water manometers. Any detected leaks were fixed before the experiments were started.

A.3 Sampling and GC calibration

The concentration of toluene in the gas stream is measured using gas chromatography (Varian CP-3800) with a flame ionization detector capillary column (Chrompack Cp-Sil 5 CB) and helium as the carrier gas. The temperature of the injector, oven and detector are 220, 180 and 200 ^{0}C, respectively. Gas samples of 0.2 ml are taken at the inlet and outlet of the reactor using a 1ml gas tight syringe (SGE).

A calibration curve was made using a known amount of liquid toluene in a known volume of air in a Tedlar bag. Details can be seen in Table A.1 and results in Fig. A.1. This curve was used to correct all toluene concentrations in the experiments.

***Table A.1**: The GC calibration curve.*

Concentration (ppm)	**Liquid toluene (µl)**	**Air (ml)**	**Average peak area**
50	0.43	2000	8808 ± 306
100	0.87	2000	18126 ± 426
200	1.74	2000	36585 ± 618
500	4.35	2000	88961 ± 588
1000	8.69	2000	186628 ± 2475

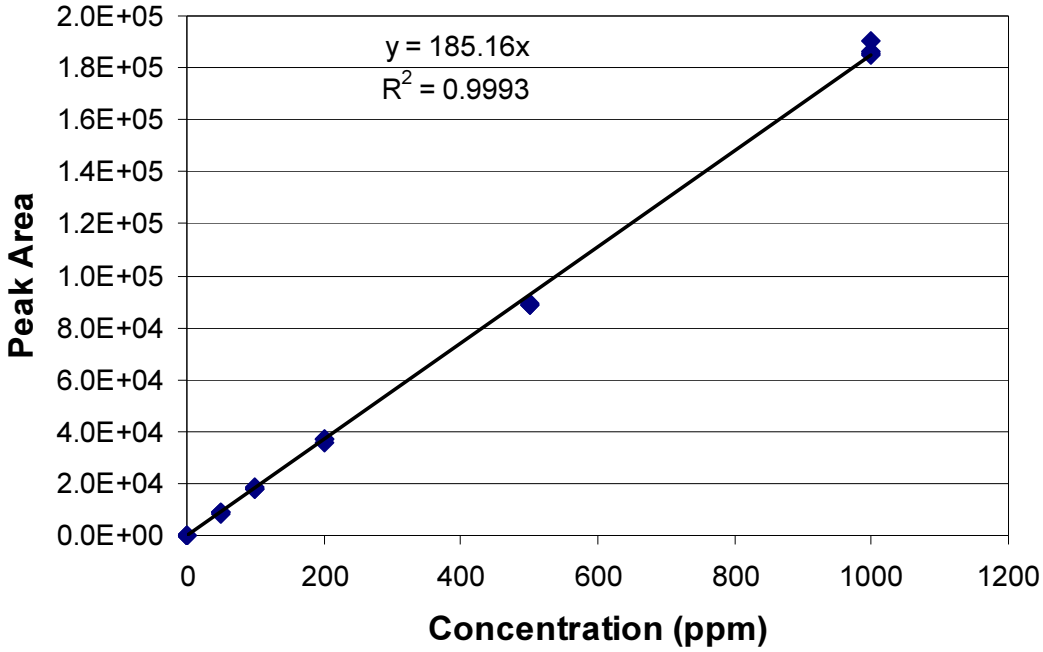

***Figure A.1**: The GC calibration curve. The equation is based on a linear fit through the origin.*

A.4 Mass balance discrepancy

The first control experiment was done without any compost to identify abiotic toluene loss. The results show (Fig. A.2) that there was a discrepancy between the inlet and outlet concentration, even when the large error of sampling is taken into consideration.

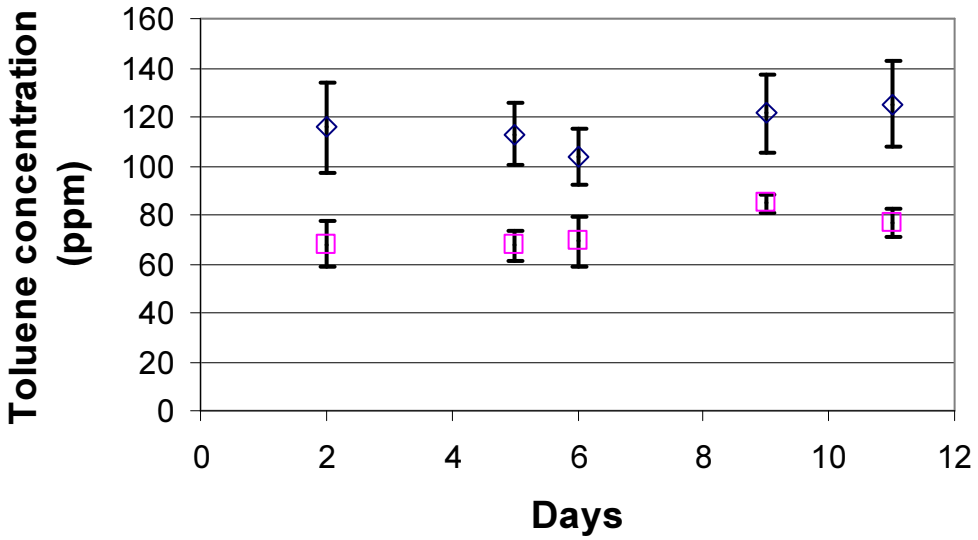

***Figure A.2**: The losses in the blank run caused by a biofilm growing on the bottom (water side) of the membrane. Concentrations are normalized to 100 ppm. The open circles (○) represent the inlet and the open squares (□) represent the outlet concentration. The error bars represent one standard deviation over all samples (9 or more).*

After the run, the reactor was disassembled and inspected. The mixed cellulose membrane was removed from the mesh and upon closer inspection a slimy layer was discovered on the water side of the membrane. This appeared to be a biofilm that could have removed the toluene from the reactor. No experiment to confirm the nature of slimy layer was attempted. Handling of the reactor components along with non-sterile air potentially caused the contamination. The reactor and water were autoclaved (121°C for 20 min) and the experiment was repeated. No significant losses after this were observed (Fig. A.3).

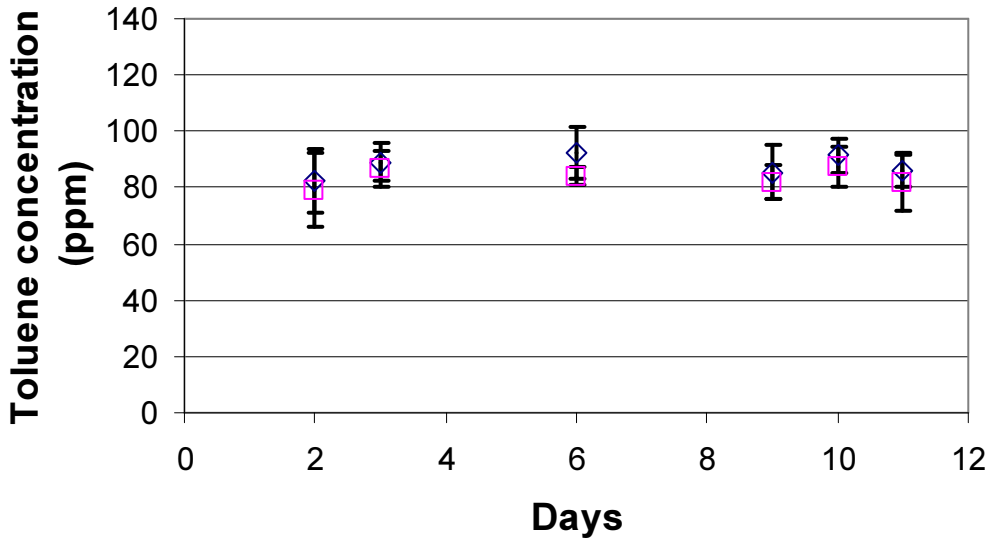

***Figure A.3**: Inlet and outlet concentration of the blank after cleaning and autoclaving. Concentrations are normalized to 100 ppm. The open circles (○) represent the inlet and the open squares (□) represent the outlet concentration. The error bars represent one standard deviation over all samples (9 or more).*

A.5 Diffusion tube

A diaphragm pump was used to provide head space mixing in Reactor 1. An experiment was conducted where the concentration generated by the diffusion tube was monitored without and without the diaphragm pump for head space mixing. The results of this experiment can be seen in Fig. A.4.

The circulation pump added both a vibration and a pulsation to the system. Both of these can increase mass transfer rates (Baird and Garstang, 1972). The accuracy of the concentration generated by the diffusion tube is directly linked to the stability of the flow rate. A stable concentration is important in acquiring reliable steady state removal rates.

In order to keep Reactor 1 operating with the diaphragm recirculation pump, bottled compressed air with a known amount of toluene was used to feed the reactor. But as the diffusion tube system adds flexibility to the overall experimental system, Reactors 2 and 3 were designed using direct agitation.

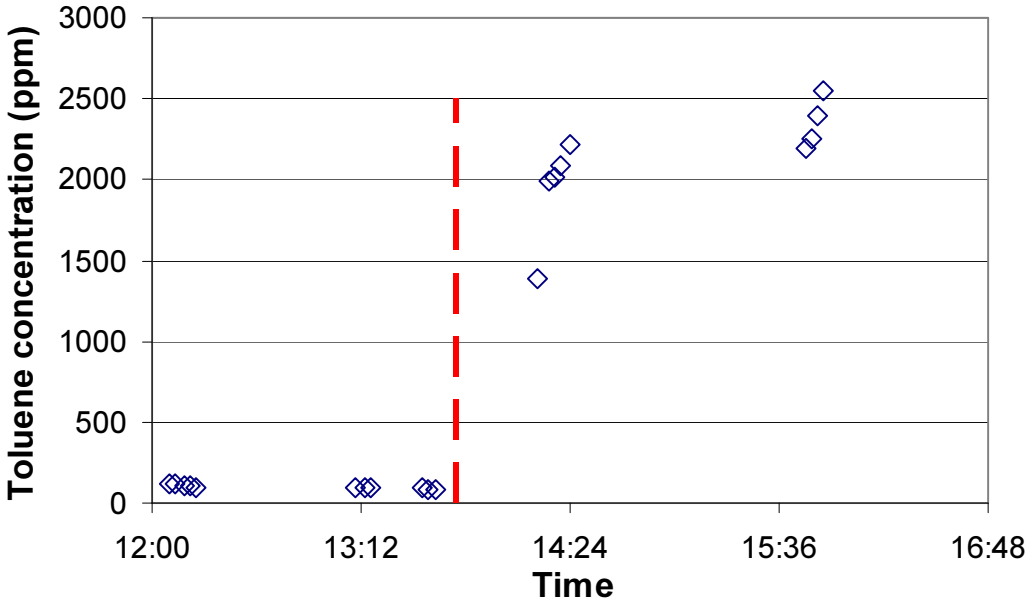

***Figure A.4**: Effect of the circulation pump on the diffusion tube output. The pump has been switched on at the red dotted line. This leads to a 20-fold increase in the toluene concentration.*

A.6 Gas bottles

The first (Table A.2) gas bottle that was purchased from BOC was a small (D size) bottle. The concentration in the bottle was similar to samples prepared by mixing a known amount of liquid toluene in a Tedlar bag. For Reactor 1, a larger (G size) bottle was purchased. The concentration in this bottle was found to be almost 5 times smaller than in the first bottle. After contacting BOC with this problem, they sent a new one. They suggested that the bottle be kept warm in order to prevent any toluene condensation and reducing the gas phase concentration. The concentrations of the bottles used with Reactor 1 were based on a calibration curve from known toluene concentrations in a Tedlar bag.

***Table A.2**: The standard gas bottles used in the experiments with Reactor 1.*

Size	Recipe	Used	Labeled (ppm)	Measured (ppm)
D	MB 83263	21-3-2006	102 +- 9	90
G	MB 84084	3-4-2006	100 ± 10	20
G	MB 84084	19-6-2006	102 ± 10	60
G	MB 84084	12-12-2006	100 ± 10	40
G	MB 84084	4-7-2007	100 ± 10	50
G	MB 84081	19-12-2007	500 ± 10	40
G	MB 84081	10-1-2008	505 ± 30	20

The biggest discrepancies in the concentration were with the 500 ppm toluene in air bottles. Both bottles had significantly lower concentrations than was ordered. After informing BOC in the matter, they never provided a satisfying answer and eventually started not answering enquiries.

A.7 Humidifier

The humidifier was capable of handling air flows up to 10 L min^{-1}. In this application, the flow rate did not exceed 50 ml min^{-1}.and therefore should have easily generated air at close to 100% relative humidity. In order to confirm this, the water consumption rates over time were monitored. The humidifier was connected in the siphon mode (Sec. 2.4). Instead of a large water reservoir, a 5 ml graduated glass pipette was used to accurately monitor water consumption.

To calculate the theoretical water consumption rate the modified Clausius Clayperon equation over liquid water was used (Eq. A.1).

$$\ln e_s = 53.67957 - \frac{6743.769}{T} - 4.8451 \cdot \ln T \qquad [A.1]$$

Using Eq. A.1 and the ideal gas law (Eq. A.2), the concentration of the water in the air was calculated. In combination with the gas flow rate, a theoretical water consumption rate (Eq. A.3) was determined.

$$c = \frac{n \cdot M_w}{V} = \frac{e_s}{RT} \qquad [A.2]$$

$$Consumption = c \cdot F_g \cdot t \qquad [A.3]$$

The consumption rate was monitored for 18 days for an average time between 16 and 90 hours. The water consumption on average was 60% higher than theory predicted. On average 0.021 ml hr^{-1} of water was missing at a consumption rate of 0.058 ml hr^{-1} (theoretical consumption 0.038 ml hr^{-1}).

An explanation of this discrepancy was that there is a small leak to the outside in the humidifier and tubing. The leak was so small that all the water leaked evaporated and therefore was not visible. A second explanation was that liquid water slowly diffused through the Nafion membrane and formed a film of water inside the tube. The water film slowly built up and the air flow dragged the liquid water along into the reactor. The extra water consumption was so small that it was unlikely to influence the results in the reactor in any way. Even if excess water fell into the reactor, it would drain away through the membrane.

A.8 Mass transfer within the compost layer

This experiment was designed to validate the assumption that the compost layer of 3 mm thickness had no external mass transfer limitations. A layer of Plus Extra compost was loaded on top of the membrane in Reactor 3. A mass of 6.10 g of wet compost (53.3% or 1.14 g water g^{-1} dry compost, is 2.85 g dry compost) was loaded into a 53 mm diameter and 5.0 mm high stainless steel ring, and lightly tamped down to the height of the ring. The ring was subsequently removed. The reactor was reassembled and operated at 30 °C, a matric potential of -20 cm, a gas flow rate of 22 ml min^{-1} and a toluene inlet concentration of 66 ppm.

A steady state was reached after 550 hr and monitored to 930 hr. After which 2.817 g of wet compost was removed from the reactor. The water content was 62.2%. The remaining compost (1.79 g dry) was lightly packed into a 53 by 3.0 mm SS ring. The reactor was reassembled and the conditions were kept as before.

After 1338 hr, the reactor was opened again and 2.92 g (water content 2.2 g water g^{-1} dry compost) wet compost was removed. The remaining compost (0.91 g dry compost) was padded into a 53 by 1.6 mm SS ring. The reactor was reassembled and the conditions were kept as before. The inlet and outlet concentrations were measured as described before. The amount of compost loaded was not only to be described by the volume, but also the weight of it (Table A.3). With the weight the bulk density can be calculated and these are similar for all three experiments

Table A.3*: Values of the compost loaded into 55 mm packing rings.*

Ring depth (mm)	Dry weight (g)	Volume (cm^3)	Dry bulk density (g cm^{-3})
5.0	2.85	11.0	0.26
3.0	1.79	6.62	0.27
1.6	0.88	3.53	0.25

After the first steady state was reached, compost was removed and the water content measured. At a matric potential of 20 cm the water content was 62.2% or 1.65 g water g^{-1} dry compost. The average water content from the control experiments at 20 cm was 1.44 g water g^{-1} dry compost.

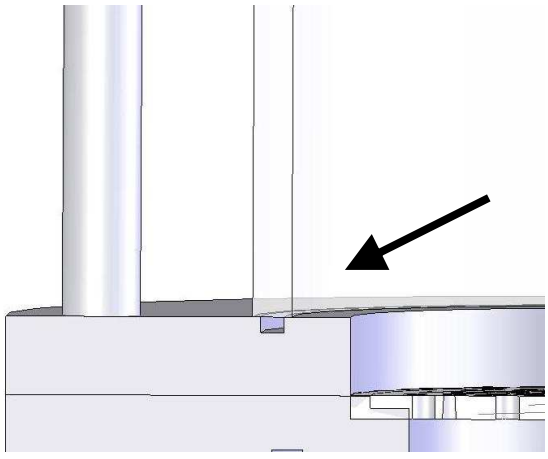

Figure A.5*: Open cut drawing of the ridge of R3, where water accumulated.*

At the second steady state more compost was removed. This compost had a very high water content of 2.20 g water g^{-1} dry compost. The stainless steel ring that clamps the Viton o-ring onto the membrane and where the top glass sits onto has a ridge (Fig. A.5) where water collected due to condensation. After moving the reactor out of the temperature controlled box, some of the water leaked on top of the compost,

increasing the water content. During normal operation, excess water that builds up on the ridge fell off the sides directly on the membrane. Between the edge of the compost and the SS ring was an 11 mm open space for the water to land and drain off.

During the experiments the inlet concentration (40 ± 2 ppm) and flow (22 ± 1 ml min^{-1}) were kept constant. The change in load (Fig. A.6) is caused by the reduction of the volume of the compost.

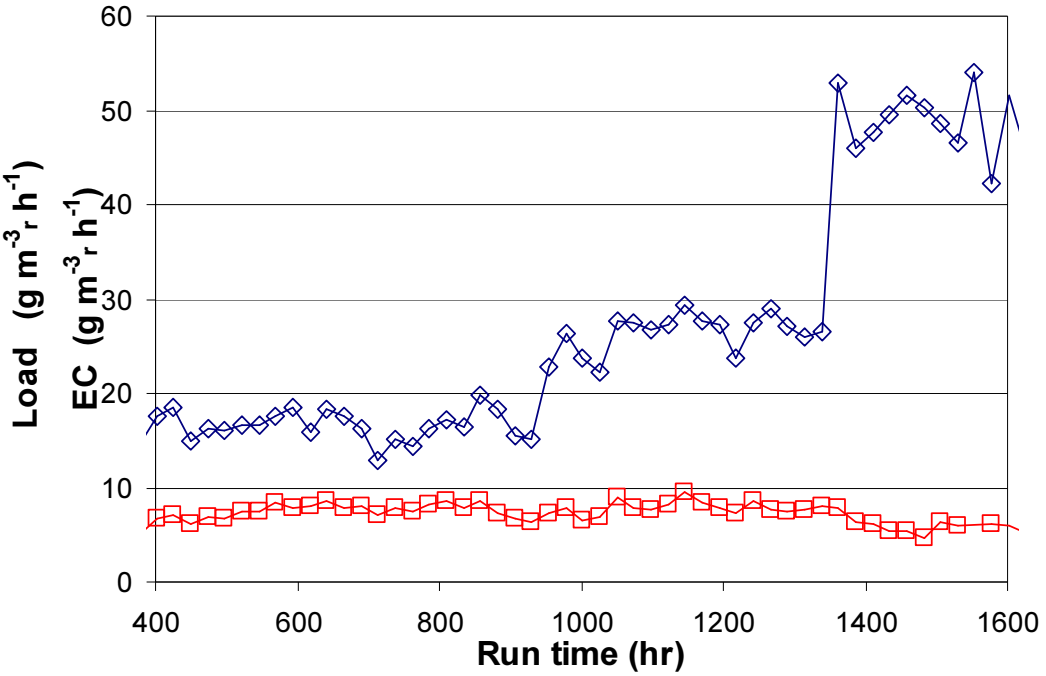

***Figure A.6**: Load and EC's of the layer thickness experiment in R3. Elimination capacity (open red squares (□) and load (open blue diamonds (◊).*

The results from Fig. A.6 can be summarized into Fig A.7. Although the EC at a layer thickness of 1.6 mm is ~ 25% lower then at 3 and 5 mm, the bulk density was similar.. As the EC of the thinnest layer was actually lower than with the thicker layers, it was concluded interparticle mass transfer did not restrict the EC. Therefore, no significant concentration gradient existed through the gas phase of the compost layer.

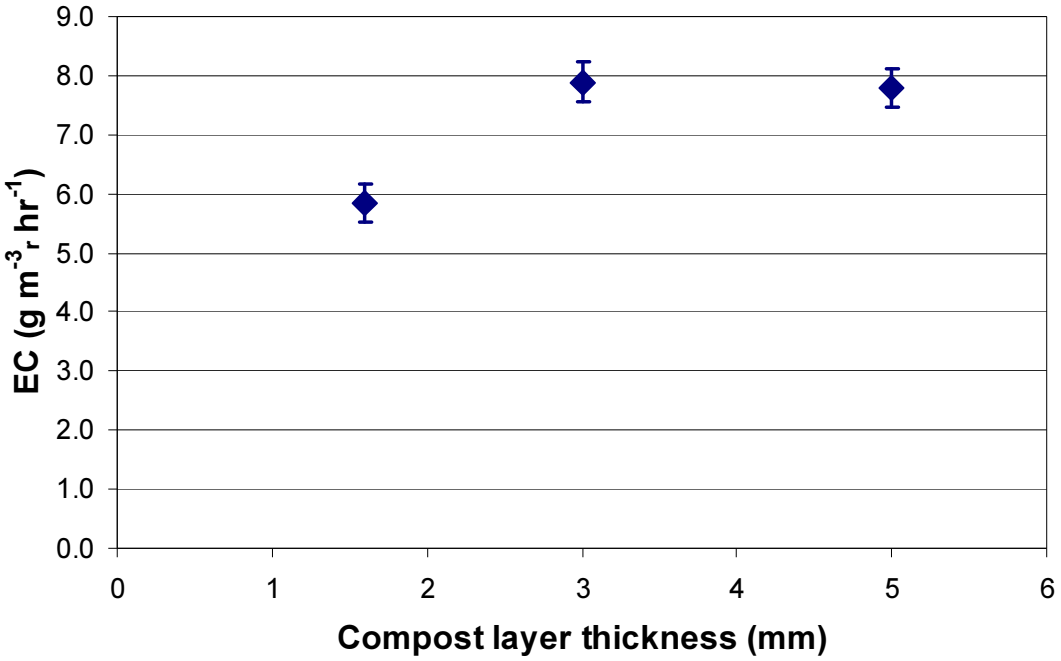

***Figure A.7**: The EC as function of the layer thickness in Reactor 3. The error bars represent 955 confidence interval.*

A.9 Water retention curves

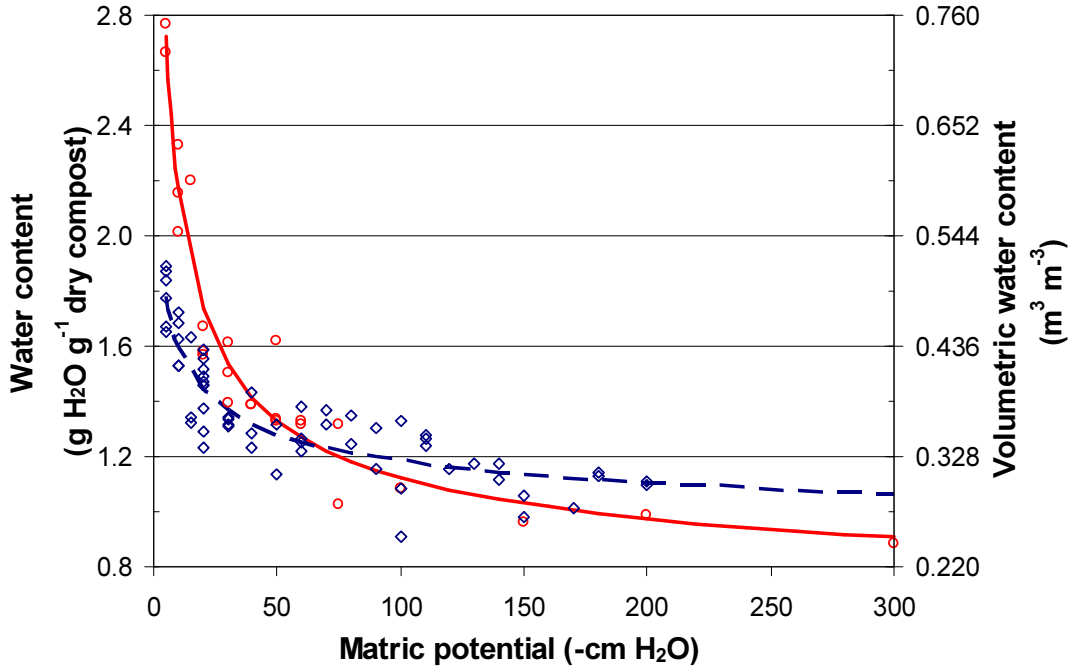

***Figure A.8**: Water retention curves with the Van Genuchten model fit for Compost 1 (red solid line and circles) and compost 2 (blue broken line and diamonds). The bulk density used is 270 kg m^{-3}.*

A.10 Experimental flow diagrams

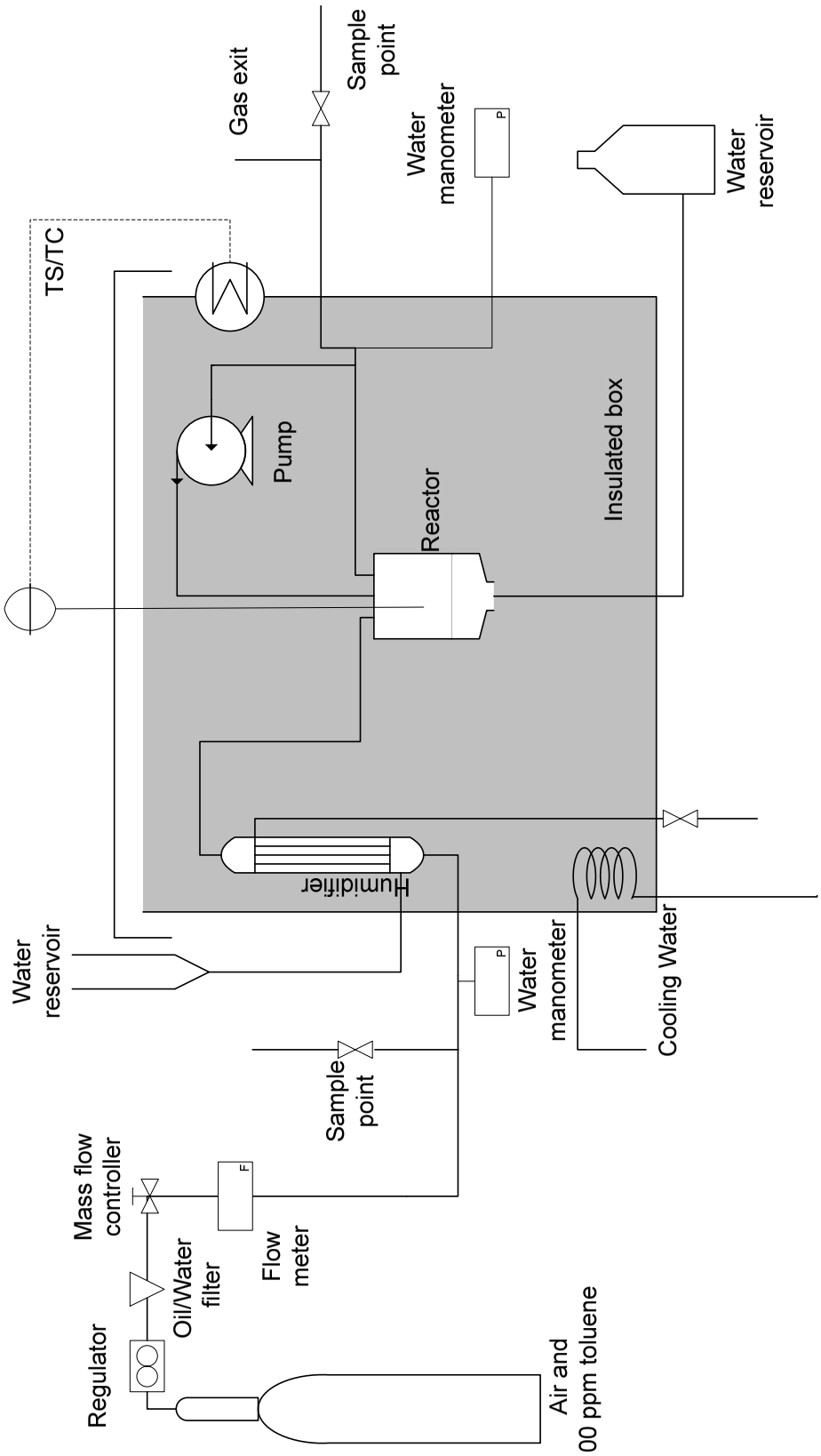

***Figure A.9**: The experimental setup of Reactor 1.*

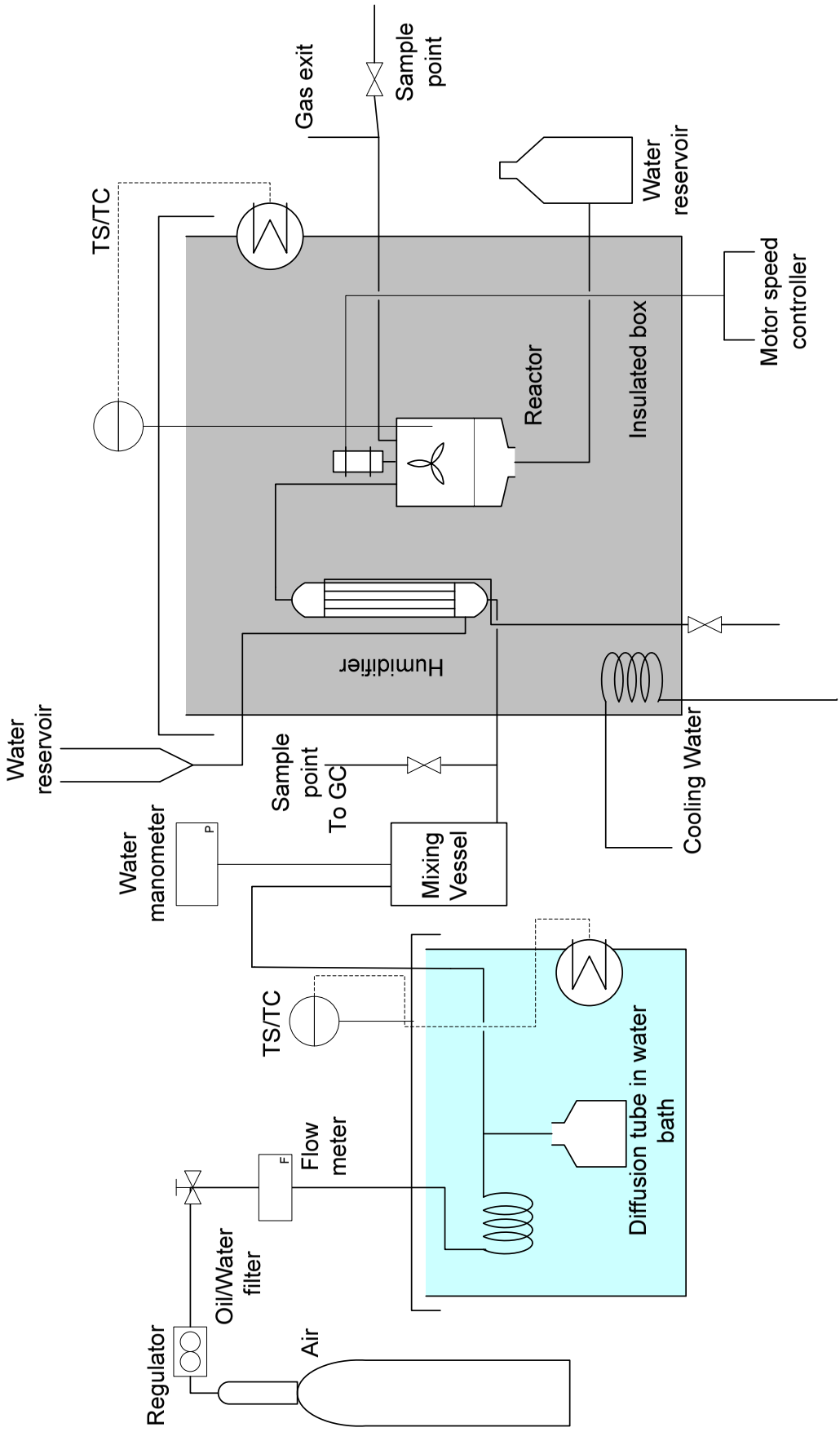

***Figure A.10**: The experimental setup of Reactor 2.*

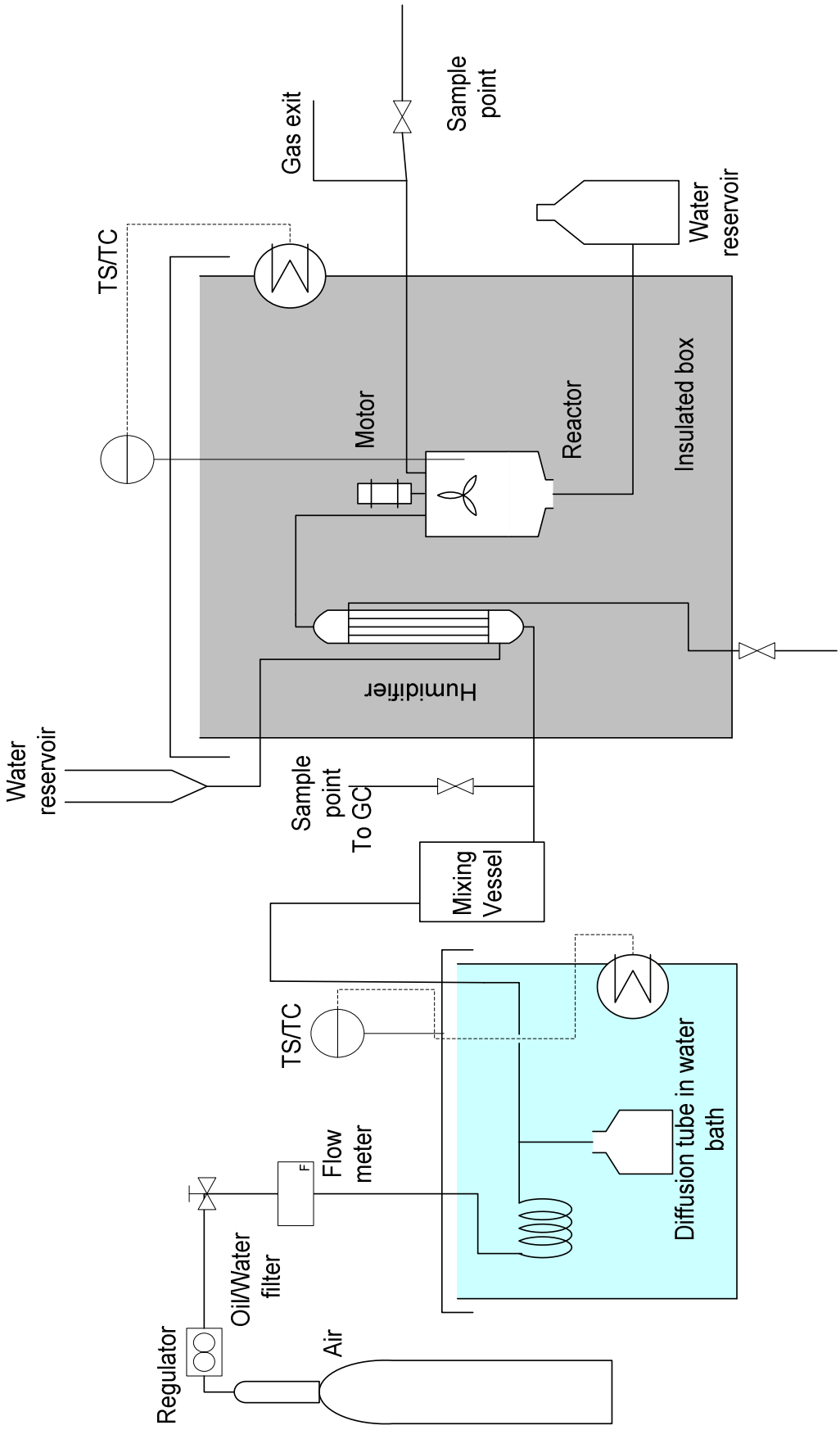

***Figure A.11**: The experimental setup of Reactor 3.*

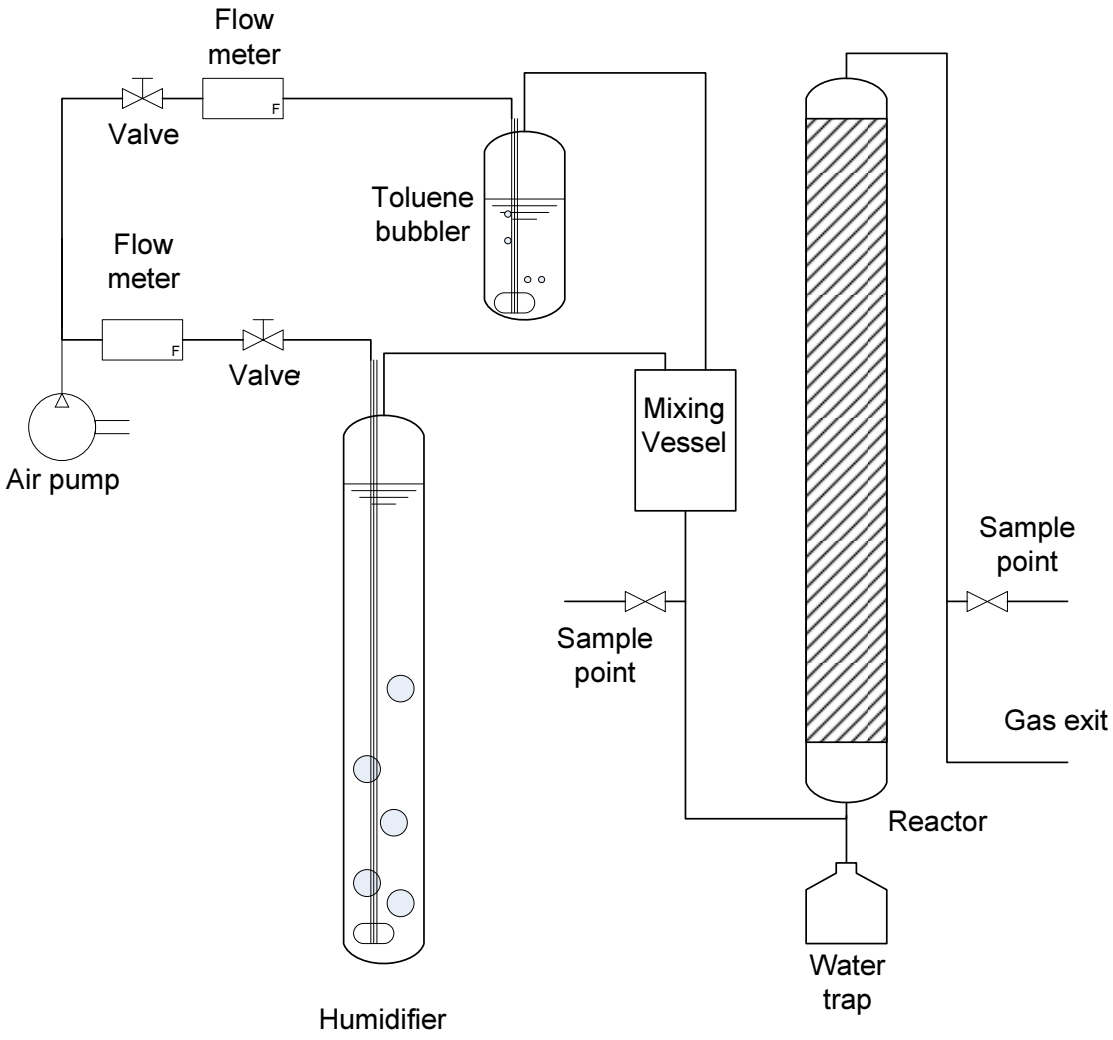

***Figure A.12**: The experimental setup of the Column Reactor.*

A.11 Nomenclature

c	concentration water in gas phase	$g_w\ m^{-3}{}_g$
e_s	saturation vapor pressure	mbar
F_g	gas flow rate	$m^3{}_g\ hr^{-1}$
M_w	molecular weight of water	$g\ mol^{-1}$
n	moles of water	-
R	gas constant	$J\ K^{-1}\ mol^{-1}$
T	temperature	K
t	time	hr
V	volume of gas	m^3

Subscripts

g	of gas
r	of reactor
w	of water

A.12 References

Baird, M. H. I., and J. H. Garstang. 1972. Gas absorption in a pulsed bubble column. *Chemical Engineering Science* 27: 823-833.

Appendix B

B.1 Growth medium

The medium chosen was based on the hydrocarbon degradation medium (HDM) described by Shen *et al.* (1998).

***Table B.1**: Medium composition adapted from Shen et al. (1998)*

Chemical	**Concentration (g l^{-1})**
$NaNO_3$	4.0
NaH_2PO_4	2.6
K_2HPO_4	1.2
$FeSO_4 \cdot 7H_20$	0.0035
$MgSO_4 \cdot 7H_20$	0.4
$CaCl_2 \cdot 2H_20$	0.02

Medium adjusted from pH= 6.1 to 7.03 with NaOH.

B.2 Direct Inoculation

Serum bottles (160 ml) were chosen because an atmosphere of toluene could easily be maintained and monitored. A volume of 25 ml medium (Table B.1) was transferred into serum bottles and closed with a butyl stopper and an aluminium cap. Five serum bottles were autoclaved at 121 °C for 20 minutes. The serum bottles were inoculated per the schedule in Table B.2 and incubated at 30 °C.

***Table B.2**: The inoculation schedule of the five serum bottles*

Bottle	Medium ml	Supernatant[a] µl	Spatula[b]	Compost[c] g	Toluene µl
1	25	150			25
2	25		V		25
3	25		V		25
4	25			0.09	25
5[d]	25				25

[a] 1 gram of compost was combined in 1 ml DI water in a 1.5 ml microtube, then shaken on a mechanical shaker and centrifuged for 60 seconds at 10,000 g. 150 µl of supernatant was used to inoculate serum bottle 1.

[b] Spatula: A stainless steel spatula was stirred through the compost for 10 seconds. Any compost attached to the surface was brushed off, and the spatula was dipped in the medium in the serum bottle and stirred around.

[c] The amount of wet compost directly added to the serum bottle.

[d] Control experiment.

B.3 Agar plates

Toluene degraders were selectively grown on agar plates in a toluene rich environment. The agar plates were prepared by combining 3.2 g agar with 170 ml medium. The agar was autoclaved for 20 min at 121 °C. The warm agar was poured into non-sterile glass Petri dishes. After cooling, the plates were inoculated according to Table B.3. The liquid was spread evenly over the agar using a glass rod.

***Table B.3**: Plates streaked*

Plate	Inoculated from
A	Water from Biomix, Plus Extra and Bioblend composts
B	Water from Results compost
C	Spatula stirred through Plus compost/mulch
D	1 ml aliquot from bottle 4
E	Water from composted garden soil
F	Left on bench for 30 min and touched with fingers

The plates were placed on a metal grid suspended in a glass desiccator chamber. The desiccator provided an enclosed environment for toluene-laden air. A small amount of water was added to cover the bottom of the desiccator to provide moisture in the air phase. Liquid toluene (150 µl) was added to the desiccator as the only carbon source. The desiccator with the plates was incubated at 30 °C. Small amounts of liquid toluene (100 µl) were added daily or when the desiccator was opened to inspect the plates.

After three days colonies appeared on plate A and a day later all plates had growth. After 7 days the plates were inspected and photos were taken (Fig. B.1).

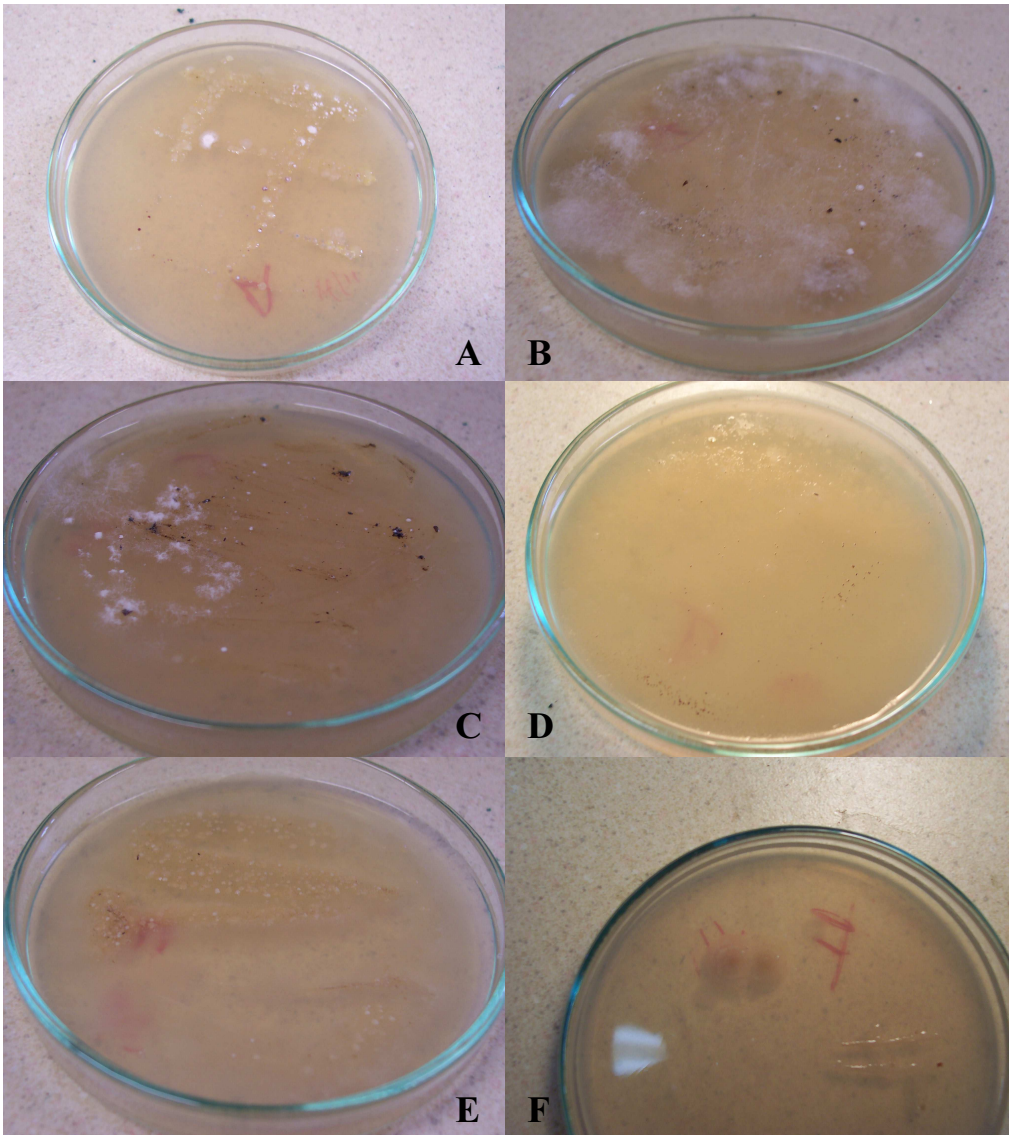

***Figure B.1**: Photos of the plates from Table B.3 after 7 days of incubation with toluene.*

B.4 Microbial growth in serum bottles

Liquid cultures were grown in serum bottles to generate sufficient biomass to inoculate the reactor. The medium used can be found in Table B.4. To the 499 ml of medium 1 ml of trace element solution (Table B.5) was added and the pH was adjusted to 7.05 with NaOH.

***Table B.4**: Medium composition*

Chemical	**Concentration (g l^{-1})**
$NaNO_3$	4.0
NaH_2PO_4	2.6
K_2HPO_4	1.2
$FeSO_4 \cdot 7H_20$	0.0008
$MgSO_4 \cdot 7H_20$	0.2
$CaCl_2 \cdot 2H_20$	0.009

***Table B.5**: Trace element solution composition*

Chemical	**Concentration (g l^{-1})**
$CoSO_4$	0.236
$CuSO_4$	0.395
EDTA	2.499
$FeSO_4 \cdot 7H_20$	5.019
$ZnSO_4$	11.054
$MnCl_2$	1.747

Four serum bottles with 30 ml of medium were inoculated taking a sample of the colonies according to Table B.6 and placed in an incubator / shaker (Minitron, Infors AC, Switzerland) at 30 °C. Gas samples were taken at the start and certain intervals using the method described in App. A.3.

***Table B.6**: Serum bottles pure culture*

Bottle	Inoculated from Plate	Liquid toluene (µl)
A	A	10
B	B	10
E	E	10
F	F	10

After three days in the incubator gas samples were taken and analyzed on the GC. A volume of 10 µl liquid toluene was added to bottle E, and 25 ml of sterile air (0.45 µm syringe filter) was added to all four. The bottles were returned to the incubator. The bottles were analyzed a month later and fresh sterile air (60 ml) and 5 µl liquid toluene was added to all four bottles.

At t = 0 the bottles are prepared as described before. After incubation at 30 °C for 11 days, the toluene concentration was measured. All bottles except for bottle F had approximately 0.02 % of the initial toluene present. In Fig. B.2 the relative removal of toluene is presented at one month after inoculation of the bottle cultures.

Toluene was added (day 49) to achieve a gas phase concentration of 14,000 ppm. After three days the concentration in the bottles was halved. Hardly any toluene was removed in the four days thereafter. Oxygen limitation was suspected to be the cause. To remove 22,000 ppm of toluene, stoichiometrically nine times the amount of oxygen is needed (see Sec. 4.2.2). At an initial oxygen concentration of 20%, most of the oxygen would have been depleted.

Red colonies were discovered on Plate F and were used to inoculate a serum bottle with 20 ml medium and 5 µl liquid toluene on day 44. The bottle was named R. Toluene was added to the bottles as in Table B.7.

***Table B.7**: Toluene addition to the serum bottles*

Time days	Liquid toluene added µl	To bottles
38	10	A, B, E
38	7	R
38	4	F
49	5 (+air)	A, B, E, F and R
52	5	B and R
53	5	B, E and R

After 57 days the overpressure was relieved and the bottles were flushed three times with fresh air. The bottles were pressurised to approximately 1.5 atm. The added toluene was depleted in bottles B and R within 2 days. The freshly added toluene was removed in the day after. No significant removal was seen in bottles A and F. The first 2 days after the adding the air, bottle E did not remove any toluene. But a day later 93% was removed.

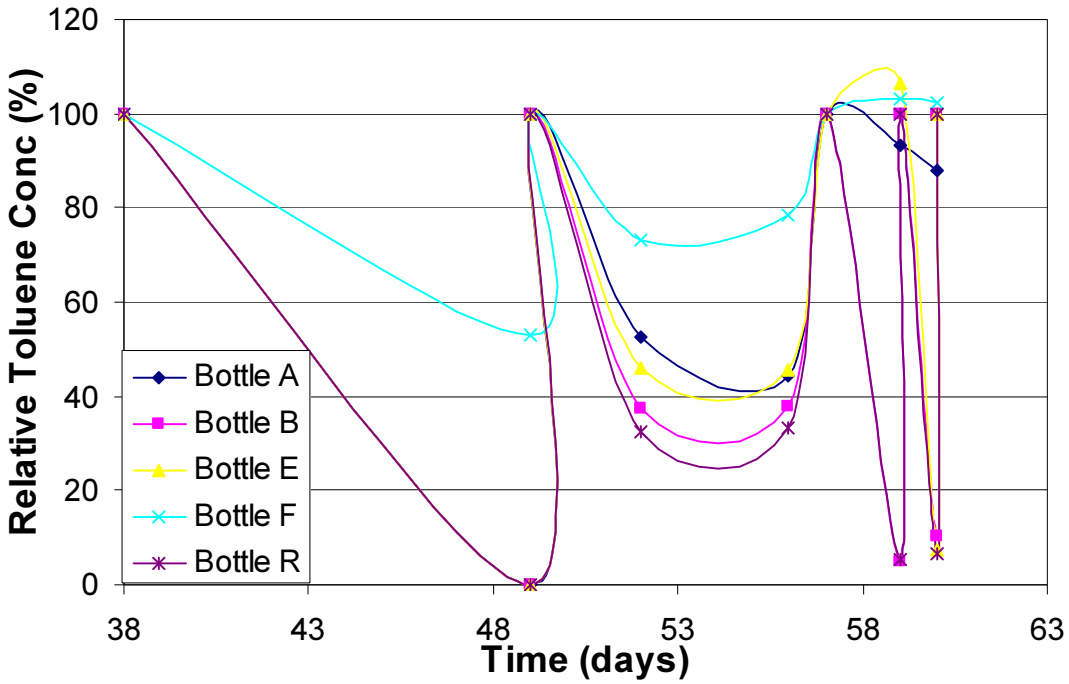

***Figure B.2**: The removal of toluene using the suspended cultures in serum bottles. The corresponding toluene additions are in Table B.7*

The microbial suspensions in the serum bottles were kept alive for more than a year. Even after ignoring them for 8 months, the capacity to remove toluene was still present.

Fresh air and toluene were added on day 287, which was removed by bottles A and B within 48 hours (Fig B.3). Two days later bottle E also picked up the removal, although F and Red did not remove any significant amounts

***Table B.8**: Toluene addition to the serum bottles*

Time days	Liquid toluene added µl	To bottles
289	2	A, B, E, F, Red
290	5	A, B, E, F, Red
291	5	A, B, E, F, Red

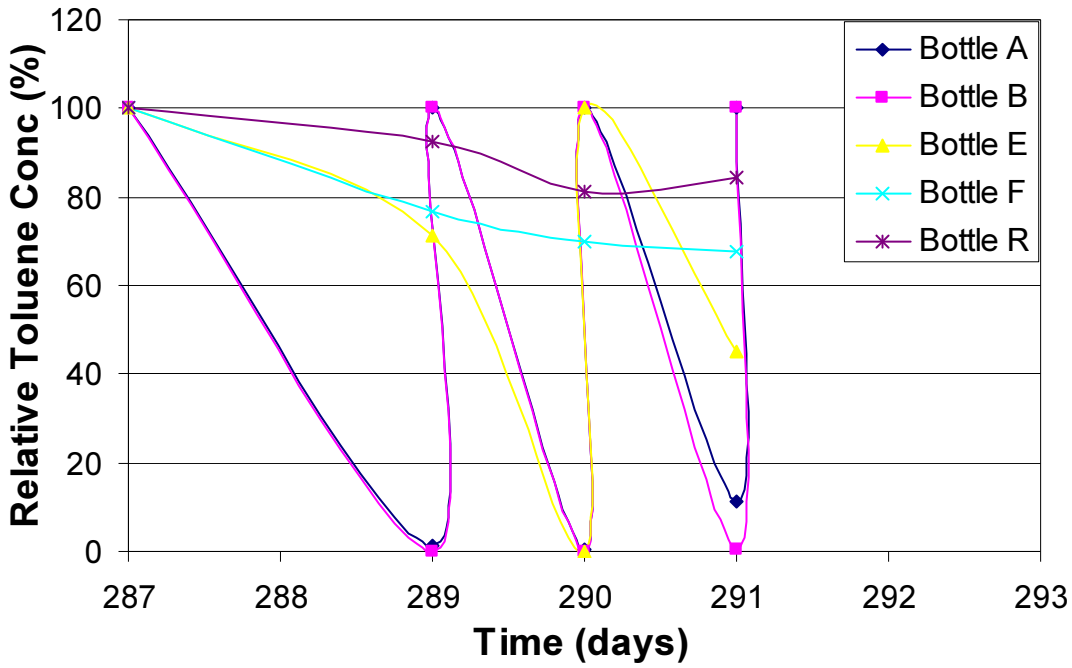

***Figure B.3**: The removal of toluene using the suspended cultures in serum bottles. The corresponding toluene additions are in Table B.8*

Three more serum bottles were prepared to increase the microbial stock. The most active cell suspensions are used to inoculate new serum bottles (Table B.9).

***Table B.9**: Sub-cultures of the serum bottles.*

Bottle	Medium ml	Inoculum ml	Source of inoculum	Toluene µl	Air ml
1A	20	5	A	1	50
1B	20	5	B	1	50
1E	20	5	E	1	50

The bottles were kept into the incubator for two weeks. Fresh air and toluene were added after 305 days (Table B.10). The bottles were sampled regularly (Fig. B.4). The suspensions chosen for inoculation of run 1 were bottles A, 1A and 1E. Bottles B, E and F were less active, so were not considered. Bottles Red and 1B were not used as 30 ml of cell suspension was considered a large enough inoculum to see a significant removal rate.

***Table B.10**: Toluene addition to the serum bottles*

Time days	Liquid toluene added µl	To bottles
305	5	A, B, E, 1A, 1B and 1E
305	3	F and Red
306	5	1A
306	4	1B
306	3	1E
307	5	B, Red and 1A
307	4	E
308	5	A, B, E and F
308	8	Red, 1A, 1B and 1C
310	5	A,B,E, Red,1B and1E

After run 1 failed, fresh sterile air and 5 µl of liquid toluene was added to the bottles after 366 days and the toluene concentration was monitored for three days (data not shown). On day 368 15 ml of cell suspension from bottle 1E was used to inoculate run 2.

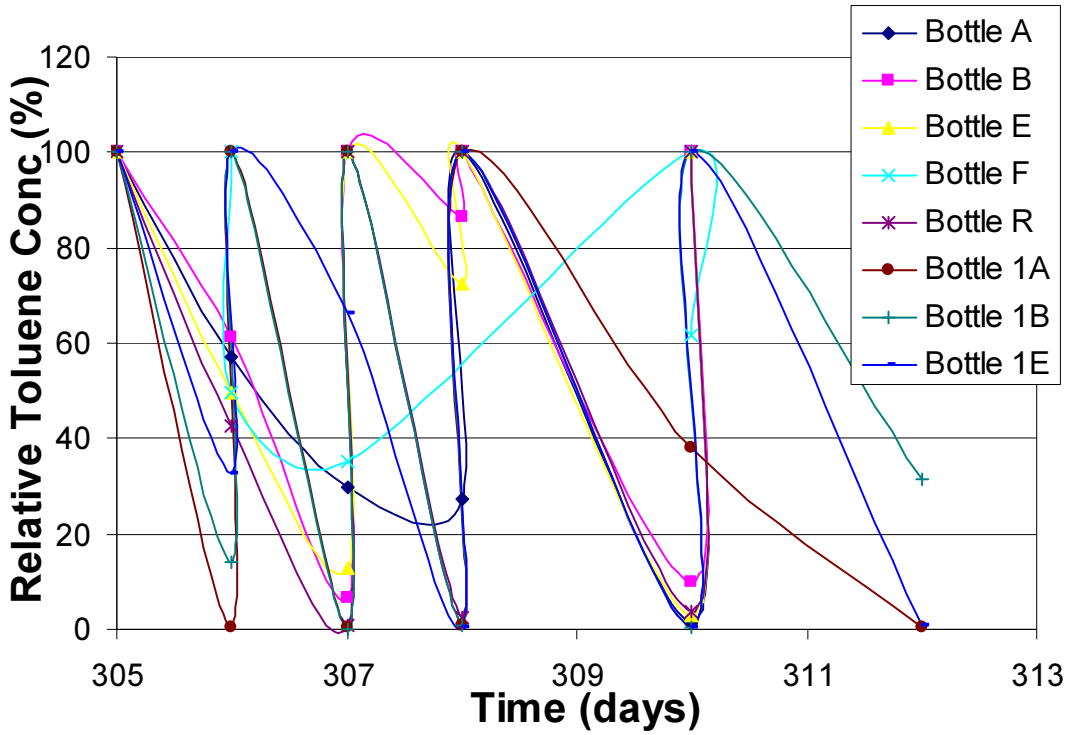

***Figure B.4**: The removal of toluene using the suspended cultures in serum bottles. The corresponding toluene additions are in Table B.10.*

B.5 References

Shen, Y., L. G. Stehmeier, and G. Voordouw. 1998. Identification of hydrocarbon-degrading bacteria in soil by reverse sample genome probing. *Applied and Environmental Microbiology* 64: 637-645.

Appendix C

C.1 Variation of toluene concentration in the reactor

The variation of the toluene inlet concentration was accomplished using three diffusion tubes and adjusting the water bath temperature to achieve the desired concentration. The concentration was controlled from 15.5 ±1.2 ppm to 638 ±22 ppm. The toluene concentration was measured using a GC and method as described in App. A.3. The concentrations did agree (Fig. C.1) for the small and medium diffusion tube with the theoretical concentrations (gas flow = 22 ml min^{-1}) using the method outlined in Sec. 2.3. The theory over-predicts the toluene concentration generated by the large diffusion tube. No explanation for the discrepancy was found. But concentrations generated by diffusion tubes are very sensitive to minor fluctuations in physical dimensions in Fig. 2.14.

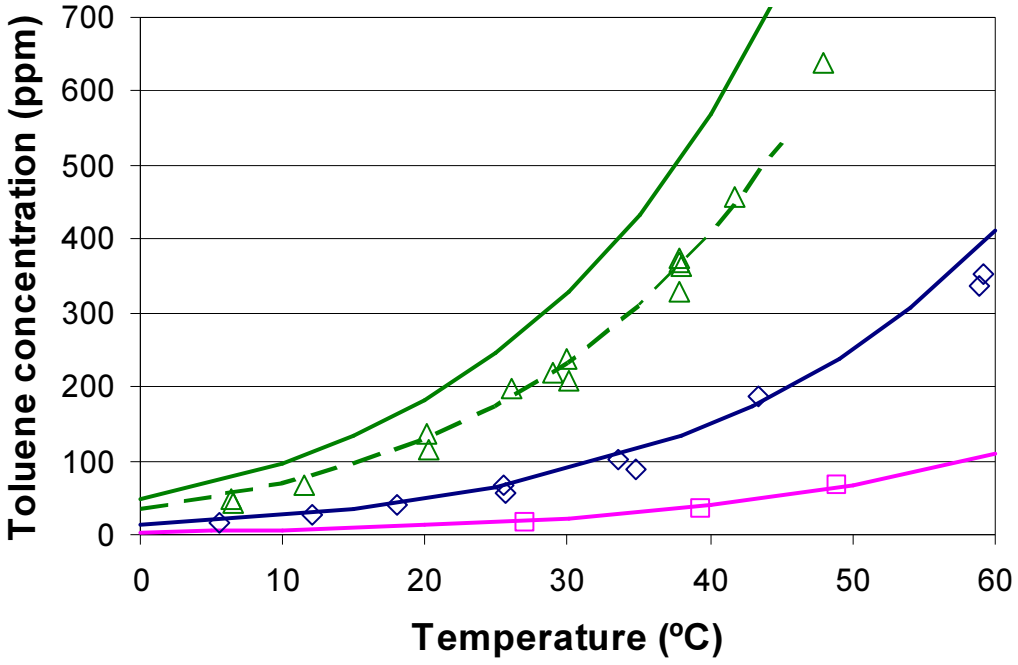

***Figure C.1**: Toluene concentration generated by the diffusion tubes (Large are the green triangles Δ, Medium: blue diamonds ◊ and Small: pink squares □) at different water bath temperatures. The solid lines are the prediction by the theory in Sec 2.3. The broken line is the prediction with an adjusted diameter for the large diffusion tube. Tube dimensions are described in Table 2.2.*

By adjusting the large diffusion tube diameter from 0.64 cm to 0.54 cm, the theoretical values calculated by Eq. 2.5 (green broken line in Fig C.1) agree with the experimental values. Additionally, minor non-idealities in the connection of the diffusion tube to the main air flow line can impact the concentration due to induced turbulence at the junction. This sensitivity means diffusion tubes will probably always need to be calibrated after construction.

C.2 The effect of toluene concentration on EC

The relationship between the outlet concentration (i.e. residual concentration) and the EC was explored (Fig. 5.5 to 5.7). In Fig. C.2 to C.4 all the separate data points that form the averages were included. After initially exploring the range of toluene concentrations (Fig C.2), an increase in biomass was suspected and a new curve was explored (Fig. C.3). Nitrate was added temporarily to the water reservoir to stimulate growth and increase EC. The nitrate was removed and the system stabilised with a new biomass level (Fig. C.4).

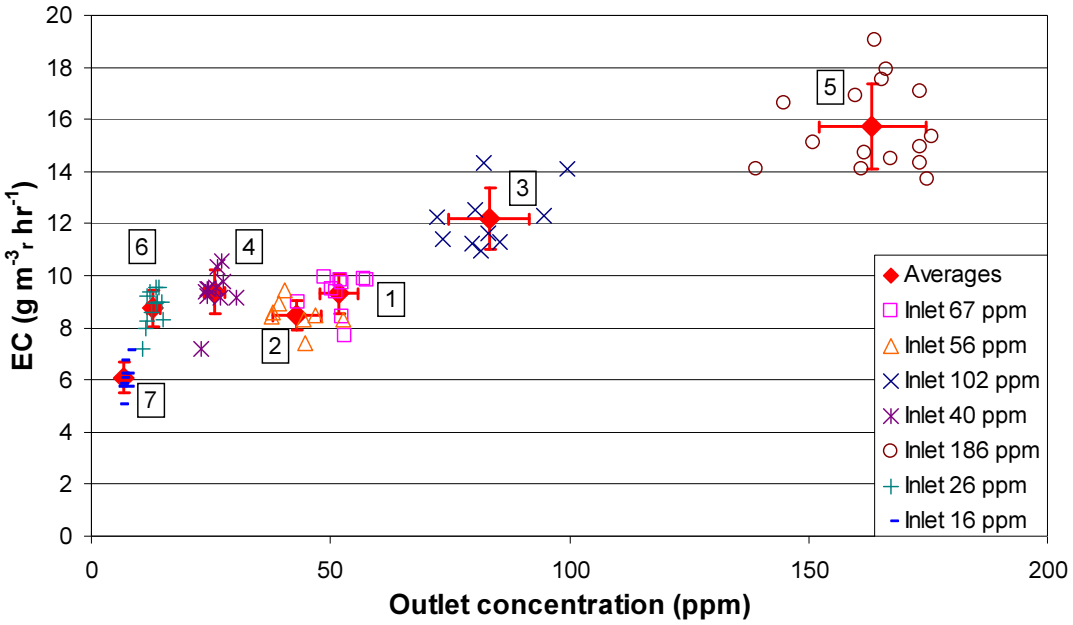

***Figure C.2**: The relationship between the outlet (or residual) concentration on the EC. The numbers represent the order in which the curve was generated. The red diamonds are the averages of between 8 and 15 samples, the error bars are one standard deviation. This sample set is called Low and was obtained between hour 2,000 and 5,000.*

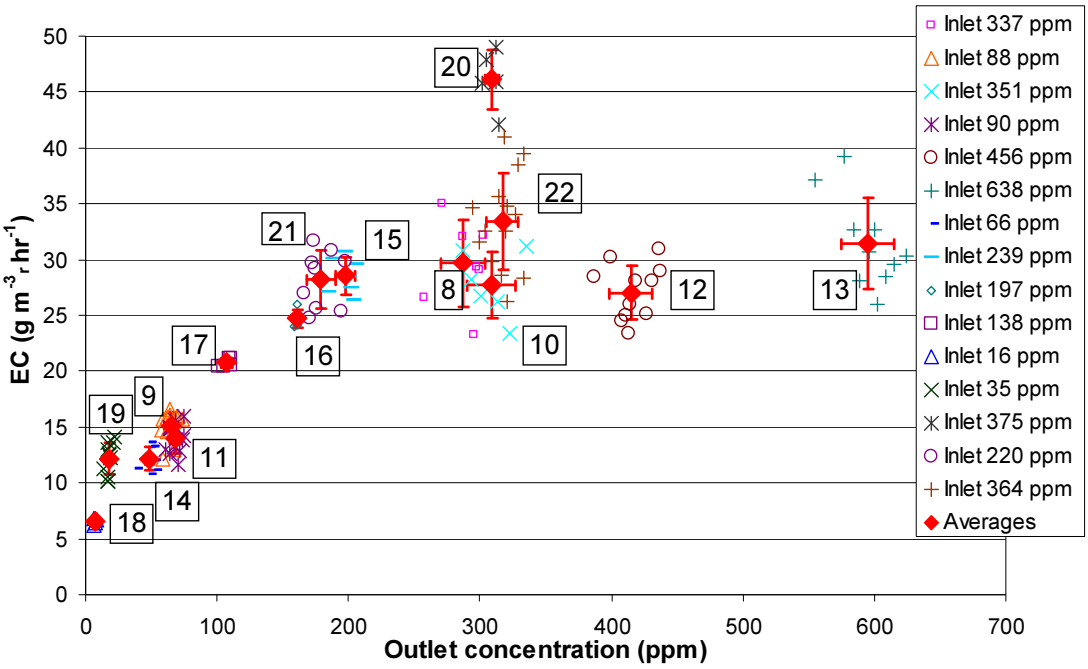

Figure C.3: *The relationship between the outlet (or residual) concentration on the EC. The numbers represent the order in which the curve was generated. The red diamonds are the averages of between 4 and 15 samples, the error bars are one standard deviation. The sample set is called High and was obtained between hour 5,000 and 9,600.*

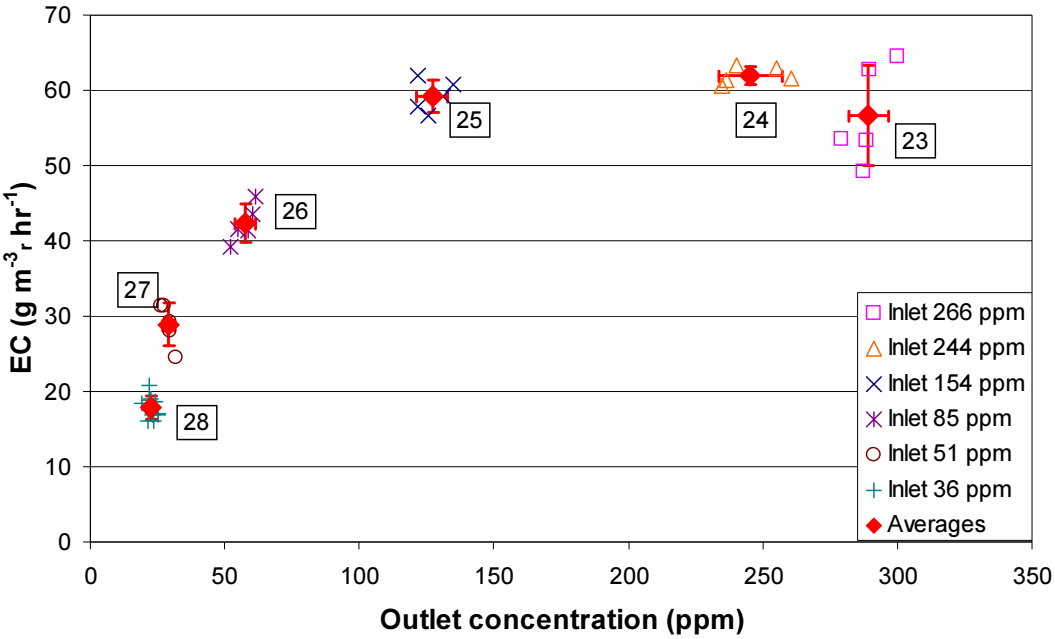

***Figure C.4**: The relationship between the outlet (or residual) concentration on the EC. The numbers represent the order in which the curve was generated. The red diamonds are the averages of between 5 to 11 samples, the error bars are one standard deviation. This sample set is called NO_3 and was obtained between hour 9,600 and 10,700.*

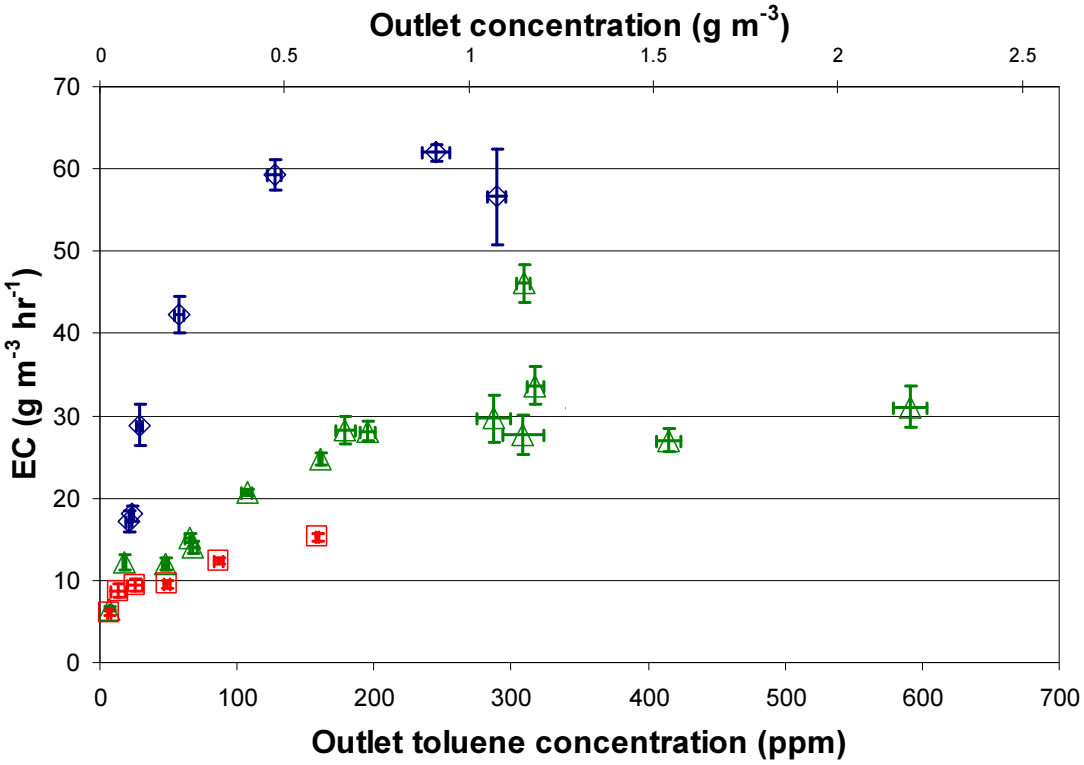

Figure C.5: *The relationship between the outlet (or residual) concentration on the EC for all three data sets. Low is the red open squares (□), High is the open green triangles (Δ) and NO_3 is the open blue diamonds (◊). The error bars represent 95% confidence interval.*

C.3 Fitting of the models

The known parameters can be found in Table 5.2. This leaves five unknown parameters: C_{crit}, EC_{crit}, L_F, A_F and K_s described Eqs. C.1 to C.9. The model was solved in the following steps:

1. From the three data sets initially, a C_{crit} and EC_{crit} were determined graphically (Table C.1). The C_{crit} is the lowest concentration where the maximal EC was reached.

Table C.1: *Initial values for C_{crit} and EC_{crit} obtained graphically from Figs C.2 – C.4,*

Parameter	**Low (Fig. C.2)**	**High (Fig. C.3)**	**NO_3 (Fig. C.4)**	**Units**
C_{crit}	80	175	100	ppm
EC at C_{crit}	15	29	60	$g\ m^{-3}_r\ hr^{-1}$

2. At C_{crit} the penetration thickness δ is equal to the biofilm thickness L_F (Eq. C.1).

$$L_F = \sqrt{\frac{2D_i \cdot \frac{C_{crit}}{m}}{q_{\max} \cdot X}} \qquad [C.1]$$

3. Subsequently, the biofilm area A_F can be calculated using Eq. C.2

$$A_F = \frac{F(C_{g,in} - C_{crit})}{q_{\max} X L_F} \qquad [C.2]$$

4. With these initial values, the variable residual gas concentration C_g (= $m \cdot C_{i,0}$) and a first guess of the K_s value (0.1 $g\ m^{-3}_g$ or 27 ppm, (Moller *et al.*, 1996; Vinage and von Rohr, 2003b)), the model can be solved by solving for the zero order flux (Eq. C.3 or Eq. C.4), the first order flux (Eq. C.5 and Eq. C.6). With the two fluxes, the composite flux can be calculated (Eq. C.7)

$$J_{F,i}^{0} = \sqrt{2D_i \cdot q_{\max,i} \cdot X} \cdot \sqrt{C_{i,0}} \qquad L_F > \delta \qquad [C.3]$$

$$J_{F,i}^{0} = L_F \cdot q_{\max,i} \cdot X \qquad L_F < \delta \qquad [C.4]$$

$$J_{F,i}^{1} = \frac{q_{\max,i} \cdot X \cdot L_F \cdot C_{i,0}}{K_s} \alpha \qquad [C.5]$$

Where

$$\alpha = \frac{\tanh \beta}{\beta} \quad \text{and} \quad \beta = \sqrt{\frac{q_{\max,i} \cdot X \cdot L_F}{D_i \cdot K_s}} \qquad [C.6]$$

$$J_{F,i} = \left(\frac{C_{i,0}}{C_{i,0} + K_s} \right) J_{F,i}^{0} + \left(1 - \frac{C_{i,0}}{C_{i,0} + K_s} \right) J_{F,i}^{1} \qquad [C.7]$$

With the composite flux, Eq. 5.38 can be reorganised to obtain the inlet gas concentration $C_{g,in}$ (Eq. C.8).

$$C_{g,in} = \frac{J_{F,i} A_F}{F} + mC_{i,0} \qquad [C.8]$$

And finally the EC can be calculated using Eq. C.9.

$$EC = \frac{(C_{g,in} - C_g)F}{V} \qquad [C.9]$$

5. With the first guess of K_s, the best values for the C_{crit} and EC_{crit} can be found. First the R^2 (Eq. C.11) value for every data set is calculated. The R^2 uses the y (measured EC's), $\bar{y}$ (the average of the measured EC's) and y (the predicted EC's by the model) The R^2 value is between 0 (worst fit) and 1 (perfect fit). Then the sum of the three data sets (R^2_{total}, Eq. C.12) is maximised using the Solver function in Excel.

$$R^2 = \frac{\sum (y - \bar{y})^2 - \sum (y - y)^2}{\sum (y - \bar{y})^2} \quad [C.11]$$

$$R^2_{total} = R^2_{Low} + R^2_{High} + R^2_{NO_3} \quad [C.12]$$

6. The K_s is assumed to be constant for the three data sets, as the biomass in the biofilm is assumed to be constant in concentration and composition. To optimise the K_s value, first the least squares (LSM) for every data set are calculated. This is the sum of the squared difference between y (measured EC) and the EC's predicted by the model (y) (Eq. C.10). The LSM is calculated for all three data sets and added together. This sum is minimised by changing the K_s using the Solver function in Excel

$$LSM = \sum (y - y)^2 \quad [C.10]$$

$$LSM_{total} = LSM_{Low} + LSM_{High} + LSM_{NO_3} \quad [C.11]$$

7. With new value of $K_{s\ t}$, steps 5 and 6 are repeated until the conditions in Eqs. C.13 and C.14 are met. With j the number of iteration steps.

$$\frac{R^2_{total,j+1} - R^2_{total,j}}{R^2_{total,j}} \cdot 100\% \leq 10^{-2}\% \quad [C.13]$$

$$\frac{LSM_{total,j} - LSM_{total,j+1}}{LSM_{total,j}} \cdot 100\% \leq 10^{-3}\% \quad [C.14]$$

8. With the sum of squares (Eq. C.15), the sum of squares of the 95% confidence intervals can be calculated with Eq. C.16.

$$S_R = \sum (y - y)^2 \quad [C.15]$$

$$S_{95} = S_R\left[1 + \frac{p}{n-p} F_{0.05}(p, n-p)\right] \quad [C.16]$$

With the optimal, C_{crit} and EC_{crit} final the biofilm thickness L_F and biofilm area A_F are recalculated with Eqs. C.1 and C.2. The final values are reported in Table C.2 and C.3.

***Table C.2**: Values used for the fitting of the zero order model.*

Parameter	**Low**	**High**	**NO_3**	**Units**
C_{crit}	109	266	136	ppm
Inlet concentration at C_{crit} (C_{in})	132	314	225	ppm
EC at C_{crit}	15.4	32.5	59.3	g m^{-3}_r hr^{-1}
Biofilm area (A_F)	9.5 10^{-4}	1.3 10^{-3}	3.3 10^{-3}	m^2
Biofilm thickness (L_F)	8.6 10^{-5}	1.3 10^{-4}	9.6 10^{-5}	m
Sum of squares (S_R)	25	278	115	-
Sum of squares within 95% confidence interval	381	441	84	-
EC_{crit} boundaries 95% confidence interval	8-14	25-34	45-59	g m^{-3}_r hr^{-1}
E_{crit} boundaries 95% confidence interval	10-275	159-403	78-194	ppm
R^2 zero order	0.53	0.81	0.95	-

***Table 5.3**: Values used for the fitting of the composite model. The R^2 value for the first order part of the composite model is not shown because of the poor fit.*

Parameter	**Low (Fig. 5.8)**	**High (Fig. 5.9)**	**NO_3 (Fig. 5.10)**	**Units**
C_{crit}	69.0	268	127	ppm
Inlet concentration at C_{crit} (C_{in})	86.7	312	205	ppm
EC at C_{crit}	11.9	29.5	52.1	g m^{-3}_r hr^{-1}
Biofilm area (A_F)	$9.3\ 10^{-4}$	$1.2\ 10^{-3}$	$3.0\ 10^{-3}$	m^2
Biofilm thickness (L_F)	$6.8\ 10^{-5}$	$1.3\ 10^{-4}$	$9.2\ 10^{-5}$	m
K_s	$1.27\ 10^{-1}$			g m^{-3}
Sum of squares (S_R)	40	296	83	-
Sum of squares within 95% confidence interval (S_{95})	236	553	496	-
EC_{crit} boundaries 95% confidence interval	7-17	28-36	52-66	g m^{-3}_r hr^{-1}
E_{crit} boundaries 95% confidence interval	1-103	175-374	101-203	ppm
R^2 composite	0.26	0.80	0.96	-
R^2 zero order of composite	0.31	0.76	0.88	-
Iteration result (j = 4) Eq. C.13	$8.6\ 10^{-3}$			%
Iteration result (j = 4) Eq. C.14	$5.2\ 10^{-5}$			%

The values for the biofilm thickness L_F and area A_F can be checked if they are realistic. The physical dimensions of the compost layer restrict these values. Compost has a specific area between 300 and 1000 m^2 m^{-3} (Ottengraf and Konings, 1991). The area of compost surface in the reactor is therefore between $1.9\ 10^{-3}$ and $6.6\ 10^{-3}$ m^2. The estimated area of the biofilm should be within this range (Table C.2). As well as the total biofilm volume cannot exceed the total volume of the compost layer. With a

porosity of 0.3 (Choi and Myung, 2004), the volume of pores is 2.0 10^{-6} m^3. The total biofilm volume for the three runs is 6.3 10^{-8}, 1.6 10^{-7} and 2.8 10^{-7} m^3, which is well below the pore volume.

C.4 Nomenclature

A_F	area of the biofilm	m^2
C_{crit}	concentration of full penetration	g m^{-3}_g
$C_{g,in}$	inlet concentration in the gas phase	g m^{-3}_g
D_i	diffusion coefficient of *i*	m^2 h^{-1}
F	gas flow rate	m^3_g h^{-1}
j	number of iteration steps	-
K_s	Toluene half-saturation constant	g m^{-3}_g
L_F	biofilm thickness	m
m	Henry distribution coefficient	-
n	number of samples	-
p	number of parameters	-
q_{max}	maximum specific degradation rate of *i*	g m^{-3} h^{-1}
S_R	Sum of squares	-
S_{95}	Sum of squares for the 95% confidence Interval	-
X	biomass concentration	g m^{-3}_b
y	data point (EC)	g m^{-3}_r h^{-1}
$\bar{y}$	average of all data points (EC)	g m^{-3}_r h^{-1}
y	predicted value by model (EC)	g m^{-3}_r h^{-1}
δ	penetration depth	m

Subscripts

b	of biomass
g	of gas
r	of reactor

C.5 References

Choi, H. S., and S. W. Myung. 2004. Numerical and experimental study on the biofiltration of toluene vapor. *Korean Journal of Chemical Engineering* 21: 680-688.

Moller, S., A. R. Pedersen, L. K. Poulsen, E. Arvin, and S. Molin. 1996. Activity and three-dimensional distribution of toluene-degrading *Pseudomonas putida* in a multispecies biofilm assessed by quantitative in situ hybridization and scanning confocal laser microscopy. *Applied and Environmental Microbiology* 62: 4632-4640.

Ottengraf, S. P. P., and J. H. G. Konings. 1991. Emission of microorganisms from biofilters. *Bioprocess Engineering* 7: 89-96.

Vinage, I., and P. R. von Rohr. 2003. Biological waste gas treatment with a modified rotating biological contactor. II. Effect of operating parameters on process performance and mathematical modeling. *Bioprocess and Biosystems Engineering* 26: 75-82.